BNL 51232

[redacted]

FINAL REPORT OF THE EVALUATION OF VAPOR TAGGANTS AND SUBSTRATES FOR THE TAGGING OF BLASTING CAPS

GUNNAR I. SENUM, ROBERT P. GERGLEY, EUGENE M. FERRERI,
MARGARET W. GREENE AND RUSSELL N. DIETZ

MARCH 1980

SPONSORED BY THE
BUREAU OF ALCOHOL, TOBACCO AND FIREARMS
OF THE U.S. DEPARTMENT OF THE TREASURY

UNDER THE DIRECTION OF
THE AEROSPACE CORPORATION

DEPARTMENT OF ENERGY AND ENVIRONMENT

BROOKHAVEN NATIONAL LABORATORY
UPTON, NEW YORK 11973

EVALUATION OF VAPOR TAGGANTS AND SUBSTRATES FOR THE TAGGING OF BLASTING CAPS

Gunnar I. Senum, Robert P. Gergley, Eugene M. Ferreri,
Margaret W. Greene and Russell N. Dietz

March 1980

Sponsored by the
the Bureau of Alcohol, Tobacco and Firearms
of the U.S. Department of the Treasury

under the direction of
The Aerospace Corporation

Leonard Newman - Division Head

ENVIRONMENTAL CHEMISTRY DIVISION

DEPARTMENT OF ENERGY AND ENVIRONMENT
BROOKHAVEN NATIONAL LABORATORY
ASSOCIATED UNIVERSITIES, INC.

Under Contract No. DE-AC02-76CH00016 with the
UNITED STATES DEPARTMENT OF ENERGY

NOTICE

This report was prepared as an account of work sponsored by the United States Government. Neither the United States, nor any agency thereof, nor any of their employees, makes any warranty, express or implied, or assumes any legal liability or responsibility for the accuracy, completeness, or usefulness of any information, apparatus, product, or process disclosed, or represents that its use would not infringe privately owned rights. Reference herein to any specific commercial product, process, or service by trade name, mark, manufacturer, or otherwise, does not necessarily constitute or imply its endorsement, recommendation, or favoring by the United States Government or any agency thereof. The views and opinions of authors expressed herein do not necessarily state or reflect those of the United States Government or any agency thereof.

ABSTRACT

Efforts for the predetonation tagging of electric blasting caps have been focused on the investigation of appropriate vapor taggant chemicals and elastomeric substrates. Atlas Powder Company, Hercules, Inc., and duPont are the three principal manufacturers of blasting caps for use as items of commerce in the explosives industry. However, electric blasting caps represent a common key component of clandestine bombs. Therefore, Brookhaven National Laboratory was placed under contract to investigate methods to successfully tag blasting caps, at the time of manufacture, with a distinctive chemical. This chemical, when subsequently detected by sensitive instruments at a security checkpoint, would indicate the presence of a clandestine bomb.

In order to accomplish this objective, several performance criteria had to be simultaneously optimized.

During this evaluation, approximately 20 vapor taggant chemicals and 6 elastomeric substrate materials useful as blasting cap end closures were evaluated.

Five chemicals have passed the vapor taggant chemical selection criteria:

- perfluorodimethylcyclobutane (PDCB),
- perfluoromethylcyclohexane (PMCH),
- perfluorodimethylcyclohexane (PDCH),
- perfluorohexylsulfur pentafluoride (L-4412), and
- perfluorodecalin (PFD).

None of the elastomers presently used by the blasting cap manufacturers passed the substrate selection criteria. Only highly fluorinated

elastomers such as Viton or Fluorel were acceptable. The selected vapor taggants were incorporated into these elastomers. No pairing directly satisfied the performance criteria when suitable vapor taggant chemicals were solubilized into selected elastomers. Marginal satisfaction of the emission rate and useful lifetime criteria were met by pairing L-4412 with Viton.

Due to technical difficulties encountered in the direct solubilization of detection taggants in elastomers of blasting caps, a second method of vapor tagging explosive products was studied. Through the use of microencapsulation technology, a vapor taggant chemical is enclosed in small (5 to 35 μm) diameter particles. The microcapsule wall chemical composition and size characteristics control the subsequent release of vapor taggant chemical. The microcapsules can be added to packaged, cap-sensitive explosives at the time of manufacture as a free-flowing powder at 0.05 to 0.10 percent by weight. Brookhaven has measured the emission rate of several prepared microcapsule batches and sticks of simulated explosives tagged with 0.05 to 0.10 percent by weight of microcapsules.

GLOSSARY

A	the total area of the cracks in the barrier (cm^2)
a	attenuation factor due to surface adsorption
$a_{0 \cdots n}$	power series expansion coefficient
c	empirical constant associated with the adsorption phenomena
C(t)	the taggant concentration (ppt) inside the scenario at time (t)
$C(\infty)$	steady-state taggant concentration (ppt)
$C_o(t)$	the concentration of taggant in the scenario with no barrier
Cen(t)	the concentration of taggant (ppt) inside the barrier at time (t)
D	the taggant diffusion constant in air (cm^2/min)
DFBP	decafluorobiphenyl
DFCH	decafluorocyclohexene
2,4-DNT	2,4-dinitrotoluene
EGDN	ethylene glycol dinitrate
f	the volume fraction of the taggant in the air leaving the scenario
f(s)	the Laplace transform of V(t)
FC-72	3M Company Fluorinert liquid, average molecular weight-340
FC-78	3M Company Fluorinert liquid, average molecular weight-300
FC-77	3M Company Fluorinert liquid, average molecular weight-415
Freon E-1	duPont Freon
Freon E-2	duPont Freon
g(s)	Laplace transform of V_{en} (t)

HFB	hexafluorobenzene
k	barrier constant (1/min)
L	average depth (cm) of a crack in the barrier
L-4412	perfluorohexylsulfur pentafluoride
NG	nitroglycerin
OFCP	octafluorocyclopentene
OFN	octafluoronaphthalene
OFT	octafluorotoluene
P	partial pressure (torr) of the taggant chemical
P_o	equilibrium vapor pressure (torr) of taggant chemical
PDCB	perfluorodimethylcyclobutane (mixture of 1,2- and 1,3-isomers)
PDCH	perfluorodimethylcyclohexane (mixture of 1,3- and 1,4-isomers)
PETN	pentaerythritol tetranitrate
P_{ext}	ambient pressure (torr)
PFD	perfluorodecalin
PFP	pentafluoropyridine
PFX	perfluoroxylene
PMCH	perfluoromethylcyclohexane
ppb	parts per billion (volume per volume)
ppt	parts per trillion (volume per volume)
Q	the permeability coefficient cm^3 (STP) cm/sec-cm^2 torr
r_1	coefficient of the Laplace transform
r_2	coefficient of the Laplace transform

R_{ad}	rate of taggant chemical loss due to adsorption (d Vad/dt)-(l/min)
R_{cap}	taggant emission rate (l/min)
RDX	1,3,5-trinitro-1,3,5-triazacyclohexane
$R_{en}(t)$	taggant emission rate from the barrier into the scenario (l/min)
R_{ex}	chamber ventilation rate (l/min)
t	time (min)
TNT	2,4,6-trinitrotoluene
t_v	turnover or ventilation time (min) of the scenario
V	taggant volume (l) inside the barrier at time t = 0
Vad	volume of taggant contained in the Langmuir adsorption isotherm (l)
V_{ch}	volume (l) of scenario
$\overset{*}{V}_{en}$	initial non-zero taggant volume (l) inside the barrier
V_{en}	volume (l) of barrier
$V_{en}(t)$	the taggant volume (l) inside the barrier at time (min)
v_m	gas volume (l) necessary to cover the absorbing surface with a monolayer
$V_o(t)$	taggant volume (l) present in scenario at time (t)
V(t)	taggant volume (l) inside the scenario at time (t)
β	ratio of barrier air exchange rate to scenario ventilation rate, i.e., k/R_{ex} (dimensionless)
γ	ratio of barrier volume to scenario volume, i.e., V_{en}/V_{ch} (dimensionless)
τ	turnover time factor, t/t_v (dimensionless)

atmospheric ionization mass spectroscopy techniques. These three detection mechanisms are under consideration. The three methods utilize negative ion formation from the fluorocarbon taggant chemical and utilize this feature for subsequent detection.

The solubilization of a vapor taggant into a blasting cap end closure requires the selection of a perfluorinated vapor taggant that has appropriate solubility characteristics and emission rates of vapor taggant from the end closure. The taggant emission rate must be high enough to be detected in various envisioned scenarios and yet low enough for the solubilized taggant to be effective for a period of from 5 to 10 years. Ideally, 5 to 10 percent by weight (25 to 50 mg) of vapor taggant would be solubilized into an end closure which would have an emission rate in the 0.5 to 5 nl/min (2 to 20 μg per day) in order to be detected in most scenarios during a 5- to 10-year emitting lifetime.

The perfluorinated vapor taggant selection program was experimentally investigated in three steps. The first step was an initial screening of perfluorinated compounds for those that had the requisite solubility in the currently used electric blasting cap end closures and in other substitute elastomeric substrates. Vapor taggants and substrates which satisfied the first step were prepared as tagged dummy blasting caps. In the second step, the emission rates of the vapor taggants from these caps where then monitored over several months in order to evaluate each taggant/substrate combination. Finally, as step 3, each successful taggant/substrate pair was evaluated with respect to adsorption loss in a typical detection scenario.

A large number of perfluorinated compounds were examined. The range of perfluorinated compounds included perfluoroalkanes, perfluorocycloalkanes, perfluoroalkenes, fluoroaromatics, inorganic fluorides, and other miscellaneous fluorides. The solubilities were determined by

exposing the substrates to the perfluorinated compounds at a variety of temperatures and pressures. The abbreviations for the perfluorinated compounds of interest are given in Table 1. The compounds

Table 1. Abbreviations for the Perfluorinated Compounds

Abbreviation	Chemical Name
OFN	Octafluoronaphthalene
HFB	Hexafluorobenzene
OFT	Octafluorotoluene
DFBP	Decafluorobiphenyl
PDCB	Perfluorodimethylcyclobutane
PMCH	Perfluoromethylcyclohexane
PDCH	Perfluorodimethylcyclohexane
SF_6	Sulfur hexafluoride
PFX	Perfluoroxylene
PFP	Pentafluoropyridine
DFCH	Decafluorocyclohexene
OFCP	Octafluorocyclopentene
PFD	Perfluorodecalin
L-4412	Perfluorohexylsulfur pentafluoride

which have at least 5 percent solubility (by weight) in the substrate in either one of the three present blasting cap end closures (Buna (DuPont), Rubber (Atlas) and Kraton (Hercules)) or in Viton (DuPont) or equivalently Fluorel (3M) are tabulated in Table 2. Negative solubilities represent a leaching of the substrate by the perfluorinated compound; other methods were used to verify negligible solubilities when they occurred.

atmospheric ionization mass spectroscopy techniques. These three detection mechanisms are under consideration. The three methods utilize negative ion formation from the fluorocarbon taggant chemical and utilize this feature for subsequent detection.

The solubilization of a vapor taggant into a blasting cap end closure requires the selection of a perfluorinated vapor taggant that has appropriate solubility characteristics and emission rates of vapor taggant from the end closure. The taggant emission rate must be high enough to be detected in various envisioned scenarios and yet low enough for the solubilized taggant to be effective for a period of from 5 to 10 years. Ideally, 5 to 10 percent by weight (25 to 50 mg) of vapor taggant would be solubilized into an end closure which would have an emission rate in the 0.5 to 5 nl/min (2 to 20 g per day) in order to be detected in most scenarios during a 5- to 10-year emitting lifetime.

The perfluorinated vapor taggant selection program was experimentally investigated in three steps. The first step was an initial screening of perfluorinated compounds for those that had the requisite solubility in the currently used electric blasting cap end closures and in other substitute elastomeric substrates. Vapor taggants and substrates which satisfied the first step were prepared as tagged dummy blasting caps. In the second step, the emission rates of the vapor taggants from these caps where then monitored over several months in order to evaluate each taggant/substrate combination. Finally, as step 3, each successful taggant/substrate pair was evaluated with respect to adsorption loss in a typical detection scenario.

A large number of perfluorinated compounds were examined. The range of perfluorinated compounds included perfluoroalkanes, perfluorocycloalkanes, perfluoroalkenes, fluoroaromatics, inorganic fluorides, and other miscellaneous fluorides. The solubilities were determined by

exposing the substrates to the perfluorinated compounds at a variety of temperatures and pressures. The abbreviations for the perfluorinated compounds of interest are given in Table 1. The compounds

Table 1. Abbreviations for the Perfluorinated Compounds

Abbreviation	Chemical Name
OFN	Octafluoronaphthalene
HFB	Hexafluorobenzene
OFT	Octafluorotoluene
DFBP	Decafluorobiphenyl
PDCB	Perfluorodimethylcyclobutane
PMCH	Perfluoromethylcyclohexane
PDCH	Perfluorodimethylcyclohexane
SF_6	Sulfur hexafluoride
PFX	Perfluoroxylene
PFP	Pentafluoropyridine
DFCH	Decafluorocyclohexene
OFCP	Octafluorocyclopentene
PFD	Perfluorodecalin
L-4412	Perfluorohexylsulfur pentafluoride

which have at least 5 percent solubility (by weight) in the substrate in either one of the three present blasting cap end closures (Buna (DuPont), Rubber (Atlas) and Kraton (Hercules)) or in Viton (DuPont) or equivalently Fluorel (3M) are tabulated in Table 2. Negative solubilities represent a leaching of the substrate by the perfluorinated compound; other methods were used to verify negligible solubilities when they occurred.

Table 2. Solubility of Various Perfluorinated Compounds in the Present Electric Blasting Cap End Closures and in Viton or Fluorel in percent by weight

	End Closure Substrates (% by weight)			
Perfluorinated Compounds	DuPont Buna	Atlas Rubber	Hercules Kraton	Viton or Fluorel
OFN	60.3	25.6	182.6	107.2
HFB	22.0	28.6	26.4	85.9
OFT	5.7	10.3	-10.4	60.5
DFBP	11.2	27.8	-4.6	60.1
PDCB	-5.7	-0.2	-2.0	8.9
PMCH	-5.3	1.7	-5.6	7.6
PDCH	-6.1	0.6	-6.6	7.9
SF_6	-0.9	1.5	2.0	7.0
PFX	8.0	6.9	-10.3	7.3
PFP	40.9	11.5	3.0	139.0
DFCH	-2.0	6.1	-1.8	20.0
OFCP	-3.0	6.6	-6.8	24.3
PFD	-1.4	3.4	2.1	2.4
L-4412	17.1	0.97	--	1.8

The results of this initial solubility screening indicate that most perfluorinated compounds have a high degree of solubility in the Viton and Fluorel fluoroelastomers whereas only the fluoroaromatics have appreciable solubilities in the present electric blasting cap end closures.

Dummy tagged blasting caps were prepared from taggant/substrate combinations which were chosen on the basis of the solubility results. The end closure substrates were obtained from the blasting cap manufacturers, and the Viton and Fluorel substrates from rubber compounders. The end closure test pieces were the same size as are presently used. The taggants were impregnated into the elastomeric substrates using procedures to ensure uniform impregnation of the substrate. The resulting end closures were crimped into blank electric blasting cap shells with a duPont crimper in order to simulate, as closly as possible, the present manufacturing techniques. Triplicate sets of tagged blasting caps were prepared for emission rate determinations at room temperature, 45°C and 65°C. The tagged caps were tare weighed periodically on a microbalance for a period of several months in order to determine gravimetric loss data (i.e., the rate of weight loss of the tagged cap due to vapor taggant emission). Occasionally the emission rates determined from the gravimetric loss data were verified by a chromatographic determination of the emission rates with good agreement between the two methods.

The taggant emission rates as derived from the gravimetric loss data were obtained over a time period up to 6 months. In order to fully evaluate the various taggant/substrate combinations, an emission rate model was derived which would be able to predict emission rates at time periods up to 5 years based on a few months of gravimetric loss data. The taggant emission rate model was derived by applying the diffusion equation to the geometry of a tagged blasting cap with the following model assumptions.

1. The rate of taggant emission from the tagged blasting cap is determined by:

    - The rate of taggant diffusion in the substrate plug as characterized by a taggant/substrate diffusion constant.

- The rate of taggant mass transfer across the substrate plug end as characterized by a taggant mass transfer coefficient.

2. The taggant diffusion constant is independent of the initial taggant concentration in the substrate plug.

3. The substrate plug is impregnated uniformly with the taggant, at least in the axial direction, at the time of impregnation.

Solution of the differential diffusion equation with these model assumptions leads to the following expression for the taggant emission rate

$$\frac{dc(t)}{dt} = - \frac{c(o)}{Z_0} \left(\frac{D}{\pi t}\right)^{1/2} \left(1+2 \sum_{n=1}^{\infty} (-1)^n \exp\left[- \frac{n^2 Z_0^2}{Dt}\right]\right) \qquad (1)$$

where: $dc(t)/dt$ = the taggant emission rate (milligrams of taggant/sec)

$c(o)$ = the amount of taggant impregnated into the substrate plug (milligrams of taggant)

D = the taggant/substrate diffusion constant (cm^2/sec)

t = the age of the tagged blasting cap, i.e., the elapsed time after impregnation (sec).

This solution reflects the experimental observation that the taggant mass transfer rate across the plug end is negligible when compared to the taggant diffusion rate in the substrate plug. In most situations, the emission rate expression (1) can be approximated by the first term,

$$\frac{dc(t)}{dt} \approx -\frac{c(o)}{Z_0}\left(\frac{D}{\pi t}\right)^{1/2} \qquad (2)$$

yielding a simple inverse square root of time dependence for the taggant emission rate.

Integration of (2) leads to the following approximate expression for c(t), the total amount of taggant remaining in the substrate plug as a function of elapsed time after impregnation, i.e.,

$$c(t) \approx c(o) - 2c(o)(Dt/\pi Z_0^2)^{1/2} \qquad (3)$$

This expression is used to obtain the taggant/substrate diffusion constants from the experimentally obtained gravimetric loss data. With this diffusion constant, (1) permits the prediction of the taggant emission rates from a tagged blasting cap up to 5 to 10 years after impregnation based on data from a few months of following the weight change of tagged blasting caps.

Taggant/substrate combinations which meet the taggant emission rate requirements (0.5 to 5 nl/min over a 5- to 10-year period) are presented in Table 3. None of the pairings of end closures and vapor taggant chemicals satisfy the solubility requirements of 5 to 10 percent by weight, and an emission rate of greater than 0.5 nl/min at the end of 5 years.

In a separate study, the vapor taggant chemical candidates were experimentally evaluated for comparative performance with respect to adsorption on surfaces or penetration of barriers. In the penetration of barriers studies, it was assumed that the most volatile vapor taggant, PDCB, has no appreciable surface interaction reducing its available vapor phase taggant concentration.

Table 3. Most Promising End Closure Taggant Combinations

End Closure/Taggant	Diffusion Constant (10^{-9} cm^2/sec)	Emission Rate (nl/min)		
		1 yr	2 yr	4 yr
DuPont Buna/OFN	3.23	1.82	1.15	0.490
DuPont Buna/DFBP	32.2	1.70	0.359	0.016
Kraton/PFD	17.8	2.28	1.06	0.230
Kraton/OFN	9.99	1.93	1.17	0.445
Atlas/OFCP	15.8	2.90	1.35	0.294
Atlas/DFBP	21.6	1.90	0.670	0.083
Atlas/PDCH	23.5	1.57	0.506	0.052
Atlas/L-4412	11.4	1.38	0.642	0.140
Viton/SF_6	3.4	2.12	1.50	1.01
Viton/PFP	3.07	1.74	1.23	0.844
Viton/PFD	20.7	0.984	0.208	0.044
Viton/HFB	3.25	1.63	1.15	0.782
Viton/OFT	1.74	0.939	0.664	0.469
Viton/L-4412	3.20	0.674	0.476	0.337
Fluorosilicone 70/PMCH	25.7	1.77	0.512	0.042
Fluorosilicone 70/PDCB	25.7	2.07	0.597	0.050

Several potential vapor taggants were experimentally examined for their vapor concentration depletion by adsorption in a typical scenario. Three potential vapor taggants, perfluorodimethylcyclobutane (PDCB), perfluoromethylcyclohexane (PMCH), and perfluorodimethylcyclohexane (PDCH) were determined to have a negligible adsorption loss. Perfluorodecalin (PFD) and perfluorohexylsulfur pentafluoride (L-4412) were determined to have moderate adsorption losses of 66 and 40 percent, respectively. Three other potential taggants, decafluorobiphenyl (DFBP), octafluoronaphthalene (OFN), and octafluorotoluene (OFT) have significant adsorption losses (greater than 80 percent) that we believed would preclude their use as effective vapor taggants. Thus, the list of acceptable taggant/substrates in Table 3 is severely reduced with only PDCB, PMCH, PDCH, PFD, and L-4412 being the most acceptable taggants.

The second type of taggant attenuation in the scenario is independent of the choice of taggant but dependent on the tagged explosive enclosure. Six enclosures were examined experimentally for their ability to contain taggant vapors. Of these, a box filled with styrofoam packing, a suitcase, a heat-sealed polyethylene bag, and an attache case provided no significant impediment to the release of the vapor taggant into the detection scenario, i.e., these enclosures had a negligible degree of airtightness. The remaining two enclosures examined, a paint can and a zip-lock plastic bag, showed significant vapor containment and thus possibly could hinder the vapor detection of explosives. These results were further corroborated by two field experiments involving the detection of vapor tagged simulated explosives in various luggage items. The various types of baggage, ranging from a soft suitcase to an aluminum suitcase with a rubber gasket, did not possess any significant degree of airtightness so as to impede the detection of the vapor taggant.

These field experiments served to verify the conclusions of a theoretical model of barrier enclosed explosives: The taggant concentration within briefcases and suitcases containing a tagged explosive emitting at 1 nl/min is of the order of ppb. This concentration allows real-time continuous detection of the taggants using a taggant detection system with a ppt limit of detection and a sampling system having a dilution factor up to 1000. The model predicted that the taggant concentration attained in a moderately sized room and a severe barrier containing a taggant source of 1 nl/min emission rate in it 1 hour earlier is detectable 15 min after introduction. A moderate barrier, such as a suitcase or box, would allow almost real-time continuous detection under the same circumstances.

For the second method of vapor tagging studied, namely incorporation of microencapsulated taggants into packaged explosives, over 50 microencapsulated taggant samples were examined for suitability with respect to the specified taggant emission rate; namely 1 to 10 nl/min-g. Most microcapsules were found experimentally to be fragile or to have too low a taggant emission rate. One microencapsulated sample, L-4445, as supplied by 3M, provided an acceptable PDCH taggant emission rate when mixed with simulated explosives. These explosives tagged with L-4445 microcapsule successfully demonstrated the viability of vapor tagging of explosives with microencapsulated PDCH. The demonstrations involved the detection of the vapor tagged explosives (1) aboard an aircraft and (2) in luggage (by means of a baggage examiner). The results of these field tests indicate a successful predetonation detection of concealed explosive vapor tagged by microencapsulated vapor taggants.

CONTENTS

ABSTRACT		iii
GLOSSARY		v
EXECUTIVE SUMMARY		ix
I.	INTRODUCTION	1-1
II.	SOLUBILITY OF VAPOR TAGGANTS IN BLASTING CAP END CLOSURES	2-1
III.	ELECTRON CAPTURE DETECTION	3-1
	A. Theoretical Considerations	3-1
	B. Continuously Operating Perfluorocarbon Sniffer	3-17
IV.	AMBIENT ATMOSPHERIC BACKGROUNDS OF PROPOSED VAPOR TAGGANTS	4-1
V.	TAGGANT DETECTABILITY	5-1
	A. Adsorption Losses	5-1
	B. Theoretical Model of Taggant Considerations from Barrier-Enclosed Vapor Tagged Explosives	5-19
	C. Experimental Results: Taggant Concentration from Barrier-Enclosed Vapor-Tagged Explosives	5-51
VI.	ENVIRONMENTAL EFFECTS OF VAPOR TAGGANTS	6-1
	A. Toxicity of Vapor Taggants	6-1
	B. Detonation End Products from PDCH Tagged Explosives	6-2
VII.	SOLUBILIZED VAPOR TAGGANT EFFECT ON END CLOSURE MECHANICAL PROPERTIES	7-1
VIII.	TAGGANT EMISSION RATES FROM VAPOR TAGGED BLASTING CAPS	8-1
	A. Theoretical Diffusion Model	8-1
	B. Experimental Results	8-7

CONTENTS (concluded)

IX. TAGGANT EMISSION RATES FROM MICROENCAPSULATED VAPOR TAGGANTS 9-1

A. Gelatin Walled Microcapsule: Sample Batch Numbers AC1093 and AC1094 9-1
B. National Cash Register (NCR) Coated Labels 9-4
C. 3M Microcapsules 9-6
D. Capsulated Systems, Inc. (CSI), Microencapsulated Perfluorocarbon Samples 9-6
E. Microcapsule Tagged Cap-Sensitive, Packaged Explosive Simulants 9-14
F. Microcapsule Blended in Blasting Cap End Closures 9-15

X. CONCLUSION 10-1

A. Solubilization of the Vapor Taggant into the Blasting Cap End Closure 10-2
B. Blending of Packaged, Cap-Sensitive Explosives with Microencapsulated Vapor Taggants 10-5
C. Microencapsulated Vapor Taggants Blended in Blasting Cap End Closures 10-5
D. Detection of Vapor Tagged Explosives Contained in Barriers 10-6

XI. REFERENCES 11-1

APPENDIX A. Scenario Taggant Concentrations from Barrier Enclosed Vapor Tagged Explosives: Solution of the Two Coupled Differential Equations A-1

APPENDIX B. Taggant Emission Rates from Vapor Tagged Blasting Caps: Mathematical Solution of the Diffusion Model B-1

APPENDIX C. Taggant Concentrations in Detection Scenarios Enclosed in Various Barriers: Theoretical Modeling of the Adsorption Losses C-1

APPENDIX D. Evaluation and Field Testing of Vapor Taggants for Predetonation Detection of Explosives D-1

I. INTRODUCTION

An effective technique for detecting concealed explosives prior to detonation is to vapor tag the explosive components with a material that can be detected as a trace vapor. The technique is accomplished by the incorporation of specific compounds--vapor taggants--into the explosives at the time of manufacture effecting a subsequent slow vapor taggant release from the explosive over a long time period. Concealed explosives so tagged can be detected by the presence of the taggant vapor in scenarios such as rooms, buildings, aircraft, etc.

Three methods have been proposed for vapor taggant incorporation:

- Solubilizing the vapor taggants into blasting cap end closures with the consequent diffusion of the taggant,

- Blending microencapsulated vapor taggants with explosives with the consequent permeation of taggant from the microcapsule, and

- Blending microencapsulated taggants with blasting cap end closures during manufacture with the consequent permeation and diffusion of the taggant end closure.

Other methods for vapor tagging explosives have been proposed; however, these three methods were examined in the experimental program reported herein. These methods for vapor predetonation detection of explosives have been considered because of the inability to successfully detect the natural vapors emitted by explosives, (EGDN, NG, 2,4-DNT, 2,4,6-TNT, RDX, PETN) with the required detection sensitivity (Pate, 1976; McReynolds et al., 1975).

Solubilization was the method primarily investigated in this effort, which was a continuation of an earlier program at Brookhaven (Dietz et al., 1976). This earlier program demonstrated the possibility of tagging blasting caps using sulfur hexafluoride, but more importantly, it demonstrated the general concept of vapor tagging. Sulfur hexafluoride, however, was inadequate as a vapor taggant and consequently other vapor taggants had to be examined, which was the initial purpose of this program. As this program proceeded, the other two vapor tagging methods appeared more viable alternatives, and the program emphasis was shifted to an examination of these vapor tagging methods.

Certain criteria were formulated in order to evaluate the proposed vapor taggant methods. The selection criteria for vapor taggant chemicals were:

1. 5 to 10 percent soluble by weight in elastomers.

2. The vapor taggant must have certain molecular properties that lend themselves to instrumental detection at the required detection sensitivity. For illustration, a real-time continuous detection of the vapor taggant at concentration of the order of a part per trillion (ppt) with a signal-to-noise (S/N) ratio greater than two.

3. A low ambient vapor taggant background is necessary to ensure the detection of the vapor taggant in all detection scenarios. A high ambient background would mask the presence of a vapor tagged explosive and impede their detection.

4. The vapor taggant should be sufficiently volatile so as to minimize adsorption losses, i.e., the taggant vapors emitted

into a detection scenario can be potentially diminished by taggant adsorption onto adsorptive surfaces present in the detection scenario.

5. The vapor taggants should have a low toxicity and not exhibit mutagenicity or carcinogenicity. In addition, the vapor taggant should not cause any adverse environmental impact.

The selection criteria for elastomer substrates requires that:

6. The incorporation of the vapor taggants into the explosives should be compatible with the present manufacturers products and processes.

And finally, the criteria of performance for vapor taggant chemical solubilization in an elastomer are:

7. The taggant emission rate from a vapor tagged explosive must be in the 0.5- to 5-nl/min range, and

8. The useful lifetime of vapor tagged explosives is to be 5 years after fabrication in order for the vapor taggants to be detectable in most scenarios.

An effect common to any method of vapor tagging for prediction detection is the retention of the vapor taggant in an airtight enclosure in which the vapor tagged explosives might be concealed. This effect has been modeled and the results are given in this report (Appendix A, B and C). A limited series of field test evaluations of vapor taggants in checked luggage and aircraft scenarios are described in Appendix D.

The vapor taggants that were considered as alternatives to SF_6 are tabulated in Table 1-1 with their abbreviations. Additional vapor taggants have been considered by Toy et al. (1978) specifically for the tagging of blasting caps. The potential vapor taggants were evaluated with respect to the individual criteria for vapor taggants as discussed in the following chapters and applied specifically to the tagging of blasting caps. Some physical properties of the proposed taggants are given in Table 1-2.

The proposed vapor taggants will be evaluated with respect to the above criteria and are discussed more fully in the following sections. Parts of the final report, especially those sections regarding the barrier and adsorption loss effects have been presented in an earlier informal report (Senum et al., 1979a). An earlier report of the results was given at the New Concepts Symposium and Workshop on the Detection and Identification of Explosives in November 1978 (Senum et al., 1978a).

Table 1-1. Potential Vapor Taggants

Compounds	Abbreviation
Fluoroaromatics	
Pentafluoropyridine	PFP
Hexafluorobenzene	HFB
Octafluorotoluene	OFT
Decafluoroxylene	PFX
Decafluorobiphenyl	DFBP
Octafluoronaphthalene	OFN
Fluorocyloalkenes	
Decafluorocyclohexene	DFCH
Octafluorocyclopentene	OFCP
Perfluorocycloalkanes	
Perfluorodimethylcyclobutane	PDCB
Perfluoromethylcyclohexane	PMCH
Perfluorodimethylcyclohexane	PDCH
Perfluorodecalin	PFD
Perfluoroalkanes	
Perfluorooctane	PFO
Perfluoropentane	PFPT
Others	
Fluorinert Liquid*, Average molecular weight - 340	FC-72
Fluorinert Liquid*, Average molecular weight - 300	FC-78
Fluorinert Liquid*, Average molecular weight - 415	FC-77
duPont Freon**	Freon E-1
duPont Freon**	Freon E-2
Perfluorohexylsulfur pentafluoride*	L-4412

*Proprietary compounds developed by 3M.
**Proprietary compounds developed by duPont.

Table 1-2. Physical Properties of the Proposed Vapor Taggants

Taggant	Melting Point °C	Boiling Point °C	Vapor Pressure at 25°C;atm
PDCB	-32	45	0.50
PMCH	-30	76	0.14
PDCH	-70	102	0.046
HFB	4	80.2	0.11
OFT	20	105	-
DFBP	93	206	-
OFN	88	80(at 0.02 atm)	0.0001
PFD	0	142	0.0087
L-4412	-31	118	0.024
OFCP	-	27	-
DFCH	-50	53	-
Freon E-1	-154	41	0.53
Freon E-2	-123	104	0.4
FC-72	-90	56	0.31
PFX	-	-	-
PFP	-	84	-

II. SOLUBILITY OF VAPOR TAGGANTS IN BLASTING CAP END CLOSURES

One method to vapor tag electric blasting caps is to solubilize a vapor taggant into the blasting cap end closure. Thus, one of the necessary criteria for the selection of a vapor taggant is that it has 5- to 10-percent solubility in the end closure. The solubilized end closure preferably should be the present electric blasting cap end closure; specifically, Buna rubber (DuPont), an unspecified rubber (Atlas), and Kraton (Hercules). If no proposed vapor taggant has a sufficient solubility in the present end closures, then other elastomeric materials would have to be used as substitute end closures. In addition to solubility, the other criteria that dictate taggant properties (and these taggants having these properties) might require the use of substitute end closures because the present end closures are incompatible with these taggants. Consequently, a large set of proposed vapor taggants and present and substitute end closures were examined.

The selection of proposed vapor taggants was initially limited to fluorinated compounds which, as a class, have a relatively high sensitivity to detection by electron capture detectors (ECD). The technical brochures (I.S.C. Chemicals, 1974; duPont, 1968a; 1968b; 3M Company, 1976) of the manufacturers of the fluorinated compounds provided some data regarding the solubility of some fluorinated compounds in various elastomers. This led to the choice of several fluoroelastomers and fluoroplastics for examination as substitute end closures based on the possibility that they might have the required 5- to 10-percent taggant solubility.

The solubility criteria were used to determine the maximum solubility of the various proposed vapor taggants in the present and substitute end closures. This was experimentally accomplished by immersing the end closures with the correct dimensions (1/4-in. diameter by 1/2-in.

length) in a proposed vapor taggant. The end closures were weighed to record their weight gain until the maximum weight gain was reached, from which the maximum solubility was calculated. This procedure required one to two days at room temperature for vapor taggants which had a relatively large diffusion constant (approximately 10^{-6} cm^2/sec) in the end closure. For other taggants with lower diffusion constants (10^{-7} to 10^{-10} cm^2/sec), solubilization required a correspondingly longer time, up to one month at room temperature. This process was accelerated by raising the temperature to 45°C. The diffusion constants, as tabulated in Section VII were determined subsequent to the solubility experiments.

The resulting maximum solubilities are tabulated in Table 2-1 for the present end closures and in Table 2-2 for the substitute end closures. (Other potential vapor taggants and substitute end closures have been obtained by Toy et al. (1978).) There are several negative solubilities displayed in the tables. These signify that the particular vapor taggant solution had leached some soluble material out of the end closure elastomer.

Several fluoropolymer candidates (Teflons) were eliminated as substitute end closures, due to their propensity to cold flow. Fluorosilicone 35 was eliminated due to its softness, because an end closure requires a durometer Shore 2A hardness of 70 ± 5. Kel-F 3700 was eliminated due to its low taggant solubilities. Kel-F 3700 was also considered by Toy et al. (1978). Sulfur hexafluoride, when solubilized into various types of candidate end closures, causes them to bubble and tear due to the high room temperature vapor pressure of SF_6. It consequently destroys the end closures, and this feature eliminates SF_6 as a possible vapor taggant.

Based on the solubility results, it appears that the fluoroaromatic and to some extent the fluorocycloalkenes could be suitable as vapor

Table 2-1. Maximum Solubility of Various Perfluorinated Compounds in the Present Electric Blasting Cap End Closures (percent by weight)

Vapor Taggants	duPont Buna	Atlas Rubber	Hercules Kraton
Fluoroaromatics			
PFP	40.9	11.5	3.0
HFB	25.6	28.6	26.4
OFT	5.7	10.3	-10.4
PFX	8.2	7.6	-10.3
DFBP	11.1	27.8	-4.6
OFN	60.3	25.6	182.6
Perfluorocyclo-alkanes			
PDCB	0.7	0.6	-2.0
PMCH	0.8	1.7	1.5
PDCH	0.8	1.2	-6.6
PFD	-1.4	3.4	2.1
Perfluorocyclo-alkenes			
DFCH	-2.0	6.4	-1.8
OFCP	-3.0	6.6	-6.8
Others			
FC-72	-6.7	-7.4	-10.9
FC-77	-6.6	-10.5	0.8
FC-78	-6.2	-5.4	3.3
E-1	-6.5	1.0	-3.5
E-2	-6.2	1.2	-0.5
SF_6	-9.9	1.5	2.0
L-4412	-0.71	0.97	---

Table 2-2. Maximum Solubility of Various Perfluorinated Compounds in the Substitute End Closures (percent by weight)

Vapor Taggant	Viton A	Fluorel 2176	Fluoro-silicones 35	Fluoro-silicones 70	Kel-F 3700	Teflons PFA	Teflons FEP	Teflons TFE
Fluoroaromatics								
PFP	139.0							
HFB	85.9							
OFT	60.5							
PFX	8.5							
DFBP	60.1							
OFN	107.2							
Perfluorocyclo-alkanes								
PDCB	8.9	7.4	10.3	7.9	3.0	6.4	8.1	4.6
PMCH	7.6	5.3	10.0	7.6	3.1	6.2	10.2	5.4
PDCH	7.9	4.9		7.1	3.9	5.8	10.7	4.9
PFD	2.4							
Perfluorocyclo-alkenes								
DFCH	20.3							
OFCP	24.3							
PFO	3.8							
PFPT	3.0							
Other Candidates								
FC-72	5.2	5.5	4.6	2.0	3.9	7.3	8.0	8.8
FC-77	6.0	5.9	5.3	3.9	4.3	8.5	9.3	10.3
FC-78	8.6	8.8	8.7	5.6	6.1	8.8	10.3	6.2
E-1	7.9	7.9	7.9	5.8	5.0	4.5	5.3	3.6
E-2	7.4	7.0	7.5	5.8	3.7	3.4	4.8	3.4
SF_6	7.0	4.4	10.1	10.1	1.9	9.2	9.1	5.0
L-4412	1.8							

taggants for the present end closures. The perfluorocycloalkane vapor taggants show sufficient solubility in selected substitute end closures, such as the Vitons, Fluorels, and fluorosilicones. The large difference between the solubility of the fluoroaromatics and perfluorocycloalkanes in the various end closures can be qualitatively described by the following equation (Prins, 1967):

$$\ln S \approx -4.5 + X + \frac{10T_b}{T} \qquad (2\text{-}1)$$

where:

S = solubility (cm^3 of vapor taggant in cm^3 of end closure),
T_b = the vapor taggant boiling point, and
X = the Flory-Huggins interaction coefficient.

This coefficient is zero when there is no chemical interaction between the taggant molecule and enclosure elastomers. As a consequence of this equation, taggants with similar boiling points (e.g., the perfluoroalkanes and the fluoroaromatics) should have similar solubilities in the same end closure if there is no chemical interaction (i.e., $X = 0$). However, the fluoroaromatics, representing a fully unsaturated cyclic group of compounds, have a greater solubility than the perfluorocycloalkanes (a fully saturated cyclic group of compounds) in almost all of the examined end closures. These results indicate a chemical interaction ($X>0$) between the fluoroaromatic taggants and the end closures. This concept is in agreement with the fluoroalkene vapor taggants, partially unsaturated cyclic compounds, as having an intermediate solubility in some end closures when compared to the fluoroaromatic and the perfluoroalkanes solubilities.

As noted in the results (given in Tables 2-1 and 2-2), the fluoroaromatics have an appreciable solubility in the present end closures and, in most instances, several times more than the required 5- to

10-percent solubility. To solubilize the vapor taggant at the 5- to 10-percent solubility level when the maximum solubility is 10 to 20 times greater, the vapor taggant could be immersed for a proportionally shorter period than required for maximum solubility. However, only the exterior layers of the end closure will have been solubilized to the maximum extent, while the interior could have a slight degree of solubilization. The potential non-uniform solubilization could shorten the effective taggant emission lifetime of the tagged electric blasting caps. The end closures require uniform solubilization for the maximum emission lifetime.

Two other techniques are available that uniformly solubilize the taggant at the required solubility. The first technique is to make use of the decreasing maximum solubility with increasing temperature (equation 2-1); however, this is impractical because the exposure to higher temperatures could damage the mechanical properties of the end closures. Another potential technique makes use of the concept that the equilibrium solubility is proportional to the mole fraction of the taggant solute; e.g., by exposing the end closure to a solution of 0.5-mole-fraction taggant (inert solvent having no solubility), then the end closure will have a uniform solubility of half the maximum. This technique was verified with use of the HFB taggant in a hexane solution and the duPont Buna end closure as displayed in Figure 2-1; indeed, the equilibrium solubility is proportional to the HFB mole fraction as evidenced by the straight line fit. Thus, this technique provides a method to prepare a uniform solubilized end closure.

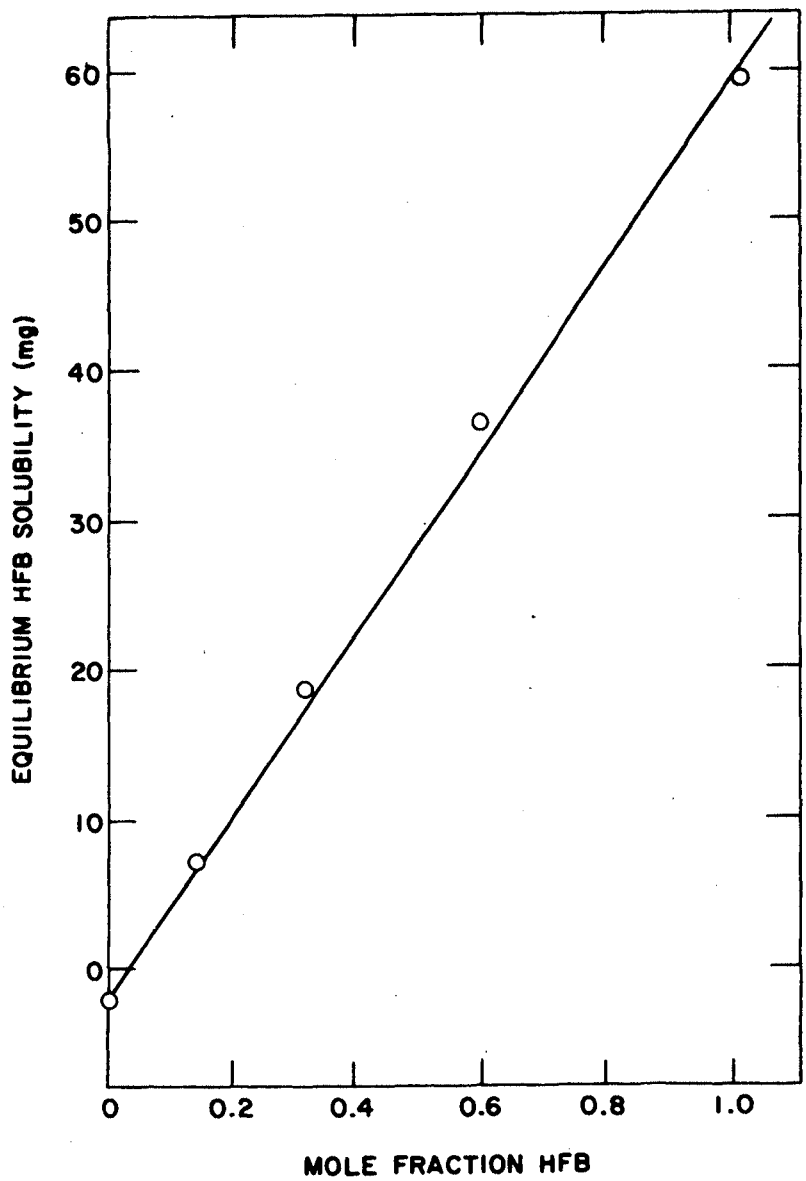

Figure 2-1. Equilibrium Solubility of HFB in duPont Buna as a Function of HFB Mole Fraction

III. ELECTRON CAPTURE DETECTION

A. THEORETICAL CONSIDERATIONS

For successful vapor tagging of explosives, an anaytical detection technique capable of detecting the vapor taggant at a required sensitivity is necessary. In practice, the taggant and the analytical technique are chosen to mutually maximize taggant detectability. The detection technique considered is electron capture detection (ECD). This method potentially will allow a coulometric detection response for certain compounds whereby one electron is reacted with each molecule at the maximum theoretical rate. It is this consequent electron loss via reaction which is measured and related to the compound concentration in the detector.

Basically, an ECD cell has a source of electrons and a method of electron collection that determines their concentration in the cell. A cross-section view of a typical ECD cell is given in Figure 3-1. The source of electrons is a radioactive foil which is a beta emitter, generally either tritium chemisorbed on titanium or scandium or simply a Ni^{63} foil. The beta particles (which are high energy electrons) collide with an inert gas, either N_2 or a Ar/CH_4 mix, which thermalizes the electrons. This thermalization process reduces the electron kinetic energy to equilibrium with room temperature particles. During this process, more electrons are formed by ionization of the inert gas along with an equal number of positive ions (e.g., N_2^+, N_4^+, etc.). In the presence of only the inert gas, the predominant modes of electron removal are (1) collision at the cell walls and (2) mutual positive ion-electron neutralization. Thus, a steady-state concentration of electrons and positive ions will be maintained. The electron concentration can be measured by periodically applying a quick voltage pulse across the cell with the resulting current being proportional to the electron concentration.

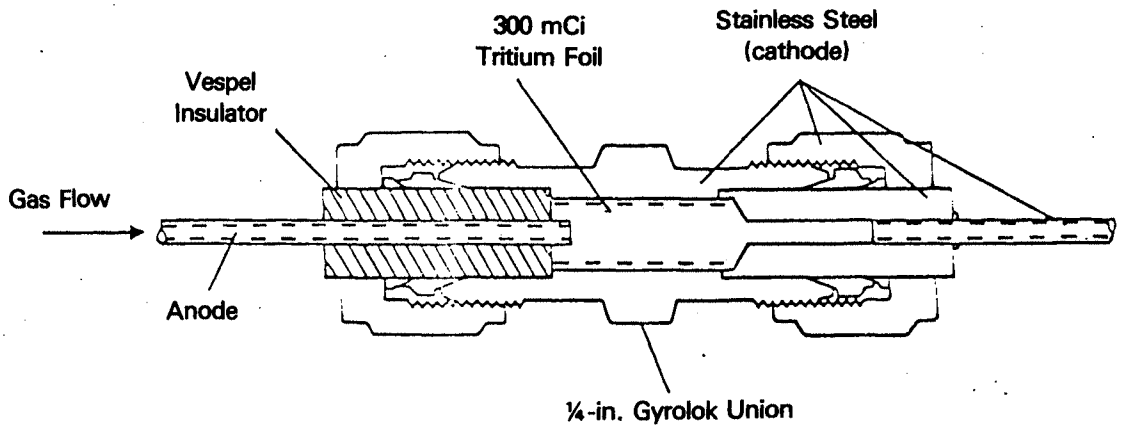

Figure 3-1. Cross Section of Electron Capture Detector

As certain compounds with a high reactivity with electrons pass through the ECD cell, the electron concentration will be lowered. This depletion is due to electron attachment to the compound because of the inherent electron affinity or the reaction of the compound with the electrons to form other species. Regardless of the mechanism, electrons are removed from the cell due to the presence of these ECD-sensitive compounds. The periodic sampling voltage pulse showing a decreased current will then measure the decreased electron concentration. The consequent current change (from the initial steady state to that when an ECD-sensitive compound is present in the cell) will be proportional to the concentration of that ECD-sensitive compounds.

In practice, there are three modes of sampling the ECD electron concentration: d.c. mode, fixed-frequency pulsed mode, and a variable--frequency constant-current pulsed mode. The latter two modes are more versatile. The fixed-frequency pulsed mode samples the ECD cell by applying a voltage pulse (50 volts) with a sufficiently narrow pulse width (1 to 3 μsec) to collect the very mobile electrons but not the heavier, slower ions. The pulse is applied with a selected frequency to allow a steady-state electron concentration to build up between the sampling pulses ($\sim$150 μsec). The variable-frequency constant-current mode decreases the time in between the sampling pulses as the electron concentration is decreased due to passage of an ECD-sensitive compound through the cell. The degree of increase in the pulse frequency is such that the total collected current is constant. The frequency change is then proportional to the sample concentration. A schematic of this mode is given in Figure 3-2.

Both pulsed modes, fixed-frequency and variable-frequency, have nearly equivalent ultimate sensitivities (approximately 0.1 ppt) at a S/N = 2 for the strongest electron capturing compounds, but the variable-frequency mode has the greater linear response range (approximately 10^4) (Patterson, 1977).

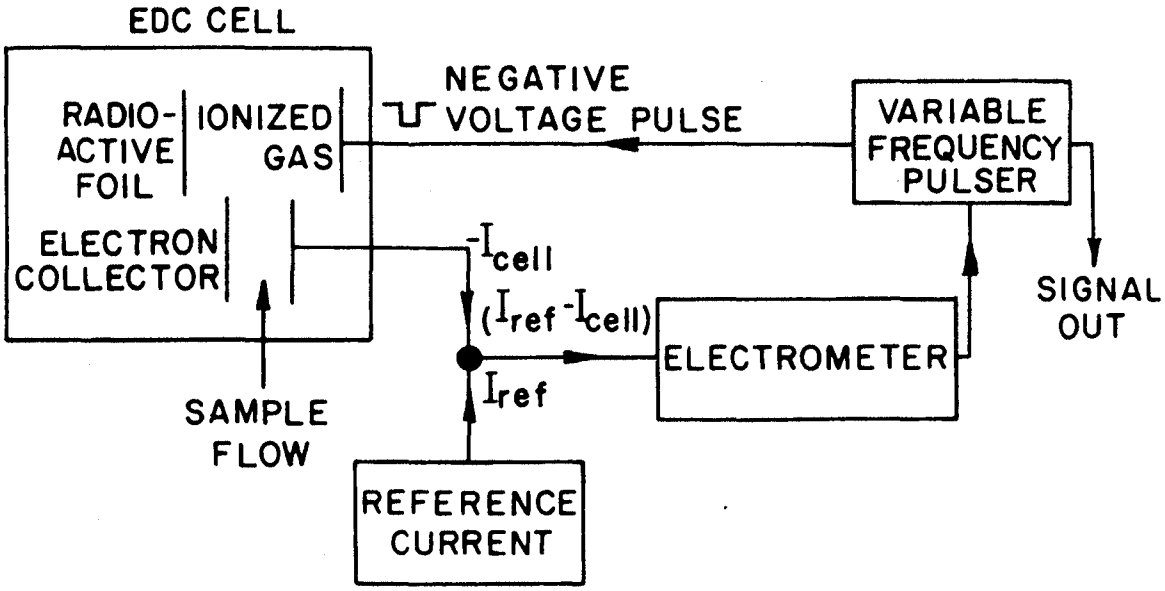

Figure 3-2. Block Diagram of the Constant Current Detection Mode

Generally, compounds having electronegative moieties will react favorably with electrons, e.g., halogenic, olefinic and aromatic moieties. A convenient measure of the ECD sensitivity of a particular compound is its thermal electron reaction cross-section. Preferably, compounds with the greatest thermal electron cross section should be chosen as vapor taggants.

To see if the chosen taggant compounds are highly ECD sensitive, it is convenient to calculate the maximum theoretical thermal electron capture (EC) cross section. Christodoulides (1979) expresses it simply as

$$\sigma_{max} = \pi \lambda\!\!\!^{-2} = \frac{1.197 \times 10^{-15}\ cm^2}{\epsilon} \qquad (3\text{-}1)$$

where: $\lambda\!\!\!^{-2}$ = the DeBroglie wavelength of the electrons (e.g., λ = 10 Å for thermal electrons)

ϵ = 0.038 eV.

This equation assumes the interaction between the electron and molecule to be pointlike. A simplistic modification which takes into account the molecular size is (Davis et al., 1972)

$$\sigma_{max} = \pi(\lambda\!\!\!^{-} + S)^2 \qquad (3\text{-}2)$$

where: S = an effective radius of the molecule.

The value σ_{max} is based on the assumption that once an electron collides with the molecule it will remain attached or otherwise react with the molecule. There are of course, other factors which determine the actual thermal EC cross sections, which in most instances are very small compared to the maximum theoretical cross section.

Thermal EC cross sections have been determined for a large number of compounds by three techniques, some of which predate the ECD. These techniques are ion cyclotron resonance, microwave conductivity, and electron swarm techniques. Table 3-1 lists several thermal EC cross sections which have been determined by these techniques and also by a fourth method, namely extrapolation from measured ECD sensitivities. Also listed are the ambient atmospheric backgrounds for several of these compounds (Singh et al., 1978). These tables allow the choice of compounds with the highest EC cross sections which are not already present in the atmosphere.

These experimental EC cross sections can be compared with the theoretical maximum EC cross section as calculated by equation (3-2); this is given in Table 3-2. It is seen that it is possible to have compounds with an EC cross section approaching the maximum theoretical values. Thus, it is certain that the chosen taggant compounds are optimum for electron capture detection methods.

However, it is not solely the thermal EC cross section that determines the ultimate sensitivity of an ECD. There are three other factors which will significantly change the apparent ECD sensitivity for many compounds: the relative large electron concentration which allows pseudo-first-order kinetics to occur, the effect of the molecular ECD residence time, and the effect of impurities in the inert carrier gas, specifically O_2 and H_2O.

The observed ECD response will depend on both the compound and electron concentrations in the ECD cell. The electron concentration is generally 10^{10} to $10^{11}/cm^3$, three to four orders greater than the minimum detectable molecular concentrations. Thus depending on the molecular residence time in the ECD, many strong and moderate EC-sensitive compounds will have nearly an equal response and ultimate

Table 3-1. Thermal Electron Capture Cross Sections (cm^3/sec)

Compound	Cross Section (298°K)	Ambient Background (ppt)	Reference
	A. Ion Cyclotron Resonance Techniques		
CCl_4	4.1×10^{-7}	123.6 ± 8.3	Mothes et al., 1972; Schultes et al., 1975
SF_6	2.6×10^{-7}	0.27 ± 0.03	Mothes et al., 1972
BrCN	1.8×10^{-7}	--	Mothes et al., 1972
$c\text{-}C_4F_8$	1.1×10^{-7}	--	Mothes et al., 1972
CCl_3F	1.0×10^{-7}	126.5 ± 12.4	Schumacher et al., 1978
PMCH	5.2×10^{-8}	--	Mothes et al., 1972
$COCl_2$	5.0×10^{-8}	15.4 ± 4.2	Schultes et al., 1975
N_2F_4	3.8×10^{-9}	--	Mothes et al., 1972
$CHCl_3$	2.6×10^{-9}	19.9 ± 5.1	Schultes et al., 1975; Christodoulides et al., 1975a
ICN	2.1×10^{-9}	--	Mothes et al., 1972
Cl_2	1.1×10^{-9}	--	Schultes et al., 1975; Christodoulides et al., 1975b
CCl_2F_2	8.3×10^{-10}	220.5 ± 19.8	Mothes et al.; 1972; Schumacher et al., 1978
NOCl	6.9×10^{-10}	--	Schultes et al., 1975
C_2H_3Cl	4×10^{-10}	--	Schultes et al., 1975
ClF_3	3.6×10^{-10}	--	Christodoulides et al., 1976
$C_2F_4Cl_2$	1.2×10^{-10}	11.9 ± 5.2	Mothes et al., 1972
CNCl	1.1×10^{-10}	--	Mothes et al.; 1972; Schultes et al., 1975
HBr	9.6×10^{-11}	--	Mothes et al., 1972
HCN	9.1×10^{-11}	--	Mothes et al., 1972
C_2H_3CN	5.6×10^{-11}	--	Mothes et al., 1972
$(CN)_2$	4.6×10^{-11}	--	Mothes et al., 1972
NO_2	4.5×10^{-11}	<5000	Schumacher et al., 1977
NF_3	2.4×10^{-11}	--	Mothes et al., 1972

Table 3-1. Thermal Electron Capture Cross Sections (cm^3/sec)(continued)

Compound	Cross Section (298°K)	Ambient Background (ppt)	Reference
	A. Ion Cyclotron Resonance Techniques (continued)		
CH_3CN	7.2×10^{-12}	--	Mothes et al., 1972
C_2ClF_3	6.6×10^{-12}	--	Christodoulides et al., 1976
CH_2Cl_2	4.1×10^{-12}	44.8 ± 21.5	Schultes et al., 1975; Christodoulides et al., 1975a
CH_3Br	3.2×10^{-12}	--	Mothes et al., 1972
$CHCl_2F$	1.5×10^{-12}	5.0 ± 1.9	Christodoulides et al., 1978
$CHClF_2$	$< 3.3 \times 10^{-13}$	20 to 30	Christodoulides et al., 1978
HCl	2×10^{-13}	--	Christodoulides et al., 1975b
$CClF_3$	7×10^{-14}	--	Schumacher et al., 1978
CHF_3	3.6×10^{-14}	--	Christodoulides et al., 1978
CH_3Cl	5×10^{-15}	733.3 ± 134.1	Schultes et al., 1975; Christodoulides et al., 1975b
CF_4	$< 10^{-16}$	--	Schumacher et al., 1978
	B. Microwave Conductivity Techniques		
SF_6	2.2×10^{-7}	0.27 ± 0.03	Fessenden and Bansal, 1970; Bansal and Fessenden, 1973
$c\text{-}C_4F_6$	1.4×10^{-7}	--	Bansal and Fessenden, 1973
$2\text{-}C_4F_8$	4.9×10^{-8}	--	Bansal and Fessenden, 1973
$c\text{-}C_4F_8$	1.2×10^{-8}	--	Bansal and Fessenden, 1973
CF_2Cl_2	1.3×10^{-9}	220.5 ± 19.8	Bansal and Fessenden, 1973
$n\text{-}C_4F_{10}$	9.6×10^{-12}	--	Fessenden and Bansal, 1970
CH_2Cl_2	4.7×10^{-12}	44.8 ± 21.5	Fessenden and Bansal, 1970
$CClF_3$	5.2×10^{14}	126.5 ± 12.4	Fessenden and Bansal, 1970
CHF_3	7.6×10^{-14}	--	Fessenden and Bansal, 1970
CH_3CF_3	4.3×10^{-14}	--	Fessenden and Bansal, 1970
$c\text{-}C_3F_6$	$< 3 \times 10^{-14}$	--	Bansal and Fessenden, 1973

Table 3-1. Thermal Electron Capture Cross Sections (cm^3/sec)(continued)

Compound	Cross Section (298°K)	Ambient Background (ppt)	Reference
	B. Microwave Conductivity Techniques (continued)		
CH_2F_2	1.6×10^{-14}	—	Fessenden and Bansal, 1970
C_2H_5F	$< 5 \times 10^{-15}$	—	Fessenden and Bansal, 1970
CH_3F	$< 10^{-15}$	—	Fessenden and Bansal, 1970
C_3F_8	$< 10^{-15}$	—	Fessenden and Bansal, 1970
C_2F_6	$< 10^{-15}$	—	Fessenden and Bansal, 1970
CF_4	$< 10^{-16}$	—	Fessenden and Bansal, 1970
	C. Direct Electron Capture Detection		
CCl_4	2.2×10^{-7}	123.6 ± 8.3	Lovelock and Watson, 1978
$CFCl_3$	1.26×10^{-7}	126.5 ± 12.4	Lovelock and Watson, 1978
CF_2BrCl	1.18×10^{-7}	—	Lovelock and Watson, 1978
CH_3CCl_3	2.4×10^{-8}	110.7 ± 18.1	Lovelock and Watson, 1978
$CF_2ClCFCl_2$	7.6×10^{-9}	22.6 ± 4.8	Lovelock and Watson, 1978
$CHCl_3$	4.5×10^{-9}	19.9 ± 5.1	Lovelock and Watson, 1978
CF_3CFCl_2	3.2×10^{-9}	11.9 ± 5.2	Lovelock and Watson, 1978
	D. Electron Swarm Techniques		
DFCH	3.67×10^{-7}	—	Davis et al., 1972; Pai et al., 1979
OFCP	3.59×10^{-7}	—	Davis et al., 1972; Pai et al., 1979
CCl_4	3.55×10^{-7}	123.6 ± 8.3	Davis et al., 1972; Cristophorou, 1976
OFT	2.60×10^{-7}	—	Davis et al., 1972; Pai et al., 1979

Table 3-1. Thermal Electron Capture Cross Sections (cm^3/sec)(continued)

Compound	Cross Section (298°K)	Ambient Background (ppt)	Reference
	D. Electron Swarm Techniques (continued)		
PDCB	1.46×10^{-7}	2.2×10^{-3}	Pai et al., 1979
c-C_4F_6	1.29×10^{-7}	--	Christodoulides, 1979
1,3-C_4F_6	1.19×10^{-7}	--	Christodoulides, 1979
HFB	1.02×10^{-7}	--	Davis et al.; 1972; Gant and Christophorou, 1976
PDCH	7.68×10^{-8}	1.2×10^{-2}	Pai et al., 1979
CH_3I	7.1×10^{-8}	4.8 ± 2.9	Christophorou, 1976
1-C_4F_6	5.18×10^{-8}	--	Christodoulides, 1979
2-C_4F_8	4.37×10^{-8}	--	Davis et al., 1972; Christodoulides and Christophorou, 1979
PMCH	4.0×10^{-8}	1.5×10^{-3}	Davis et al., 1972; Christodoulides and Christophorou, 1979
c-C_4F_8	1.39×10^{-8}	--	Christodoulides, 1979; Davis et al., 1972; Christophorou et al., 1974
Perfluoro-heptene	4.10×10^{-9}	--	Christodoulides and Christophorou, 1979
C_2HCl_3	2.4×10^{-9}	11.5 ± 1.0	Christophorou, 1976;
SeF_6	1.27×10^{-9}	--	Davis et al., 1972
Cyclo-octa-tetraene	7.7×10^{-10}	--	Davis et al., 1972
SO_2F_2	5.8×10^{-10}	--	Davis et al., 1972
TeF_6	2.0×10^{-11}	--	Davis et al., 1972
C_2ClF_5	6.2×10^{-12}	--	Davis et al., 1972
$C_2H_4F_2$	1.6×10^{-12}	--	Davis et al., 1972

Table 3-1. Thermal Electron Capture Cross Sections (cm^3/sec)(continued)

E. Extrapolated from EC Sensitivity Studies		
Compound	Cross Section (298°K)	Ambient Background (ppt)
CCl_4	4.4×10^{-7}	123.6 ± 8.3
$CFCl_3$	1.1×10^{-7}	126.5 ± 12.4
C_2Cl_4	9.1×10^{-8}	33.4 ± 4.6
$CHClCCl_2$	1.7×10^{-9}	11.5 ± 1.0
$CHCl_3$	1.5×10^{-9}	19.9 ± 5.1
trans-$CH_2ClCHCHCH_2Cl$	1.0×10^{-9}	--
CH_2CCl_2	2.9×10^{-10}	--
CF_2Cl_2	2.3×10^{-10}	220.5 ± 19.8
ph-CH_2Cl	1.5×10^{-11}	--
meta ph-Cl_2	7.5×10^{-12}	--
ortho ph-Cl_2	3.7×10^{-12}	--
CH_3Br	3.0×10^{-12}	--
para ph-Cl_2	1.1×10^{-10}	--
CF_3Cl	4.8×10^{-13}	--
CH_2CHCH_2Cl	3.4×10^{-13}	--
1,2 dichloroethane	2.2×10^{-13}	--
CH_2Cl_2	1.5×10^{-13}	44.8 ± 21.5
2-Bu-Cl	1.3×10^{-13}	--
1,4 dichlorobutane	1.3×10^{-13}	--
n-Bu-Cl	6.0×10^{-14}	--
1,3 dichloropropane	5.5×10^{-14}	--
CHF_2Cl	4.5×10^{-14}	20 to 30
EtCl	5.0×10^{-14}	--

Table 3-1. Thermal Electron Capture Cross Sections (cm^3/sec)(continued)

E. Extrapolated from EC Sensitivity Studies (continued)		
Compound	Cross Section (298°K)	Ambient Background (ppt)
n-PrCl	4.5×10^{-14}	--
i-prCl	4.5×10^{-14}	--
t-BuCl	3.3×10^{-14}	--
trans-CHClCHCl	3.3×10^{-14}	--
CH_3Cl	3.0×10^{-14}	733.3 ± 134.1
cis-CHClCHCl	1.7×10^{-14}	--
CH_2CClCH_3	4.6×10^{-16}	--
ph-Cl	1.4×10^{-17}	--
$CHClCHCH_3$	2.6×10^{-19}	--

Table 3-2. Comparison of the Experimental and Theoretical Electron Capture Cross Section (S - molecular radius) (10^{-8}cm = 1, Angstrom = Å)

Compound	S(Å)	σ_{max} ($10^{-14}cm^2$)	k_{th} ($10^{-7}cm^3$/sec)	K_{meas} ($10^{-7}cm^3$/sec)	k_{meas}/k_{th}
CCl_4	2.94	5.26	6.05	4.1	0.68
SF_6	2.48	4.89	5.62	2.6	0.46
OFT	3.51	5.75	6.61	2.6	0.39
PDCB	3.51	5.73	6.59	1.46	0.22
HFB	3.34	5.58	6.42	1.02	0.16
CCl_3F	2.27	4.73	5.43	1.0	0.18
PDCH	3.92	6.08	6.99	7.68	0.11
PMCH	3.70	5.89	6.77	0.52	0.077
CCl_2F_2	2.41	4.84	5.57	8.3×10^{-3}	0.0015

sensitivity. This is due to the pseudo-first-order kinetics situation which exists because of the excess of electrons over molecules in the ECD cell. Under certain flow conditions, the response will be coulometric for a large range of EC-sensitive compounds. One electron is depleted for each molecule present in the cell, as long as the electron concentration is in excess over the molecular concentration.

The second effect concerns the ultimate fate of the electron-attached species. There are essentially two fates, either the electron-attached molecule dissociates into other species or the electron is autodetached after a certain lifetime from the molecule thus regenerating the original molecule and the electron. Examples of the first fate are most chlorinated hydrocarbons (Johnson et al., 1976).

$$CCl_4 + e^- \longrightarrow CCl_3 + Cl^-$$

with the resulting dissociation products having no EC sensitivity. An example of the second fate is (Christodoulides and Christophorou, 1979)

$$PMCH + e^- \longrightarrow [PMCH]^-$$

with $[PMCH]^-$ having an autodetachment lifetime of 0.775 ± 0.025 msec. If during that lifetime $[PMCH]^-$ happens to collide with a positive ion (an equal number of positive ions and electrons exist in an ECD cell), they will be mutually neutralized. PMCH will be regenerated. but not an electron. The regenerated PMCH will again be available for another electron attachment if the molecular ECD residence time is sufficiently long. This consideration can increase the effective response of PMCH and other compounds with long autodetachment lifetimes. Table 3-3 tabulates some known autodetachment lifetimes. With flow conditions which might ordinarily give coulometric response, these molecules will yield a supercoulometric response with several electrons depleted for each compound molecule.

Table 3-3. Electron Autodetachment Lifetimes for EC-Sensitive Compounds

Species	Autodetachment Lifetime (μsec)	Reference
c-C_4F_6	8 ± 3	Naff et al., 1968; Thynne, 1972; Sauers et al., 1973
HFB	12 ±	Naff et al., 1968
2-C_4F_6	13 ± 5	Thynne, 1972; Sauers et al., 1973
C_2Cl_4	14 ± 3	Johnson et al., 1976
c-C_4F_8	2.3 ± 2.4	Naff et al., 1968; Sauers et al., 1973; Harland and Thynne, 1973
2-C_4F_8	20.6 ± 14	Thynne, 1972; Sauers et al., 1973
OFT	25 ± 18	Naff et al., 1968; Thynne, 1972
OFCP	38 ± 17	Naff et al., 1978; Thynne, 1972
SF_6	41 ± 24	Compton et al., 1966; Harland and Thynne, 1970
DFCH	110 ± 5	Naff et al., 1968; Thynne, 1972
PDCB	34 ± 150	Naff et al., 1968; Thynne, 1972
PMCH	775 ± 25	Naff et al., 1968
1,3-C_4F_6	710 ± 4	Sauers et al., 1973

The effect of slight impurities in the ECD inert carrier gas (N_2) can significantly increase the EC response of many compounds as has been shown recently by Grimsrud et al. (Miller and Grimsrud, 1979; Grimsrud and Stebbins, 1978; Grimsrud and Miller; 1978; Grimsrud and Kim, 1979). These studies were primarily concerned with O_2 doping of the N_2 carrier gas at the 2000-ppm level. In all the compounds which have been examined, the effect of the addition of O_2 is to increase the apparent ECD response of the compound. The response enhancement is especially large (approximately 200-fold enhancement) for compounds that have a low

sensitivity for EC detection, but only a slight enhancement for those compounds with a high EC sensitivity (e.g., CCl_4, $CFCl_3$, etc.). Table 3-4 presents a range of compounds and their response enhancements due to 2000-ppm O_2 doping. The mechanism for the response enhancement as stated by Grimsrud et al. is that O_2 is a slight EC-sensitive compound and will capture an electron to form O_2^-. Consequently, O_2^- forms a steady-state concentration in the ECD and provides another source of electrons for EC sensitive compounds, i.e.,

$$O_2^- + X \longrightarrow O_2 + X^-$$

via a charge transfer reaction. Compounds with a high EC sensitivity will capture electrons by direct electron capture, and consequently, the O_2 response enhancement should be slight. Compounds with a low EC sensitivity now have two routes for capturing electrons, directly and

Table 3-4. ECD Response Enhancement due to 2000 ppm O_2

Compound	Thermal Electron Cross Section (cm^3/sec)	Response Enhancement at 250°C (2000 ppm O_2 in N_2)
CCl_4	4.1×10^{-7}	1.9
$CFCl_3$	1.0×10^{-7}	2.2
$CHCl_3$	2.6×10^{-9}	4.8
$CHClCCl_2$	2.4×10^{-9}	2.9
CF_2Cl_2	8.3×10^{-10}	3.4
CH_2CHCl	4×10^{-10}	107
CH_2Cl_2	4.1×10^{-12}	108
CH_3Br	3.6×10^{-12}	55
CH_3Cl	5×10^{-15}	189

from O_2^-, thus with O_2 doping, the ECD response should be greater. The optimum O_2 doping was determined to be about 2000 ppm which is a trade-off between the O_2 response enhancement and the ECD electron concentration depletion due to O_2 (standing current reduction).

Based on the above effects and discussion, the operating conditions of an ECD should depend on the class of compounds being detected. There are two basic detection modes for an ECD: (1) as a general all purpose chromatographic detector or (2) as a detector for a specific set of compounds such as a taggant detector.

The optimum ECD operation conditions for an all-purpose detector would be: (1) high electron concentrations in the ECD (tritium source preferable to a Ni^{63} source), (2) a long residence time of the compound in the ECD, and (3) carrier gas doping with O_2. These three conditions maximize the detection of compounds with either high or low EC sensitivities.

The optimum ECD conditions for a specific taggant detector would be: (1) low electron concentrations in the ECD (Ni^{63} preferable to a tritium source), (2) a long residence time of the compound in the ECD, and (3) no carrier gas doping -- low O_2 impurity levels in the carrier gas. These conditions maximize the detection of compounds with a high EC sensitivity but to some extent minimize the detection of all other compounds. These operating conditions would be optimal for an explosives taggant ECD detector. These conditions minimize the detection of the ambient Freons, many of which have a low EC sensitivity.

A list of potential taggant compounds, extracted from Table 3-1, is given in Table 3-5. These taggants were selected based on the criteria of a high EC detection sensitivity ($> 10^{-8} cm^3/sec$) and a negligible ambient background concentration (< 0.1 ppt).

Table 3-5. Potential Explosives Taggants

Compound	Thermal Electron Cross Section ($10^{-7}cm^3/cm$)	Autodetachment Lifetime ($10^{-6}sec$)
Decafluorocyclohexene (DFCH)	3.67	100 ± 5
Octafluorocyclopentene (OFCP)	3.59	38 ± 17
Octafluorotoluene (OFT)	2.6	25 ± 18
Perfluorodimethylcyclobutane (PDCB)	1.46	340 ± 150
Hexafluorocyclobutene (c-C_4F_6)	1.4	8 ± 3
Hexafluorobutadiene (1,3-C_4F_6)	1.19	10 ± 4
Hexafluorobenzene (HFB)	1.02	12
Perfluorodimethylcyclohexane (PDCH)	0.76	--
Perfluoromethylcyclohexane (PMCH)	0.52	775 ± 25
Hexafluorobutyne (2-C_4F_6)	0.52	13 ± 5
Octafluorobutene (2-C_4F_8)	0.49	20.6 ± 14
Perfluorocyclobutane (c-C_4F_8)	0.12	12.3 ± 2.4

B. CONTINUOUSLY OPERATING PERFLUOROCARBON SNIFFER

Brookhaven, under contract to National Oceanic and Atmospheric Administration (NOAA), has developed a continuously operating perfluorocarbon sniffer (COPS) for air monitoring studies (Dietz et al., 1976b). The COPS device is also suitable for vapor taggant chemical detection at low part-per-trillion lower limits of detection. The portable detector that was used to conduct limited field testing is described below. These tests for the detection tagging effort used the U.S. Customs Service Baggage Examiner; they are described in greater detail in Appendix D.

The COPS operates by drawing in air continuously with a sampling pump, combusting the oxygen component of the air with hydrogen over a catalyst, drying the gas, passing it through an electron capture detector, and monitoring the output signal. The pneumatics system (pump, gases, reactor, and dryer) and the electronics system (detector and electrometer) are described below. The parameters of operation and limits of sensitivity and drift are given in Table 3-6 and the specific details of construction.

1. Pneumatic System

A diagram of the pneumatic system is given in Figure 3-3 and a list of flow rates, pressures and other pertinent parameters are included in Table 3-6. The temperatures are controlled by a d.c. power proportional controller manufactured by Oven Industries.

(a) Sampling Pump. The pump must be capable of supplying at least 1 l/min at a pressure great enough to get the required flow into the reactor. The size and power consumption are subject to the type and bulk of the instrument.

(b) Gas Supply. The gases used in addition to the sample air are fuel, purge gas, and nitrogen. The fuel is hydrogen (prepurified or better quality). Other fuel gases may work but have not been tried. The purge gas may be nitrogen, hydrogen, or any other inert gas not containing oxygen. Oxygen or air permeates through the Nafion to give about 100 ppm O_2 which would be unacceptably high for the detector. Ultrapure nitrogen is used to purge the detector in the standby mode to maintain standing current.

Table 3-6. Instrument Parameters of the Continuously Operating Perfluorocarbon Sniffers (COPS)

Parameter	Setting or Measured Value
Pressure	
P1	--
P2	15 to 20 psig
P3	3 psig
P4	1 to 15 psig
P5	--
Flows at Restrictions	
R1	at least 2 times flow out of Reactor
R2	1/2 R3
R3	20 to 30 cm^3/min
R4	50 to 60 cm^3/min
R5	= detector at 15 psig on R5
Detector	16 to 24 cm^3/min
Sensitivity (minimum)	10 mV/ppt
Standing Current (min)	3 V (full sensitive)
Base line drift (shortterm)	<+ 0%/hr
Span drift	<5%/8 hr

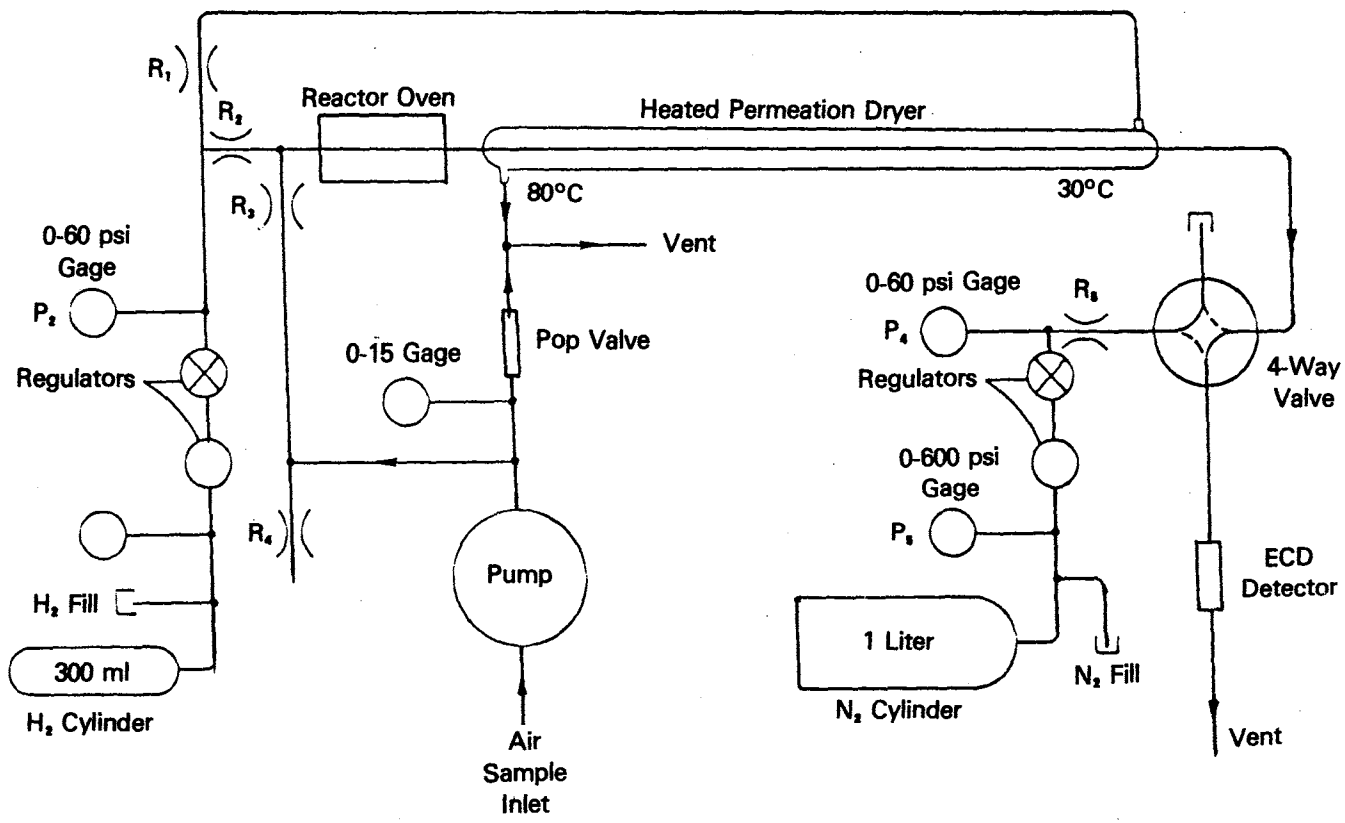

Figure 3-3. Continuous Electron Capture Detector — Components Diagram

The reactor consists of 3 to 5 percent palladium supported on asbestos or molecular sieve 5A (30-35 mesh), approximately 1-in. long, and 1/8-in. outside diameter. The temperature should be maintained between 175° and 200°C with a maximum variation of ±0.1°C/min.

The effectiveness of the catalyst is determined using an oxygen analyzer on the effluent of the catalyst; the oxygen level should be less than 10 ppm. After 2 years of intermittent use, there has been no occurrence of catalyst degradation or poisoning, so no catalyst has yet needed regeneration. The hydrogen fuel is blended in at a rate of half the air sample flow rate before the reactor oven; the catalyst in the oven should have little pressure drop, i.e., less than 0.3 psig at 20 ml/min.

Nafion Dryer. The dryer is similar to Perma Pure Model MD-125-48F (Perma Pure Products, Inc., Oceanport, NJ 07757) with heating zoned for the inlet half of its length to maintain the gas above the dew point temperature of 65°C (usually about 75° to 80°C). The flow of the purge gas has to be greater than 2 times the sample gas flow. The pressure drop of the sample gas in the 4-ft model is approximately 1 psig. The sample gas leaving the dryer must have a dew point temperature less than 0°C. With this Perma Pure dryer, the dew point was generally less than -30°C.

The efficiency of drying was checked by passing the dried gas through a weighed drierite tube and reweighing after a period of time; the increase in weight is proportional to the moisture content of the gas. It was found that the moisture content was not much greater than that of the drier counter current purge gas. The only failures of the dryer have been due to overheating in the initial heating zone (greater than 120°C). In those cases the dryer was reconstructed with new Nafion tubing.

2. Electronics System

Electron Capture Detector. The detector has been described in the literature (Dietz et al., 1976c) and a cross-section view of the detector is given in Figure 3-1. The detector is operated at ambient temperatures, but insulated to smooth and dampen temperature changes. Caution must be exercised when using Vespel SP 1 as the insulator because electronic noise is transmitted in some circumstances.

Electrometer. The detector body was pulsed with a negative 15-V pulse having a width of 2 μsec and a period of 35 μsec. The changes in the standing current were sensed with an electrometer with RC filtering of 1 sec. A block diagram of the electronics is shown in Figure 3-4.

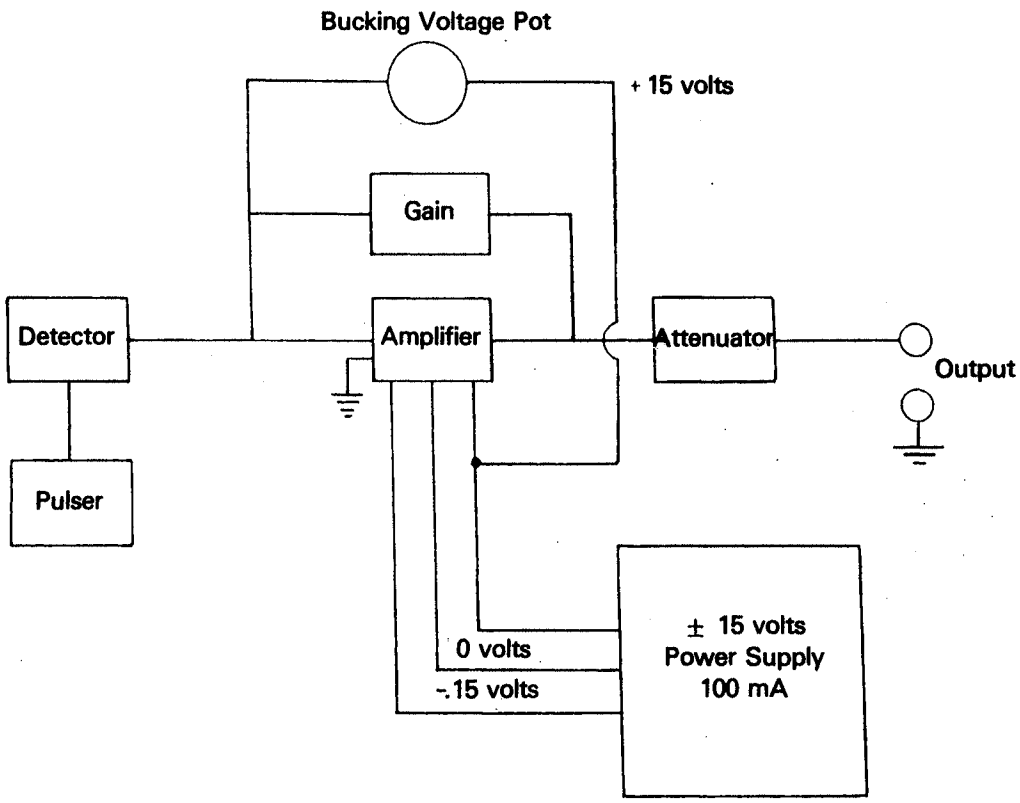

Figure 3-4. Electrometer Board Block Diagram

IV. AMBIENT ATMOSPHERIC BACKGROUNDS OF PROPOSED VAPOR TAGGANTS

All of the proposed vapor taggants, with the exception of PDCB, PMCH, and PDCH, have had little industrial use, and consequently they have negligible ambient atmospheric backgrounds. The three exceptions have received limited industrial use as coolants, and there has been a sufficient amount released into the environment to produce a measureable background. An ambient PDCH background concentration of 23.8 ± 2.5 ppq (part per quadrillion) has been measured in Chester, New Jersey by the Environmental Measurements Laboratory (DOE)(Lagmarsino, 1977). This is near the value of 30.3 ± 1.7 ppq measured in September 1979 for PDCH at Yaphank, a rural central Long Island, New York, site (Senum et al., 1979b). Concentrations of 7.9 ± 1.8 ppq and 2.7 ± 0.3 ppq were measured for PDCB and PMCH, respectively, at the same Yaphank site. These background concentrations are two to three orders of magnitude lower than the SF_6 ambient background. The low ambient backgrounds for PDCB, PMCH, and PDCH could be expected to have a negligible effect on the detectability of vaport tagged explosives in all but the more extreme detection scenarios, e.g., a Boeing 727 aircraft. See Appendix D, Senum et al. (1979b), for a more complete discussion for this scenario.

V. TAGGANT DETECTABILITY

A. ADSORPTION LOSSES

To ensure that there will be negligible taggant adsorption losses on the various surfaces which are present in detection scenarios (clothing inside suitcases, packing material inside boxes, etc.), any proposed vapor taggant must be sufficiently volatile. This mechanism for taggant depletion from the detection scenario via adsorption has been mathematically treated in Appendix C. A major conclusion is that, for adsorption losses, the initial rate of taggant buildup in the scenario is reduced by an adsorption attenuation factor, i.e.,

$$(1 + v_m c P_{ext}/V_{ch} P_o) \qquad (5\text{-}1)$$

where:

- v_m = the gas volume necessary to cover the adsorbing surface with a complete monolayer,
- c = an empirical constant of the order of ten,
- P_{ext} = the ambient pressure,
- P_o = the equilibrium vapor pressure of the taggant, and
- V_{ch} = the volume of the scenario.

The conclusion of this derivation is that the adsorption losses are greatest when: (1) v_m is large (a large surface area is available for adsorption) and (2) P_o is small (the adsorbate, the vapor taggant, is nonvolatile).

This attenuation can be quantified if v_m, c, and P_o are known for a particular vapor taggant and known surface. In the majority of realistic situations, however, these parameters are unknown, and thus, it is more appropriate to select vapor taggants that will have negligible

adsorption loss in the majority of scenarios (very volatile taggants). The question then becomes, how volatile must a taggant be to have a negligible taggant adsorption loss in most scenarios? This has been determined experimentally for a series of proposed vapor taggants with a test scenario consisting of a towel enclosed vapor taggant source which is placed in a cloth suitcase. This arrangement was chosen as the test scenario because it is representative of a number of expected detection scenarios, and the test arrangement is reasonably reproducible. If the proposed vapor taggants have a negligible adsorption loss in this test scenario, it is expected that it will have a negligible (or at most a small) loss in most other scenarios.

The experimental procedure was to place the entire cloth suitcase in a 422-liter sampling chamber having a constant ventilation rate of 200 cm^3/min. The taggant source was a vapor tagged blasting cap with a predetermined taggant emission rate. The taggant concentrations in the sampling chamber were determined chromatographically every half-hour after the test suitcase had been placed in the chamber. The adsorption experiment for each potential vapor taggant was performed in two parts. First, the tagged source was placed in the chamber without the suitcase and measurements were performed. Then the experiment was repeated with the source in the test suitcase. The difference in results was related to adsorption losses. In the experiment without the above test suitcase, only the vapor tagged sources were suspended in a wire cage in the sampling chamber in order to provide the identical source of vapor taggant for both parts of the adsorption experiments.

To provide a direct comparison between the results for each of the potential vapor taggants (see Table 1-1), the resulting vapor taggant concentrations inside the chamber were normalized by dividing the measured taggant concentration, $C(t)$, by the calculated steady-state taggant concentration, $C(\infty)$, i.e.,

$$\text{normalized concentration} = C(t)/C(\infty): \qquad (5\text{-}2)$$

in which

$$C(\infty) = R_{cap}/R_{ex} \qquad (5\text{-}3)$$

where: R_{cap} = the taggant emission rate of the source and
R_{ex} = the chamber ventilation rate.

The elapsed time was normalized in terms of turnover times, i.e., divided by the chamber turnover time, the length of time required to entirely ventilate the chamber volume. This turnover time is obtained from the quotient of the chamber volume and the chamber ventilation rate. In realistic scenarios, turnover times generally range from 20 to 60 minutes for ventilated areas in modern buildings.

1. Suitcase Scenario

The potential vapor taggants which were tested are listed in Table 5-1 and the results for each taggant are discussed in the following paragraphs.

PDCB Taggant. A PDCB tagged blasting cap vapor source with an emission rate of 0.55 nl/min was used in both parts of the experiment. The results are shown in Figure 5-1 with the measured normalized PDCB concentration $C(t)/C(\infty)$ plotted on the vertical axis and the normalized elapsed time expressed as the number of turnover times plotted on the horizontal axis. As shown in the figure, there is negligible PDCB adsorption loss in the test towel/suitcase adsorption scenario; the resulting concentrations from both parts of the experiment are nearly coincident. In fact, it appears that the taggant concentrations for the adsorbent part of the experiment are slightly higher than for the no adsorbent part. The most likely cause of this result was a decrease in the in-house compressed air supply used to ventilate the chamber which

Table 5-1. Vapor Taggants Used for Adsorption Studies

Chemical Name	Abbreviation
Perfluorodimethylcyclobutane	PDCB
Perfluoromethylcyclohexane	PMCH
Perfluorodimethylcyclohexane	PDCH
Octafluoronaphthalene	OFN
Octafluorotoluene	OFT
Decafluorobiphenyl	DFBP
$SF_5C_6F_{13}$	L-4412
Perfluorodecalin	PFD

increased the measured taggant concentration. Ideally, the chamber ventilation rate was to be a constant throughout the entire series of adsorbent experiments; however, due to length of time required for each experiment (1 to 3 days), the chamber ventilation rate would often vary after the experiment had begun, consequently affecting the chamber taggant concentrations. Nevertheless, the results do indicate that, within the precision of the experiment, there was a negligible PDCB adsorption loss in the test scenario. This result was further validated in the no barrier and barrier experiments in which the PDCB concentrations were coincident when the barrier contained a significant adsorption surface, e.g., polystyrene packing material.

PMCH Taggant. For the PMCH taggant, a tagged blasting cap source with an emission rate of 0.17 nl/min was used. The results, shown in Figure 5-2, indicate negligible PMCH adsorption loss on the test scenario as is evidenced by the near coincidence of the resulting PMCH concentrations for both parts of the experiment.

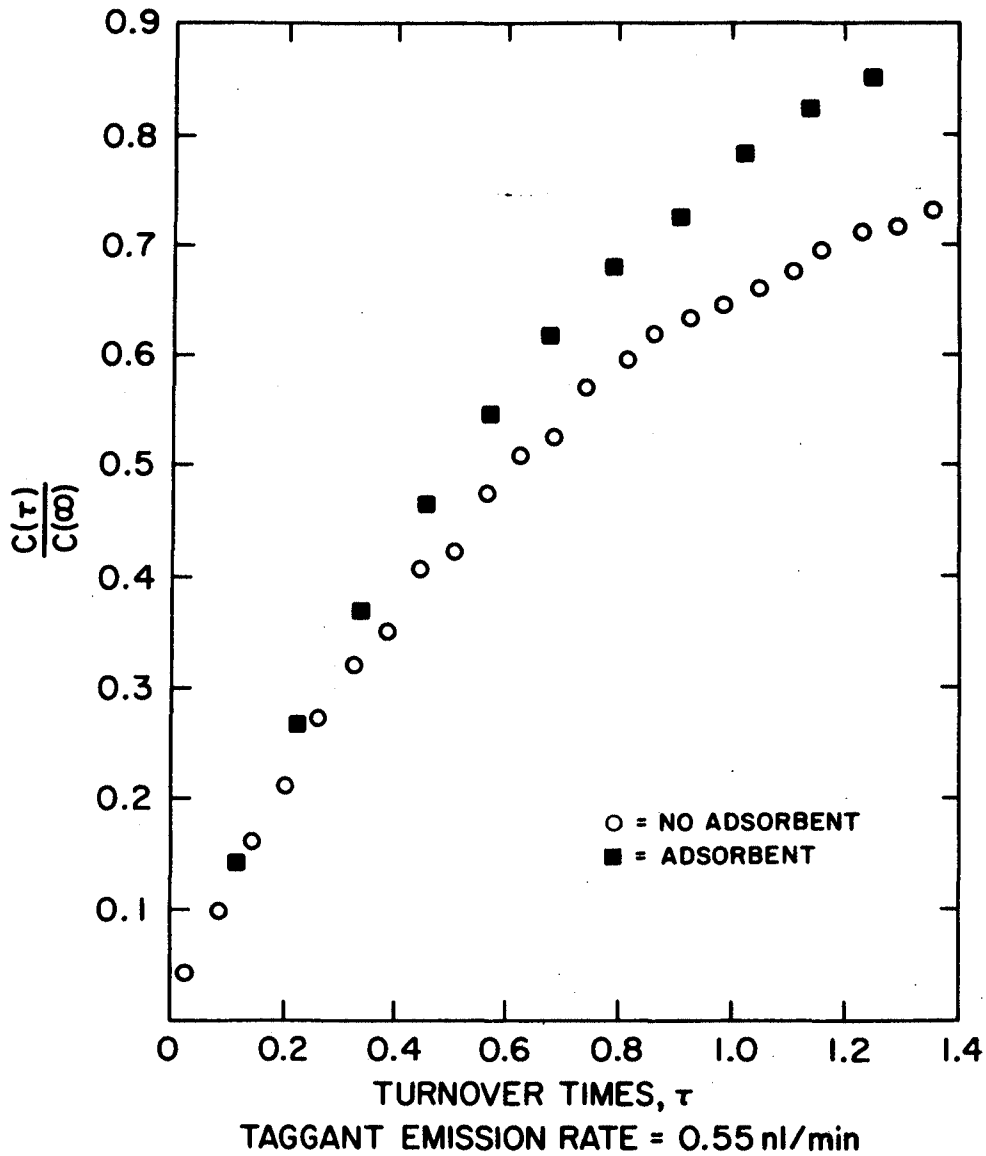

Figure 5-1. PDCB Adsorption Experiment

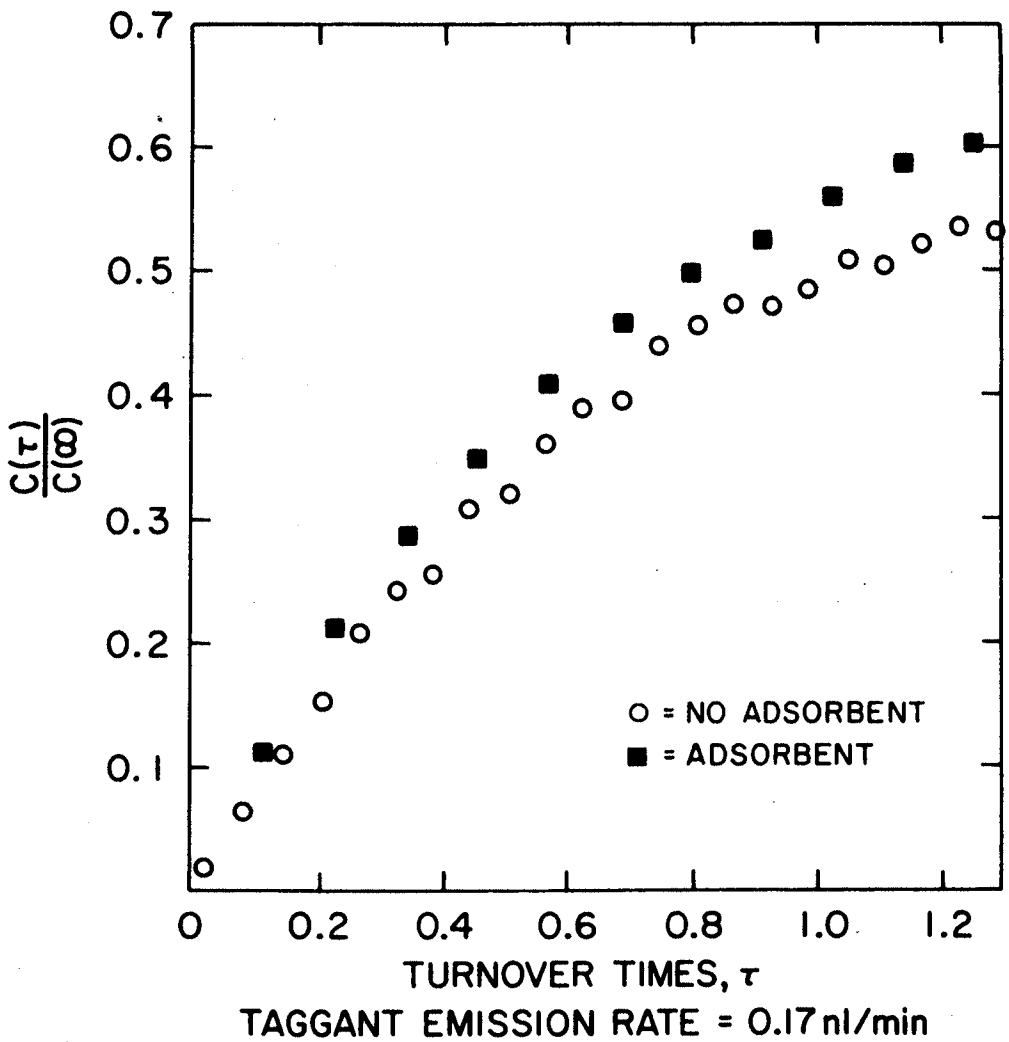

Figure 5-2. PMCH Adsorption Experiment

PDCH Taggant. Figure 5-3 gives the results for the PDCH taggant. The data indicate a lack of PDCH adsorption loss on the test scenario. As with the PDCB taggant, the adsorbent part of the experiment yielded higher PDCH concentrations than the no adsorbent part. This is again ascribed to a decrease (by approximately 20 percent) in the chamber ventilation rate which increased the PDCH taggant concentration for the adsorbent part of the experiment.

PFD Taggant. The results of the perfluorodecalin tagged blasting cap, as shown in Figure 5-4, indicate a slight degree of PFD adsorption loss in the test towel/suitcase scenario. This adsorption loss can be quantified by comparing the initial slopes of both parts of the experiment in order to determine the adsorption attenuation factor ($1 + v_m c P_{ext}/V_{ch} P_o$). This comparison gives the factor as 1.50 ± 0.21. It is not possible to determine the individual terms in this factor, therefore only the total adsorption attenuation term is given.

This degree of adsorption loss for PFD is slight and does not preclude its use as a vapor taggant; however, the scenario taggant concentrations will be reduced slightly due to adsorption. In this test towel/suitcase scenario, it was initially reduced to 50 percent of its expected concentration. However, as is seen in the mathematical derivation in Appendix C, adsorption losses only affect the initial taggant concentration. Given sufficient lapsed time, the taggant concentration will reach the same steady-state concentration regardless of the taggant volatility and the amount of adsorptive surface. The significant effect of an absorptive surface is only to slow the initial rate of taggant increase in the scenario, which for most detection schemes is the most important time.

L-4412 Taggant. The taggant L-4412 also exhibits a slight degree of adsorption loss as is indicated from the results displayed in Figure

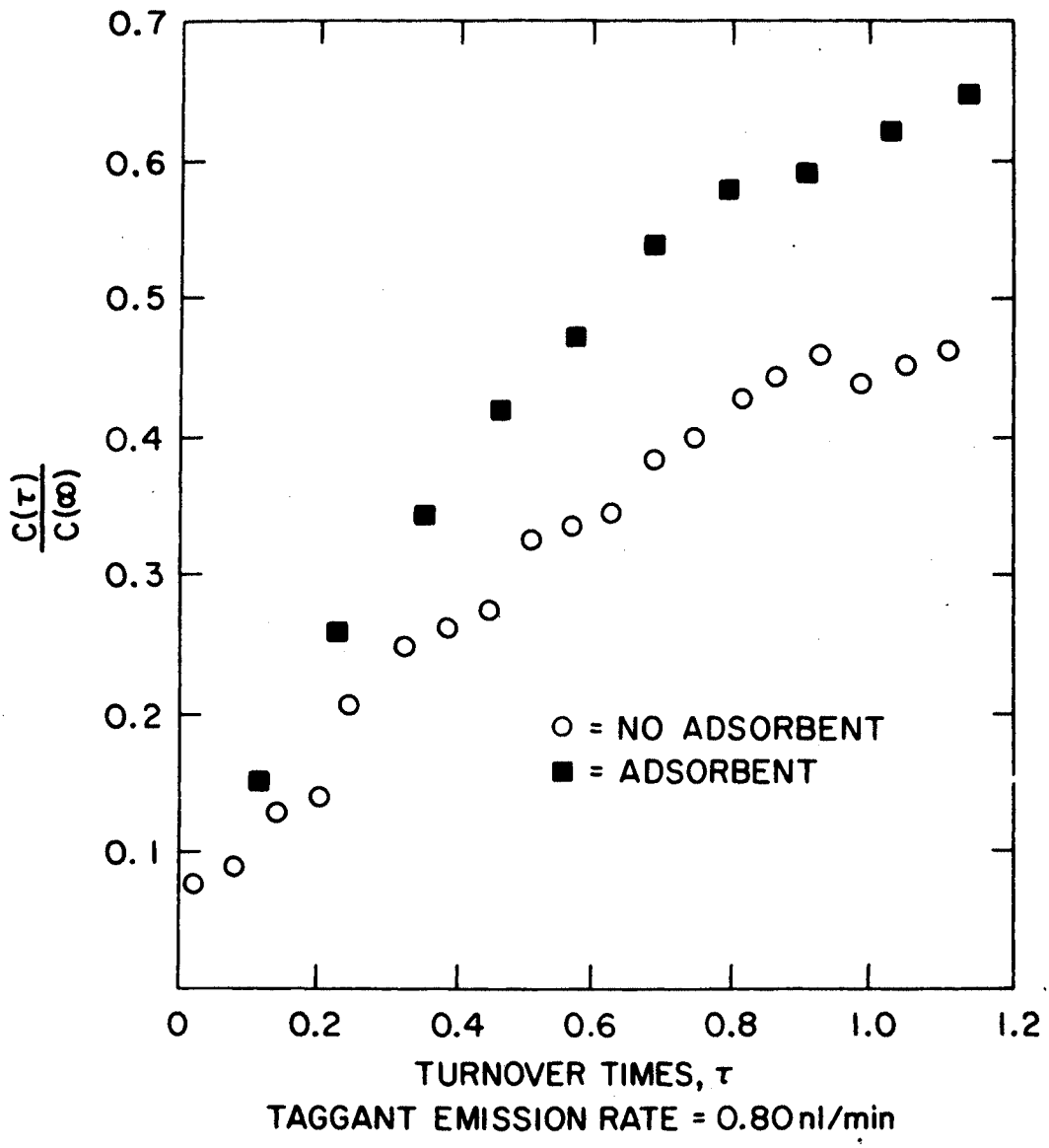

Figure 5-3. PDCH Adsorption Experiment

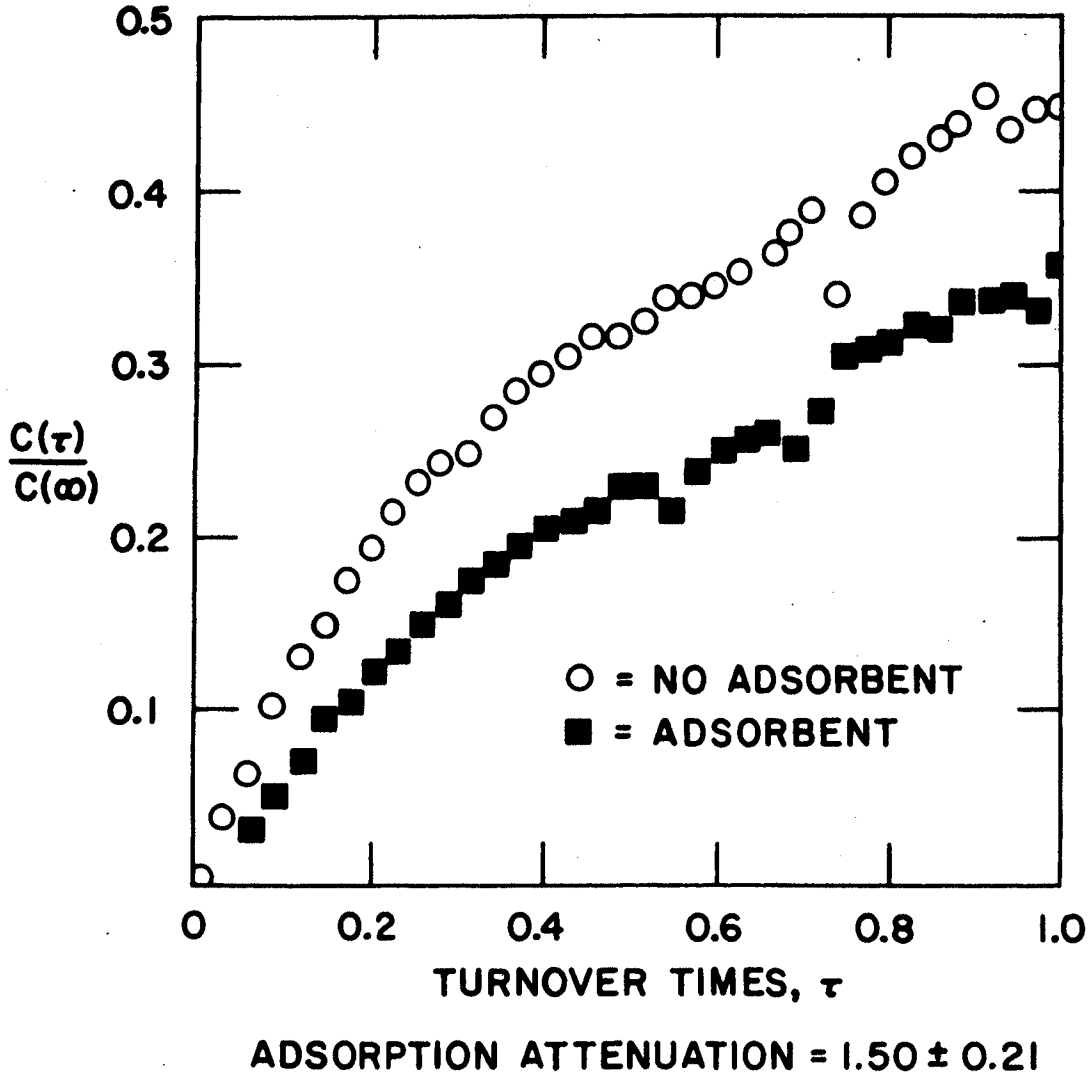

Figure 5-4. Perfluorodecalin Adsorption Experiment, Suitcase/Towel Absorbent

5-5. The adsorption attenuation factor as obtained from the initial slopes is 1.63 ± 0.36 which indicates an initial 40 percent decrease in taggant concentration due to adsorption of L-4412 in the towel/suitcase scenario. As with PFD, this does not necessarily preclude the use of PFD as a vapor taggant, provided this loss can be tolerated.

DFBP Taggant. A large adsorption loss was obtained for the DFBP taggant as is shown in Figure 5-6. The adsorption attenuation factor was determined to be 4.3 ± 1.0 indicating that approximately 80 percent of the taggant emitted from the taggant source is being adsorbed on the towel/suitcase surfaces. This adsorption loss is sufficiently great so as to remove DFBP as a potential vapor taggant.

OFN Taggant. OFN was also determined to have a large adsorption attenuation (13.2 ± 2.0) which effectively precludes its use as a vapor taggant. The results are displayed in Figure 5-7 and indicate that approximately 93 percent of the OFN is being adsorbed on the suitcase/towel surfaces at the start of the experiment.

OFT Taggant. Octafluorotoluene (OFT) was also determined to have a large adsorption loss with an observed adsorption attenuation factor of 13.5 ± 5.8 as shown in Figure 5-8. This large degree of adsorption loss for OFT similarly precludes its use as a vapor taggant.

2. Charcoal Scenario

The suitcase/towel test scenario was considered to be an average of all possible scenarios which might introduce adsorption losses. All taggants, regardless of their volatility, will adsorb to some extent. There are scenarios that are highly adsorptive that might possibly be used to hinder taggant detection such as a box containing activated charcoal. Activated charcoal has an extremely large surface area (v_m in

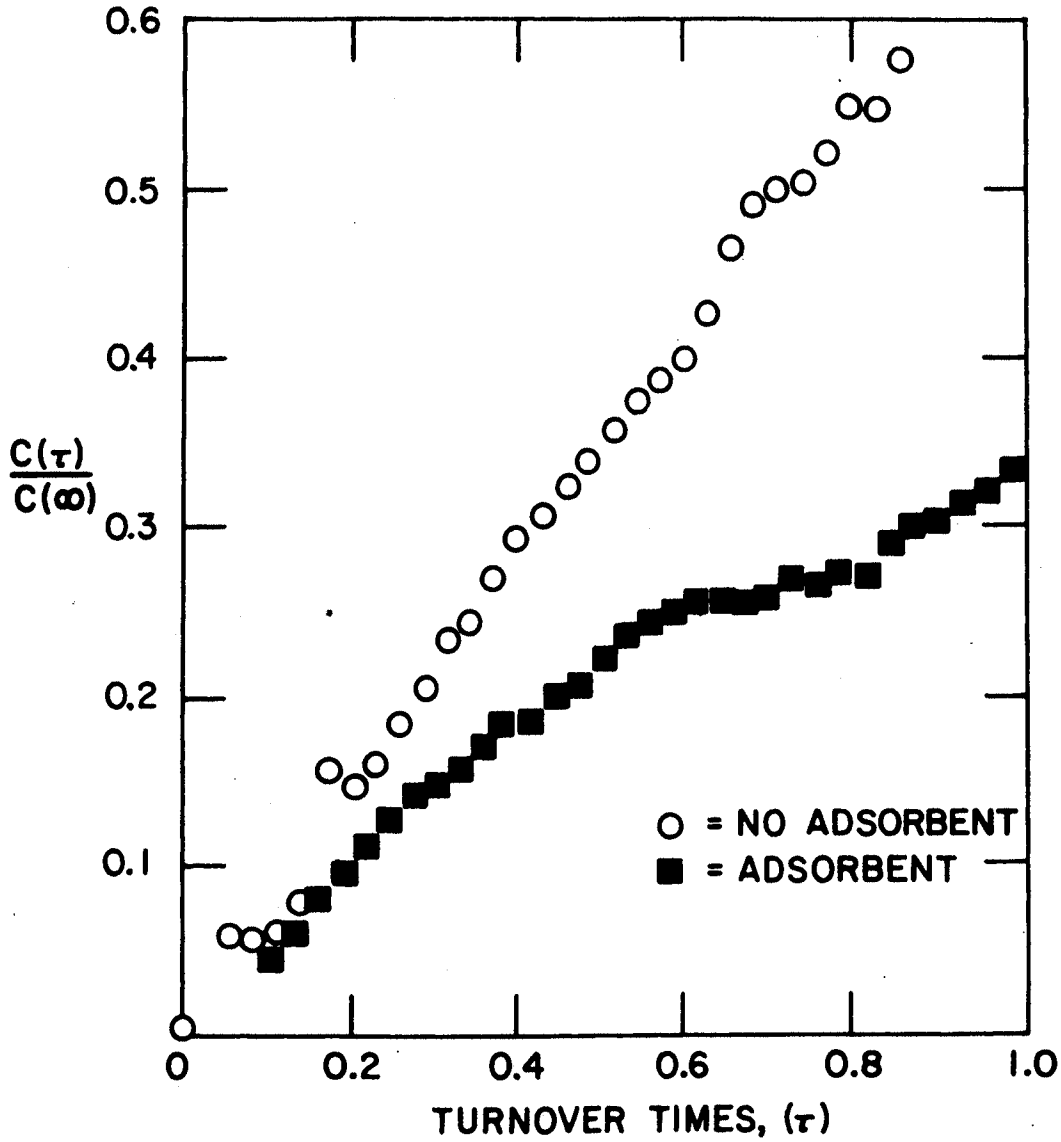

ADSORPTION ATTENUATION = 1.63 ± 0.36

Figure 5-5. L-4412 Adsorption Experiment, Suitcase/Towel Adsorbent

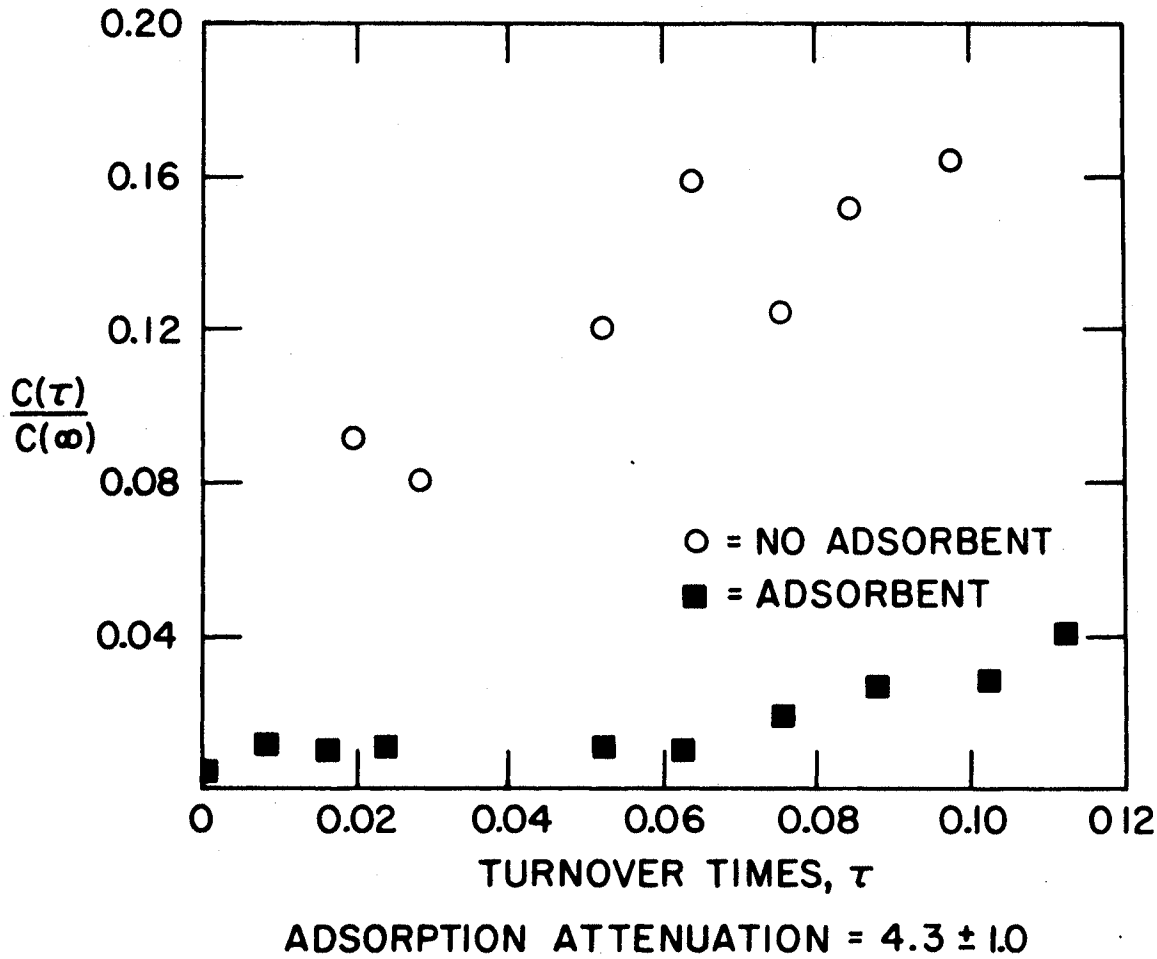

Figure 5-6. DFBP Adsorption Experiment ,
Suitcase/Towel Absorbent

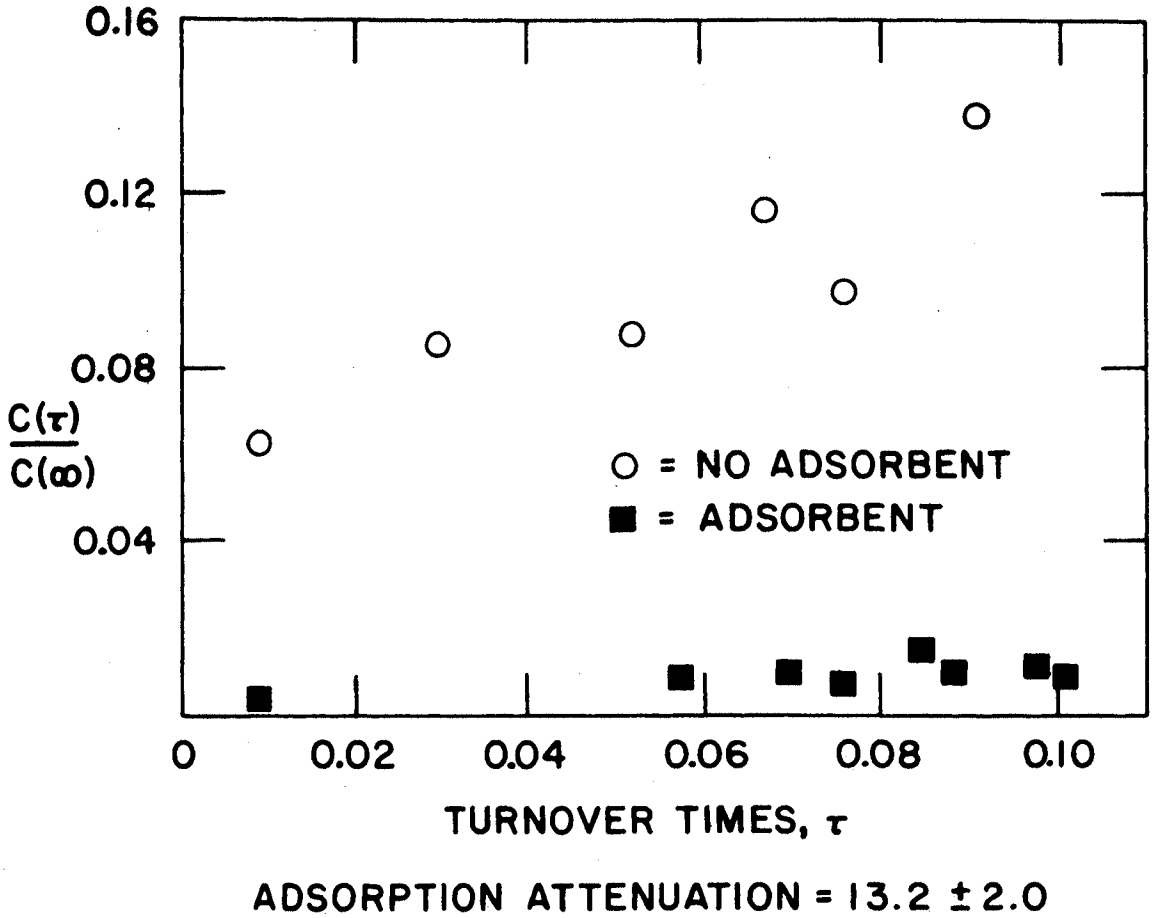

Figure 5-7. OFN Adsorption Experiment ,
Suitcase/Towel Absorbent

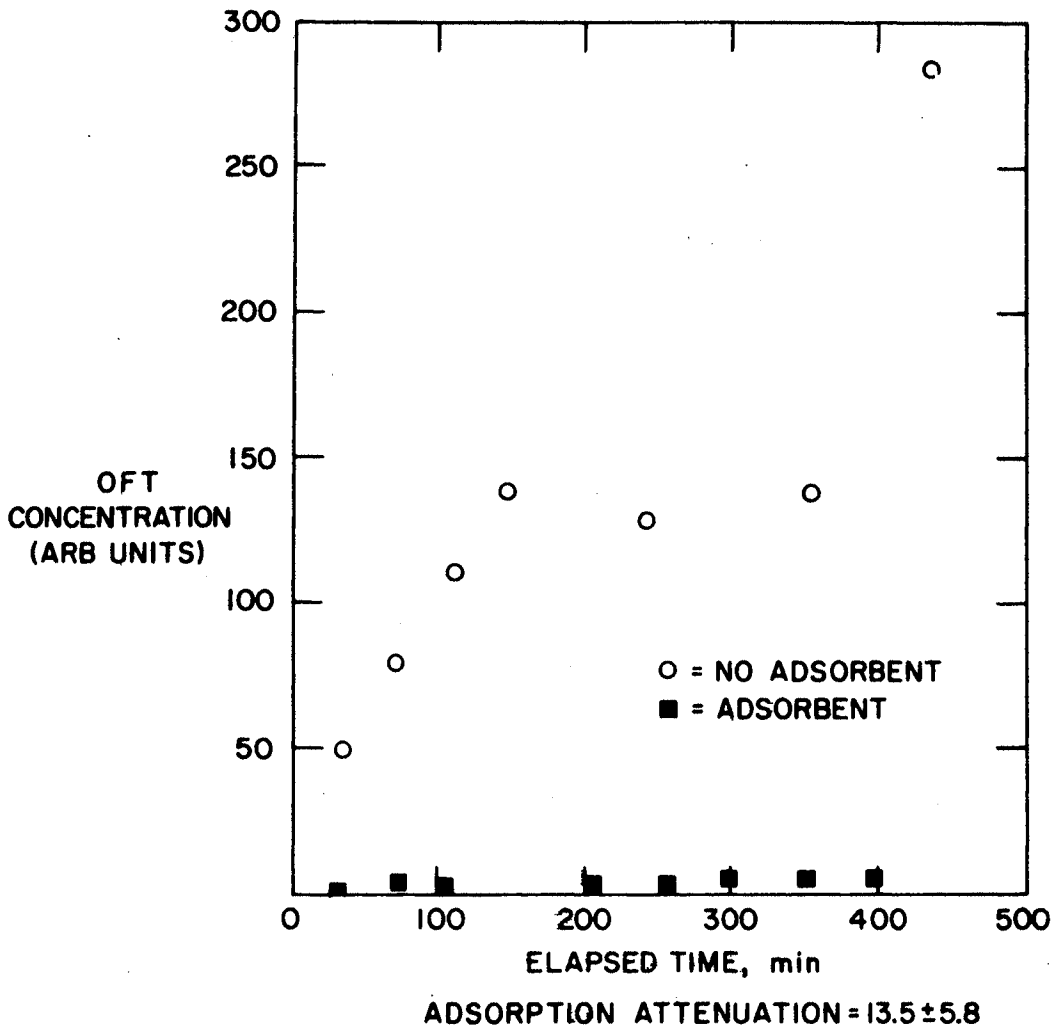

Figure 5-8. OFT Adsorption Experiment, Suitcase/Towel Barrier

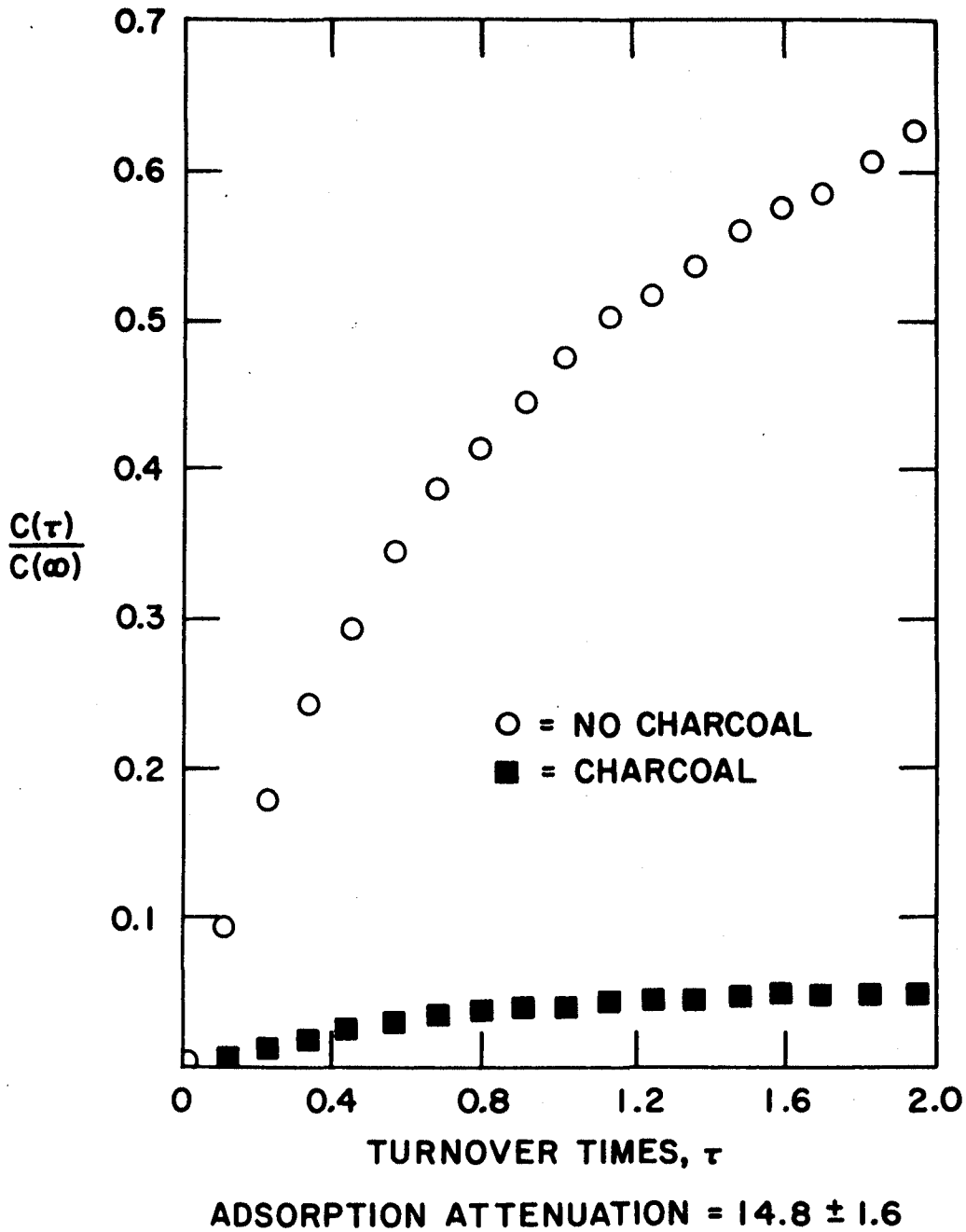

Figure 5-10. PMCH Adsorption Experiment, Charcoal Adsorbent

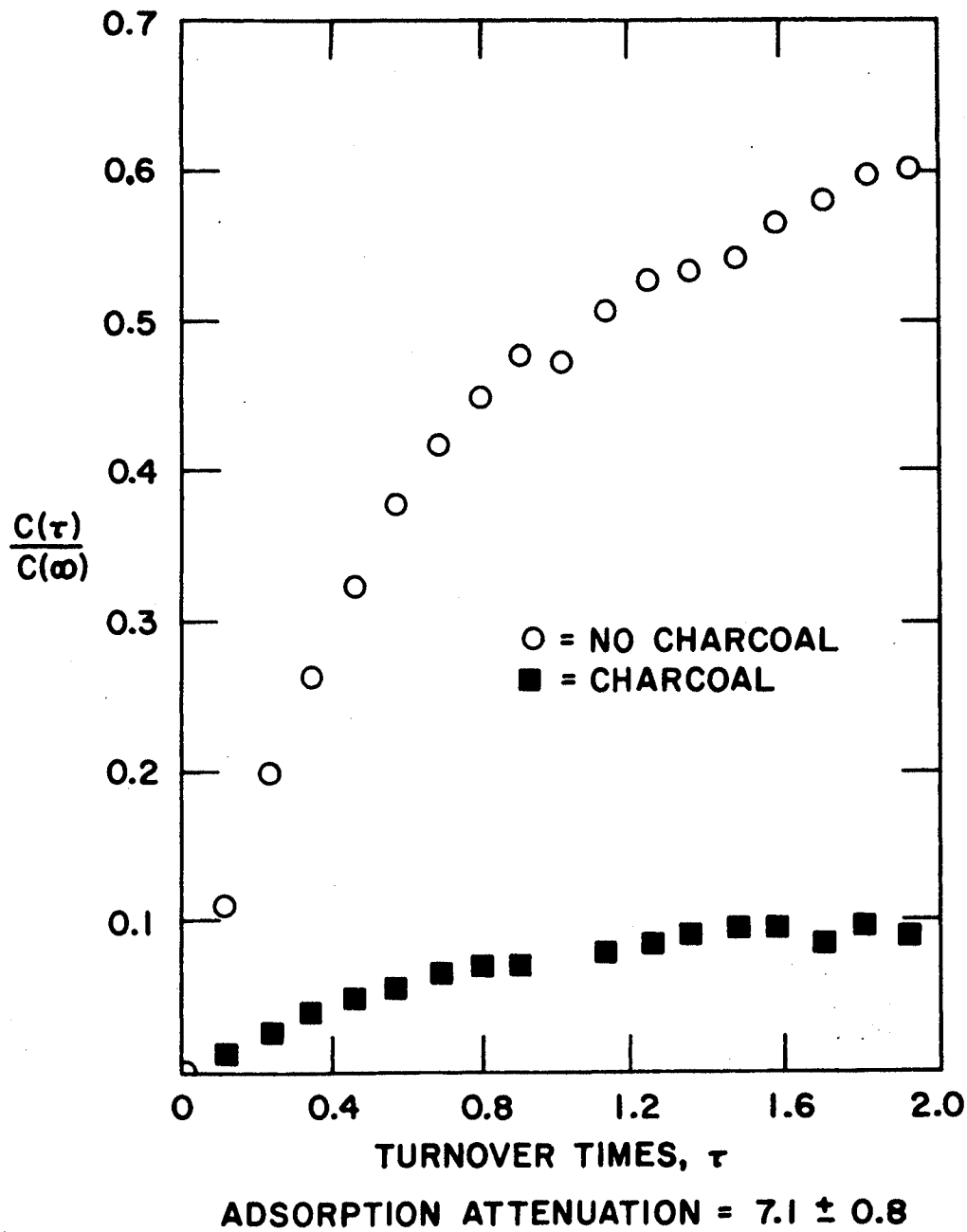

Figure 5-11. PDCH Adsorption Experiment, Charcoal Adsorbent

Table 5-3. Taggant Adsorption Losses

Taggant	Adsorption Attenuation Factor	Suitability
PDCB	1.0 ± 0.2	Yes
PMCH	1.0 ± 0.2	Yes
PDCH	1.0 ± 0.2	Yes
PFD	1.50 ± 0.21	Maybe
L-4412	1.63 ± 0.36	Maybe
DFBP	4.3 ± 1.0	No
OFN	13.2 ± 2.0	No
OFT	13.5 ± 5.8	No

B. THEORETICAL MODEL OF TAGGANT CONCENTRATIONS FROM BARRIER-ENCLOSED VAPOR TAGGED EXPLOSIVES

The ultimate success of the vapor tagging of explosives is dependent on the ability to detect the taggants in various detection scenarios. To assess realistically the detectability of tagged explosives, expressions were derived which predict the taggant concentrations in the various detection scenarios. The detectability is dependent on the taggant emission rates from the tagged explosives and other scenario and barrier parameters. The expressions derived are as general as possible so as to be applicable to the majority of realistic scenarios. The expected taggant concentrations obtained with use of the derived expressions along the detection limits of the various taggant detection methods allow an assessment of the feasibility of detecting tagged explosives in various scenarios.

Table 5-3. Taggant Adsorption Losses

Taggant	Adsorption Attenuation Factor	Suitability
PDCB	1.0 ± 0.2	Yes
PMCH	1.0 ± 0.2	Yes
PDCH	1.0 ± 0.2	Yes
PFD	1.50 ± 0.21	Maybe
L-4412	1.63 ± 0.36	Maybe
DFBP	4.3 ± 1.0	No
OFN	13.2 ± 2.0	No
OFT	13.5 ± 5.8	No

B. THEORETICAL MODEL OF TAGGANT CONCENTRATIONS FROM BARRIER-ENCLOSED VAPOR TAGGED EXPLOSIVES

The ultimate success of the vapor tagging of explosives is dependent on the ability to detect the taggants in various detection scenarios. To assess realistically the detectability of tagged explosives, expressions were derived which predict the taggant concentrations in the various detection scenarios. The detectability is dependent on the taggant emission rates from the tagged explosives and other scenario and barrier parameters. The expressions derived are as general as possible so as to be applicable to the majority of realistic scenarios. The expected taggant concentrations obtained with use of the derived expressions along the detection limits of the various taggant detection methods allow an assessment of the feasibility of detecting tagged explosives in various scenarios.

Conceptually, the detection of vapor taggants will be formulated as follows: a tagged explosive with a predetermined taggant emission rate is placed within an enclosure, realistic examples of which include boxes, cans, plastic bags, and suitcases. The enclosure, acting as a barrier to detection of the vapor taggant, is placed within a scenario. (Scenario refers to a defined space with a known volume and ventilation rate in which the taggant will be detected. Examples of scenarios are lockers, rooms, and buildings. The ventilation rate is the constant exchange of air within the scenario with air from outside the scenario.)

Barriers were considered with respect to their degree of "airtightness." A more airtight barrier decreases the rate of taggant release into the scenario. The airtightness of various barrier enclosures is compared to that of a reference barrier enclosure which is the case where no barrier is present to enclose the tagged explosive. The reference barrier enclosure (no barrier) allows the fastest taggant release and represents the most detectable scenario. In any scenario, a steady-state taggant concentration will be reached eventually regardless of the degree of airtightness of the barrier.

In most realistic cases, the tagged explosives will be prepared, placed in a barrier, and then subsequently placed in some scenario. This time delay between the introduction of the tagged explosive into the barrier and the introduction of the barrier into the final scenario affects the rate of taggant release into the scenario. In actuality, this time delay is on the order of 1 hour and is taken into account in the examples. The equations derived were used to predict the taggant concentrations inside a briefcase, in a room containing a briefcase with tagged explosives, and in a building and an airplane containing an enclosure with tagged explosives.

Conceptually, the detection of vapor taggants will be formulated as follows: a tagged explosive with a predetermined taggant emission rate is placed within an enclosure, realistic examples of which include boxes, cans, plastic bags, and suitcases. The enclosure, acting as a barrier to detection of the vapor taggant, is placed within a scenario. (Scenario refers to a defined space with a known volume and ventilation rate in which the taggant will be detected. Examples of scenarios are lockers, rooms, and buildings. The ventilation rate is the constant exchange of air within the scenario with air from outside the scenario.)

Barriers were considered with respect to their degree of "airtightness." A more airtight barrier decreases the rate of taggant release into the scenario. The airtightness of various barrier enclosures is compared to that of a reference barrier enclosure which is the case where no barrier is present to enclose the tagged explosive. The reference barrier enclosure (no barrier) allows the fastest taggant release and represents the most detectable scenario. In any scenario, a steady-state taggant concentration will be reached eventually regardless of the degree of airtightness of the barrier.

In most realistic cases, the tagged explosives will be prepared, placed in a barrier, and then subsequently placed in some scenario. This time delay between the introduction of the tagged explosive into the barrier and the introduction of the barrier into the final scenario effects the rate of taggant release into the scenario. In actuality, this time delay is on the order of 1 hour and is taken into account in the examples. The equations derived were used to predict the taggant concentrations inside a briefcase, in a room containing a briefcase with tagged explosives, and in a building and an airplane containing an enclosure with tagged explosives.

1. Derivation of the Expressions

Expressions for the scenario taggant concentrations are derived with the following assumptions: (1) the taggant emission rate from the tagged explosive is constant over the time interval from the introduction of the tagged explosive into the barrier to the detection of the taggant in the scenario; (2) the emission of the taggant from the barrier is diffusion controlled, (best described by Fick's first law of diffusion); (3) there is uniform mixing of the taggant with the air in the barrier and in the scenario; and (4) the air exchange rate due to ventilation of the scenario is constant with time.

a. No-Barrier or Reference Case

The method for the derivation of an expression for the taggant concentration in a scenario containing no barrier is simple. Let $V_o(t)$ be the volume of taggant present in the scenario at time t, with $V_o(t = 0) = 0$. The volume of taggant $V_o(t)$ is effected by two rate processes: (1) the emission of taggant from the tagged explosive in the scenario (taggant source) and (2) the removal of the taggant from the scenario by the ventilation (a taggant sink). This is conveniently expressed as a balance between the various rate processes

$$dV_o(t)/dt = \underbrace{R_{cap}}_{\text{Source}} - \underbrace{f\ R_{ex}}_{\text{Sink}} \qquad (5\text{-}4)$$

where: R_{cap} = the taggant emission rate of a tagged explosive present in the scenario (liters/min),

R_{ex} = the ventilation rate of the scenario, and

f = the volume fraction of the taggant in the air leaving the scenario

i.e., $f = V_o(t)/V_{ch}$ (5-5)

where: V_{ch} = the volume of the scenario.

Substituting for the volume fraction and noting the time independence of R_{cap} and R_{ex}:

$$dV_o(t)/dt = R_{cap} - (R_{ex}/V_{ch})V_o(t) \quad (5\text{-}6)$$

with the initial condition

$$V_o(t = 0) = 0. \quad (5\text{-}7)$$

The solution of this integral equation is

$$V_o(t) = (R_{cap}V_{ch}/R_{ex})\ (1 - \exp\left[-\ (R_{ex}/V_{ch})t\right]). \quad (5\text{-}8)$$

This may be re-expressed in terms of a taggant concentration in parts per part and in terms of a characteristic ventilation time t_v,

$$t_v = V_{ch}/R_{ex}, \quad (5\text{-}9)$$

as

$$C_o(t) = (R_{cap}/R_{ex})\ \left[1 - \exp\ (-\ t/t_v)\right] \quad (5\text{-}10)$$

where: $C_o(t)$ = the concentration of taggant in the scenario.

The characteristic time t_v is the time required to completely exchange the total volume of air in the scenario by ventilation -- the turnover time. The turnover time t_v is generally 1/2 to 1 hour for most rooms and buildings as recommended by various building ventilation standards.

The steady-state taggant concentration in the scenario is the taggant emission rate divided by the scenario ventilation rate

$$C_o(t \rightarrow \infty) = R_{cap}/R_{ex} \tag{5-11}$$

Thus, for the reference barrier (no-barrier) enclosure, in one turnover time t_v, the taggant concentration in the scenario is approximately 63 percent of its steady-state value.

b. Barrier Case with No Time Delay

The method for the derivation of expressions for the taggant concentration in a scenario with the tagged explosives enclosed in a barrier is similar to the previous example. Two taggant volumes are defined: $V_{en}(t)$, the volume of taggant inside the barrier, and $V(t)$, the volume of the taggant inside the scenario. The balances for the various rates in the barrier and scenario respectively are expressed as:

$$dV_{en}(t)/dt = \underbrace{R_{cap}}_{\text{source}} - \underbrace{R_{en}(t)}_{\text{sink}} \tag{5-12}$$

$$dV(t)/dt = \underbrace{R_{en}(t)}_{\text{source}} - \underbrace{f\ R_{ex}}_{\text{sink}} \tag{5-13}$$

where: $R_{en}(t)$ = the taggant emission rate from the barrier into the scenario and

f = the volume fraction as defined earlier.

Substituting for the volume fraction and noting which rates are time independent:

$$dV_{en}(t)/dt = R_{cap} - R_{en}(t) \tag{5-14}$$

$$dV(t)/dt = R_{en}(t) - (R_{ex}/V_{ch})V(t) \tag{5-15}$$

Assuming that the taggant emission rate from the barrier is diffusion controlled and best described by Fick's first law:

$$R_{en}(t) = k\ (V_{en}(t)/V_{en} - V(t)/V_{ch}) \tag{5-16}$$

where: V_{en} = the volume of the barrier and
k = a constant dependent only on the barrier.

This barrier constant, k, can be thought of as an "air exchange" rate between the air in the barrier and the air surrounding the barrier and is due to diffusion of air in and out of the barrier through any minute openings in the barrier. This can be made more apparent by considering the example when the air surrounding the barrier has no taggant concentration, ($V(t) = 0$). The taggant emission rate from the barrier becomes the product of the air exchange rate k and the taggant concentration in the air:

$$R_{en}(t) = k\ V_{en}(t)/V_{en} \tag{5-17}$$

When there is a taggant concentration present in the scenario, then equation (5-16) is appropriate. (The units for k are liters/minute.) By substituting the expression for $R_{en}(t)$ into the two mass balance equations, the result is

$$dV_{en}(t)/dt = R_{cap} - (k/V_{en})\ V_{en}(t) + (k/V_{ch})\ V(t) \qquad (5\text{-}18)$$

$$dV(t)/dt = (k/V_{en})\ V_{en}(t) - (k/V_{ch})\ V(t) - (R_{ex}/V_{ch})\ V(t) \qquad (5\text{-}19)$$

The associated initial conditions are

$$V_{en}(t = 0) = 0 \qquad (5\text{-}20)$$

and

$$V(t = 0) = 0 \qquad (5\text{-}21)$$

In these equations (5-20 and 5-21), the taggant concentrations in the barrier and scenario are zero at the time of introduction of the explosive into the scenario and the barrier.

The solution of these coupled differential equations is given in Appendix A and the solution for V(t) is

$$V(t) = \frac{R_{cap}V_{ch}}{R_{ex}} \left[1 - \frac{r_2 \exp[-\ r_1 t] - r_1 \exp[-\ r_2 t]}{r_2 - r_1}\right] \qquad (5\text{-}22)$$

in which

$$\begin{matrix} r_1 \\ r_2 \end{matrix} = \left(\frac{R_{ex}}{V_{ch}}\right)\left((\beta + \beta/\gamma + 1) \mp ([\beta + \beta/\gamma + 1]^2 - 4\ \beta/\gamma)^{1/2}\right)\Big/2 \qquad (5\text{-}23)$$

where: $\beta = k/R_{ex}$, the ratio of the barrier air exchange rate to the scenario ventilation rate and

$\gamma = V_{en}/V_{ch}$, the ratio of the barrier volume to the scenario volume.

The taggant concentration inside the scenario is simply

$$C(t) = V(t)/V_{ch}. \qquad (5\text{-}24)$$

Several important limits of C(t) can be derived. First, as $t \rightarrow \infty$, the taggant concentration in the scenario approaches the steady-state concentration of

$$C(t \rightarrow \infty) = R_{cap}/R_{ex} \tag{5-25}$$

which is identical to that for the no-barrier case. Thus the steady-state concentration is independent of the degree of barrier airtightness, and the only effect of a barrier is to attenuate the rate of taggant release into the scenario. This effect is dependent on the value of k, the barrier parameter, with smaller values of k corresponding to a more airtight barriers.

As stated, barrier air exchange rates k are related (in some way) to the size of air leaks of barriers. Two visualizations for the barrier air leak parameter are considered: holes or cracks and permeation. The hole, crack or microcrack barrier parameter can be expressed as

$$k = AD/L \tag{5-26}$$

where: A = the total area of the cracks in the barrier,
L = an average depth of the cracks, and
D = the taggant-air diffusion constant.

This barrier parameter is consistent with barriers such as boxes, briefcases, and pipebombs. It can be seen that this barrier parameter is nearly independent with respect to the choice of taggant because D, the taggant-air diffusion constant, differs very slightly from taggant to taggant.

The permeation barrier parameter can be expressed as

$$k = QA/L \tag{5-27}$$

where: A = the total surface area of the barrier,
L = the average thickness of the barrier wall, and
Q = the permeability coefficient expressed in appropriate units.

This barrier parameter depicts extremely well-sealed plastic bags, various waxes, and other materials which coat a barrier. With the permeation barrier parameter, there should be no dependence of k on the specific taggant due to the near constancy of Q with respect to differing taggants.

These expressions for k (eq. 5-26 and 5-27) are appropriate for obtaining an order of magnitude value of k for various barriers; however, it is more convenient to determine k experimentally for a series of barriers with the use of the derived expressions and experimentally measured taggant concentration in a scenario from a tagged source inserted in the barrier.

In this derivation, it is assumed that both the barrier and scenario taggant concentrations are zero at the time of introduction (t = 0) of the barrier into the scenario (eq. 5-20 and 5-21). In most realistic scenarios, however, the tagged explosive will be placed in the barrier and then subsequently placed in the scenario. There may be several hours delay between placing the tagged explosive in the barrier and placing the barrier in the scenario. Thus a more realistic initial condition for $V_{en}(t)$ is

$$V_{en}(t = 0) = V^{*}_{en} \tag{5-28}$$

setting the concentration of taggant inside the barrier to some non-zero value. The situation where both concentrations are zero at t = 0, however, is convenient to analyze and experimentally to realize in the laboratory for the determination of the barrier parameter for the various barriers. The situation with

$$V_{en}(t = 0) = V^{*}_{en} \tag{5-29}$$

is discussed in the next section.

c. Barrier with Time Delay Case

For the more realistic situation of a non-zero initial taggant concentration in the barrier, the coupled differential equations for the taggant volume in the scenario are the same; however, an additional term, the initial taggant volume inside the barrier, is added to the differential equation for $V_{en}(t)$. An estimation of the initial taggant concentration in the barrier can be derived from the first of the coupled differential equations. Assume the barrier enclosure is in an environment in which the taggant concentration is effectively zero (V(t) = 0 for all times). Then the concentration of taggant inside the barrier is given by

$$C_{en}(t) = V_{en}(t)/V_{en} = (R_{cap}/k)\left[1 - \exp(- kt/V_{en})\right] . \tag{5-30}$$

Thus, an appropriate initial taggant concentration is

$$V^{*}_{en} = V_{en}(t = 0) = V_{en}C_{en}(t = t_{delay}) \tag{5-31}$$

in which t_{delay} is the time between the placing of the tagged explosive in the barrier and the placing of the barrier in the scenario.

The coupled differential equations can now be solved with the inclusion of the initial barrier taggant volume. The explicit solution is given in Appendix A and is

$$V(t) = \frac{R_{cap}V_{ch}}{R_{ex}} \left[1 - \frac{r_2 \exp(-r_1 t) - r_1 \exp(-r_2 t)}{r_2 - r_1} \right]$$

$$+ k\, C_{en}(t_{delay}) \left[\frac{\exp(-r_1 t) - \exp(-r_2 t)}{r_2 - r_1} \right] . \qquad (5\text{-}32)$$

The taggant concentration in the scenario, $V(t)/V_{ch}$, with time delay, is composed of two terms: (1) the taggant concentration in the scenario without time delay (the case considered in Section 5.1.b) and (2) an additional term which is positive for all times. Thus, the effect of a time delay or, equivalently, an initial taggant concentration inside the barrier, is to increase the rate of taggant release into the scenario. Note that this additional term is proportional to the derivative of the first term; it is greatest when the taggant concentration (for the no time delay case) is rapidly increasing at a time when the barrier has just been placed in the scenario. These physical conclusions are reasonable because the emission rate of taggant from the barrier enclosure is dependent on the concentration inside the barrier enclosure and thus the rate of taggant release into the scenario should be increased.

The taggant concentration in the scenario for this case has the same steady-state value as found for the other cases:

$$C(t \rightarrow \infty) = V(t \rightarrow \infty)/V_{ch} = R_{cap}/R_{ex} \qquad (5\text{-}33)$$

2. Application and Discussion of the Derived Expressions

The expressions for the scenario taggant concentrations as derived in the previous section are discussed generally and applied to various scenarios.

a. No Barrier Case

The scenario taggant concentration is given by

$$C_o(t) = (R_{cap}/R_{ex}) \left[1 - \exp(- t/t_v)\right] \qquad (5\text{-}34)$$

where: $t_v = V_{ch}/R_{ex}$.

The approach to the steady-state concentration of R_{cap}/R_{ex} is exponential in nature. The quantity t_v is the turnover time of the scenario, the time required to completely exchange the air in the scenario with fresh air.

b. Barrier Case

The ranges defined in Table 5-4 are defined for the barrier parameter k for barrier cracks and are based on experimental evidence. A physical interpretation for these barrier parameters can be derived from equation (5-26):

$$k = AD/L$$

as defined earlier. The total area of cracks in the barrier for the various degrees of barrier airtightness severity, assuming the taggant--air diffusion constant to be approximately 5 cm^2/min and the cracks to be 1 mm in depth, were obtained and are listed in Table 5-4.

Table 5-4. Barrier Crack Parameter and Crack Area

Degree of Barrier Airtightness	Barrier Parameter k (l/min)	Total Crack Area
Severe	2×10^{-4}	0.004 cm^2
Moderate	2×10^{-2}	0.4 cm^2
Slight	2	40 cm^2

An example of a severe microcrack barrier is a 6-inch-high paint can with a 1-μm crack about the circumference of the lid. In this case, the crack area is 0.0048 cm^2.

An estimation of the barrier permeation parameter was also made and this corresponds to a barrier enclosure such as a well-sealed plastic bag. In this instance, the barrier permeation parameter:

$$k = QA/L$$

Assuming a permeation coefficient of 0.1×10^{-10} cm^3 (STP)cm/sec-cm^2 Δtorr, such as for polyethylene with a thickness of 2 mil, $k = 1 \times 10^{-10}$ l/min is obtained, a value several orders of magnitude lower than for a severe microcrack barrier. In most instances, however, small cracks in the seal of the plastic bag and pinhole leaks will be the predominant mode of taggant loss from plastic bags. For example, a single pinhole with a diameter of 0.16 mm in this polyethylene bag will give a barrier parameter of 2×10^{-4} l/min, several orders of magnitude greater than the barrier parameter that results for permeation alone.

The effect of a barrier on the scenario taggant concentration in the no time delay case is shown in Figure 5-12, a plot of the normalized

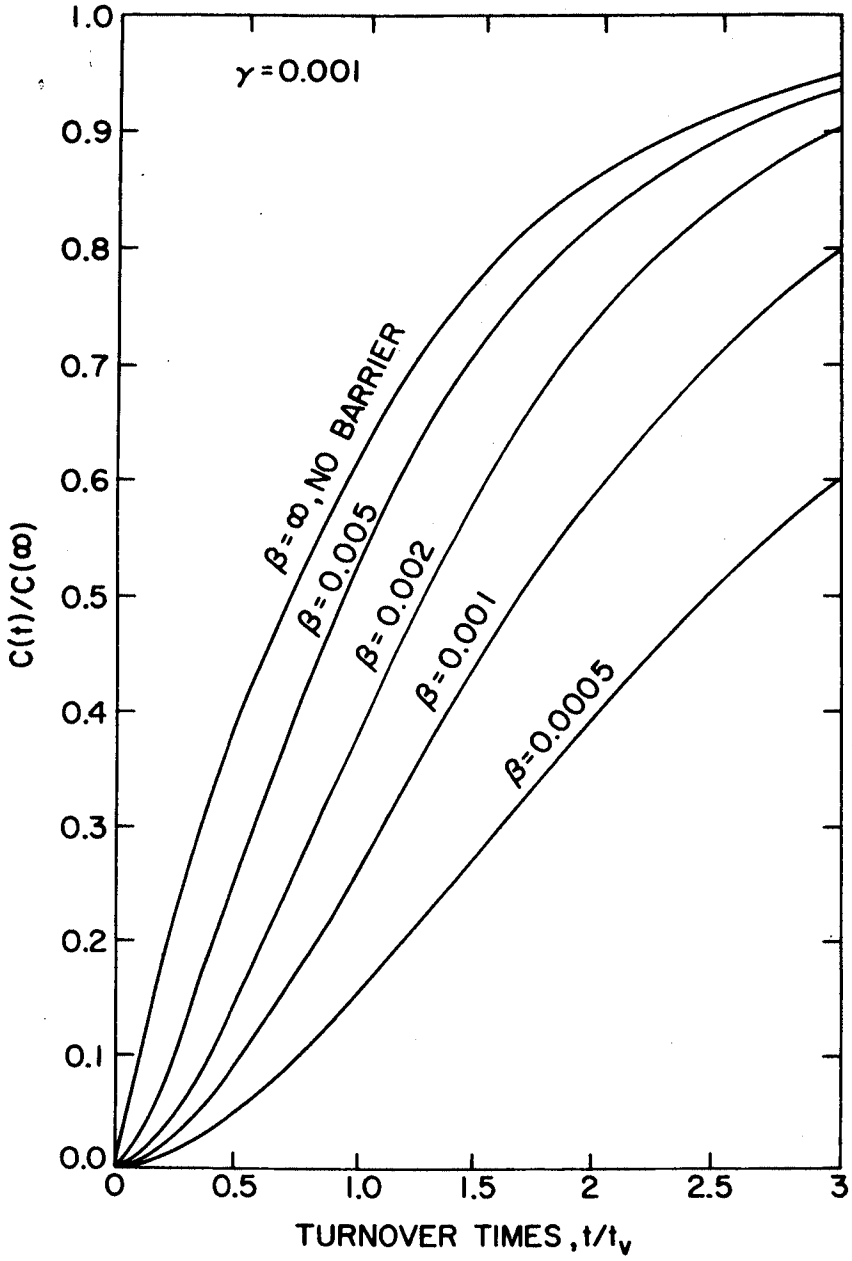

Figure 5-12. Fractional Scenario Taggant Concentrations

scenario taggant concentration (normalized with respect to the steady-state concentration, R_{cap}/R_{ex}) versus time. The various curves correspond to differing values of the barrier parameter k, expressed in the figure as the dimensionless parameter $\beta = k/R_{ex}$ with $\beta = \infty$ corresponding to the no barrier situation and decreasing β corresponding to an increased airtightness of the barrier. As expected, the effect of the barrier is to decrease the rate of taggant release into the scenario from the barrier-enclosed explosive. Note that β must be less than γ before there is any noticeable effect of the barrier on the rate of taggant release into the scenario. Equivalently this means when $k/V_{en} < R_{ex}/V_{ch}$ (the turnover time for the air in the scenario is greater than the turnover time for the air in the barrier), the taggant will be removed at a rate from the scenario faster than the barrier can release taggant. Consequently the rate of taggant release in the scenario will be attenuated.

There is also a dependence of the scenario taggant concentration on γ, the ratio of the volume of the barrier enclosure to the volume of the scenario ($\gamma = V_{en}/V_{ch}$). It can be seen in comparing Figures 5-12 and 5-13 that, for equivalent values of the barrier parameter, the attenuation in the taggant emission rate from the barrier is less with the smaller barrier enclosure volume. Figure 5-13 represents the situation where the barrier enclosure volume has been decreased by a factor of 10 compared to that in Figure 5-12. In the limit, as β goes to zero (the barrier becoming more airtight), a decrease in barrier enclosure volume by a factor of 10 will increase the rate of taggant release into the scenario by a factor of 10. This is physically reasonable because the taggant emission rate from the barrier enclosure is dependent on the taggant concentration inside the enclosure which will increase with decreasing barrier enclosure volume. In the other limit, that of no barrier, the volume of the barrier is inconsequential.

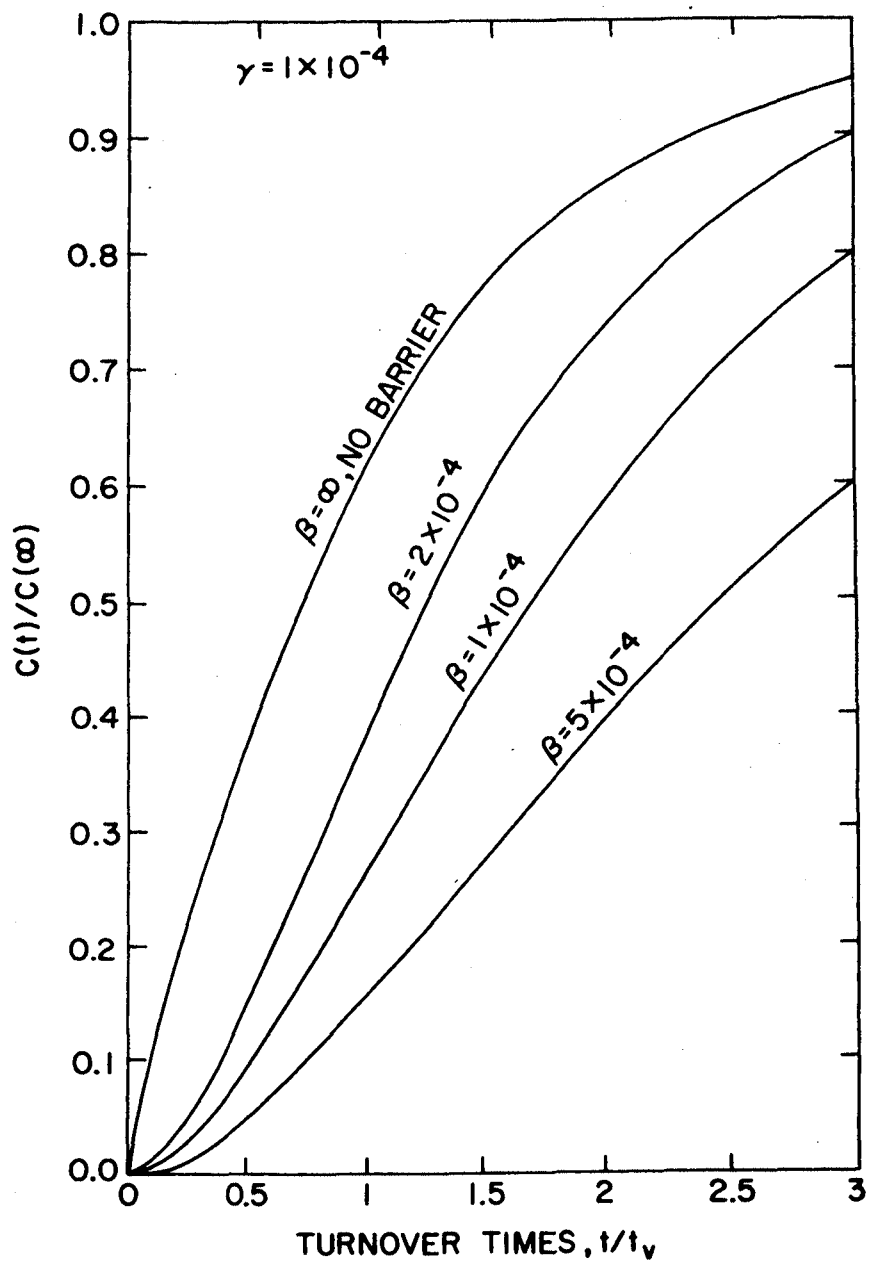

Figure 5-13. Fractional Scenario Taggant Concentrations

Several other observations for the no time delay barrier case can be made in the limit of a severe barrier. In this limit, $\gamma > \beta$, or equivalently, $k/V_{en} < R_{ex}/V_{ch}$.

- The taggant emission rate from the barrier enclosure is more or less constant after an initial period (normalized taggant concentration more than 0.1) -- the scenario taggant concentration increases linearly with time. However, the taggant emission rate during this initial period is approximately linear with time -- the scenario taggant concentration increases quadratically with time. This can best be seen in Figure 5-14, which is an expanded version of Figure 5-12.

- The taggant emission rate after the initial period is more or less linearly proportional to the barrier parameter k -- a factor of 2 decrease in k will decrease the emission rate from the barrier by a factor of 2. This can be seen in comparing the slopes in Figure 5-14.

These observations together can provide a general rule for a barrier scenario with no time delay: In the limit of a severe barrier, the taggant emission rate from the barrier is proportional to $kV_{ch}/R_{ex}V_{en}$.

It was also observed that the taggant scenario concentration always approaches the steady-state concentration, R_{cap}/R_{ex}, regardless of the degree of airtightness of the barrier. The principal effect of a barrier is to delay the approach of the taggant concentration toward its steady-state concentration as illustrated in Figure 5-15. The more airtight the barrier, the greater the delay in the approach of the taggant concentration toward its steady-state concentration. This is consonant with the idea of a lag time before the appearance of taggant concentration in the scenario.

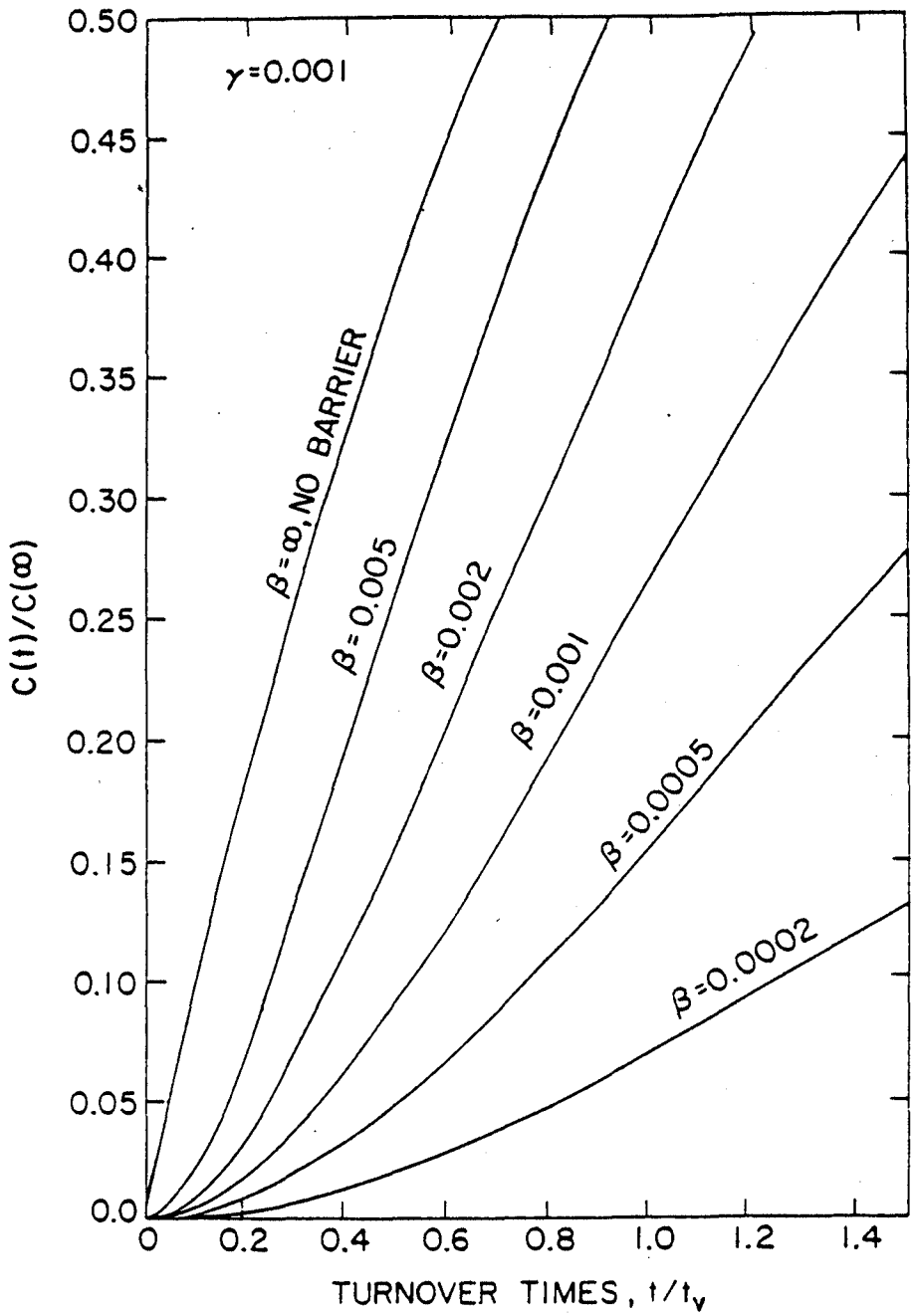

Figure 5-14. Expanded Fractional Scenario Taggant Concentrations

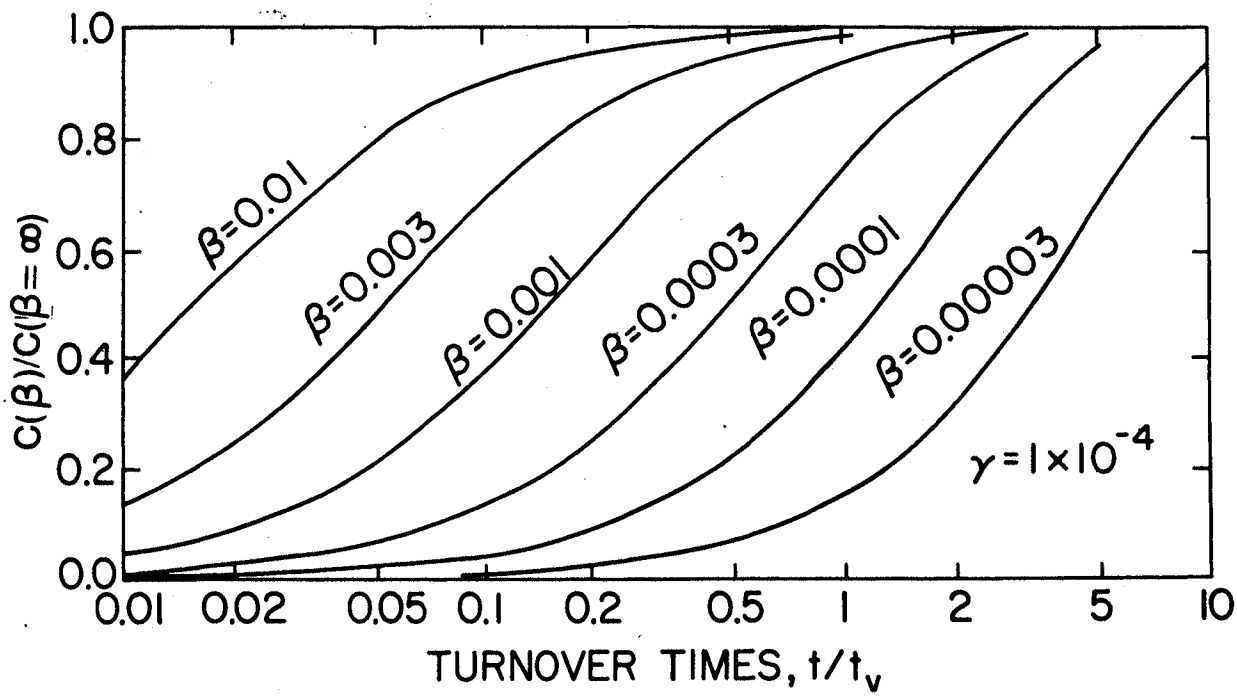

Figure 5-15. Approach to Taggant Steady State

c. Specific Examples

(1) Taggant Concentrations Inside a Briefcase. For estimating taggant concentrations in a briefcase, it is assumed that a tagged explosive has been placed within a luggage item and that the luggage has not been exposed for any length of time to any defined volume in which the taggant concentration can accumulate (the briefcase is constantly in an environment that is well ventilated). The only mechanism assumed for the loss of taggant vapors from the briefcase is diffusion through the briefcase seams. The relevant equation for the taggant concentration inside the briefcase is equation (5-30). Table 5-5 gives the results of the calculation for a standard size briefcase for three degrees of airtightness.

Table 5-5. Taggant Concentration Inside a Briefcase Having Various Degrees of Airtightness
$R_{cap} = 1 \times 10^{-9}$ 1/min
$V_{en} = 11.33$ liters

Time Elapsed	Taggant Concentration, parts per billion (ppb) Severe Barrier $k = 2 \times 10^{-4}$ (1/min)	Moderate Barrier $k = 2 \times 10^{-2}$ (1/min)	Slight Barrier $k = 2$ (1/min)
15 min	1.32	1.31	0.46
30 min	2.65	2.58	0.50
1 hr	5.29	5.02	0.50
2 hr	10.6	9.54	0.50
5 hr	26.4	20.6	0.50
10 hr	52.7	32.7	0.50
1 day	125	46.1	0.50
2 day	248	49.1	0.50

The results show that the taggant concentrations inside a briefcase are at least in the ppb range. Thus, if the taggant vapors are diluted by a factor of 1000 by some sort of briefcase/suitcase sampling scheme, it is possible to detect the taggant vapors with a real-time continuous instrument that has a taggant detectability of one part per trillion. (The dilution factor will be greater for a severe barrier enclosure than for a slight one.) This calculation neglects the effects of taggant adsorption onto material that might be present in the briefcase. But, this can be neglected if the taggants are sufficiently volatile. Using the U.S. Customs Service Baggage Examiner and the Brookhaven continuously operating perfluorocarbon sniffer (COPS) as described in Section 3, this scenario has been characterized. Appendix D.1 and D.2 give the full details of these investigations conducted with luggage and vapor tagged simulated explosives.

(2) Volume Sampling (A moderately sized room). For this scenario, a tagged explosive contained within a briefcase-size barrier is placed into a moderately sized room (10 x 20 x 8 ft or 1600 ft^3). The calculation is performed assuming various time delays ranging from zero to 24 hours between the introduction of the tagged explosive into the briefcase and the introduction of the briefcase into the scenario. The calculation is performed with the use of equation (5-32), the barrier with time delay equation and equation (5-30) for the taggant concentration inside the briefcase. Various degrees of barrier airtightness and a ventilation rate corresponding to a complete turnover time of 30 minutes with fresh air are assumed. The calculational results for a severe barrier ($k = 2 \times 10^{-4}$ 1/min) containing a tagged explosives with an emission rate of 1 nl/min are given in Table 5-5.

A typical time delay is from 1/2 to 1 hour. As shown in the table, all of the taggant concentrations are within the detectability of a concentrating taggant detection system -- greater than parts per 10^{17}.

Table 5-5. Scenario Taggant Concentrations in a Moderately Sized Room with a Severe Barrier

Time after Introduction of Barrier into Scenario	Taggant Concentration, pp10^{12} (ppt)						
	No Barrier	Barrier with No Time Delay	Barrier with Time Delay				
			1 hr	2 hr	4 hr	10 hr	24 hr
15 min	0.260	0.0000374	0.000313	0.000589	0.00113	0.00279	0.00658
30 min	0.418	0.000129	0.000572	0.00102	0.00189	0.00456	0.0106
1 hr	0.572	0.000398	0.00100	0.00161	0.00282	0.00646	0.0148
2 hr	0.650	0.00106	0.00174	0.00247	0.00386	0.00792	0.0162
4 hr	0.662	0.00245	0.00315	0.00385	0.00525	0.00944	0.0191
10 hr	0.662	0.00663	0.00732	0.00802	0.00941	0.0136	0.0231
1 day	0.662	0.0163	0.0169	0.0176	0.0190	0.0231	0.0325
2 day	0.662	0.0325	0.0332	0.0338	0.0352	0.0392	0.0483
Barrier Taggant Concentration at Time of Introduction into the Scenario		0	5290	10,600	21,100	52,700	125,500

Emission Rate of Tagged Cap = 1×10^{-9} l/min
Volume of the Scenario = 1600 ft^3
Volume of the Barrier Enclosure = 0.4 ft^3
Barrier Parameter = 2×10^{-4} l/min
Turnover Time = 30 min
Ventilation Rate = 53.3 ft^3/min

The greater the time delay the faster the initial approach to the taggant steady-state concentration.

Table 5-6 presents the results for the same briefcase scenario assuming moderate airtightness and all other conditions being the same as considered in Table 5-5. In this instance, the scenario taggant concentrations are almost in the range of the real-time continuous taggant detectors -- a part per 10^{12}. They would be in the range if the taggant emission rate from the cap were a factor of 2 or 3 higher (2 or 3 nl/min -- the scenario taggant concentrations are proportional to the taggant emission rates of the tagged explosives).

Table 5-7 lists the results for the briefcase scenario with a slight airtightness, again assuming all other conditions are the same as in Tables 5-5 and 5-6. The taggant concentrations are also approximately in the range for real-time continuous taggant detector, and in this case, the rate of taggant release is as though there were no barrier present, especially when the time delay is greater than an hour.

In the three briefcase examples, the taggant concentrations in the scenarios will approach the steady-state value of 0.66 ppt given sufficient time. This steady-state concentration is equal to R_{cap}/R_{ex}. In all detection scenarios, it is not possible to change R_{cap}, the taggant emission rate from the explosive, but it is possible to change R_{ex}, the ventilation rate of the scenario. Thus a very good detection strategy is to shut off the ventilation system in the area where tagged explosives are being attempted to be detected. The scenario taggant concentration will then be higher than those already given in the examples because the taggant emission rate from the barrier enclosure will approach a constant rate when the ventilation of the scenario is stopped.

Table 5-6. Scenario Taggant Concentrations in a Moderately Sized Room with a Moderate Barrier

Time after Introduction of Barrier Into Scenario	Taggant Concentration, pp 10^{12} (ppt)						
	No Barrier	Barrier With No Time Delay	Barrier with Time Delay				
			1 hr	2 hr	4 hr	10 hr	24 hr
15 min	0.260	0.00370	0.0295	0.0527	0.0924	0.172	0.240
30 min	0.418	0.0127	0.0535	0.0902	0.153	0.278	0.387
1 hr	0.572	0.0382	0.0919	0.140	0.223	0.387	0.531
2 hr	0.650	0.910	0.147	0.196	0.282	0.458	0.607
4 hr	0.662	0.204	0.250	0.291	0.362	0.503	0.626
10 hr	0.662	0.420	0.444	0.466	0.504	0.578	0.643
1 day	0.662	0.607	0.613	0.618	0.626	0.643	0.658
2 day	0.662	0.658	0.658	0.659	0.659	0.661	0.662
Barrier Taggant Concentration at Time of Introduction into the Scenario		0	5020	9530	17,300	32,700	46,100

Emission Rate of Tagged Cap = 1×10^{-9} l/min
Volume of the Scenario = 1600 ft^3
Volume of the Barrier Enclosure = 0.4 ft^3
Barrier Parameter = 2×10^{-2} l/min
Turnover Time = 30 min
Ventilation Rate = 53.3 ft^3/min

Table 5-7. Scenario Taggant Concentrations in a Moderately Sized Room with a Slight Barrier

Time after Introduction of Barrier into the Scenario	Taggant Concentration, pp 10^{12} (ppt)				
	No Barrier	Barrier with No Time Delay	Barrier with Time Delay		
			1 hr	2 hr	4 hr
15 min	0.260	0.178	0.260	0.260	0.260
30 min	0.418	0.363	0.418	0.418	0.418
1 hr	0.572	0.552	0.572	0.572	0.572
2 hr	0.650	0.647	0.650	0.650	0.650
4 hr	0.662	0.662	0.662	0.662	0.662
Barrier Taggant Concentration at Time of Introduction into the Scenario		0	500	500	500

Emission Rate of Tagged Cap = 1×10^{-9} 1/min
Volume of the Scenario = 1600 ft^3
Volume of the Barrier Enclosure = 0.4 ft^3
Barrier Parameter = 2 1/min
Turnover Time = 30 min
Ventilation Rate = 53.3 ft^3/min

(3) Volume Sampling (A DC-8 Aircraft). For the volume sampling scenario where the detection of a tagged explosive had been placed in an aircraft, the calculation is performed for a tagged explosive (with a taggant emission rate of 1 nl/min) placed within a briefcase-sized barrier with varying degrees of barrier airtightness. Table 5-8 contains the results for a barrier with an airtightness of the order of a pipebomb or similar enclosure. In almost all examples of time delay and time after placing the explosive on the aircraft, it is nearly impossible to detect the taggant because the taggant concentrations are of the order of the ambient taggant concentrations assuming an ambient concentration of 0.03 ppt for PDCH. If the taggant emission rate were increased by two orders of magnitude, it would be conceivable to detect the explosives in this scenario with a concentrating nonreal-time taggant detection system.

The results for a barrier of moderate airtightness (such as a very tightly sealed box) is given in Table 5-9. In this case, it is possible to detect the explosives with a concentrating detection system. If the taggant emission rate were increased by two orders of magnitude, it would be possible to detect the taggant with a real-time detection instrument.

The results for a slight barrier (briefcases, suitcases, etc.) are presented in Table 5-10. Here the barrier provides a negligible attenuation on the taggant emission rate, and it is possible to detect the tagged explosive within 5 minutes with the use of a concentrating instrument.

As in the other large volume detection scenario, if the ventilation rate could be reduced, the taggants could be detected more easily, because the taggant concentrations would be increased. The results predicted have been corroborated by a series of limited field tests

Table 5-8. Taggant Concentrations in a DC-8 from a Tagged Explosive Enclosed in a Severe Barrier

Time after Introduction of Barrier into Scenario	Taggant Concentration, parts per part						
		Barrier With	Barrier with Time Delay				
	No Barrier	No Time Delay	1 hr	2 hr	4 hr	10 hr	24 hr
5 min	1.47(-14)	7.03(-19)*	1.63(-17)	3.19(-17)	6.27(-17)	1.56(-16)	3.70(-16)
10 min	2.33(-14)	2.41(-18)	2.70(-17)	5.17(-17)	1.01(-16)	2.47(-16)	5.86(-16)
15 min	2.83(-14)	4.70(-18)	3.46(-17)	6.46(-17)	1.24(-16)	3.02(-16)	7.14(-16)
30 min	3.39(-14)	1.31(-17)	4.90(-17)	8.50(-17)	1.56(-16)	3.70(-16)	8.64(-16)
1 hr	3.52(-14)	3.16(-17)	6.88(-17)	1.06(-16)	1.80(-16)	4.03(-16)	9.15(-15)
2 hr	3.57(-14)	6.89(-17)	1.06(-16)	1.44(-16)	2.18(-16)	4.40(-16)	9.54(-16)
5 hr	3.53(-14)	1.80(-16)	2.17(-16)	2.54(-16)	3.28(-16)	5.50(-16)	1.06(-15)
12 hr	3.53(-14)	4.41(-16)	4.78(-16)	5.15(-16)	5.88(-16)	8.08(-16)	1.32(-15)
Barrier Taggant Concentration at Time of Introduction into the Scenario		0	5.29(- 9)	10.6(- 9)	21.1(- 9)	52.7(- 9)	12.5(- 8)

Taggant Emission Rate = 1×10^{-9} 1/min
Volume of the DC-8 = 9,300 ft^3
Volume of the Barrier Enclosure = 0.4 ft^3
Barrier Parameter = 2×10^{-4} 1/min
Turnover Time = 9.3 min
Ventilation Rate = 1000 ft^3/min
*7.03(-19) = 7.03×10^{-19}

Table 5-9. Taggant Concentrations in a DC-8 from a Tagged Explosive Enclosed in a Moderate Barrier

Time after Introduction of Barrier into Scenario	Taggant Concentration, parts per part						
	No Barrier	Barrier With No Time Delay	Barrier with Time Delay				
			1 hr	2 hr	4 hr	10 hr	24 hr
5 min	1.47(-14)	7.03(-17)*	1.54(-15)	2.85(-15	5.12(-15)	9.62(-15)	1.35(-14)
10 min	2.33(-14)	2.39(-16)	2.55(-15)	4.62(-15)	8.20(-15)	1.53(-14)	2.14(-14)
15 min	2.83(-14)	4.66(-16)	3.26(-15)	5.76(-15)	1.01(-15)	1.86(-14)	2.61(-14)
30 min	3.39(-14)	1.29(-15)	4.56(-15)	4.50(-15)	1.26(-14)	2.26(-14)	3.13(-14)
1 hr	3.52(-14)	3.02(-15)	6.26(-15)	9.14(-15)	1.42(-14)	2.41(-14)	3.28(-14)
2 hr	3.57(-14)	6.25(-15)	9.17(-15)	1.18(-14)	1.63(-14)	2.52(-14)	3.30(-14)
5 hr	3.53(-14)	1.42(-14)	1.63(-14)	1.82(-14)	2.15(-14)	2.80(-14)	3.37(-14)
12 hr	3.53(-14)	2.52(-14)	2.67(-14)	2.71(-14)	2.87(-14)	3.18(-14)	3.45(-14)
Barrier Taggant Concentration at Time of Introduction into the Scenario		0	5.02(- 9)	9.53(- 9)	1.73(- 8)	3.27(- 8	4.61(- 8)

Taggant Emission Rate = 1×10^{-9} 1/min
Volume of the DC-8 = 9,300 ft^3
Volume of the Barrier Enclosure = 0.4 ft^3
Barrier Parameter = 2×10^{-2} 1/min
Turnover Time = 9.3 min
Ventilation Rate = 1000 ft^3/min
*7.03(-17) = 7.03×10^{-17}

Table 5-10. Taggant Concentrations in a DC-8 from a Tagged Explosive Enclosed in a Slight Barrier

Time after Introduction of Barrier into the Scenario	Taggant Concentration, parts per part				
	No Barrier	Barrier With No Time Delay	Barrier with Time Delay		
			15 min	30 min	1 hr
5 min	1.47(-14)	5.30(-15)*	1.39(-14)	1.47(-14)	1.47(-14)
10 min	2.33(-14)	1.39(-14)	2.25(-14)	2.33(-14)	2.33(-14)
15 min	2.83(-14)	2.12(-14)	2.77(-14)	2.83(-14)	2.83(-14)
30 min	3.39(-14)	3.20(-14)	3.38(-14)	3.39(-14)	3.39(-14)
1 hr	3.52(-14)	3.52(-14)	3.52(-14)	3.52(-14)	3.52(-14)
2 hr	3.53(-14)	3.53(-14)	3.53(-14)	3.53(-14)	3.53(-14)
Barrier Taggant Concentration at Time of Introduction into the Scenario		0	0.46(-9)	0.50(-10)	0.50(-10)

Taggant Emission Rate = 1×10^{-9} l/min
Volume of the DC-8 = 9,300 ft^3
Volume of the Barier Enclosure = 0.4 ft^3
Barrier Parameter = 2 l/min
Turnover Time = 9.3 min
Ventilation Rate = 1000 ft^3/min
*5.30(-15) = 5.03×10^{-15}

using a DC-9 and Boeing 727 aircraft with vapor tagged explosive simulants on board. Using a concentrating analysis scheme, vapor taggants were readily detectable. Appendix D.3 and D.4 provide full descriptions of these limited field tests.

The experimental program effort required the quantative analysis of the proposed taggants in air at concentrations of 1×10^{-12} to 1×10^{-15} parts per part. This was performed by gas chromatography. Aliquots of air samples containing the vapor taggant were injected into a nitrogen carrier stream by a sampling value. The stream was subsequently mixed with hydrogen in order to prepare a 30 percent hydrogen gas mixture and passed through a 3 inch length of 5 percent Palladium on 4A Molecular sieve column (Dietz et al., 1978a). The column combusted the O_2 and ambient Freons present in the air sample to H_2O and HF; otherwise these would interfer with the electron capture detector. The column temperature was set at approximately 180°C, sufficient to combust the O_2 and Freons, but not the vapor taggants. The H_2O and HF were subsequently removed by a 3-foot length of a Permapure permeation drier, maintained at 86°C, in order to prevent H_2O condensation in the drier. Any residual H_2O and HF was removed by a column of Ascarite. Subsequently, the sample is chromatographed on a column of Porosil F with the chromatographic parameters listed in Table 5-11 for the respective taggants and detected by a Ni^{63} ECD at 200°C. The ECD output was displayed on a strip chart recorder and integrated by an electronic integrator. Such analyses are standardized by either of two methods. An air standard is made for the more volatile taggants (e.g., PDCB, PMCH, and PDCH) and calibrated by chromatographic analysis against the liquid taggant using a thermal conductivity detector. A tagged blasting cap prepared with those taggants which are less volatile provided a calibrated source of vapor taggant, with blasting cap taggant emission rate being determined gravimetrically over a several month period.

Table 5-11. Chromatographic Parameters for the Various Taggants

Taggant	Column Temperature* (°C)	Column Length (ft)	Retention Time (sec)	Relative ECD Response** (PDCB = 1)
PDCB	40	3	33	1
PMCH	40	3	34	0.46
PDCH	40	3	38	1.24
HFB	70	3	77	4.75
OFT	100	3	38	12.5
DFBP	70	3	60	1.21
OFN	200	1	126	2.04

*80/100 mesh Porosil F in 1/8-in. S.S. tubing
**Ni^{63} electron capture detector at 200°C with a 30% H_2/70% N_2 carrier gas at 20 ml/min.

(4) Summary. Several general and specific conclusions regarding taggant concentration in various scenarios can be made.

1. The scenario taggant concentrations will always approach a steady--state concentration of R_{cap}/R_{ex}, the taggant emission rate from the tagged explosive divided by the ventilation rate of the scenario, regardless of any barrier. The effect of a barrier is to delay the approach to this steady-state concentration. The more severe the barrier, the longer this delay.

2. The effect of a time interval between the introduction of the tagged explosive into the barrier enclosure and the barrier enclosure into the scenario is to hasten the initial approach to the steady-state concentration. The longer the time interval, the greater is the rate of initial increase in the scenario taggant concentration.

3. The taggant concentration within briefcases/suitcases from a 1-nl/min tagged explosive is of the order of parts per 10^9 for almost all degrees of briefcase/suitcase barrier airtightness. This will allow real-time continuous detection of the taggants with a sampling system tolerating a dilution factor up to 1000.

4. The scenario taggant concentrations in a moderate size room is sufficient to detect a 1-nl/min taggant emitting explosive with a concentrating detection scheme within 15 minutes after introduction of a severe barrier enclosure containing the explosive which had been placed into it 1 hour earlier. A moderate barrier will almost allow real-time continuous detection under the same circumstances.

5. The scenario taggant concentrations in a DC-8 will allow the detection of a 1-nl/min tagged explosive contained in a slight to

moderate airtightness barrier within 15 minutes using a concentrating non-real-time taggant detection system.

C. EXPERIMENTAL RESULTS: TAGGANT CONCENTRATION FROM BARRIER-ENCLOSED VAPOR TAGGED EXPLOSIVES

The rate of taggant release from a barrier-enclosed tagged explosive is dependent on two parameters as has been described in the previous section. Specifically these are β -- the ratio of the barrier constant k to the scenario ventilation rate (R_{ex}) -- and γ -- the ratio of the barrier enclosed volume (V_{en}) to the volume of the scenario (V_{ch}). Of these, only k, the barrier constant, is unknown for various common barriers, such as suitcases, boxes, and plastic bags, in which tagged explosives might be enclosed. An order of magnitude estimate of the barrier constant can be made with the use of equations (5-26) and (5-27), which are derived for the microcrack and permeation mechanisms of taggant emission through a barrier. In this section, the experimental determination of the barrier constants k for a range of various barriers (specifically, a suitcase, an attache case, an average sized box containing styrofoam chip filler, a 1-gallon paint can, a heat-sealed plastic bag, and a zip-lock plastic bag) is described. The barriers were chosen as an average representation of barriers which might be used to contain bombs.

The experimental procedure was designed to use equation (5-22) in the analysis of the experimental results. This was accomplished by enclosing a constant source of vapor taggant in one of the barriers which in turn was placed immediately in a scenario, a 422-liter chamber, with a controlled ventilation rate. The scenario taggant concentration was then recorded as a function of the elapsed time. The constant source of vapor taggant was a tagged blasting cap with a predetermined taggant emission rate. The tagged caps were sufficiently old (prepared

months previously) and had a nearly constant emission rate over the 2- to 3-day experimental period. Before the start of each experiment, it was ascertained that no initial taggant concentration existed inside either the scenario or the barrier in order that the conditions for which equation (5-22) was derived would be satisfied. With this procedure, the barrier constant for each barrier can be extracted from the results of the experiment.

The vapor taggants used, PDCB, PMCH, and PDCH, were those which had a negligible barrier adsorption loss (see Section A above) otherwise this would unnecessarily complicate the experimental results. For each experiment, the three taggant sources were enclosed in the barrier to be tested, and the scenario taggant concentrations were chromatographically obtained (periodically) for the three taggants via sampling of the scenario ventilation exhaust. For comparison, the resulting scenario taggant concentrations for each barrier-enclosed taggant source were compared against the no barrier situation. The time dependence of the scenario taggant concentration for the no barrier experiment is an exponential dilution, (as has been derived in equation 5-10).

$$C(t) = C(\infty)\left[1-\exp(-t/t_v)\right] \qquad (5\text{-}35)$$

in which $C(\infty) = R_{cap}/R_{ex}$

and $t_v = V_{ch}/R_{ex}$.

where: $C(\infty)$ = the steady-state taggant scenario concentration and
t_v = the chamber turnover time.

A comparison between the barrier and no barrier parts of the experiment provided an immediate indication of whether there was any significant barrier effect for each tested barrier.

The experimental results were normalized in the same manner as the results of the adsorption experiment. The scenario taggant concentrations C(t) were normalized by dividing by the taggant steady-state concentration $C(\infty)$, and the elapsed time was normalized by dividing by the scenario turnover time t_v. These normalizations allowed direct comparison of the results between the various barriers.

1. Styrofoam-Filled Box

Several vapor tagged blasting caps were placed inside a 7- x 9- x 12-in. box filled with a polystyrene chip packing material. The box barrier was then sealed securely with sealing tape and placed inside the scenario chamber. The caps provided the source of PDCB, PMCH, and PDCH vapor taggants. The results are displayed in Figures 5-16 through 5-18 for each of the three taggants. As is evidenced by the coincidence of the no-barrier and barrier results, it is seen that there is a negligible barrier effect exerted by the styrofoam-filled box.

The barrier constant k for this barrier is very large because this is a negligible barrier -- the box is not airtight. The precision of the experimental results does not allow a numerical value for the barrier constant to be extracted. Therefore, k can be said simply to be large (i.e., infinite) which signifies that this barrier is equivalent to the no-barrier situation which is clearly indicated in Figures 5-16 through 5-18.

2. Suitcase

A zippered cloth suitcase (22 x 8 x 16 in.) was examined in a similar manner. This is the same suitcase which had been used in the adsorption studies. As is shown in Figures 5-19 through 5-21, the suitcase has a negligible barrier effect for the three taggants. Higher

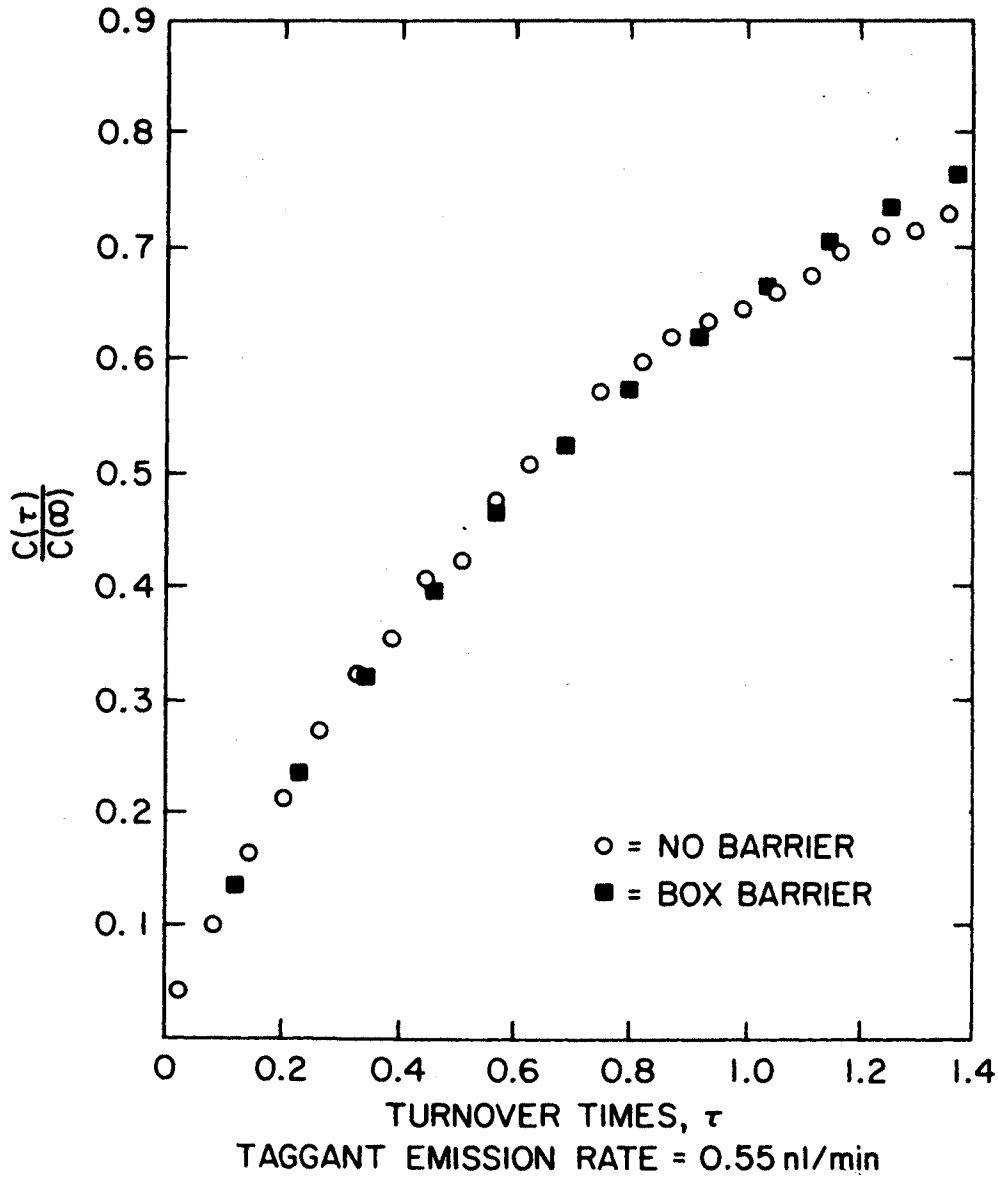

Figure 5-16. Box with Styrofoam Packing Barrier, PDCB Taggant

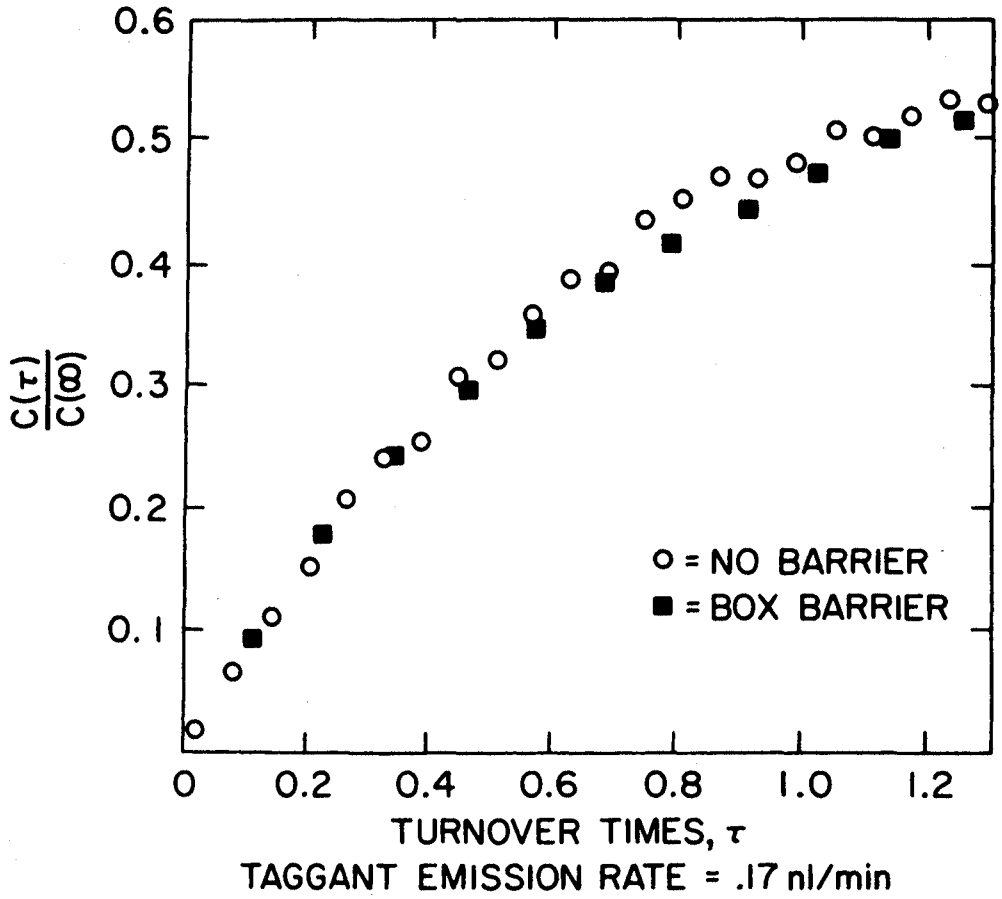

Figure 5-17. Box with Styrofoam Packing Barrier, PMCH Taggant

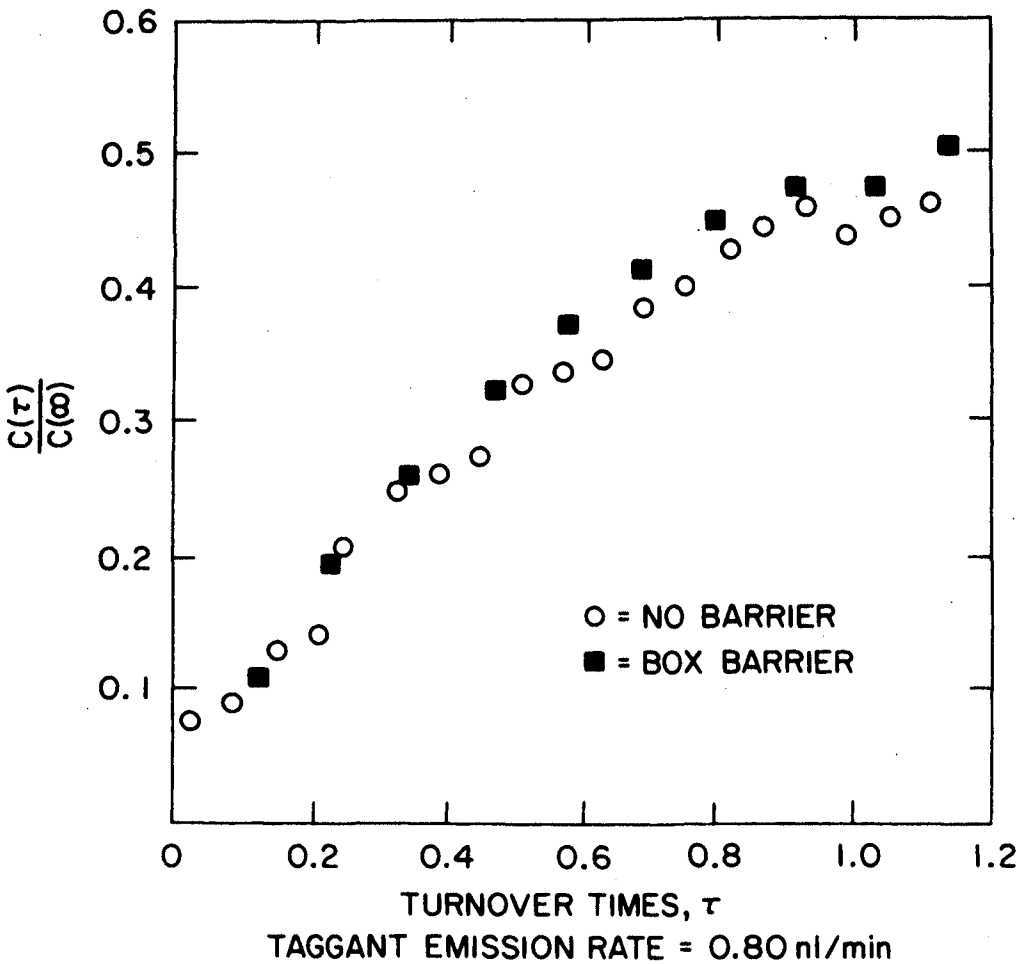

Figure 5-18. Box with Styrofoam Packing Barrier, PDCH Taggant

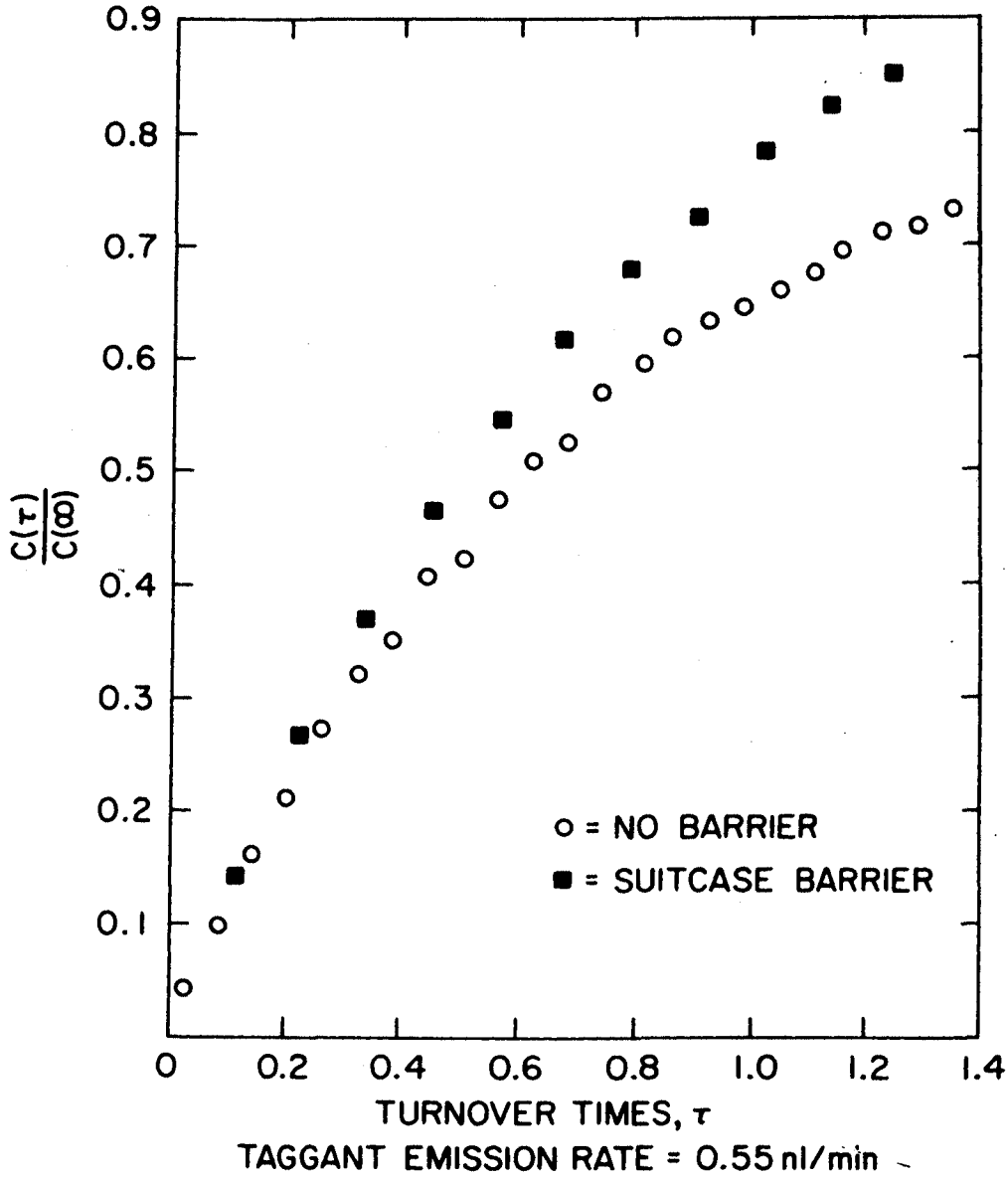

Figure 5-19. Suitcase Barrier, PDCB Taggant

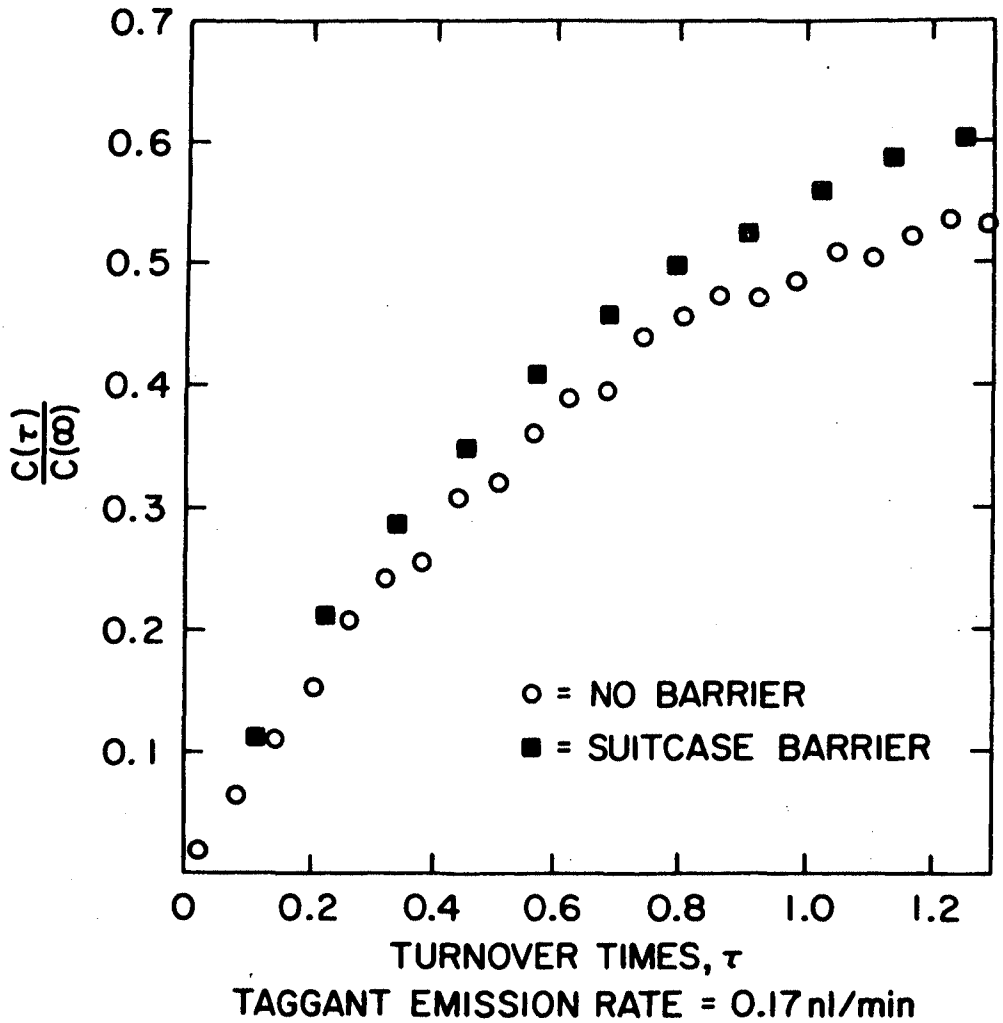

Figure 5-20. Suitcase Barrier, PMCH Taggant

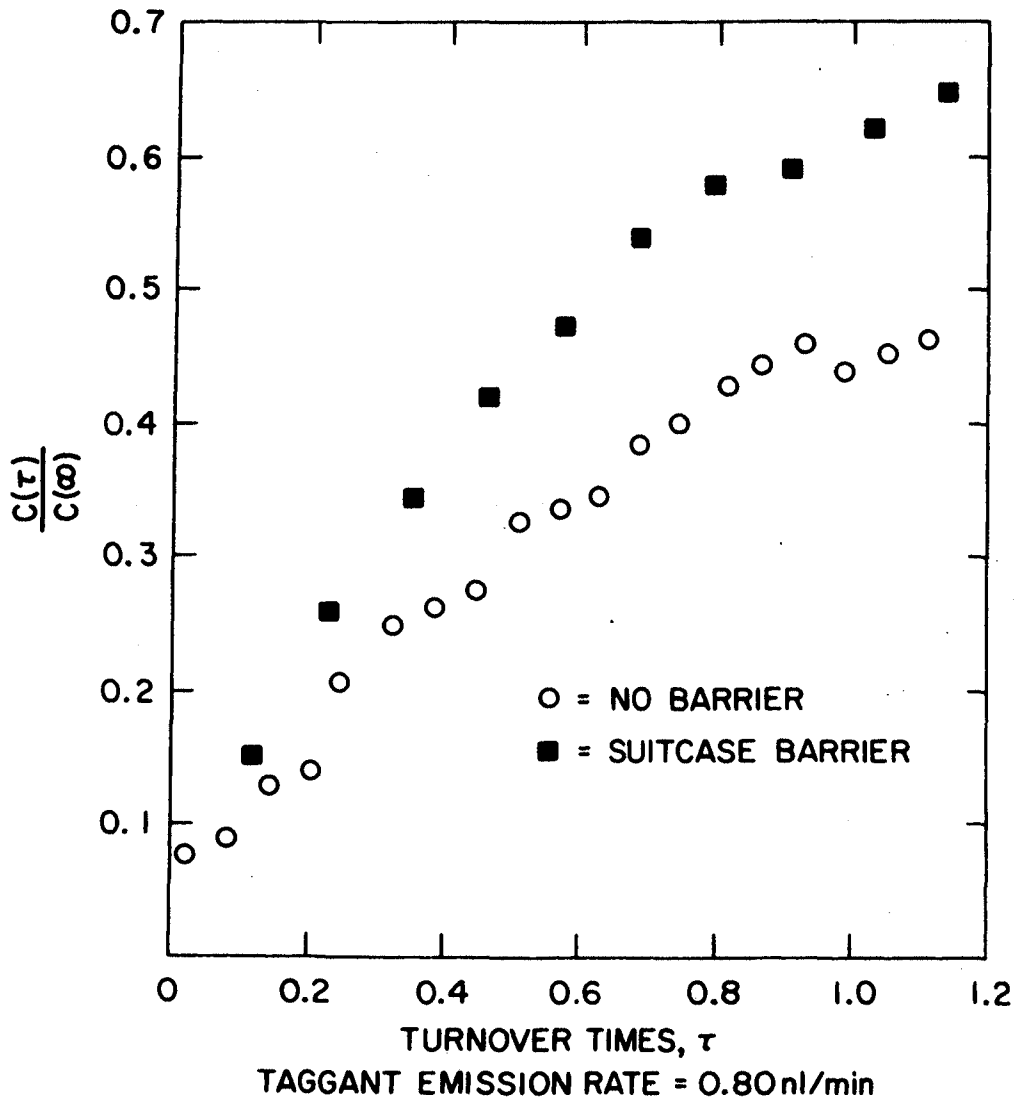

Figure 5-21. Suitcase Barrier, PDCH Taggant

taggant concentrations for all three taggants for the barrier situation as compared to the no-barrier situation are also shown in these figures, even though this is theoretically impossible. This is due, as in similar instances in the adsorption experiments, to a difference in the chamber ventilation rate between the no-barrier and barrier parts of the experiment. Although an attempt was made to use a constant ventilation rate in both parts of the experiments, the ventilation rate changed during the experiment because of insufficient flow regulation over the 2- to 3-day period. A decrease in the chamber ventilation rate proportionally increased the chamber taggant concentrations as was the case for the barrier case in this experiment. Nonetheless, the results indicate a negligible barrier effect exerted by the suitcase barrier. As in the sealed box barrier, the barrier constant for the suitcase is very large and can be assigned as infinity.

3. Heat-Sealed Polyethylene Bag

The PDCB, PMCH, and PDCH taggant sources were placed inside a 1- x 1-ft polyethylene bag which was heat-sealed several times with a small, portable heat sealer. As the results shown in Figures 5-22 to 5-24 indicate, the polyethylene bag is also a negligible barrier toward taggant release. The lack of airtightness of the heat-sealed bag is due either to imperfect heat sealing which leaves small air gaps or to small pinhole leaks. The barrier constant k for the heat-sealed polyethylene bag is very large, and is set at infinity, similar to the two other negligible barriers.

4. Attache Case

The three taggant sources were placed inside an empty attache case (4-1/2 x 17-1/2 x 13 in.) which was placed in the experimental chamber. The resulting taggant concentrations, as measured in the chamber, are

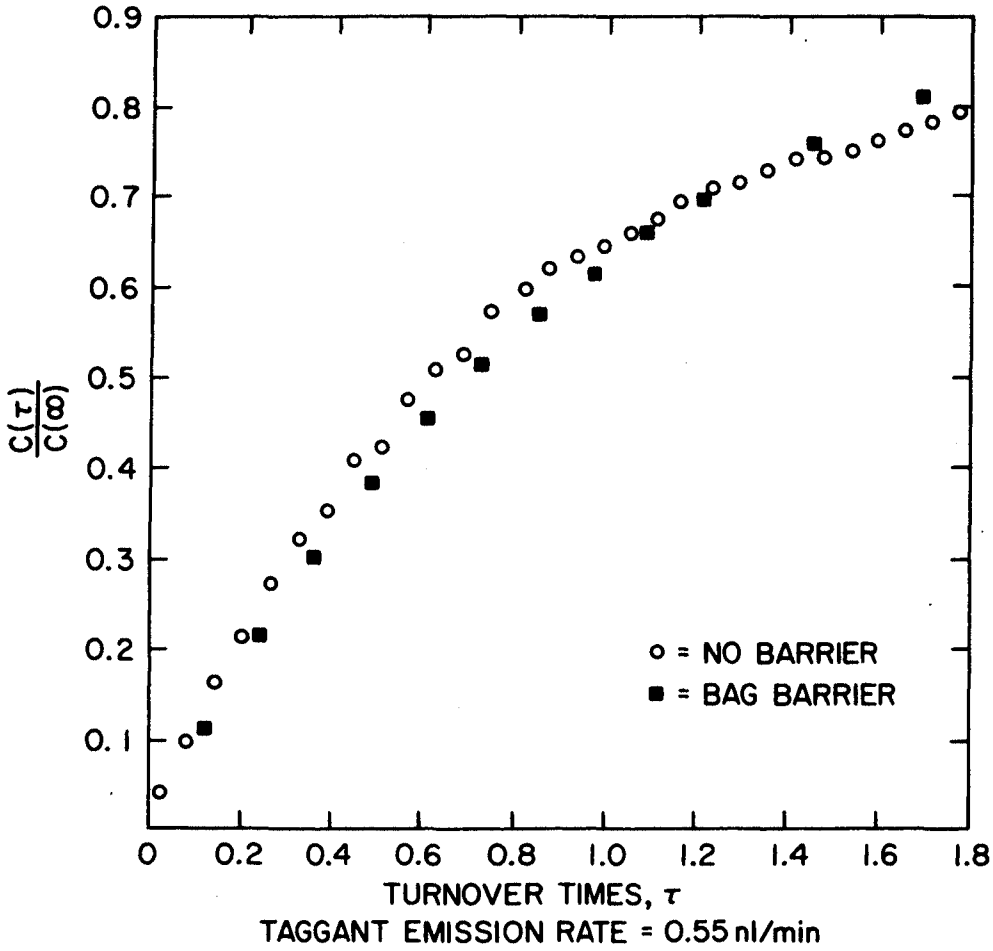

Figure 5-22. Heat Sealed Polyethylene Bag Barrier, PDCB Taggant

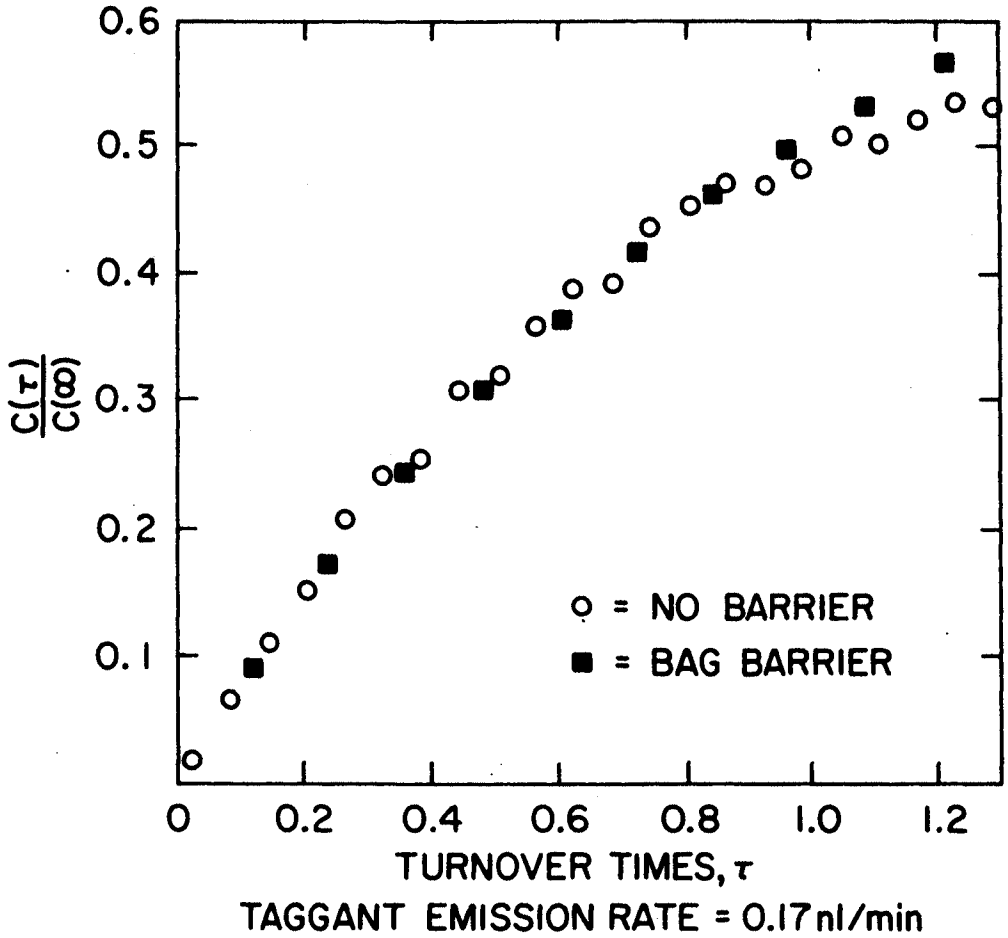

Figure 5-23. Heat Sealed Polyethylene Bag Barrier, PMCH Taggant

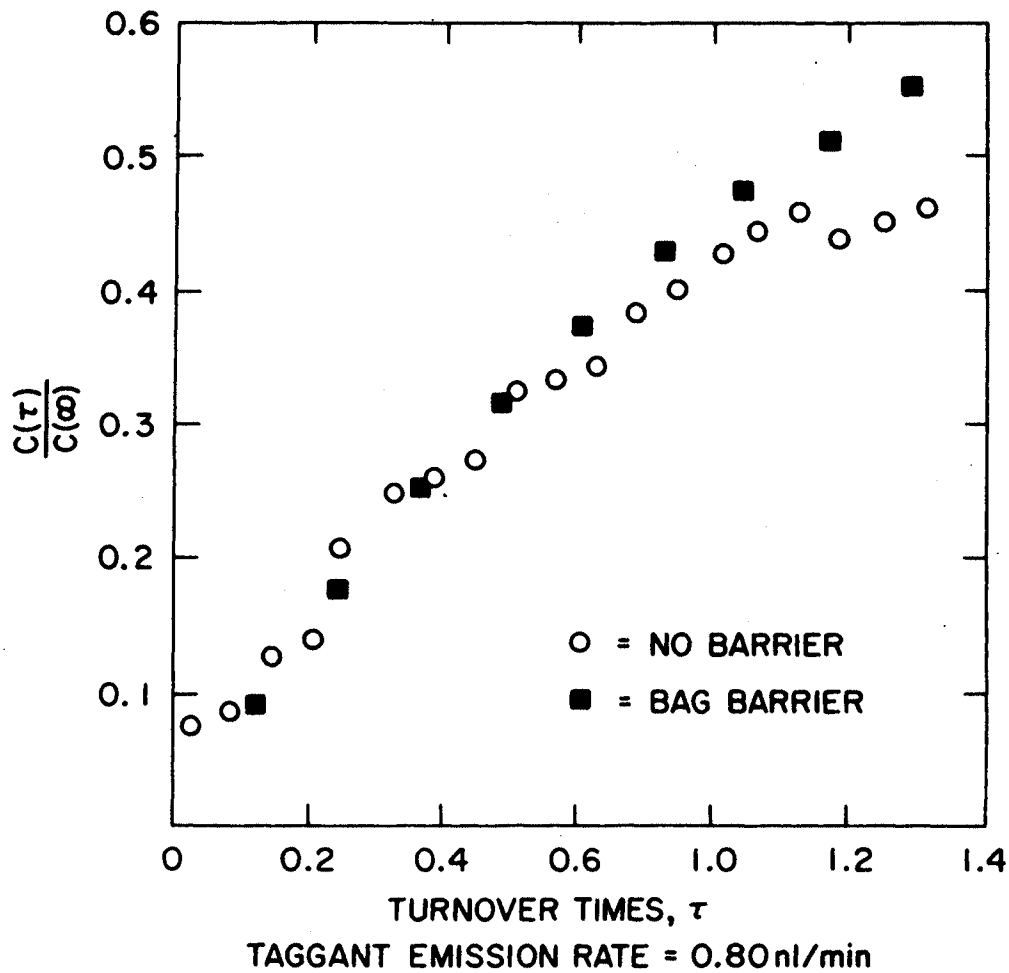

Figure 5-24. Heat Sealed Polyethylene Bag Barrier, PDCH Taggant

shown in Figures 5-25 to 5-27. The results indicate a lack of airtightness for the attache case barrier, so much that the attache case can be considered as having no barrier effect at all. Thus, the barrier constant k for the attache case is very large and is set at infinity.

The chamber ventilation rates fluctuated during this experiment due to a lack of sufficient controls. This is clearly evident in Figures 5-26 and 5-27, which show that the ventilation rate would decrease for several hours and increase the chamber taggant concentrations. Later, the ventilation rate returned to its earlier value with the consequent return of the taggant concentrations to their expected values. The source of the ventilation fluctuation was the in-house compressed air used to ventilate the chamber which varied in its supply pressure.

5. Paint Can (1-gallon)

The three taggant sources were placed inside a 1-gallon paint can with the lid tightly closed and the paint can was placed inside the experimental chamber. The resulting taggant concentrations, (Figures 5-28 to 5-30), indicate a significant barrier effect imposed by the paint can. Note in these figures that the vertical scale has been expanded by a factor of 10 and that the no-barrier taggant concentration results are entirely off-scale.

The barrier constant k was determined to be 1.2×10^{-4} l/min with the use of the theoretical barrier model. The resulting agreement, as shown in Figures 5-28 through 5-30 as a solid line, is quite good for all three taggants. The cyclical perturbation in the measured taggant concentrations is the result of a slow expansion and contraction of the paint can which allowed more or less taggant to be emitted from the paint can. The expansions and contractions were a result of a temperature fluctuations in the experimental room between day and night.

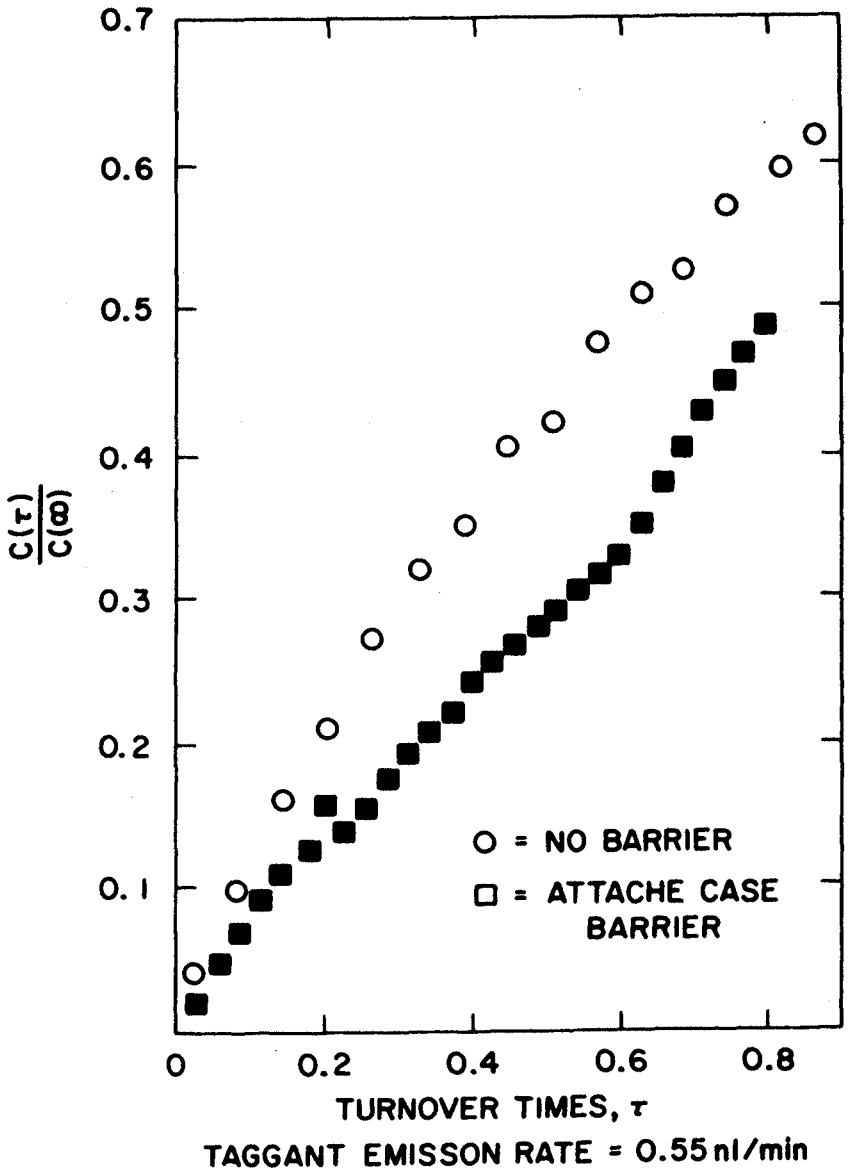

Figure 5-25. Attache Case Barrier, PDCB Taggant

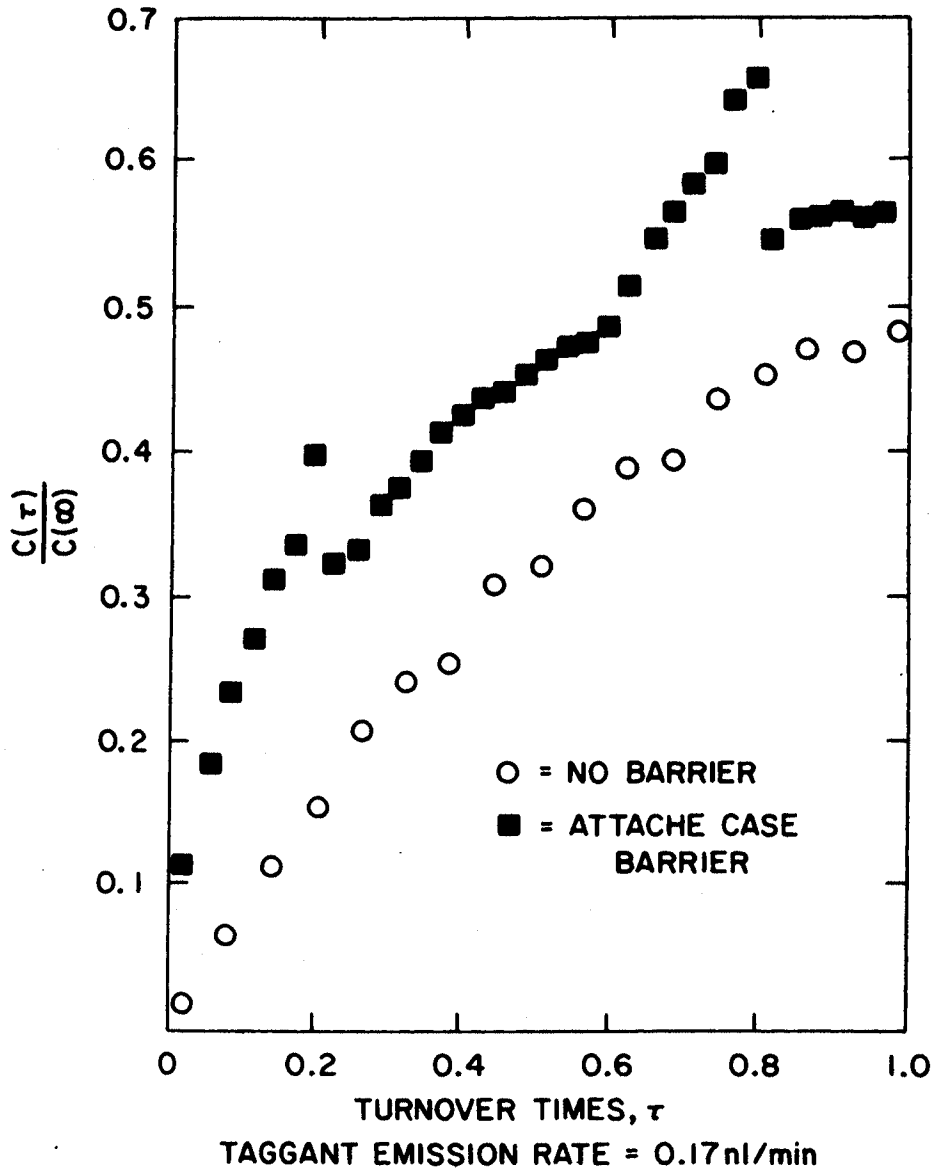

Figure 5-26. Attache Case Barrier, PDCH Taggant

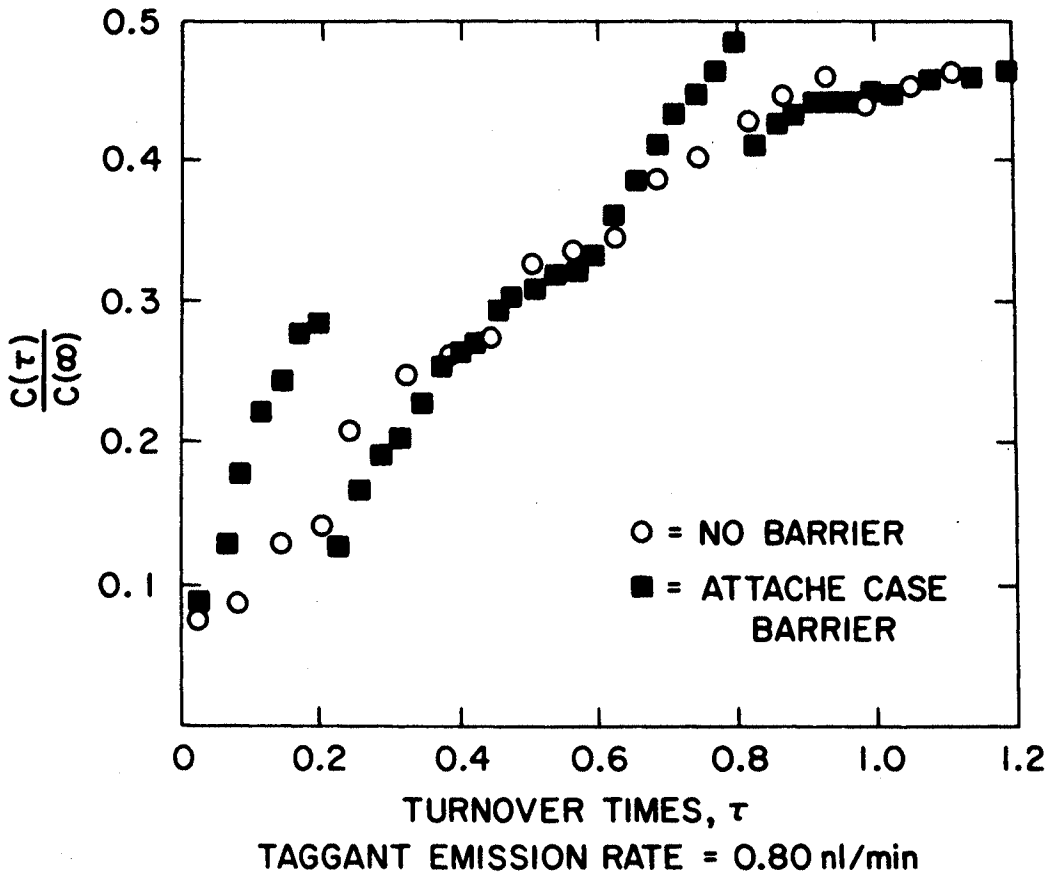

Figure 5-27. Attache Case Barrier, PDCH Taggant

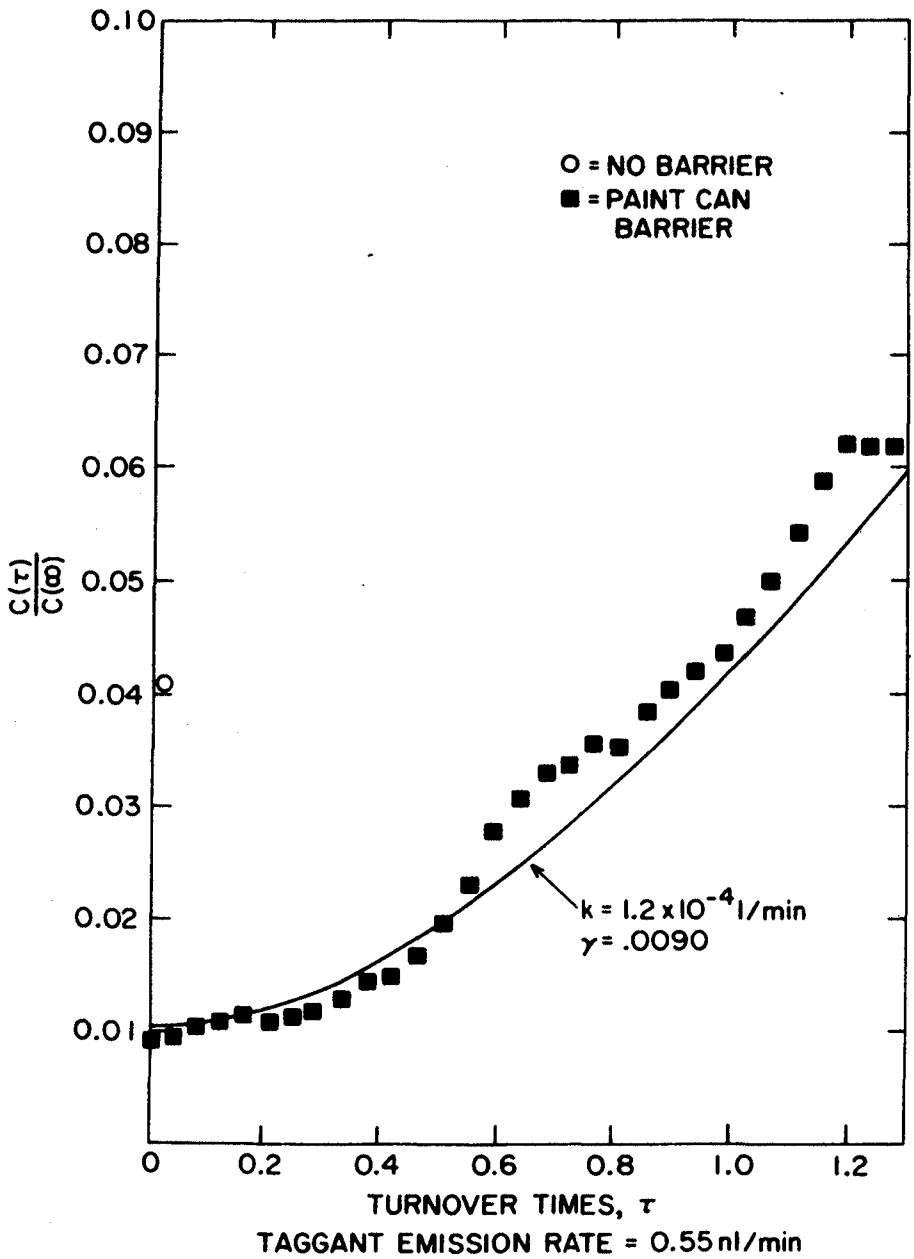

Figure 5-28. Paint Can Barrier, PDCB Taggant

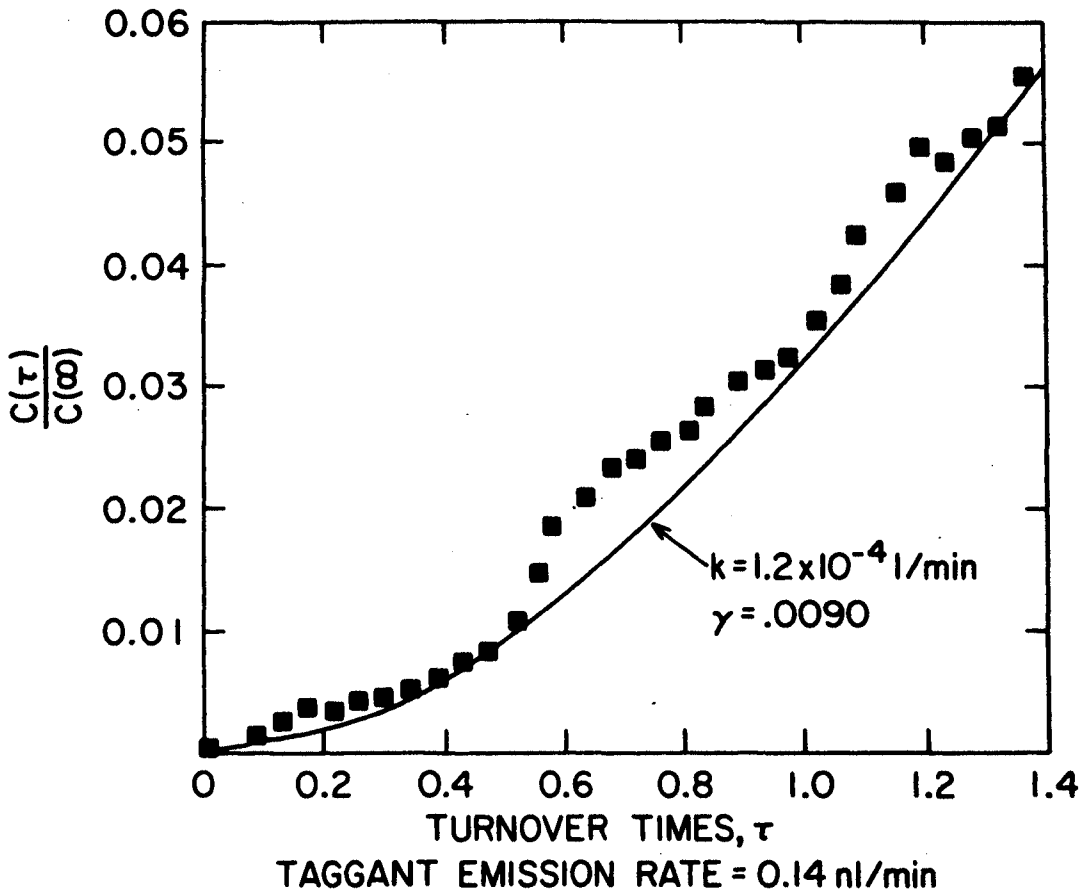

Figure 5-29. Paint Can Barrier, PMCH Taggant

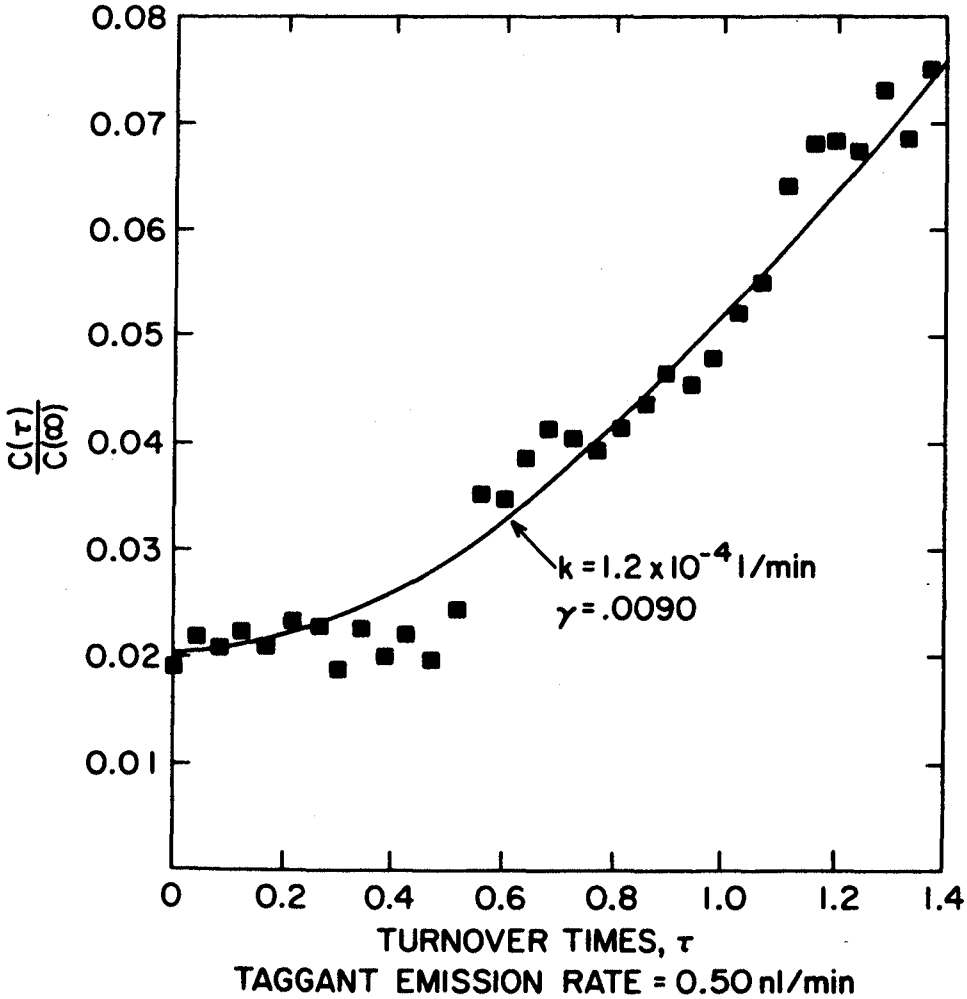

Figure 5-30. Paint Can Barrier, PDCH Taggant

The significant barrier effect will hinder the detection of vapor tagged explosives placed in the paint can. A calculation of the expected taggant concentration in a moderately sized room from a paint can with enclosed tagged explosive is given in Table 5-5. At one ventilation turnover time, the expected taggant concentration is 0.03 percent of the taggant concentration expected for no barrier.

This experiment was conducted with a new, empty paint can. It could be expected that an emptied, used paint can will not impose as great a barrier effect as a new paint can, most likely it will imposed no barrier. Realistically, a used paint can would be used more often as a barrier than a fresh, new paint can.

6. Zip-Lock Plastic Bag

A PDCB taggant source was placed inside a zip-lock plastic bag which was placed in the experimental chamber. The resulting PDCB chamber concentrations, as displayed in Figure 5-31, indicate a significant barrier effect imposed by the zip-lock plastic bag. The vertical scale of the figure has been expanded by a factor of 10 and the no-barrier PDCB chamber concentrations are off scale. The barrier constant k has been determined to be 2.7×10^{-6} 1/min using the theoretical barrier model. The resulting fit is displayed as a solid line in the figure.

Again, as with the paint can barrier, this severe degree of barrier airtightness will hinder the detection of vapor tagged explosives which are enclosed in zip-lock plastic bags. But, it can be expected that the degree of airtightness of the zip-locked bag will be degraded as the bag enclosed bomb is handled which leads to holes, tears, and other perforations in the bag. Thus, realistically, this is not a severe barrier unless it is handled with extreme care.

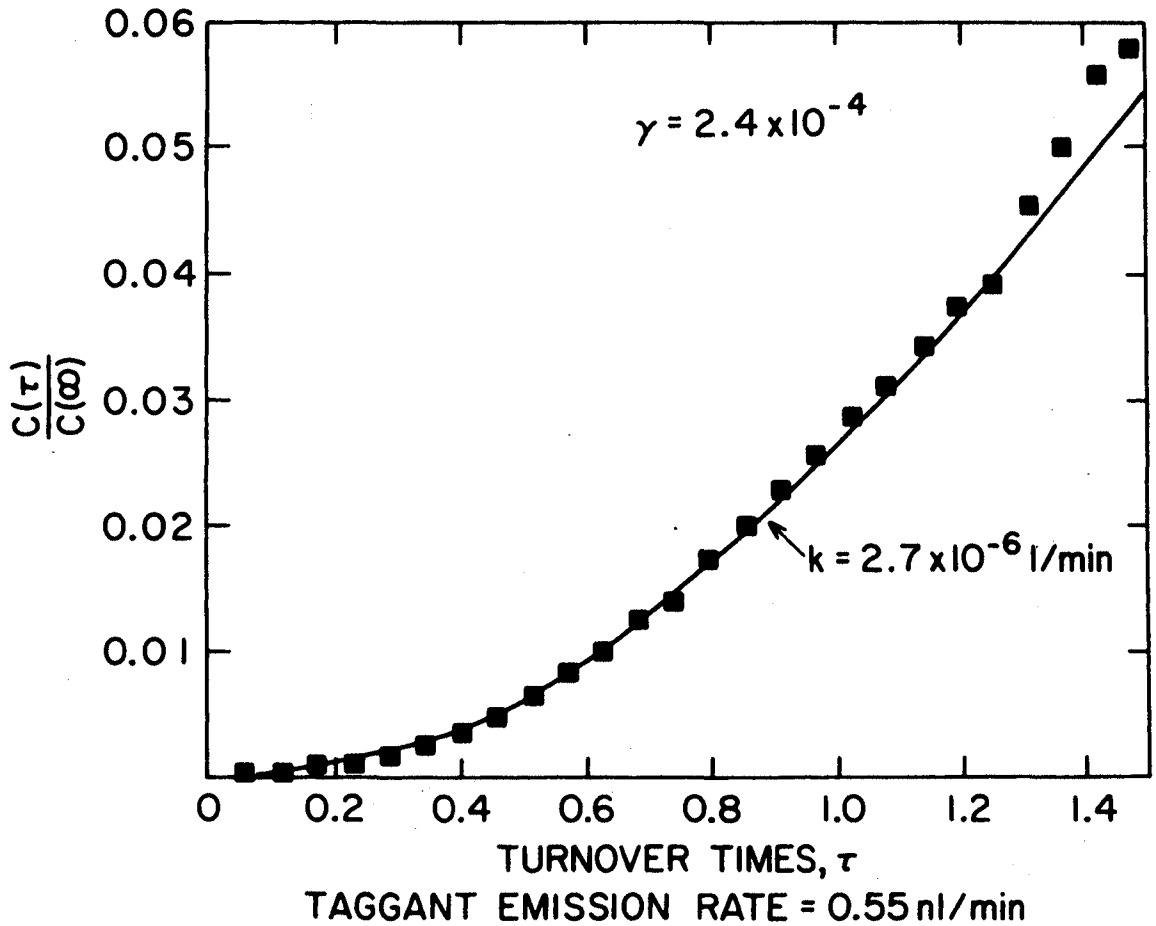

Figure 5-31. Zip-Lock Plastic Bag Barrier, PDCB Taggant

7. Summary

The principal result of these barrier experiments is that most boxes, luggage items, attache cases, and heat-sealed plastic bags will impose no significant barrier to the release of a vapor taggant because of the relative lack of airtightness of these barriers. Two other barriers, a sealed new paint can and a zip-locked plastic bag do have a significant degree of airtightness.

These results have been further corroborated by two field experiments involving the detection of vapor tagged explosives in various luggage items (Dietz et al., 1978; Senum et al., 1979c). The various types of baggage, ranging from soft suitcase to an aluminum suitcase with an O-ring gasket, did not possess any significant degree of airtightness to impede the detection of the vapor taggant.

VI. ENVIRONMENTAL EFFECTS OF VAPOR TAGGANTS

A. TOXICITY OF VAPOR TAGGANTS

Among the criteria established for explosive vapor taggants is the requirement that the taggant be relatively nontoxic. A literature search was made for available toxicity data and it is summarized in Table 6-1 for inhalation toxicity and in Table 6-2 for oral toxicity. The perfluoroalkanes are practically nontoxic, but several fluoroaromatic taggants are toxic, especially PFP (pentafluoropyridine) which was consequently eliminated as a candidate vapor taggant. In separate studies, The Aerospace Corporation has had the Ames mutagen test (Mortelmans and Simmon, 1979; Mortelmans and Marx, 1979) and the acute inhalation toxicity (Dilley, 1979) measured for several perfluorocarbon candidates.

Table 6-1. Inhalation Toxicity Data for Various Vapor Taggants

Taggant	Type*	Value	Reference
HFB	LDLo	11 ppm for 2 hr in mice	Biol.-Med. Nauk, 1965
OFT	LDLo	5000 ppm for 10 min in mice	Anesthesia, 1964
DFCH	LCLo	8000 ppm in mice	Anesthesia, 1964
OFCP	LCLo	30000 ppm in mice	Anesthesia, 1964
PDCH	No effect	4% for 6 hr in rats	Huntingdon, 1970
PMCH	No effect	2% for 6 hr in rats	Huntingdon, 1970
Freon E-1	No effect	3.3% for 4 hr in rats	duPont, 1968c

* LDLo = Lowest Published Lethal Dose
LCLo = Lowest Published Lethal Concentration

Table 6-2. Oral Toxicity Data for Various Vapor Taggants

Taggant	Oral LD50 White Mice	Toxicity rating	Reference
OFN	670 mg/kg	moderate toxic	Lapik and Zimina, 1967
PFP	280 mg/kg	very toxic	Lapik and Zimina, 1967
HFB	710 mg/kg	moderately toxic	Lapik and Zimina, 1967
PMCH	>100 g/kg	practically nontoxic	Huntingdon, 1970
PDCH	>100 g/kg	practically nontoxic	Huntingdon, 1970
Freon E1	>25 g/kg	practically nontoxic	duPont, 1968
Freon E2	25 g/kg	practically nontoxic	duPont, 1968
PFD	>200 g/kg	practically nontoxic	Huntingdon, 1970

B. DETONATION END PRODUCTS FROM PDCH TAGGED EXPLOSIVES

Survivability testing of vapor tagged explosives was conducted to determine the eventual detonation fate of the PDCH chemical vapor taggant. Three test detonations of PDCH vapor tagged Atlas 60% Extra dynamite were conducted at Rolla, Missouri, for C. T. Pate of The Aerospace Corporation. The detonation chamber at Rolla had an interior volume of 294 ft^3, and after each detonation, the chamber had a positive pressure of 4 psig. The three tests used microcapsuled PDCH added to 1-lb charges at a nominal 0.05, 0.5, and 5.0 percent by weight loading. Prior to each shot, the chamber was purged with an exhaust fan for 1 hour and air samples were withdrawn into an air sampling bag to provide a background measurement. Post-detonation gas samples were collected after each shot by the same method. At the end of the test detonations, the air sample bags were returned to BNL for analysis. An air sample remained unused (but filled with zero air) as a method blank.

The analysis for PDCH was performed chromatographically and the chromatographs were essentially clean considering the air samples contained dynamite detonation end products such as water, CO_2, and nitrates. The measured concentrations are tabulated in Table 6-3 along with the calculated vapor taggant survival results. The concentration of post-detonation PDCH was obtained from a difference of the PDCH concentration measured before and after the detonation with the latter concentration corrected for the increase in chamber pressure.

There was a negligible amount of cross contamination between the bags as indicated by the low PDCH concentration measured in bag No. 79, the method blank. Before shipping, this bag was determined to have <0.001 ppb PDCH. The degree of PDCH survival is approximately 0.1 percent for well-mixed samples of PDCH containing microcapsules and dynamite.

As noted by C. T. Pate (private communication), the dynamite samples in shots 1 and 2 were prepared by pouring the PDCH microspheres in a slit cut in the dynamite; for shot No. 3, the dynamite was removed and intimately mixed with the microcapsules. The higher survival rate for shot No. 2 is perhaps indicative of poorer mixing. The degree of survival of PMCH is approximately 0.1 percent because it is present at the same impurity level in the sample bags as in the bulk PDCH used in manufacturing the microcapsules.

Thus, it can be concluded that 99.9 percent of the PDCH vapor taggant present in microcapsule tagged explosives was destroyed during detonation. No significant increase in the ambient PDCH background is expected due to the vapor tagging of explosives.

Table 6-3. Results of PDCH Post-Detonation Analysis

Bag No.	Comments	Observed PDCH Concentration (ppb)
79	Method blank	0.034 ± 0.0016
77	Before shot No. 1	0.180 ± 0.004
76	After shot No. 1	2.20 ± 0.09
88	Before shot No. 2	9.28 ± 0.07
80	After shot No. 2	38.0 ± 0.8
87	Before shot No. 3	41.2 ± 0.3
89	After shot No. 3	227.0 ± 3.4

Calculated Results

Shot No.	Percentage Taggant	Measured PDCH Concentration (ppb)	Expected PDCH Concentration (ppb)	Survival (%)
1	0.064	2.02	1.55×10^3	0.13
2	0.46	29.0	10.97×10^3	0.26
3	5.72	185.8	138.1×10^3	0.13

VII. SOLUBILIZED VAPOR TAGGANT EFFECT ON END CLOSURE MECHANICAL PROPERTIES

The vapor taggant solubilized end closures must be able to duplicate the mechanical properties of the present nontagged end closures. Otherwise, changes in the electric blasting cap manufacturing process requiring extensive field testing of the modified blasting caps would be required. Once the taggant solubilized end closure has been incorporated into the blasting cap, it should not change (with age) the mechanical properties which otherwise could affect the performance of the blasting caps.

Early in the experimental program it was noticed that the SF_6 solubilized end closures were undergoing changes in their mechanical properties. (Bubbles were occurring beneath the end closure surface with consequent tearing of the end closures.) Thus, a limited number of experiments were performed to determine the effect of SF_6 and PDCB solubilized taggants on the tensile strength and hardness of the various end closures. Only the substitute end closures were examined due to unavailability of the present end closure test pieces large enough for testing.

Slabs of various end closures, appropriately sized for tensile strength testing, were solubilized with SF_6 and PDCB with the same techniques as described in Section 2. These test pieces were subjected to hardness and tensile strength testing. The results are given in Table 7-1 for the various unsolubilized and solubilized end closures. It is seen that the tensile strength and hardness of the various end closures is lowered when SF_6 is solubilized into the end closures. The results for PDCB, however, indicate a negligible change in tensile strength and hardness for Viton E60-C. The difference in the results for the end

Table 7-1. Change in Tensile Strength and Hardness for SF_6 and PDCB Solubilized End Closures

End Closure Material	Taggant	Percent Solubilized	Tensile Strength (psi)	Hardness (Durometer A)
Viton E60-C	none	none	1630 ± 210	76.0 ± 1.0
	SF_6	1.2	956 ± 11	61.5 ± 0.6
	SF_6	2.3	880 ± 50	61.5 ± 0.6
	SF_6	10.3	580 ± 60	--
Viton E60-C	none	none	1190 ± 130	69.7 ± 4.7
	PDCB	0.36	1140 ± 60	66.0 ± 0.6
	PDCB	1.0	1328 ± 26	69.7 ± 0.6
	PDCB	2.8	1230 ± 60	67.3 ± 0.6
Viton B	none	none	1760 ± 260	64.0 ± 3.7
	SF_6	0.09	1650 ± 150	67.7 ± 0.6
	SF_6	1.1	1940 ± 240	65.3 ± 2.1
	SF_6	11.7	910 ± 100	50.3 ± 0.6
	SF_6	12.6	1090 ± 160	47.0 ± 0.6
Viton A	none	none	1480 ± 270	71.0 ± 0.6
	SF_6	4.2	1150 ± 150	64.0 ± 1.0
Fluorel 2170	none	none	1480 ± 110	71.7 ± 0.6
	SF_6	3.0	1220 ± 120	63.3 ± 1.1
Fluorel LVS-76	none	none	1340	74
	SF_6	5.3	780 ± 80	42.7 ± 1.5
Viton E-430	none	none	580 ± 150	52.7 ± 2.5
	SF_6	5.1	490 ± 60	50.3 ± 1.6
Viton A	none	none	1110 ± 310	61.3 ± 1.1
	SF_6	8.7	580 ± 360	50.8 ± 2.0
Fluorosilicone 35	none	none	--	29.0 ± 1.0
Fluorosilicone 70	none	none	1150 ± 110	63.0 ± 1.0

closures with SF_6 or PDCB can possibly be ascribed to the difference in the equilibrium vapor pressures of SF_6 and PDCB. SF_6, with its high vapor pressure, swells slightly and tears the elastomeric end closures, thus causing the decrease in hardness and tensile strength. Thus, SF_6 and any other high vapor pressure compounds are unacceptable as vapor taggants for the tagging of blasting caps. Taggants with vapor pressure of the order of PDCB or lower should not be expected to significantly change the tensile strength or durometer hardness of the end closures.

The results also indicated an unacceptably low hardness for several studied elastomers such as Fluorosilicone 35. All elastomers presently used for electric blasting cap end closures have a durometer specification of 70 ± 5.

VIII. TAGGANT EMISSION RATES FROM VAPOR TAGGED BLASTING CAPS

A. THEORETICAL DIFFUSION MODEL

One of the criteria for the selection of optimum vapor taggant/substrate elastomer pairs is that the vapor tagged blasting cap should have a specific minimum taggant emission rate lasting several years after manufacture. The emission rates, as a minimum, should be 0.5 to 1 nl/min at 5 years after manufacture, so as to be detectable in scenarios. In order to determine optimum taggant/substrate pairs, it is required that vapor tagged sample blasting caps be prepared and the taggant emission rates be periodically monitored over a several year experimental period. However, this empirical approach is experimentally unfeasible because it would require an experimental program of a several-year duration to determine optimum taggant/substrate pairs. Thus, a theoretical model was developed and experimentally validated to allow determination of the optimum taggant/substrate pairs based on a prediction of the taggant emission rates. This model allows the calculation of the taggant emission rates based on the initial taggant loading of the elastomer.

In order to devise a model for the prediction of taggant emission rates, some understanding of the physical processes occurring in the emission of a taggant from a tagged blasting cap is required. At the time of manufacture, the vapor taggant would be solubilized into the blasting cap end closure. It is assumed the vapor taggant has been solubilized uniformly throughout the end closure. After incorporation of the taggant loaded end closure into the blasting cap, the taggant is emitted from the end of the blasting cap (see Figure 8-1). The taggant is replenished at the emitting end by diffusion of the taggant from further back in the end closure. Thus, there are two physical processes which will effect the taggant emission rate: (1) the rate of taggant

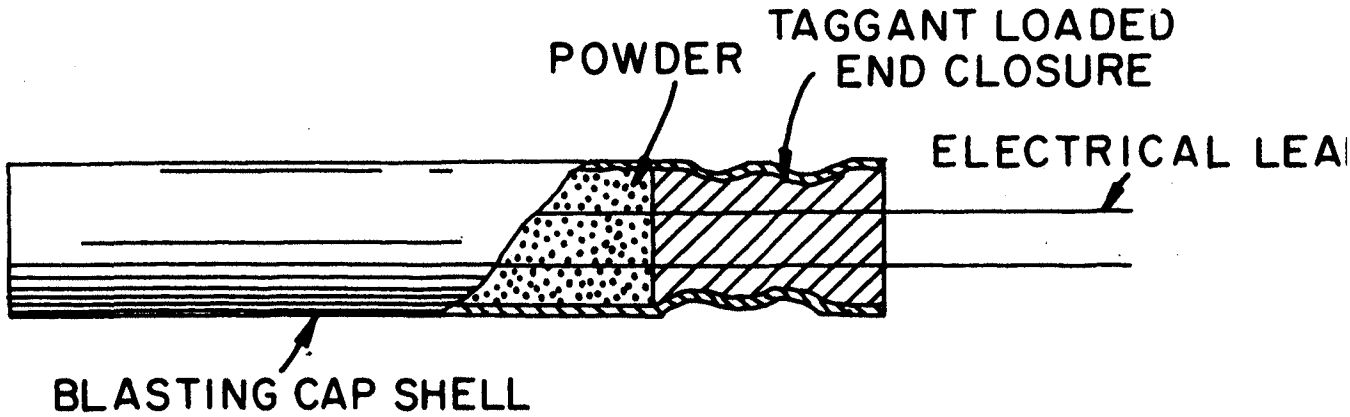

Figure 8-1. Cross-Section of a Typical Blasting Cap

mass transfer across the air-end closure interface and (2) the rate of taggant diffusion through the end closure. One of these processes will be the rate-limiting process that predominantly controls the taggant emission rate. A priori, it is impossible to state which process will be rate limiting. This depends on the relative values of the parameters which characterize the diffusion and mass transfer rates. The assumption that the taggant diffuses in the end closure as opposed to any other mechanism is valid as long as the elastomeric end closure is below its crystalline transition temperature, which is true for all the end closure substrates that have been considered in this program.

These basic physical processes can be expressed mathematically which will lead to a mathematical expression for the taggant emission rate. The rate of taggant emission from the tagged blasting cap is determined by:

- The rate of taggant diffusion in end closure as governed by Fick's law of diffusion and characterized by a taggant/substrate diffusion constant,

$$dC/dt = \nabla \cdot D \nabla C \qquad (8\text{-}1)$$

where: D = the taggant/substrate diffusion constant and
C = the taggant concentration inside the end closure as a function of position and time;

- The rate of taggant mass transfer across the end closure/air interface, mathematically expressed as a boundary condition on Fick's law of diffusion,

$$(dC/dz)_{z = z_o} = - h(C - C_e) \qquad (8\text{-}2)$$

where: C_e = the taggant concentration in the air (grams of taggant per unit volume air) and

h = mass transfer coefficient.

The taggant is emitted only from the end of the end closure ($z = z_o$) at a rate proportional to the concentration difference across the end closure/air interface.

For mathematical simplicity, two assumptions are also needed:

- The taggant/substrate diffusion constant D is independent of the taggant concentration in the end closure. This reduces equation (8-1) to the following equation:

$$dC/dt = D\nabla^2 C \qquad (8\text{-}3)$$

- The end closure is uniformly impregnated with the taggant. This can be expressed as an initial condition on Fick's law of diffusion:

$$C(r,\ t = 0) = C_o \text{ for all } r < r_o \text{ and } 0 < z < z_o \qquad (8\text{-}4)$$

where: C_o = the initial taggant solubilization with dimensions of gm taggant per unit volume of end closure and

z_o = the length of the end closure.

The differential equation (8-3) and the boundary and initial conditions (8-2 and 8-4) are explicitly solved in Appendix B in order to derive an expression for the taggant emission rate. The solution of the diffusion equation is complex and the results are shown in Figure 8-2. The fractional amount of taggant remaining in the end closure, $C^*(t)/C^*(o)$, is plotted against the square root of the reduced time

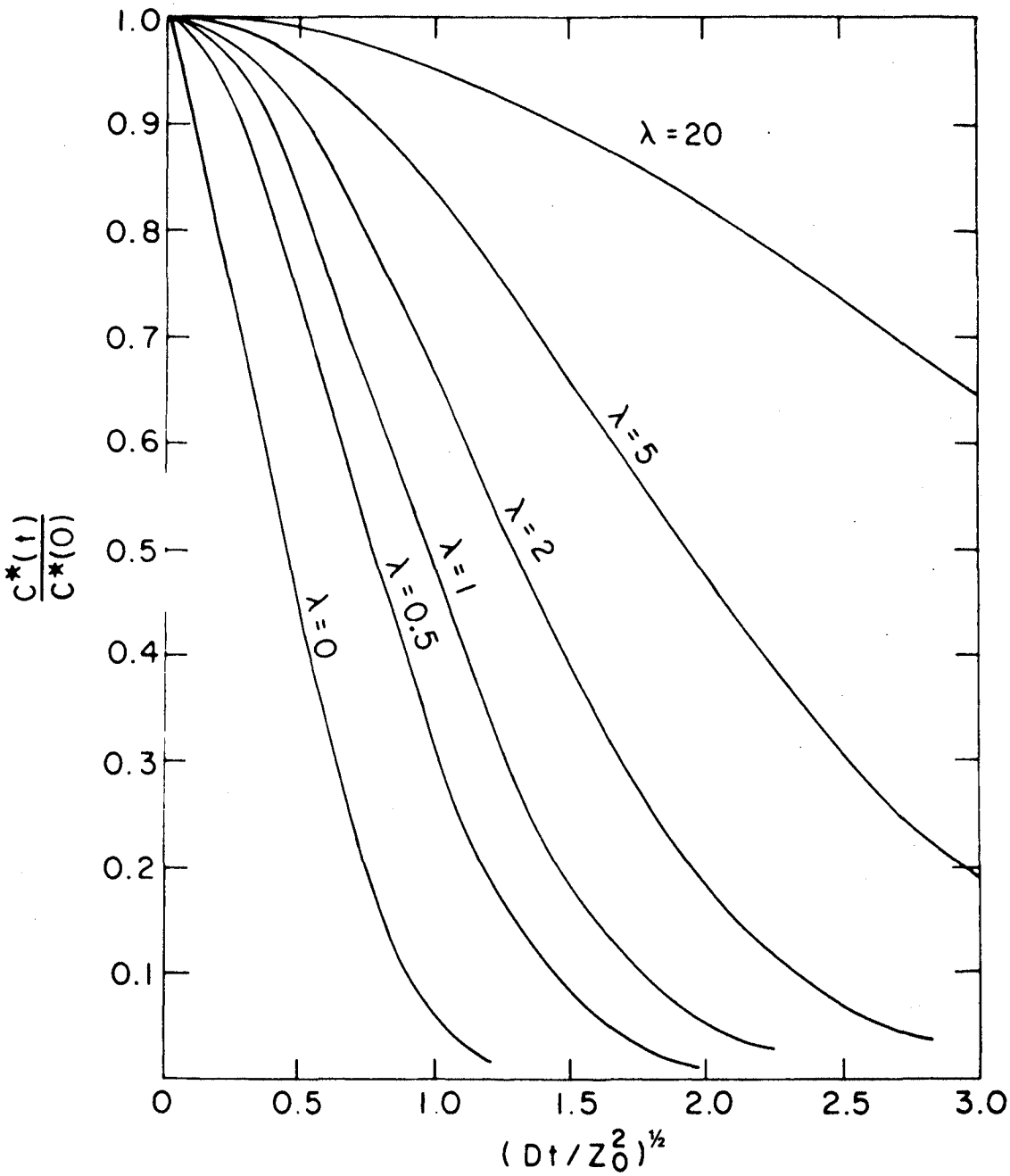

Figure 8-2. Normalized Taggant Solubility as a Function of Elapsed Time

$(Dt/z_o^2)^{1/2}$. The various curves are for different values of the mass transport coefficient h (8-2), which is expressd as a dimensionless parameter λ, where $\lambda = (hz_o)^{-1}$. The two limiting cases $\lambda = 0$ or ∞ correspond to either diffusion or mass transfer being the rate-limiting step. In almost all circumstances due to relatively small diffusion constants of the taggants in the substrates of interest in this report, it appears that the $\lambda = 0$ (diffusion-limited) case is the more relevant situation . In this instance, the expression for taggant emission rates are

$$dC(t)/dt = - (C_o - C_e)/z_o(D/\pi t)^{1/2}$$

$$\left[1 + 2 \sum_{n=1}^{\infty} (-1)^n \exp(-n^2 z_o^2/Dt)\right] \qquad (8\text{-}5)$$

or

$$dC(t)/dt = - 2(C_o - C_e)D/z_o^2$$

$$\left[\sum_{n=o}^{\infty} \exp(-(n + 1/2)^2 \pi^2 Dt/z_o^2)\right] \qquad (8\text{-}6)$$

as taken from (B-50) and (B-51) of Appendix B. Consequently, with a knowledge of the taggant substrate diffusion constant D and the initial solubilization C_o, the taggant emission rate may be predicted at any time after manufacture.

The diffusion constant D can be experimentally determined by recording the taggant emission rate for a small period of time and using equations (8-5) or (8-6) in order to determine D. An alternate method,

with greater precision, is to record the total amount of taggant emitted by periodically weighing the sample tagged cap and fitting the data to the integrated form of either (8-5) or (8-6). Thus the criteria concerning suitable taggant emission rates can be decided on the basis of the experimentally determined taggant-substrate diffusion constant D.

Figure 8-3 shows the taggant concentration as a function of the distance into the end closure (z/z_o), plotted with respect to the reduced elapsed time (Dt/z_o^2). For small elapsed time where $Dt/z_o^2 < 0.01$, most of the taggant is being emitted from the area of the end closure near the open end where ($z/z_o = 1$). As time elapses, the taggant begins to diffuse from the back of the end closure, and consequently, the taggant concentration will be depleted near the back of the end closure ($z/z_o = 0$). Convenient approximations for the total taggant concentration inside the end closure are as follows:

$$\frac{C(t) - C_e}{C_o - C_e} \approx 1 - 2/z_o(Dt/\pi)^{1/2} \qquad (8\text{-}7)$$

or

$$\frac{C(t) - C_e}{C_o - C_e} = \frac{8}{\pi^2} \sum_{n=0}^{\infty} \frac{\exp\left[-(2n+1)^2 \pi^2 Dt/4z_o^2\right]}{(2n+1)^2} \qquad (8\text{-}8)$$

Expression (8-7) is an excellent approximation when $Dt/z_o^2 \ll 1$, and (8-8) is valid for all values of Dt/z_o^2, but especially convenient when $Dt/z_o^2 > 1$.

B. EXPERIMENTAL RESULTS

The experimental procedure to determine diffusion constants for the various taggant/end closure combinations involved the preparation of taggant solubilized end closures, according to the techniques described in Section II. These tagged elastomers were subsequently crimped into an empty blasting cap shell with the use of a blasting cap crimping

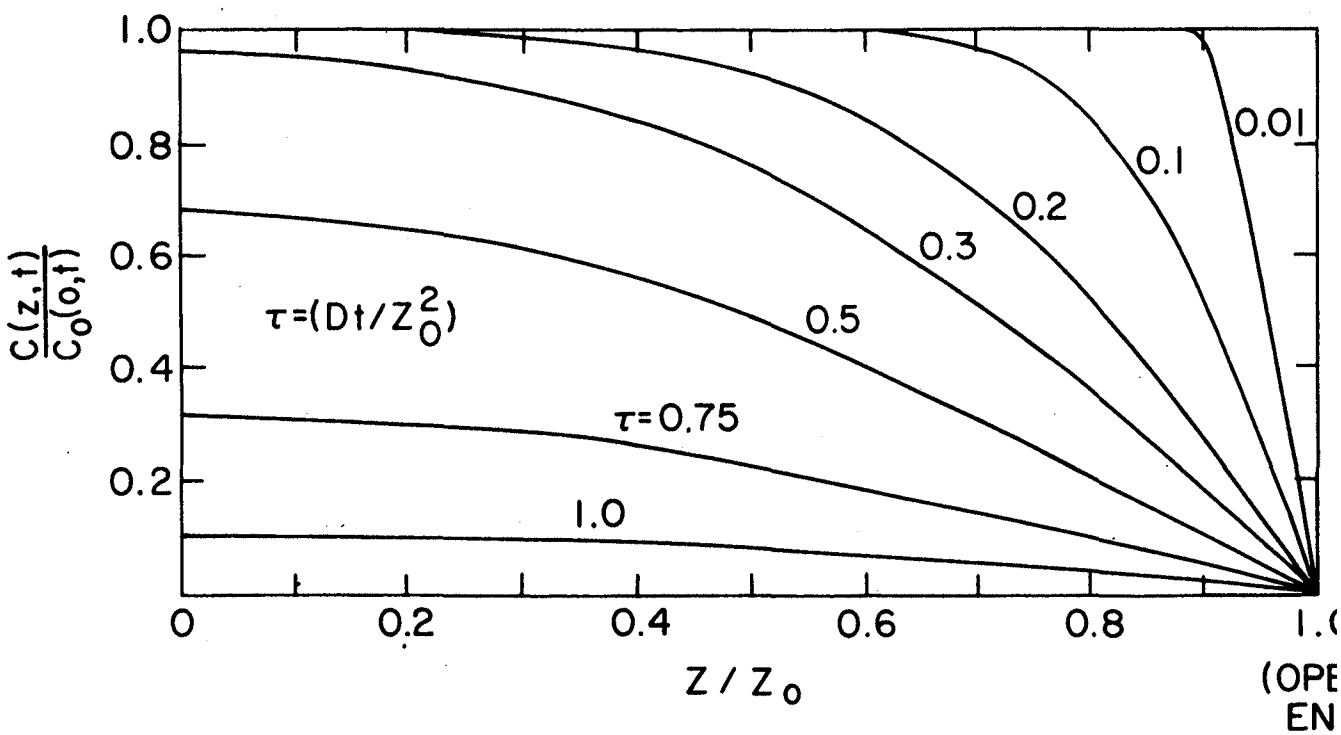

Figure 8-3. Taggant Concentration in the End Closure as a Function of Location

instrument to prepare a vapor tagged dummy blasting cap. The taggant emission rate $dC(t)/dt$) from equation (8-10) was determined from the rate of taggant loss from the tagged caps by periodically weighing the tagged caps with the use of a microbalance; however, it was more convenient to record the total taggant loss from the tagged blasting cap as a function of elapsed time after preparation. From a knowledge of $C(t)/C_o$, the diffusion constant (D) can be determined (see equation 8-10). As derived in the model, the total taggant loss should be initially proportional to the square root of the elapsed time. The initial slope is related to the taggant/end closure diffusion constant by

$$C_o - C(t) \approx 2(C_o/Z_o)(D/\pi)^{1/2} t^{1/2} \qquad (8\text{-}9)$$

where: $C_o - C(t)$ = the total taggant loss after the elapsed time, t,
Z_o = the length of the end closure,
C_o = the initial amount of solubilized taggant, and
D = the taggant/end closure diffusion constant.

This approximation is excellent when less than half of the total amount of solubilized taggant has been emitted. This expression (8-9) can be rearranged into:

$$C(t)/C_o \approx 1 - 2(Dt/\pi Z_o^2)^{1/2} \qquad (8\text{-}10)$$

where: $C(t)/C_o$ is defined as the fractional taggant loading.

This is the fraction of the initial amount of solubilized taggant still remaining in the end closure. An experimental demonstration of the square root of time dependence is shown in Figure 8-4 for the OFT/DuPont combination. In this figure, the fractional loading, as determined by periodic weighings, is plotted against the square root of the elapsed time. The straight line represents a least squares fit of the measured

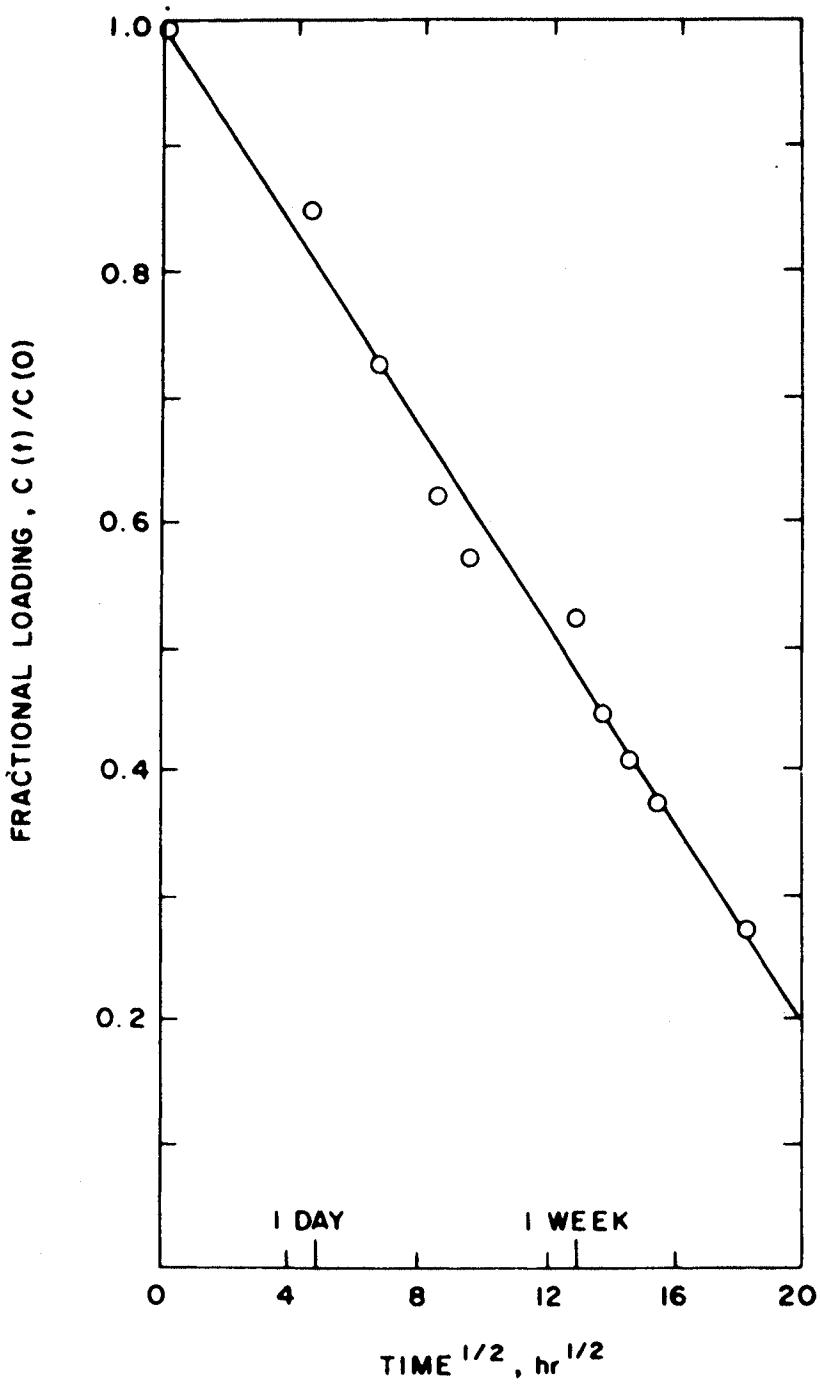

Figure 8-4. OFT Fractional Loading in duPont Buna

points from which the diffusion constant can then be obtained from the initial slope by equation (8-10). Once the diffusion constant has been obtained, the complete time dependence of the fractional loading can be calculated,

$$\frac{C(t)}{C_o} = \frac{8}{\pi^2} \sum_{n=0}^{\infty} \frac{\exp\left[-(2n+1)^2 \pi^2 Dt/Z_o^2\right]}{(2n+1)^2} \qquad (8\text{-}11)$$

(equation 8-8 of Section A above). Another example is the PDCB/Fluorosilicone 70 combination (Figure 8-5) that indicates the excellent agreement between the model calculation, the straight line (based on $D = 2.41 \times 10^{-8}$ cm^2/sec, as calculated by a least squares analysis), and the experimental points.

The square root of time dependence of the total taggant loss has been observed for all the taggant/end closures which were uniformly solubilized with taggant. A further example is displayed in Figure 8-6 for the HFB/Viton combination which has been recorded for over lapsed time of 1 year. Figure 8-7 displays the relatively nonvolatile OFN taggant loss from a duPont end closure and Figure 8-8 shows the data for the relatively slow emitting PDCB/Viton combinations.

The results of recording the cumulative weight loss of approximately 400 tagged dummy blasting caps are given in Table 8-1 for the six studied end closures. The uncertainties in the diffusion constant associated with each cap are derived from the least square analysis of the total weight loss data and are generally less than 5 percent, indicating an excellent agreement between the model and the experimental data. The apparent constancy of the diffusion constants for the HFB/duPont combinations with respect to the different amounts of initial taggant solubilized (ranging from 3.5 to 25.6 percent) verifies the assumption in the taggant emission model that the taggant diffusion constant is invariant with respect to initial degree of uniform solubilization.

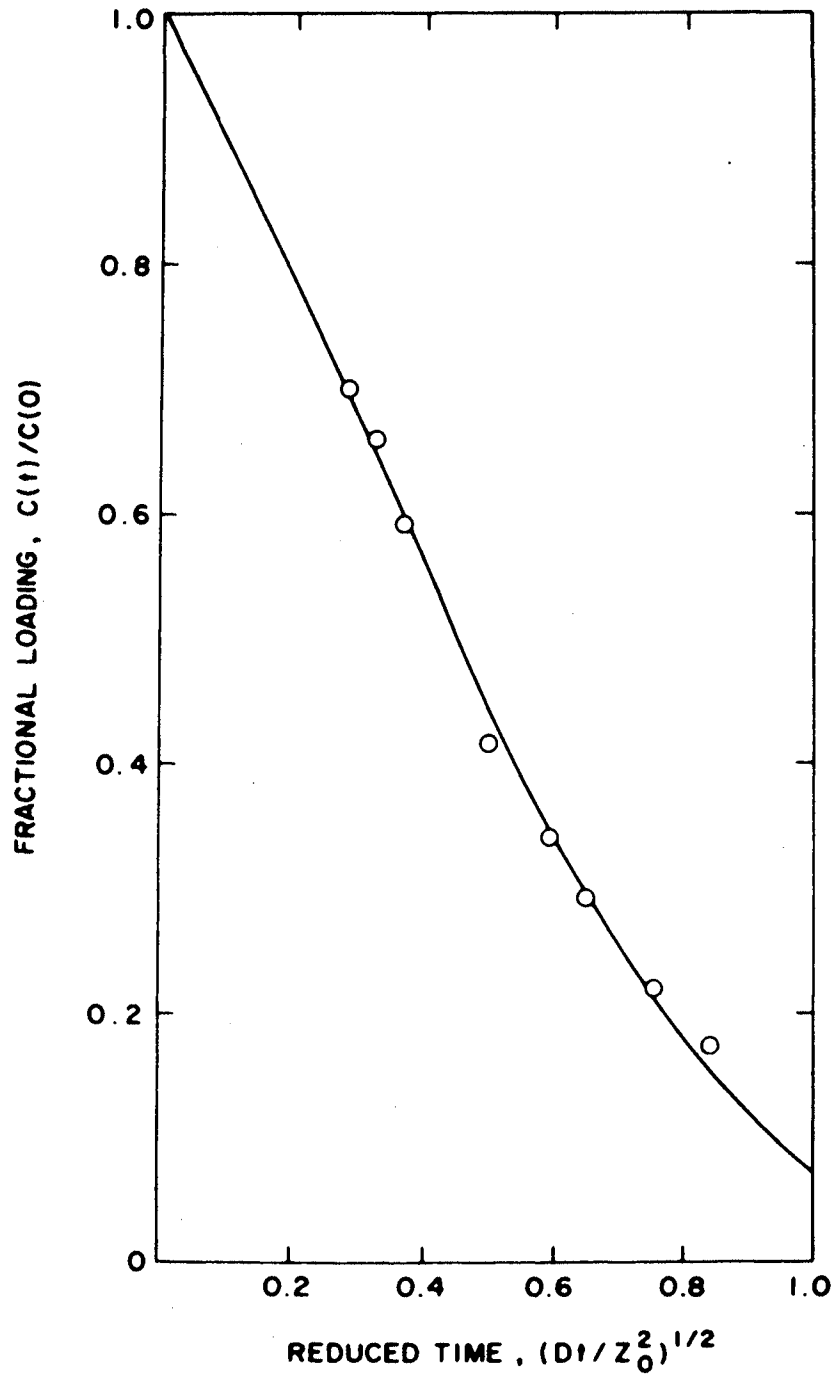

Figure 8-5. PDCB Fractional Loading in Fluorosilicone 70

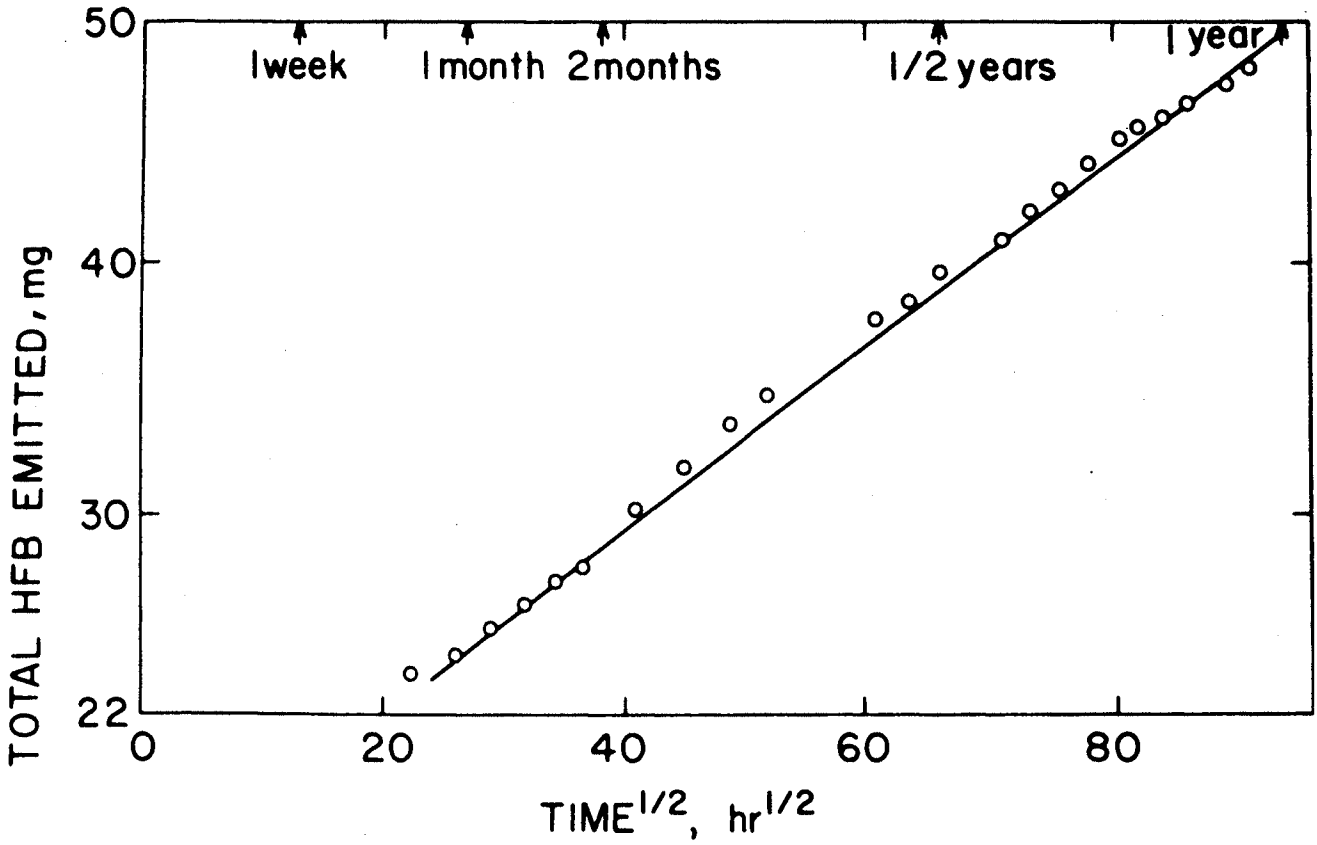

Figure 8-6. HFB Taggant Loss from Viton End Closures

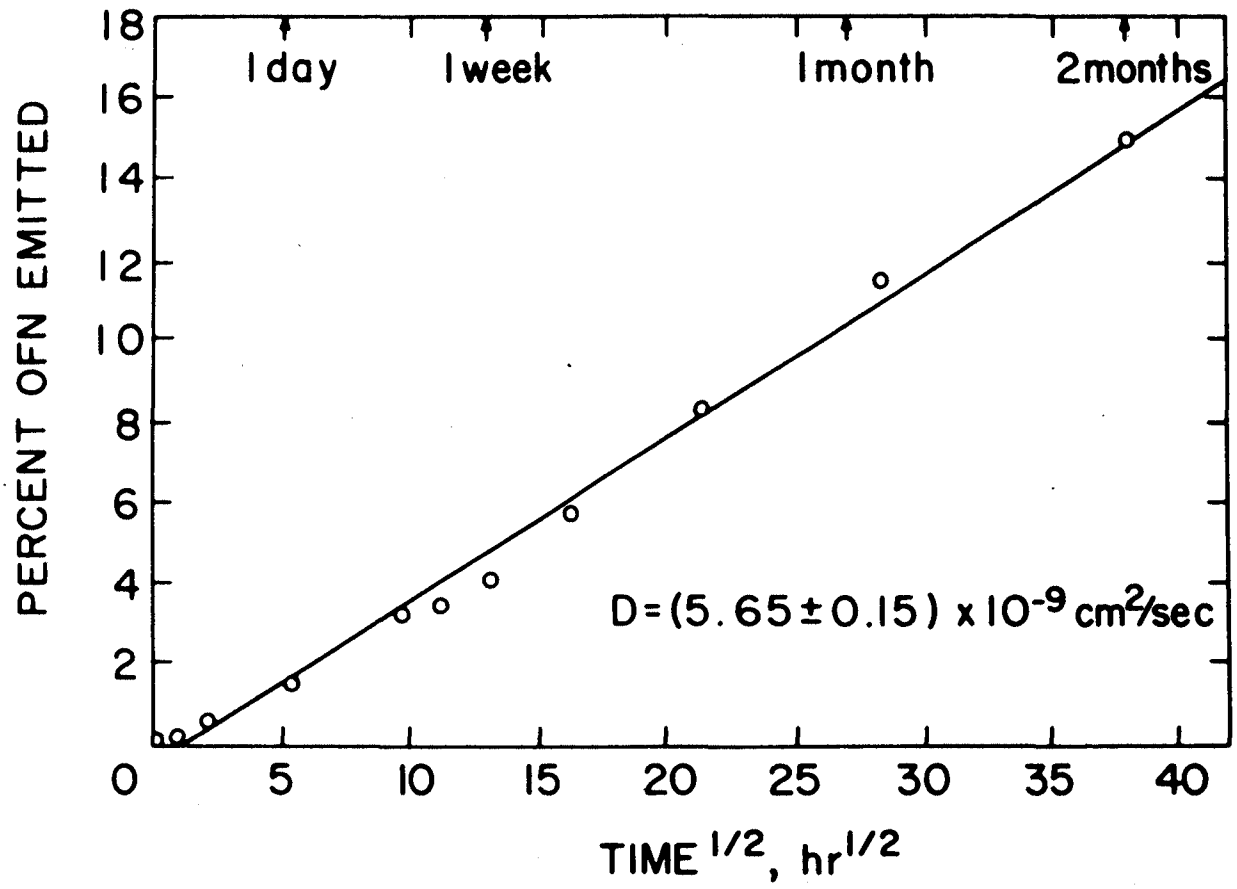

Figure 8-7. OFN Emission from an OFN/duPont Buna Cap

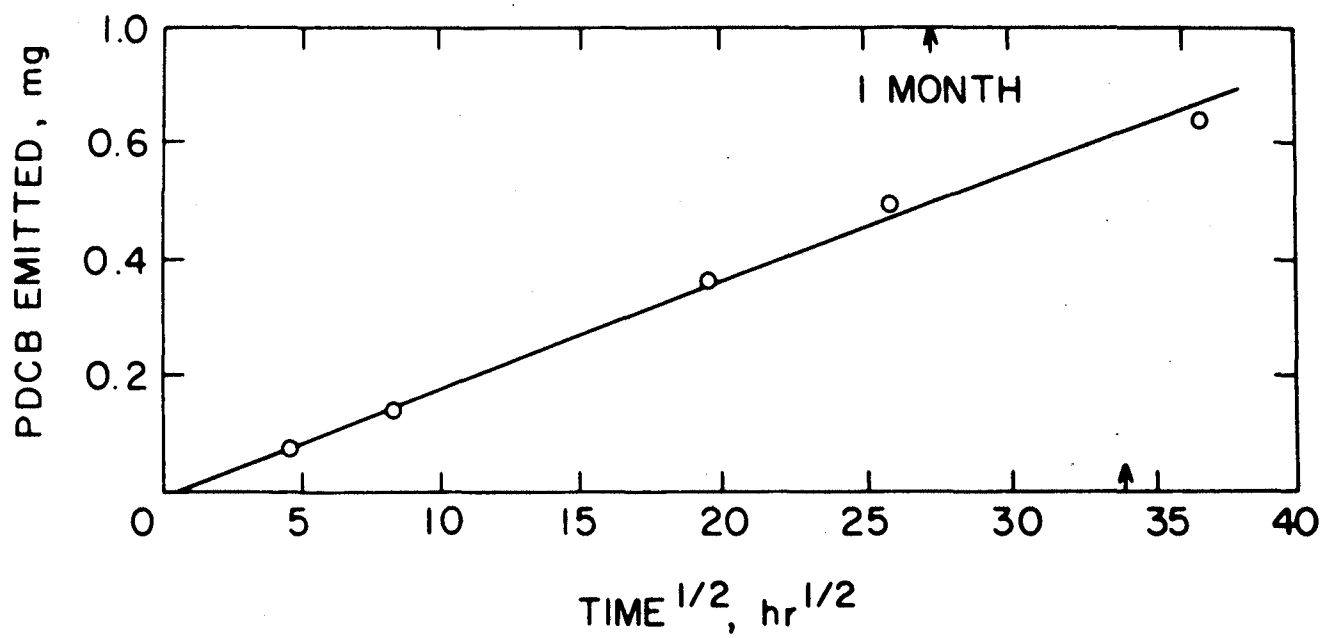

Figure 8-8. PDCB Taggant Emission from Viton End Closure

(initial PDCB solubilized = 50 mg)

Table 8-1. Taggant Diffusion Constants in End Closures

Cap Number	Taggant	Initial Taggant Solubilized (mg)	% (by weight)	Diffusion Constant (cm^2/sec)
		A. DuPont		
L-332	PFP	76.53	13.88	$(2.37 \pm 0.09) \times 10^{-6}$
L-265	HFB	20.14	3.50	$(1.22 \pm 0.05) \times 10^{-6}$
L-266	HFB	42.15	7.44	$(1.23 \pm 0.06) \times 10^{-6}$
L-267	HFB	81.44	14.56	$(1.00 \pm 0.06) \times 10^{-6}$
L-268	HFB	121.25	21.65	$(5.86 \pm 0.05) \times 10^{-7}$
---	HFB	134.48	25.60	$(1.00 \pm 0.04) \times 10^{-6}$
L-218	OFT	31.37	5.72	$(5.09 \pm 0.18) \times 10^{-7}$
L-260	PFX	45.1	8.17	$(6.05 \pm 0.15) \times 10^{-7}$
L-303	DFBP	32.39	5.76	$(3.98 \pm 0.09) \times 10^{-8}$
L-304	DFBP	36.56	6.64	$(3.72 \pm 0.11) \times 10^{-8}$
L-305	DFBP	37.25	6.77	$(4.19 \pm 0.10) \times 10^{-8}$
L-232A	DFBP	60.81	11.11	$(9.85 \pm 0.24) \times 10^{-9}$
D-17	OFN	140.82	25.1	$(6.84 \pm 0.10) \times 10^{-9}$
D-19	OFN	154.76	27.74	$(5.39 \pm 0.08) \times 10^{-9}$
L-235	OFN	170.40	31.03	$(1.66 \pm 0.10) \times 10^{-8}$
L-236	OFN	171.00	31.46	$(8.76 \pm 0.46) \times 10^{-9}$
L-234	OFN	199.5	36.31	$(1.42 \pm 0.08) \times 10^{-8}$
		B. ATLAS		
L-312	PDCB	2.18	0.56	$(1.69 \pm 0.21) \times 10^{-7}$
L-313	PDCB	2.74	0.59	$(1.13 \pm 0.09) \times 10^{-7}$
L-314	PMCH	4.96	1.06	$(2.13 \pm 0.17) \times 10^{-8}$
L-315	PMCH	2.29	0.50	$(1.55 \pm 0.08) \times 10^{-7}$
L-316	PDCH	4.49	0.93	$(2.65 \pm 0.17) \times 10^{-8}$
L-317	PDCH	5.77	1.22	$(2.04 \pm 0.14) \times 10^{-8}$
L-287	OFCP	5.69	1.13	$(1.58 \pm 0.03) \times 10^{-8}$

Table 8-1. Taggant Diffusion Constants in End Closures (continued)

Cap Number	Taggant	Initial Taggant Solubilized (mg)	% (by weight)	Diffusion Constant (cm^2/sec)
		B. ATLAS (continued)		
L-261	PFX	33.8	7.60	$(5.47 \pm 0.47) \times 10^{-8}$
L-288	DFCH	31.07	6.37	$(2.86 \pm 0.11) \times 10^{-8}$
L-247	DFBP	75.8	16.99	$(1.17 \pm 0.04) \times 10^{-8}$
L-245	PFP	34.8	7.26	$(2.24 \pm 0.12) \times 10^{-7}$
L-243	OFT	23.5	5.11	$(3.85 \pm 0.08) \times 10^{-8}$
L-248	OFN	21.9	5.02	$(3.73 \pm 0.12) \times 10^{-8}$
L-249	HFB	43.2	9.92	$(1.63 \pm 0.02) \times 10^{-7}$
	HFB	113.91	19.16	$(2.53 \pm 0.05) \times 10^{-6}$
L-389	PFD	14.6	3.35	$(4.65 \pm 0.33) \times 10^{-8}$
L-371	L-4412	9.00	0.97	$(1.14 \pm 0.08) \times 10^{-8}$
L-349	DFBP	17.43	3.67	$(2.12 \pm 0.27) \times 10^{-8}$
L-350	DFBP	18.73	4.15	$(2.44 \pm 0.26) \times 10^{-8}$
L-351	DFBP	19.96	4.36	$(1.93 \pm 0.19) \times 10^{-8}$
		C. KRATON		
L-345	PMCH	8.49	1.48	$(6.09 \pm 0.27) \times 10^{-8}$
L-346	PMCH	8.24	1.41	$(3.46 \pm 0.05) \times 10^{-8}$
L-347	PMCH	8.56	1.41	$(3.76 \pm 0.12) \times 10^{-8}$
L-289	HFB	108.53	22.3	$(2.64 \pm 0.10) \times 10^{-7}$
L-388	PFD	12.00	2.08	$(1.78 \pm 0.17) \times 10^{-8}$
L-333	OFN	63.47	10.6	$(9.34 \pm 0.36) \times 10^{-9}$
L-334	OFN	63.59	10.5	$(9.22 \pm 0.38) \times 10^{-9}$
L-335	OFN	62.65	10.7	$(1.14 \pm 0.04) \times 10^{-9}$

Table 8-1. Taggant Diffusion Constants in End Closures (continued)

Cap Number	Taggant	Initial Taggant Solubilized (mg)	% (by weight)	Diffusion Constant (cm^2/sec)
		D. VITON		
L-263	PFCP	76.7	8.20	$(3.44 \pm 0.22) \times 10^{-10}$
D-10	OFT	189.50	20.8	$(1.22 \pm 0.02) \times 10^{-9}$
L-219	OFT	188.98	19.70	$(1.15 \pm 0.02) \times 10^{-9}$
D-9	OFT	166.00	19.44	$(2.85 \pm 0.03) \times 10^{-9}$
L-233	PFP	82.84	9.42	$(3.07 \pm 0.21) \times 10^{-9}$
L-262	PFX	66.30	7.95	$(4.85 \pm 0.22) \times 10^{-10}$
L-249	DFCH	64.3	6.92	$(1.78 \pm 0.07) \times 10^{-10}$
L-92	HFB	136.51	15.61	$(3.25 \pm 0.09) \times 10^{-9}$
L-191	PDCH	42.0	4.50	$(1.40 \pm 0.10) \times 10^{-10}$
L-192	PDCH	43.2	4.32	$(2.04 \pm 0.34) \times 10^{-10}$
L-164	PMCH	38.5	4.22	$(1.32 \pm 0.14) \times 10^{-10}$
L-165	PMCH	39.4	4.20	$(7.27 \pm 0.64) \times 10^{-11}$
L-166	PMCH	38.9	4.25	$(2.83 \pm 0.24) \times 10^{-10}$
L-121	PDCB	37.0	4.51	$(4.02 \pm 0.35) \times 10^{-11}$
L-122	PDCB	40.2	4.28	$(9.15 \pm 0.54) \times 10^{-11}$
L-123	PDCB	38.3	4.46	$(8.48 \pm 1.04) \times 10^{-11}$
D-15	SF_6	11.65	1.27	$(5.41 \pm 1.07) \times 10^{-11}$
D-25	SF_6	55.94	6.03	$(3.50 \pm 0.06) \times 10^{-9}$
D-26	SF_6	43.61	4.74	$(6.96 \pm 0.24) \times 10^{-9}$
L-93	SF_6	42.50	4.47	$(2.60 \pm 0.21) \times 10^{-9}$
L-368	L-4412	16.51	1.78	$(1.93 \pm 0.11) \times 10^{-9}$
L-369	L-4412	16.57	1.87	$(4.70 \pm 0.47) \times 10^{-9}$
L-370	L-4412	17.02	1.83	$(2.97 \pm 0.14) \times 10^{-9}$
L-390	PFD	22.44	2.42	$(2.07 \pm 0.09) \times 10^{-8}$

Table 8-1. Taggant Diffusion Constants in End Closures (concluded)

Cap Number	Taggant	Initial taggant solubilized (mg)	% (by weight)	Diffusion Constant (cm^2/sec)
		E. FLUOROSILICONE 35		
D-1	PDCB	62.70	9.12	$(1.64 \pm 0.03) \times 10^{-7}$
D-2	PDCB	61.70	9.12	$(1.96 \pm 0.02) \times 10^{-7}$
D-27	PDCB	57.90	9.16	$(5.31 \pm 0.27) \times 10^{-7}$
D-28	PDCB	51.83	8.76	$(6.51 \pm 0.29) \times 10^{-7}$
D-5	PMCH	66.00	10.00	$(1.73 \pm 0.07) \times 10^{-7}$
D-6	PMCH	55.90	10.03	$(2.96 \pm 0.07) \times 10^{-7}$
D-29	PMCH	53.46	8.49	$(2.61 \pm 0.12) \times 10^{-7}$
D-30	PMCH	49.38	8.29	$(2.55 \pm 0.04) \times 10^{-7}$
D-13	SF_6	44.36	7.87	$(3.15 \pm 0.38) \times 10^{-7}$
		F. FLUOROSILICONE 70		
D-3	PDCB	43.30	5.85	$(2.41 \pm 0.03) \times 10^{-8}$
D-4	PDCB	42.80	5.89	$(2.72 \pm 0.07) \times 10^{-8}$
D-7	PMCH	53.40	7.18	$(2.13 \pm 0.05) \times 10^{-8}$
D-8	PMCH	56.20	7.24	$(3.02 \pm 0.20) \times 10^{-8}$
D-14	SF_6	34.22	4.84	$(7.67 \pm 0.19) \times 10^{-8}$
D-23	SF_6	61.38	9.37	$(6.90 \pm 0.12) \times 10^{-8}$
D-24	SF_6	69.71	10.07	$(5.54 \pm 0.07) \times 10^{-8}$
D-31	SF_6	24.26	3.39	$(4.81 \pm 0.17) \times 10^{-8}$
D-32	SF_6	22.84	2.96	$(8.58 \pm 0.21) \times 10^{-8}$
D-12	SF_6	31.60	4.30	$(6.29 \pm 0.05) \times 10^{-8}$

Thus, the taggant diffusion constants obtained for a particular initial degree of taggant solubilization can be assumed for any other degree of solubiliziation with an upper limit for this assumption being 30 percent solubiliziation.

Several tagged blasting caps were prepared for each taggant/end closure. The resulting diffusion constants were averaged and are tabulated in Table 8-2 for each combination. For each end closure, the ordering of diffusion constants for the different taggants is systematic. The fluoroaromatics have a greater diffusion constant than the fluoroalkenes which have a greater diffusion constant than the perfluoroalkanes. Within each class of taggants, the more volatile the taggant, the larger the diffusion constant.

The taggant emission rate is the most important of the criteria established for an acceptable taggant/end closure combination; this rate must be at least 0.5 to 1.0 nl/min five years from fabrication. The taggant emission rates (dC(t)/dt) can be calculated from the various taggant/end closure diffusion constants with the use of the following equation for various elapsed times after fabrication.

$$\frac{dC(t)}{dt} = -(2\,C_0 D/Z_0^2) \sum_{n=0}^{\infty} \exp\left[-(n+1/2)^2\,\pi^2\,Dt/Z^2\right] \qquad (8\text{-}12)$$

The calculated taggant emission rates are given in Table 8-3 for the three present end closures and three substitute end closures. The emission rates were calculated assuming 50 mg of initial taggant solubilization, where C_0 = 50 mg, with the diffusion constants tabulated in Table 8-2.

The taggant emission lifetimes -- the time required to completely deplete the initially solubilized taggant by emission -- ranges from one

Table 8-2. Averaged Diffusion Constants (cm^2/sec) at Room Temperature

Dupont	
PFP	2.38×10^{-6}
HFB	1.01×10^{-6}
OFT	5.09×10^{-7}
PFX	6.05×10^{-7}
DFBP	3.22×10^{-8}
OFN	3.23×10^{-9}

Viton	
PFD	2.07×10^{-8}
SF_6	3.40×10^{-9}
HFB	3.25×10^{-9}
L-4412	3.20×10^{-9}
PFP	3.07×10^{-9}
OFT	1.74×10^{-9}
PFX	4.85×10^{-10}
PFCP	3.44×10^{-10}
DFCH	1.78×10^{-10}
PDCH	1.72×10^{-10}
FC-72	1.64×10^{-10}
PMCH	1.63×10^{-10}
PDCB	7.21×10^{-11}

Fluorosilicone 35	
SF_6	6.63×10^{-8}
PDCB	3.86×10^{-7}
SF_6	3.15×10^{-7}
PMCH	2.46×10^{-7}

Atlas	
HFB	1.35×10^{-6}
PFP	2.24×10^{-7}
PDCB	1.41×10^{-7}
DFCH	1.21×10^{-7}
PMCH	8.82×10^{-8}
PFX	5.47×10^{-8}
PFD	4.65×10^{-8}
OFT	3.85×10^{-8}
OFN	3.73×10^{-8}
PDCH	2.35×10^{-8}
DFBP	2.16×10^{-8}
OFCP	1.58×10^{-8}
L-4412	1.14×10^{-8}

Kraton	
HFB	2.64×10^{-7}
PMCH	4.44×10^{-8}
PFD	1.78×10^{-8}
OFN	9.99×10^{-9}

Fluorosilicone 70	
PDCB	2.57×10^{-8}
PMCH	2.57×10^{-8}

Table 8-3. Taggant Emission Rates from Tagged Elastomers
(50 mg Taggant, Initial Solubilization)

Taggant	Emission Rate (nl/minutes) at										
	1 day	10 days	1 month	2 months	1/2 year	1 year	2 years	3 years	4 years	5 years	10 years
A. duPont Buna											
PFP	926	50.5	0.082	0.000							
HFB	549	119	7.78	0.134	0.000						
OFT	307	92.1	23.2	2.99	0.001	0.000					
PFX	276	79.4	15.5	1.36	0.000						
DFBP	54.6	17.3	9.89	6.99	3.70	1.70	0.359	0.076	0.016	0.003	0.000
OFN	35.2	11.1	6.37	4.50	2.60	1.82	1.15	0.752	0.490	0.320	0.038
B. Hercules Kraton											
HFB	329	103	40.9	14.1	0.202	0.000					
PMCH	61.1	19.3	11.1	7.82	3.62	1.24	0.146	0.017	0.002		
PMCH	61.1	19.3	11.1	7.82	3.62	1.24	0.146	0.017	0.002		
PFD	47.2	14.9	8.55	6.06	3.48	2.28	1.06	0.494	0.230	0.108	0.002
OFN	37.3	11.8	6.76	4.78	2.76	1.93	1.17	n.c.	0.445	0.275	0.025

Table 8-3. Taggant Emission Rates from Tagged Elastomers (continued)
(50 mg Taggant, Initial Solubilization)

Taggant	Emission Rate (nl/minutes) at										
	1 day	10 days	1 month	2 months	1/2 year	1 year	2 years	3 years	4 years	5 years	10 years
					C. Atlas Rubber						
HFB	634	102	2.65	0.012	0.000						
PFP	284	89.9	44.9	18.2	0.495	0.002	0.000				
DFCH	135	42.7	24.1	14.5	2.08	0.112	0.000				
PDCB	127	40.2	22.4	12.6	1.30	0.043	0.000				
PMCH	86.2	27.3	15.6	10.4	2.50	0.297	0.004	0.000			
PFX	83.1	26.3	15.1	10.6	4.26	1.14	0.081	0.006	0.000		
OFT	84.4	26.7	15.3	10.8	5.37	2.12	0.330	0.051	0.008	0.001	0.000
OFN	72.1	22.8	13.1	9.24	4.65	1.89	0.312	0.052	0.009	0.001	0.000
OFCP	60.2	19.0	10.9	7.72	4.44	2.90	1.35	0.630	0.294	0.137	0.003
PFD	47.9	15.1	8.71	6.14	2.84	0.973	0.115	0.013	0.002		
DFBP	44.7	14.1	8.11	5.73	3.25	1.90	0.670	0.536	0.083	0.029	0.000
PDCH	38.9	12.3	7.06	4.99	2.81	1.57	0.506	0.163	0.052	0.017	0.000
L-4412	28.6	9.03	5.18	3.67	2.11	1.38	0.642	0.300	0.140	0.065	0.001

Table 8-3. Taggant Emission Rates from Tagged Elastomers (continued)
(50 mg Taggant, Initial Solubilization)

Taggant	Emission Rate (nl/minutes) at										
	1 day	10 days	1 month	2 months	1/2 year	1 year	2 years	3 years	4 years	5 years	10 years
					D. Viton Substitute						
SF_6	40.6	12.8	7.36	5.20	3.00	2.12	1.50	1.01	0.856	0.376	
PFP	33.1	10.5	6.04	4.27	2.46	1.74	1.23	0.844	0.723	0.343	0.078
PFD	31.6	9.98	5.72	4.05	2.14	0.984	0.208	0.044	0.009	0.002	
HFB	31.1	9.84	5.64	3.99	2.30	1.63	1.15	0.782	0.666	0.303	0.063
OFT	17.9	5.68	3.25	2.30	1.33	0.939	0.664	0.469	0.418	0.266	0.114
L-4412	12.9	4.07	2.33	1.65	0.951	0.674	0.476	0.337	0.301	0.127	0.015
PFX	7.82	2.47	1.42	1.00	0.588	0.409	0.289	0.205	0.183	0.129	0.091
PFCP	8.89	2.81	1.61	1.14	0.658	0.464	0.329	0.232	0.208	0.147	0.104
DFCH	5.17	1.64	0.937	0.663	0.383	0.271	0.191	0.135	0.121	0.086	0.061
PDCH	3.33	1.05	0.603	0.427	0.246	0.174	0.123	0.087	0.078	0.555	0.039
FC-72	3.85	1.22	0.697	0.493	0.285	0.201	0.142	0.101	0.090	0.064	
PMCH	3.70	1.17	0.672	0.475	0.274	0.194	0.137	0.097	0.087	0.061	0.043
PDCB	2.88	0.909	0.521	0.368	0.213	0.150	0.106	0.075	0.067	0.048	0.034

Table 8-3. Taggant Emission Rates Tagged Caps (concluded)
(50 mg Taggant, Initial Solubilization)

Taggant	Emission Rate (nl/minutes) at									
	1 day	10 days	1 month	2 months	1/2 year	1 year	2 years	4 years	5 years	10 years
					E. Fluorosilicone 35					
SF_6	396	123	50.7	14.3	0.089	0.000				
PDCB	210	65.5	22.7	4.80	0.008	0.000				
PMCH	144	45.5	21.8	8.09	0.154	0.000				
					F. Fluorosilicone 70					
SF_6	179	56.7	32.5	22.5	7.64	1.54	0.063	0.000		
PDCB	54.3	17.2	9.84	6.96	3.87	2.07	0.597	0.050	0.014	0.000
PMCH	46.5	14.7	8.43	5.96	3.31	1.77	0.512	0.042	0.012	0.000

month for HFB/duPont to greater than 20 years for PDCB/Viton. The optimal taggant emission lifetime should be approximately 5 years. An examination of the emission rates in Table 8-3 reveals that a taggant/end closure diffusion constant in the range of 3×10^{-9} to 30×10^{-9} cm^2/sec provides the optimal emission lifetime of 5 years. Those taggant/end closure combinations with these optimal lifetimes are tabulated in Table 8-4. The calculated taggant emission rates at 1, 2, and 4 years after fabrication of these tagged blasting caps are given. From these data, it is seen that there are several taggants that when combined with either the present or the substitute end closures will satisfy the taggant emission rate criteria. Several of these taggant combinations, however, are unacceptable with respect to criteria other than the emission rate.

According to conventional diffusion theory, the temperature dependence of the diffusion constant should follow the Arrhenius equation form:

$$D = D_o \exp(-E_d/RT) \qquad (8\text{-}12)$$

where: D_o = a pre-exponential constant,
E_d = the activation energy of diffusion,
R = the gas constant, and
T = the absolute temperature.

The determination of the taggant/end closure diffusion constant at three elevated temperatures, 45°, 65°, and 85°C was accomplished by preparing identical sets of tagged dummy blasting caps and storing them in temperature-controlled ovens at these temperatues. The tagged caps were periodically weighed (in the same manner as for the room temperature analyses) to determine their total taggant weight loss from which the diffusion constant could be obtained.

Table 8-4. Most Promising Taggant/End Closure Combinations

Taggant/End Closure	Diffusion Constant (10^{-9} cm^2/sec)	Emission Rate (nl/min)		
		1 year	2 years	4 years
OFN/DuPont Buna	3.23	1.82	1.15	0.490
DFBP/DuPont Buna	32.2	1.70	0.359	0.016
PFD/Kraton	17.8	2.28	1.06	0.230
OFN/Kraton	9.99	1.93	1.17	0.445
OFCP/Atlas	15.8	2.90	1.35	0.294
DFBP/Atlas	21.6	1.90	0.670	0.083
PDCH/Atlas	23.5	1.57	0.506	0.052
L-4412/Atlas	11.4	1.38	0.642	0.140
SF_6/Viton	3.4	2.12	1.50	1.01
PFP/Viton	3.07	1.74	1.23	0.844
PFD/Viton	20.7	0.984	0.208	0.044
HFB/Viton	3.25	1.63	1.15	0.782
OFT/Viton	1.74	0.939	0.664	0.469
L-4412/Viton	3.20	0.674	0.476	0.337
PMCH/Fluorosilicone 70	25.7	1.77	0.512	0.042
PDCB/Fluorosilicone 70	25.7	2.07	0.597	0.050

The diffusion constants for six different taggant end closure combinations at the four different temperatures are given in Table 8-5 with the averaged value at each temperature also given. The Arrhenius dependence of the diffusion constants is verified by the straight line fit of the data as displayed in Figures 8-9 through 8-14 and the resulting least square analysis values for the pre-exponential factor D_o and the activation energy E_d is given in Table 8-6.

Table 8-5. Taggant/End Closure Diffusion Constants at Various Temperatures

Temperature (°C)	Diffusion Constants (cm^2/sec)	Averaged Values (cm^2/sec)
	A. OFN/duPont Buna	
Room Temperature	$(1.44 \pm 0.11) \times 10^{-9}$	$(3.23 \pm 1.70) \times 10^{-9}$
	$(9.54 \pm 0.28) \times 10^{-9}$	
	$(6.82 \pm 0.27) \times 10^{-9}$	
	$(6.22 \pm 0.41) \times 10^{-9}$	
45°C	$(4.84 \pm 0.04) \times 10^{-8}$	$(4.05 \pm 0.59) \times 10^{-8}$
	$(4.53 \pm 0.06) \times 10^{-8}$	
	$(3.05 \pm 0.04) \times 10^{-8}$	
65°C	$(2.09 \pm 0.02) \times 10^{-7}$	$(1.88 \pm 0.11) \times 10^{-7}$
	$(1.84 \pm 0.02) \times 10^{-7}$	
	$(1.71 \pm 0.02) \times 10^{-7}$	
85°C	$(3.94 \pm 0.17) \times 10^{-6}$	$(4.55 \pm 0.38) \times 10^{-6}$
	$(4.97 \pm 0.19) \times 10^{-6}$	
	$(5.08 \pm 0.24) \times 10^{-6}$	
	B. OFN/Hercules Kraton	
Room Temperature	$(9.34 \pm 0.36) \times 10^{-9}$	$(9.99 \pm 1.23) \times 10^{-9}$
	$(9.22 \pm 0.38) \times 10^{-9}$	
	$(1.14 \pm 0.04) \times 10^{-9}$	
45°C	$(1.22 \pm 0.04) \times 10^{-7}$	$(1.08 \pm 0.17) \times 10^{-7}$
	$(8.88 \pm 0.14) \times 10^{-8}$	
	$(1.12 \pm 0.04) \times 10^{-7}$	
65°C	$(2.07 \pm 0.04) \times 10^{-7}$	$(2.12 \pm 0.06) \times 10^{-7}$
	$(2.19 \pm 0.05) \times 10^{-7}$	
	$(2.11 \pm 0.05) \times 10^{-7}$	
85°C	$(4.13 \pm 0.09) \times 10^{-7}$	$(5.19 \pm 0.93) \times 10^{-7}$
	$(5.86 \pm 0.12) \times 10^{-7}$	
	$(5.58 \pm 0.10) \times 10^{-7}$	

Table 8-5. Taggant/End Closure Diffusion Constants at Various Temperatures (continued)

Temperature (°C)	Diffusion Constants (cm^2/sec)	Averaged Values (cm^2/sec)
	C. DFBP/Atlas Rubber	
Room Temperature	$(2.12 \pm 0.27) \times 10^{-8}$ $(2.44 \pm 0.26) \times 10^{-8}$ $(1.93 \pm 0.19) \times 10^{-8}$	$(2.16 \pm 0.26) \times 10^{-8}$
45°C	$(1.49 \pm 0.04) \times 10^{-7}$ $(1.43 \pm 0.04) \times 10^{-7}$ $(1.59 \pm 0.04) \times 10^{-7}$	$(1.50 \pm 0.08) \times 10^{-7}$
65°C	$(5.50 \pm 0.21) \times 10^{-7}$ $(4.67 \pm 0.23) \times 10^{-7}$ $(3.62 \pm 0.14) \times 10^{-7}$	$(4.60 \pm 0.94) \times 10^{-7}$
85°C	$(1.38 \pm 0.06) \times 10^{-6}$ $(1.05 \pm 0.06) \times 10^{-6}$ $(1.02 \pm 0.06) \times 10^{-6}$	$(1.15 \pm 0.20) \times 10^{-6}$
	D. DFCH/Atlas Rubber	
Room Temperature	$(4.81 \pm 0.16) \times 10^{-8}$ $(2.60 \pm 0.06) \times 10^{-7}$ $(5.57 \pm 0.21) \times 10^{-8}$	$(1.21 \pm 1.20) \times 10^{-7}$
45°C	$(2.25 \pm 0.15) \times 10^{-7}$ $(2.48 \pm 0.15) \times 10^{-7}$ $(2.49 \pm 0.14) \times 10^{-7}$	$(2.41 \pm 0.14) \times 10^{-7}$
65°C	$(3.67 \pm 0.30) \times 10^{-7}$ $(4.46 \pm 0.25) \times 10^{-7}$ $(6.17 \pm 0.67) \times 10^{-7}$	$(4.77 \pm 1.28) \times 10^{-7}$

Table 8-5. Taggant/End Closure Diffusion Constants at Various Temperatures (continued)

Temperature (°C)	Diffusion Constants (cm^2/sec)	Averaged Values (cm^2/sec)
	E. FC-72/Viton	
Room Temperature	$(2.27 \pm 0.21) \times 10^{-10}$ $(1.96 \pm 0.24) \times 10^{-10}$ $(6.99 \pm 1.15) \times 10^{-11}$	$(1.64 \pm 0.83) \times 10^{-10}$
45°C	$(5.63 \pm 0.28) \times 10^{-9}$ $(5.27 \pm 0.33) \times 10^{-9}$ $(4.53 \pm 0.27) \times 10^{-9}$	$(5.14 \pm 0.56) \times 10^{-9}$
65°C	$(3.18 \pm 0.10) \times 10^{-8}$ $(3.55 \pm 0.10) \times 10^{-8}$ $(8.00 \pm 0.42) \times 10^{-9}$	$(2.18 \pm 1.23) \times 10^{-8}$
	F. PDCB/Viton A	
Room temperature	$(4.02 \pm 0.35) \times 10^{-11}$ $(9.15 \pm 0.54) \times 10^{-11}$ $(8.48 \pm 1.04) \times 10^{-11}$	$(5.76 \pm 1.14) \times 10^{-11}$
45°C	$(1.66 \pm 0.11) \times 10^{-9}$ $(1.86 \pm 0.06) \times 10^{-9}$ $(1.56 \pm 0.06) \times 10^{-9}$	$(1.70 \pm 0.10) \times 10^{-9}$
65°C	$(6.51 \pm 0.36) \times 10^{-9}$ $(3.04 \pm 0.18) \times 10^{-9}$ $(3.76 \pm 0.09) \times 10^{-9}$	$(3.74 \pm 0.46) \times 10^{-9}$

Table 8-5. Taggant/End Closure Diffusion Constants at Various Temperatures (continued)

Temperature (°C)	Diffusion Constants (cm^2/sec)	Averaged Values (cm^2/sec)
	G. PDCB/Viton E60-C	
Room temperature	$(6.77 \pm 0.42) \times 10^{-11}$ $(8.16 \pm 0.18) \times 10^{-11}$ $(1.18 \pm 0.12) \times 10^{-10}$	$(8.02 \pm 0.51) \times 10^{-11}$
45°C	$(1.64 \pm 0.03) \times 10^{-9}$ $(3.06 \pm 0.07) \times 10^{-9}$ $(1.42 \pm 0.04) \times 10^{-9}$	$(1.72 \pm 0.33) \times 10^{-9}$
65°C	$(1.06 \pm 0.08) \times 10^{-8}$ $(7.34 \pm 0.28) \times 10^{-9}$ $(5.53 \pm 0.32) \times 10^{-9}$	$(6.82 \pm 0.93) \times 10^{-9}$
	H. PDCB/Fluorel 2170	
Room temperature	$(8.81 \pm 0.35) \times 10^{-11}$ $(7.23 \pm 0.50) \times 10^{-11}$ $(2.83 \pm 0.24) \times 10^{-10}$	$(5.08 \pm 0.86) \times 10^{-11}$
45°C	$(6.67 \pm -0.15) \times 10^{-9}$ $(2.75 \pm 0.06) \times 10^{-9}$ $(3.92 \pm 0.20) \times 10^{-9}$	$(3.33 \pm 0.93) \times 10^{-9}$
65°C	$(5.00 \pm 0.28) \times 10^{-9}$ $(6.57 \pm 0.33) \times 10^{-9}$ $(1.68 \pm 0.20) \times 10^{-8}$	$(5.78 \pm 0.99) \times 10^{-9}$

Table 8-5. Taggant/End Closure Diffusion Constants at Various Temperatures (continued)

Temperature (°C)	Diffusion Constants (cm^2/sec)	Averaged Values (cm^2/sec)
	I. PDCH/Viton A	
Room temperature	$(1.32 \pm 0.41) \times 10^{-10}$ $(7.27 \pm 0.64) \times 10^{-11}$ $(2.83 \pm 0.24) \times 10^{-10}$	$(9.41 \pm 2.07) \times 10^{-11}$
45°C	$(2.54 \pm 0.14) \times 10^{-9}$ $(2.124 \pm .039) \times 10^{-9}$ $(1.555 \pm .045) \times 10^{-9}$	$(1.70 \pm 0.10) \times 10^{-9}$
65°C	$(6.74 \pm 0.51) \times 10^{-9}$ $(5.82 \pm .433) \times 10^{-9}$ $(1.322 \pm 0.39) \times 10^{-9}$	$(9.12 \pm 1.42) \times 10^{-9}$
	J. PDCH/Viton E60-C	
Room temperature	$(1.175 \pm .089) \times 10^{-10}$ $(5.44 \pm 0.38) \times 10^{-11}$ $(1.79 \pm .087) \times 10^{-10}$	$(7.02 \pm 1.06) \times 10^{-11}$
45°C	$(2.56 \pm 0.13) \times 10^{-9}$ $(2.359 \pm .029) \times 10^{-9}$ $(3.37 \pm 0.24) \times 10^{-9}$	$(2.38 \pm 0.51) \times 10^{-9}$
65°C	$(1.34 \pm 0.12) \times 10^{-8}$ $(1.856 \pm .098) \times 10^{-8}$ $(1.537 \pm .047) \times 10^{-9}$	$(1.57 \pm 0.06) \times 10^{-8}$

Table 8-5. Taggant/End Closure Diffusion Constants at Various Temperatures (concluded)

Temperature (°C)	Diffusion Constants (cm^2/sec)	Averaged Values (cm^2/sec)
	K. PDCH/Fluorel 2170	
Room temperature	$(9.8 \pm 1.10) \times 10^{-11}$ $(4.95 \pm 0.70) \times 10^{-11}$ $(3.54 \pm 0.28) \times 10^{-11}$	$(4.06 \pm 0.59) \times 10^{-11}$
45°C	$(5.78 \pm 0.26) \times 10^{-9}$ $(6.39 \pm 0.24) \times 10^{-9}$ $(3.96 \pm 0.13) \times 10^{-9}$	$(4.71 \pm 0.42) \times 10^{-9}$
65°C	$(5.00 \pm 0.28) \times 10^{-9}$ $(2.02 \pm 0.28) \times 10^{-9}$	$(1.38 \pm 0.20) \times 10^{-9}$

Table 8-6. Activation Energies and Preexponential Factor for the Diffusion Constants (cm^2/sec)

Taggant/End Closure	E_d(kcal/mole)	ln D_o
OFN/Kraton	13.5 ± 1.1	4.64 ± 1.75
DFBP/Atlas	13.9 ± 0.7	6.01 ± 1.04
FC-72/Viton	25.0 ± 3.1	19.90 ± 4.86
DFCH/Atlas	8.33 ± 2.14	2.15 ± 3.39
OFN/DuPont	23.0 ± 1.7	19.5 ± 2.7

	Activation Energies, E_d(cal/mole) End Closure		
Taggant	Viton A	Viton E60-C	Fluorel 2170
PMCH	5830 ± 850	6900 ± 950	7500 ± 2400
PDCB	5400 ± 1700	5670 ± 1000	6100 ± 2400

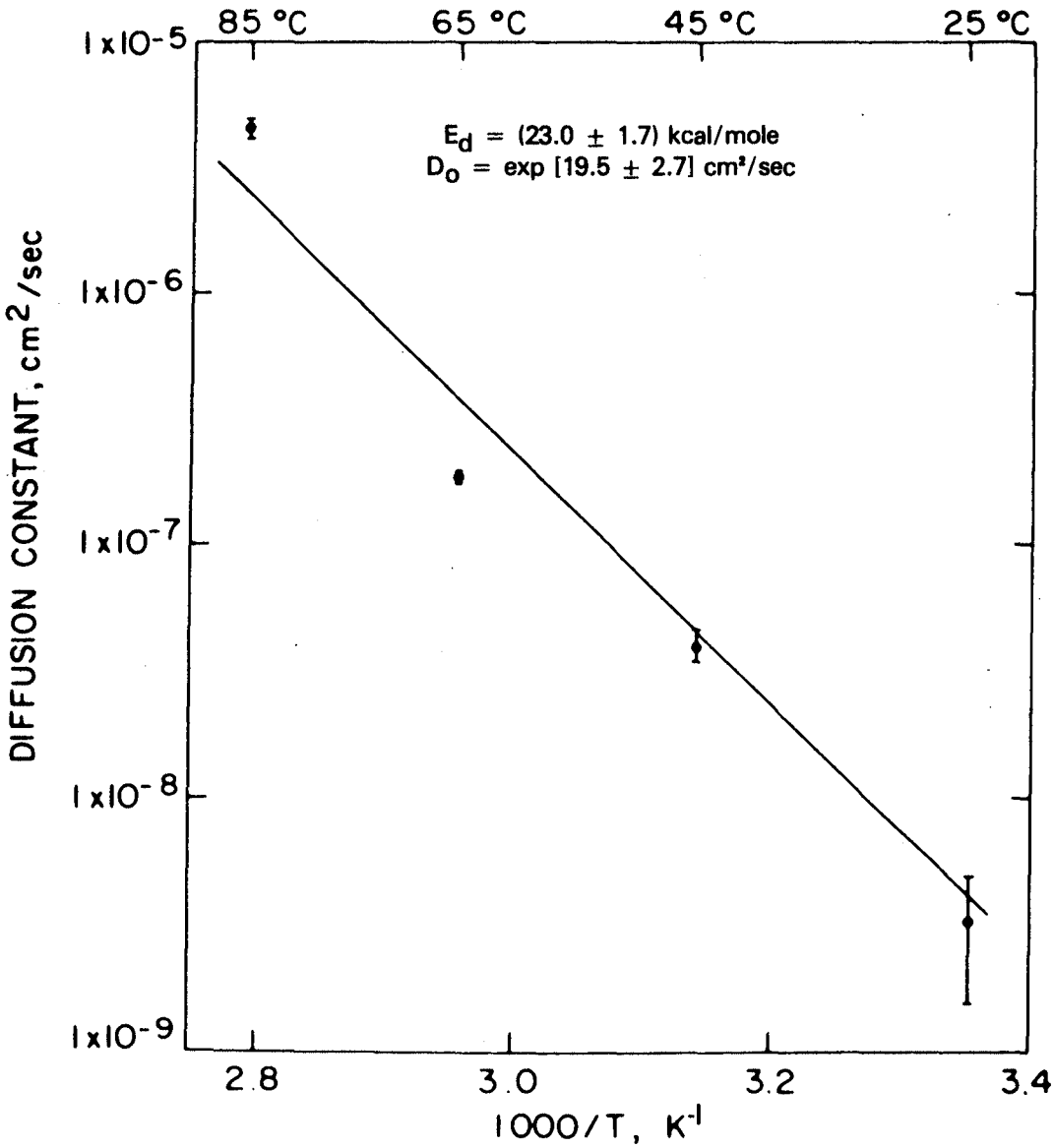

Figure 8-9. Temperature Dependence of the OFN/duPont Diffusion Constant

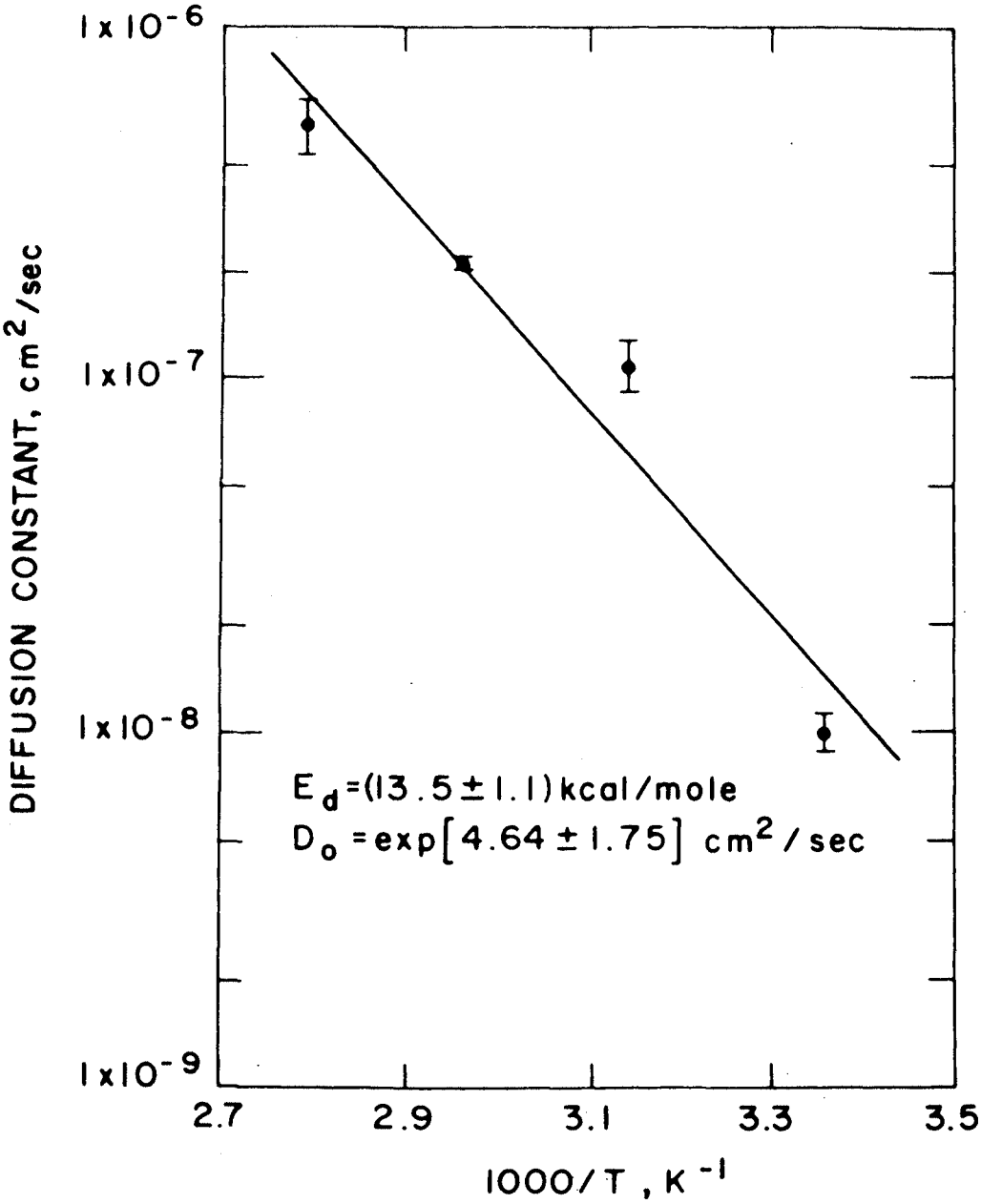

Figure 8-10. Temperature Dependence of the OFN/Kraton Diffusion Constant

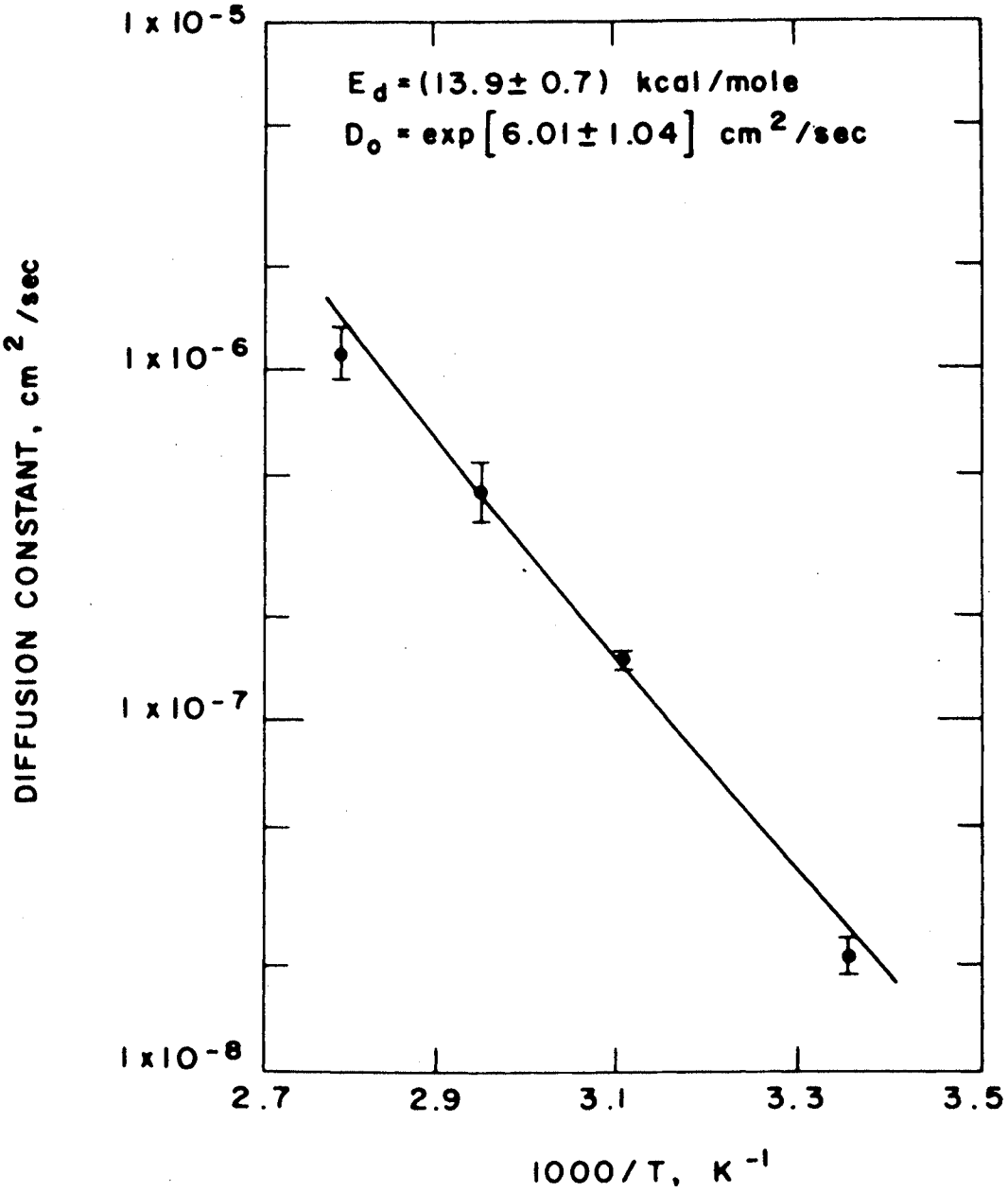

Figure 8-11. Temperature Dependence of the DFBP/Atlas Diffusion Constant

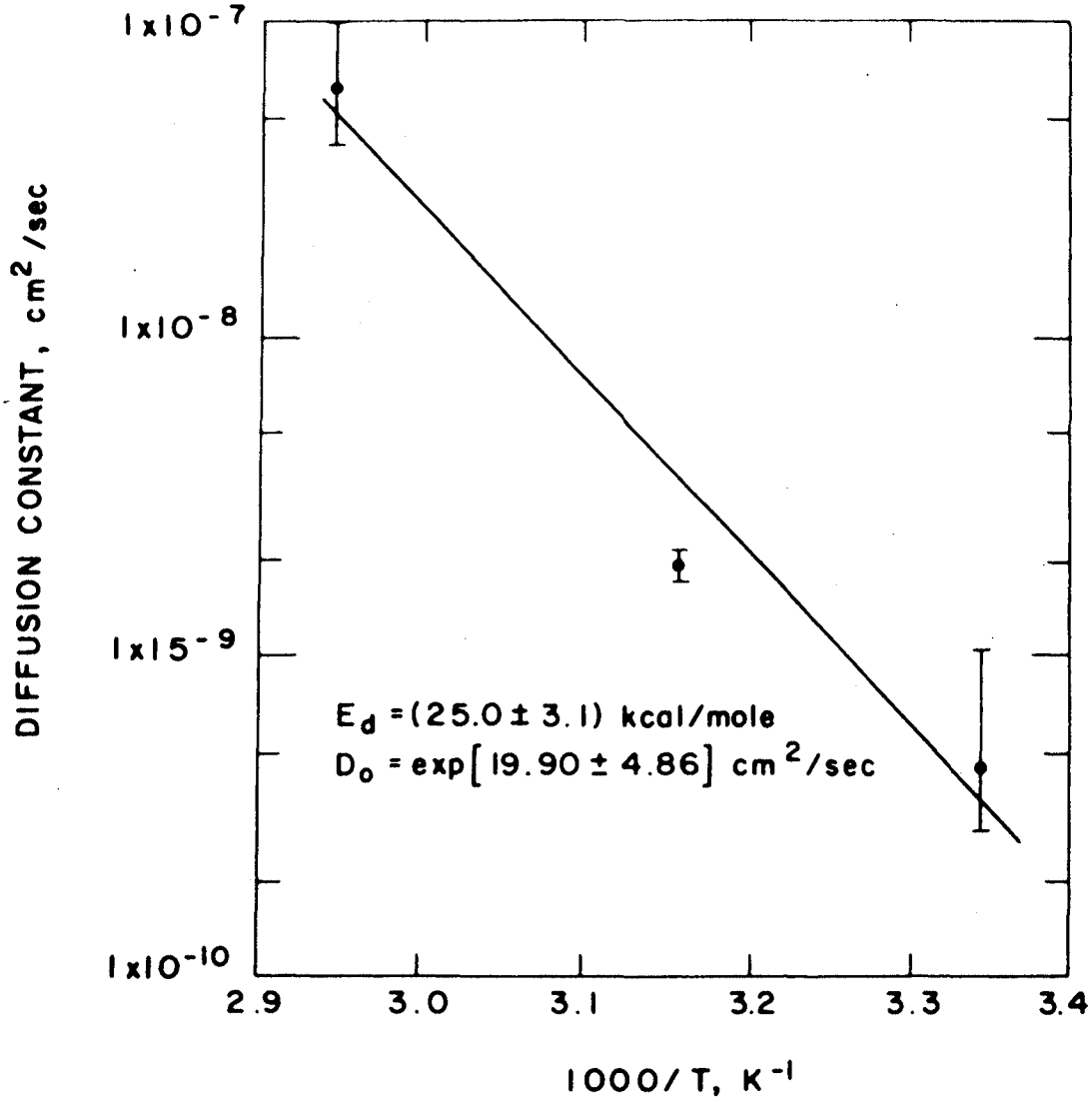

Figure 8-12. Temperature Dependence of the FC-72/Viton Diffusion Constant

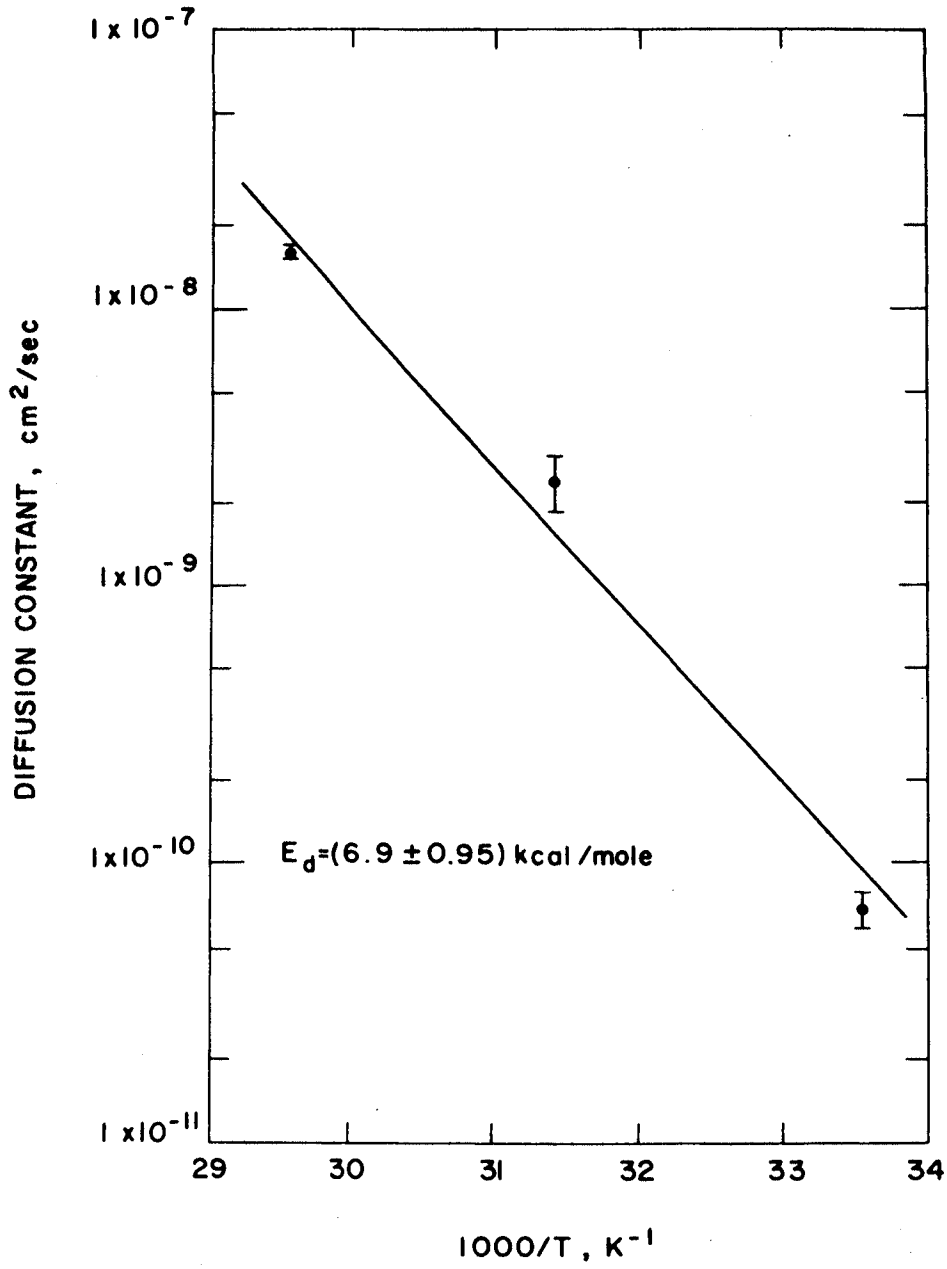

Figure 8-13. Temperature Dependence of the PMCH/Viton E60-C Diffusion Constant

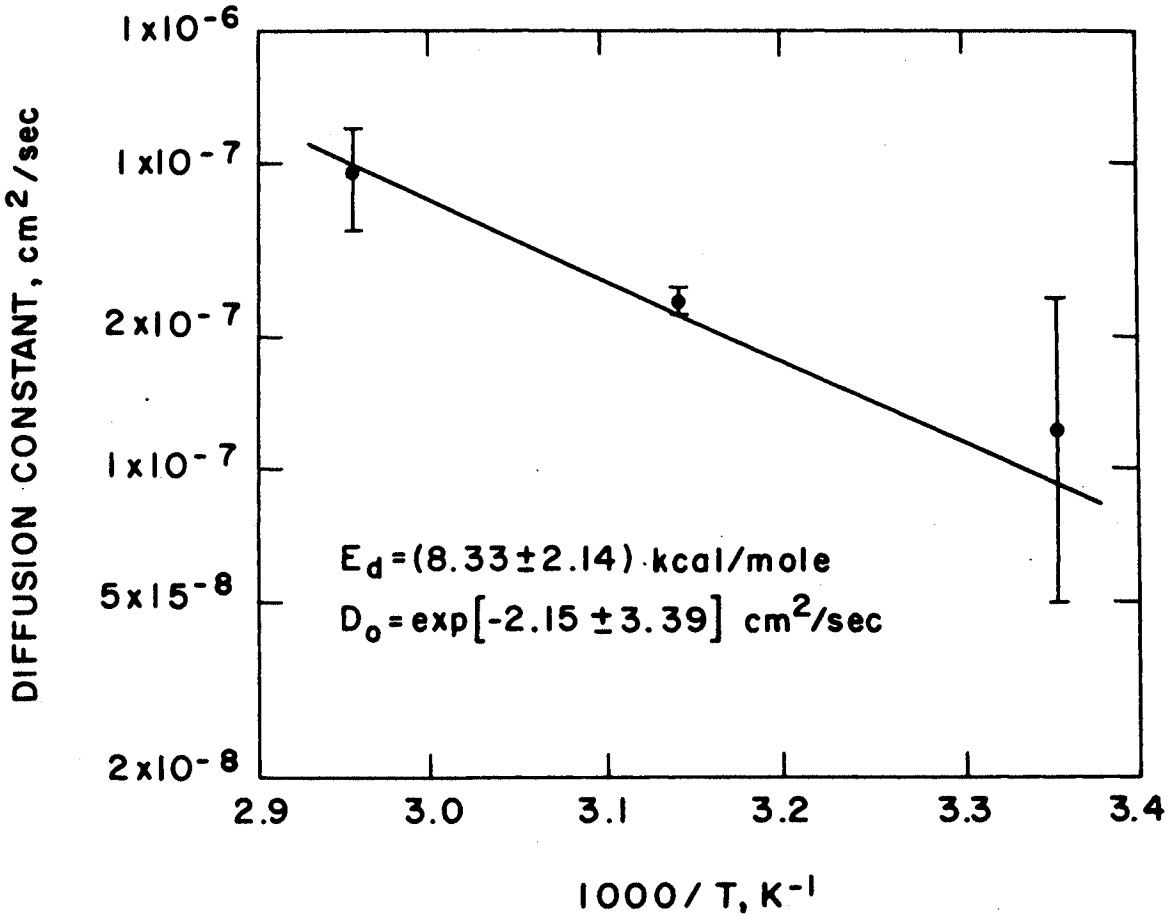

Figure 8-14. Temperature Dependence of the DFCH/Atlas Diffusion Constant

IX. TAGGANT EMISSION RATES FROM MICROENCAPSULATED VAPOR TAGGANTS

Vapor tagging of explosives for predetonation detection can be accomplished with the use of microencapsulated perfluorocarbon chemical taggants. Taggant-containing microcapsules can be blended into bulk explosives at 0.05 to 0.10 percent or into the blasting cap end closures, both at the time of manufacture. The microcapsules can also be coated on adhesive labels which adhere to bulk explosives and blasting caps. Once incorporated into or on bulk explosives, vapor taggants permeate the microcapsule membrane and provide a detectable and uniform source of vapor taggant. The vapor taggant permeation rate (emission rate) from the microcapsules is constant as long as there is vapor taggant perfluorocarbon liquid remaining inside the microcapsule. Taggant microencapsulation is a preferred mode of tagging, because taggant permeation rates are presumed constant, whereas vapor tagging by solubilization into a blasting cap end closure has a $(\text{time})^{-1/2}$ emission rate dependence. Thus, in order for this technique to be successful, microencapsule polymeric membrane chemical composition and thickness has to be selected which will provide a taggant emission lifetime of at least 5 years at a sufficient emission rate (1 to 10 nl/min).

The experiments performed led to a determination of the vapor taggant emission rates for various microencapsulated taggant batches as provided by the microcapsule manufacturers. Approximately 50 discrete microcapsule batches were examined.

A. GELATIN WALLED MICROCAPSULES: SAMPLE BATCH NUMBERS AC1093 AND AC1094

The emission rate of hexafluorobenzene (HFB) containing gelatin microcapsules, sample numbers AC1093 and AC1094, was examined chromatographically and by measurement of the increase in absolute pressure over

a microcapsule sample with a quartz spiral manometer (Dietz and Smith, 1976). The microencapsulated samples were packed in a section of 1/4-in. copper tubing.

The emission rate of sample AC1093 was examined chromatographically by flowing a stream of N_2 through the microcapsule packed tube to sweep out the permeated HFB. The emission rate ranged from about 250 nl/min-g to a low of about 10 nl/min-g and was found to be erratic with time. It was observed that the emission rate would increase sharply when the tube containing the microcapsules was slightly disturbed and would decrease again if left undisturbed. A sharp rap with the fingers on the sample tube resulted in a great increase in the emission rate (too great to be determined due to EC detector saturation) and it would take several hours before the rate would return to previous rates. Evidently, sample AC1093 was quite fragile and any slight physical disturbance would rupture some microcapsules allowing them to release their HFB loads, greatly increasing the measured emission rate. Sample AC1094 was also examined chromatographically and the emission rate was relatively constant. However when the tube containing the microcapsules was rapped the emission rate would similarly increase sharply, but to not as a great a degree as AC1093. Thus, the AC1094 sample was fragile but not as fragile as the AC1093 sample.

The HFB emission rates as determined by the quartz spiral manometer are more precise since the technique allowed the microcapsules to remain motionless, with no N_2 flowing through the microcapsules. The calculated HFB emission rates as determined by this method are given in Table 9-1. All of the experimental runs of AC1093 were characterized by two or three episodes of brief periods of high emission rates (100 to 150 nl/min-g) possibly corresponding to the disintegration of a microcapsule with its consequent release of HFB. The HFB emission rates are clearly not constant with time, decreasing over a period of a week. There were

Table 9.1. HFB Emission Rate from Gelatin Walled Microencapsulated HFB

Run No.	Date	Time	Emission rate (nl/min-g)	Length of Run (hr)
Sample AC1093 (sample size 880 mg)				
1	11/22/78	Morning	80.0 ± 10.5	4:10
2	11/22/78	Afternoon	50.3 ± 7.8	3:00
3	11/23/78	Morning	34.3 ± 6.6	3:20
4	11/23/78	Afternoon	23.4 ± 6.3	3:20
5	11/29/78	Day	10.8 ± 4.1	7:30
6	11/29-30/78	Night	40.1 ± 1.26	16:00
Average			38 ± 4	
Sample AC1094 (sample size 1309 mg)				
1	12/13-14/78	Night	4.14 ± 0.29	18.00
2	12/14-15/78	Night	2.51 ± 0.42	17:00
3	12/15-16/78	Night	2.72 ± 0.37	16:00
Average			3.4 ± 0.5	

no episodes of high emission rates with the AC1094 sample compared to the AC1093 sample. The emission rate was relatively constant from day to day.

Experimentally, the quartz manometric system can determine the emission rate down to 1 nl/min per gram of sample. With large samples (~5 g) a rate of 0.2 nl/min-g represents a lower limit of accurate determination. However for these samples, the precision of the emission rate determination was largely controlled by the fragility of the microencapsulated HFB.

Clearly, a result of this examination strongly implies that these gelatin microcapsules are too fragile to be used as microencapsulated sources of vapor taggants.

B. NATIONAL CASH REGISTER (NCR) COATED LABELS

Labels coated with vapor taggant-containing microcapsules (made by NCR) were received for chromatographic determination of their taggant emission rates. Each label was placed in a cell which was continuously purged with N_2. The N_2 exiting the cell contained the released taggant and was subsequently analyzed. The analysis was performed over a period of several months in order to examine the time dependence of the emission rate, which for permeation was expected to be constant with time. The resulting emission rates are given in Table 9-2 for the HFB microcapsule coated labels. The emission rate is indeed not constant with

Table 9-2. Hexafluorobenzene (HFB) Emission Rates from NCR Coated Labels

Sample Number	Initial HFB Loading, mg/in.^{2}	Emission rate (nl/min-in.^{2})			
		1/16	3/27	6/1	10/17
3046-L	2.3	4.5	6.0	0.085	---
3046-M	4.6	5.5	5.4	0.05	---
3046-H	6.7	4.3	12.1	0.17	---
3051-L	2.3	1.2	3.8	0.05	---
3051-M	4.6	6.2	5.8	1.01	1.19
3052-L	2.3	2.2	2.3	0.0024	---
3052-M	4.6	34.0	0.3	0.063	---
3052-H	6.7	1.5	0.5	0.31	---
3056-L	8.9	13.7	1.4	0.44	---
3056-M	13.1	17.0	10.6	2.44	3.02
3056-H	20.5	20.5	14.0	8.08	5.19

time as seen in the results. Apparently, the microcapsules are being depleted. Similar results are seen for the PDCH and DFMB (1,3 di-trifluoromethylbenzene) containing microcapsule coated labels as tabulated in Table 9-3. Thus these taggant emitting adhesive labels appear unsuitable for the vapor tagging of explosives. However, samples 3051-M, 3056-M, and 3056-H potentially could be used as taggant sources.

Table 9-3. Emission Rates from NCR Coated Labels

Sample Number	Initial PDCH Loading, mg/in.^{2}	Emission Rate nl/min-in.^{2}			"Lifetime" days*
A. Perfluorodimethylcyclohexane (PDCH) coated labels					
		3/9	6/1	8/16	
3097-L	8.8	3.8	0.03	0.67	103
3097-M	13.9	24.5	0.17	1.26	22
3097-H	17.6	5.6	0.15	0.17	19
B. 1,3 Di-trifluoromethylbenzene (DFMB) coated labels					
		3/23		8/16	
3098-L	9.1	0.06		0.25	30.2
3098-M	15.0	0.84		0.04	3.56
3098-H	22.2	0.41		0.002	10.8

*Lifetime as calculated on 3/9 in Part A and on 3/23 in Part B assuming "zero order" emission rates.

C. 3M MICROCAPSULES

Taggant containing microcapsules, manufactured by 3M, were received for examination. The capsule membrane material was a urea-formaldehyde polymer. The microcapsules were packed in 1/4-in. tubing and continuously purged with N_2 to remove the released taggant for subsequent chromatographic analysis. For the first week after receiving the samples, and for the first analysis, they were purged with dry N_2 and afterwards with 95 percent relative humidity N_2, made by bubbling dry N_2 through a saturated KNO_3 solution (List, 1971). This study was to ascertain the effect of a change in relative humidity on the emission rate.

The emission rates were found to be relatively constant over the 6-month analysis period and they are tabulated in Table 9-4. The microcapsules were not as fragile as with the earlier samples, and humidity did not seem to effect the emission rates. Sample L-4445 appears to meet the requirements for a microencapsulated taggant and consequently has been used to vapor tag some simulated bulk explosives, which are discussed in Section E. The L-4449 microcapsules containing OFT were discontinued from the study due to high OFT adsorption loss and L-4463 and L-4464 microcapsules containing L-4412 discontinued due to the low L-4412 sensitivity to ECD detection.

D. CAPSULATED SYSTEMS, INC., (CSI) MICROENCAPSULATED PERFLUOROCARBON SAMPLES

Microencapsulated samples made by CSI were received over a period of 5 months for analysis. Each sample had a slightly different membrane formulation so as to determine the optimum membrane to satisfy the emission rate requirement. When the microcapsules were initially received they were placed overnight in a vacuum oven at 40°C so as to

Table 9-4. 3M Microencapsulated Taggants

Date Analyzed	Sample Number and Taggant Core (Taggant Emission Rates (nl/min-g)				
	L-4445 (PDCH)	L-4449 (OFT)	L-4463 (L-4412)	L-4464 (L-4412)	Relative Humidity
11/15	41.6 ± 0.8	17.4 ± 2.4	--	--	0%
11/22	18.9 ± 0.5	15.5 ± 0.7	--	--	0%
12/12	0.82 ± 0.10	35.8 ± 3.7	--	--	95%
1/ 9	18.7 ± 5.3	1.22 ± 0.61	--	--	95%
3/ 8	11.9 ± 2.4	--	--	--	95%
4/12	36.3 ± 1.2	--	49 ± 6	7.4 ± 0.5	95%
Average	25 ± 5				

remove any residual taggant remaining on the outer microcapsules surfaces. Afterwards, they were placed in 1/4-in. tubing and continuously purged with N_2. For the first two weeks the N_2 was dry, but afterwards, it had a 95 percent relative humidity as described earlier. The emission rates were determined chromatographically from the N_2 purge gas.

The resulting emission rates, as tabulated in Tables 9-5a and 9-5b, show rather large variations. The large fluctuations between different determinations and the large relative standard deviations are inherent to the microcapsule samples and not the chromatographic analysis technique. Standards which were analyzed with the microcapsules showed a 5 percent analysis precision. These fluctuations may be due to the large temperature dependence of the emission rate since the analysis was done without temperature regulation. The reasons for these large fluctua-

Table 9-5. Emission Rates of CSI Microencapsulated Samples

A. PDCH Emission Rates (nl/min-g)

Set 1	Batch Numbers				
Date of Measurement	59-41A	59-42	59-43A	59-44A	Relative Humidity
12/08/78	8.8 ± 0.9	18.6 ± 1.8	0.62 ± 0.10	2.3 ± 0.9	0%
12/29/78	29 ± 5	5.8 ± 1.8	167 ± 4.4	24.2 ± 6.9	95%
01/25/79	14.6 ± 14.8	16.5 ± 3.6	55.1 ± 6.8	9.4 ± 2.7	95%
02/20/79	0.26 ± 0.06	6.3 ± 0.9	1.7 ± 0.6	6.6 ± 0.3	95%
03/08/79	2.2 ± 0.4	2.8 ± 0.4	0.34 ± 0.17	0.23 ± 0.04	95%
04/06/79	--	3.0 ± 1.1	0.37 ± 0.15	0.23 ± 0.02	95%
04/09/79	0.32 ± 0.03	--	--	--	95%

Set 2	Batch numbers				
	59-45B	59-45A	70-1B	70-4	Relative Humidity
12/26/78	9.0 ± 3.5	61 ± 5	240 ± 70	220 ± 40	0%
01/30/79	--	8 ± 7	--	--	0%
02/01/79	380 ± 100	--	350 ± 140	--	95%
02/09/79	--	11 ± 6	--	7.5 ± 0.5	95%
02/12/79	2.3 ± 1.2	--	--	--	95%
02/15/79	1.7 ± 0.4	29 ± 5	2.3 ± 1.0	9.2 ± 1.8	95%
03/07/79	1.87 ± 0.22	2.9 ± 2.1	1.06 ± 0.06	1.78 ± 0.21	95%
04/06/79	--	0.22 ± 0.02	--	0.26 ± 0.03	95%
04/09/79	0.36 ± 0.10	--	0.14 ± 0.06	--	95%
04/30/79	--	0.05	0.081 ± 0.05	0.33 ± 0.06	95%

Table 9-5. Emission Rates of CSI Microencapsulated Samples (continued)

A. PDCH Emission Rates (nl/min-g)					
Set 3	Batch Number				
Date	70-7	66-28	66-25	66-29	Relative Humidity
1/03/79	26 ± 6	10.8 ± 0.6	110 ± 40	12 ± 6	0%
1/29/79	21 ± 15	38 ± 21	47 ± 19	45 ± 51	0%
1/30/79	--	--	--	57 ± 35	0%
2/09/79	--	40 ± 15	15.8 ± 2.8	--	95%
2/12/79	--	--	--	7.3 ± 1.6	95%
2/14/79	11.6 ± 0.7	3.00 ± 0.24	--	4.5 ± 1.2	95%
3/07/79	54 ± 8	0.44 ± 0.13	--	0.68 ± 0.21	95%
3/08/79	--	--	0.24 ± 0.08	--	95%
4/06/79	43.9 ± 0.6	--	--	32 ± 12	95%
4/09/79	--	0.70 ± 0.32	6.9 ± 1.7	--	95%
4/25/79	280 ± 60	--	1.7 ± 1.6	0.65 ± 0.45	95%
4/30/79	--	0.71 ± 0.17	--	--	95%

Table 9-5. Emission Rates of CSI Microencapsulated Samples (continued)

A. PDCH Emission Rates (nl/min-g)

Set 4	Batch Number						
	66-39	66-38	66-34	66-42	70-1BH	S-11534-28*	Relative Humidity
2/16/79	19.1 ± 2.5	1.3 ± 0.4	--	4.1 ± 0.9	21 ± 7	292 ± 9	0%
2/22/79	14.5 ± 2.0	10.2 ± 1.9	281 ± 19	9.4 ± 0.7	20.5 ± 2.1	68 ± 3	95%
3/06/79	7.6 ± 0.3	0.61 ± 0.03	34 ± 7	2.51 ± 0.03	15.7 ± 3.1	23 ± 7	95%
3/08/79	1.94 ± 0.3	0.31 ± 0.04	44 ± 13	3.0 ± 0.4	20 ± 6	134 ± 17	95%
3/30/79	2.7 ± 1.5	4.6 ± 0.8	47 ± 13	3.9 ± 0.6	8.1 ± 1.2	240 ± 50	95%
4/13/79	5.6 ± 1.1	3.1 ± 0.7	55 ± 20	0.98 ± 0.11	94 ± 30	92 ± 30	95%

B. Various Taggant Emission Rates

Set 5	Batch Number and Taggant					
	73-7 (PDCH)	73-8 (PDCH)	73-9 (OFT)	73-10 (OFT)	73-11 (OFT)	Relative Humidity
2/23/79	35.5 ± 1.2	20.8 ± 1.7	--	--	--	0%
2/26/79	--	--	2.39 ± 0.09	23.6 ± 1.6	--	0%
3/02/79	--	4.1 ± 1.5	--	--	--	95%
3/05/79	0.71 ± 0.05	--	--	--	--	95%
3/21/79	--	--	--	--	19.5 ± 1.5	95%
4/16/79	4.5 ± 1.3	0.68 ± 0.08	--	--	--	95%

*SRI-supplied sample.

Table 9-5. Emission Rates of CSI Microencapsulated Samples (continued)

B. Various Taggant Emission Rates

Set 6	Batch Number and Taggant			
	73-16 (PDCH)	73-18 (PDCH)	75-3 (PDCB)	Relative Humidity
2/23/79	30.8 ± 1.8	55.7 ± 1.1	--	0%
2/26/79	--	--	0.46 ± 0.13	95%
3/02/79	12.2 ± 3.2	8.1 ± 1.4	0.12 ± 0.04	95%
4/09/79	1.26 ± 0.11	4.5 ± 0.6	--	95%
4/26/79	0.64 ± 0.18	1.7 ± 0.6	0.38 ± 0.10	95%

Set 7	Batch Number and Taggant					
	70-22 (PDCB)	70-25 (PDCB)	S-11534-30*+ (PFD)	S-11534-32* (PMCH)	S-11534-34* (PDCH)	Relative Humidity
3/27/79	39.80 ± 0.15	15 ± 4	--	262 ± 2	373 ± 23	0%
4/04/79	175 ± 23	3.9 ± 0.6	--	1450 ± 5	1500 ± 350	95%
4/20/79	303 ± 27	0.35 ± 0.07	--	101 ± 6	150 ± 40	95%
5/17/79	85 ± 6	0.11 ± 0.01	--	1084 ± 8	474 ± 3	95%

*SRI-supplied sample.
+Received, not tested.

Table 9-5. Emission Rates of CSI Microencapsulated Samples (continued)

B. Various Taggant Emission Rates

Set 8a	Batch Number and Taggant					
	70-19 (PDCB)	73-21 (PDCH)	73-25 (PDCH)	73-26 (PDCH)	73-31 (PDCH)	Relative Humidity
3/27/79	1336 ± 8	12.9 ± 1.5	114 ± 13	19 ± 5	28 ± 6	0%
4/04/79	151 ± 12	14 ± 6	3.1 ± 1.7	--	90 ± 18	95%
4/05/79	--	--	--	2.8 ± 2.0	--	95%
4/16/79	--	--	--	--	0.52 ± 0.06	95%
4/17/79	91 ± 5	0.33 ± 0.11	29 ± 14	0.66 ± 0.24	--	95%
4/30/79	0.36 ± 0.03	0.74 ± 0.26	0.85 ± 0.34	0.74 ± 0.13	0.22 ± 0.06	95%

Set 8b	Batch Number and Taggant					
	73-32 (PDCH)	73-33 (PDCH)	73-34 (PDCH)	73-35 (PDCH)	73-36 (PDCH)	Relative Humidity
3/27/79	52.7 ± 3.5	15.2 ± 3.8	18 ± 9	9.4 ± 1.5	260 ± 136	0%
4/04/79	53 ± 10	25 ± 8	--	8.6 ± 0.06	400 ± 160	95%
4/05/79	--	--	4.8 ± 0.4	--	--	95%
4/16/79	--	--	--	--	--	95%
4/17/79	450 ± 180	1.4 ± 0.5	4.4 ± 1.0	9 ± 5	4.7 ± 1.1	95%
4/30/79	0.8 ± 0.5	0.28 ± 0.05	7 ± 3	1.8 ± 0.3	1.1 ± 0.5	95%

Table 9-5. Emission Rates of CSI Microencapsulated Samples (continued)

B. Various Taggant Emission Rates							
Set 9	Batch Number and Taggant						
	73-39 (PDCH)	73-43 (PDCH)	73-42 (PDCH)	73-40 (PDCH)	73-39H (PDCH)	73.41 (PDCH)	Relative Humidity
4/03/79	600 ± 50	26.2 ± 0.7	24.7 ± 3.1	10.8 ± 1.0	777 ± 21	8.2 ± 1.2	0%
4/12/79	204 ± 26	1.64 ± 0.08	4.1 ± 0.7	68 ± 16	65 ± 10	11.7 ± 1.7	95%
4/20/79	0.80 ± 0.08	0.16 ± 0.06	8.2 ± 0.7	1.7 ± 0.7	2.1 ± 0.1	0.5 ± 0.1	95%
4/30/79	27 ± 6	0.76 ± 0.12	0.35 ± 0.14	1.18 ± 0.21	0.72 ± 0 08	3.0 ± 0.5	95%

tions are a subject of investigation by Aerospace and the microcapsule manufacturers. Purge gas relative humidity was also found to have an effect on the emission rate, initially increasing it by a factor of two or three and afterwards, over a period of several weeks, the taggants rates would decrease to their earlier levels. None of the examined CSI microcapsules had a constant taggant emission rate and all appear to be slowly approaching a very low taggant emission rate. An exception was the OFT microcapsules in which it appeared that the microcapsule membrane was slowly dissolving. Consequently, all of these CSI microcapsules are unacceptable for use as microencapsulated taggant sources in explosives.

E. MICROCAPSULE TAGGED CAP-SENSITIVE, PACKAGED EXPLOSIVE SIMULANTS

Vapor tagged cap-sensitive, packaged explosive simulants were prepared during November 1978 by incorporating the batch L-4445 microencapsulated PDCH. These simulants are described in Table 9-6 along with the amount of microencapsulated taggant that was blended into each sample, and a description of the tagged explosive wrapper marking. These samples were simulants in the sense that the EGDN or NG had been excluded during manufacture and a closely chemically related but inert compound had been substituted. The PDCH emission rates from these samples were recorded for 6 months and the chromatographically determined emission rates are tabulated in Table 9-7 with the averaged emission rates. The PDCH emission rates show a large variation from measurement to measurement which is probably due to the temperature dependence of the L-4445 PDCH permeation rate. Nonetheless, the apparent overall consistency of the PDCH taggant emission rate demonstrates the ability to tag bulk explosives by incorporation of microencapsulated taggant into the explosive. Another potential taggant, PMCH, is present as an impurity in PDCH at about 5 to 20 percent depending on the source of PDCH. Thus, the PDCH-tagged samples emit PMCH and the emission rates of PMCH as determined chromatographically are given in Table 9-8.

Table 9-6. Microcapsule Tagged Bulk Explosive Simulants (Power Primer Formula)

Sample Number	PDCH Microcapsule Weight Percent	Cartridge Wrapper (dimensions in.)	Wrapper Designation
A01	0.05	White Plastic	Power Primer
A02	0.05	Waxed Paper (1 x 12)	Powerdyn X
A03	0.10	Waxed Paper (1 x 12)	Powerdyn X
A04	0.10	Waxed Paper (1-1/2 x 12)	Extra Gelatin
A05	0.10	Waxed Paper (1 x 8)	Permissible Gelatin
A06	0.05	Waxed Paper (1 x 8)	Permissible Gelatin
A07	0.05	Waxed Cartridge (2 x 14)	Floridyn
A08	0.10	Waxed Cartridge (2 x 14)	Floridyn
A09	0.05	Waxed Cartridge (2 x 5)	Super Prime 16L
A010	0.10	Waxed Cartridge (2 x 5)	Super Prime 16L

F. MICROCAPSULE BLENDED IN BLASTING CAP END CLOSURES

Two samples of the elastomer used by Atlas in their blasting cap plugs blended with the L-4500 microcapsules (3M Company) were prepared in order to examine the feasibility of tagging blasting caps by incorporating taggant containing microcapsules. This technique overcomes the negligible solubility of several promising taggants, such as PDCB, PMCH, or PDCH, in the present blasting cap plug material. The microcapsules were blended in during the milling of the elastomer in place of the usual inert fillers. One sample was subsequently cured while the other sample remained uncured. Emission rates of the taggants from the microcapsule containing elastomers were measured gravimetrically daily.

Table 9-7. PDCH Emission Rate from the Microcapsule Tagged Bulk Explosives Simulant Sticks

Sample Number	Loading %	PDCH Emission Rate nl/min-stick 1/23-25/79	3/1/79	3/29/79	4/18-19/79	5/11-14/79	6/19-20/79	6/29/79	7/21/79	8/14/79	Averaged PDCH Emission Rate, (nl/min)
A01	0.05	—	1.74 ± 0.33	7.2 ± 1.1	1.52 ± 0.22	2.49 ± 0.35	0.91 ± 0.20	2.3 ± 0.7	0.63 ± 0.04	1.31 ± 0.29	1.6 ± 0.7
A02	0.05	20.3 ± 5.4	10.2 ± 1.1	8.38 ± 0.24	6.02 ± 0.07	16 ± 4	2.53 ± 0.20	—	0.99 ± 0.14	1.13 ± 0.35	9 ± 7
A03	0.10	23.5 ± 3.3	3.96 ± 0.32	48.7 ± 2.3	2.91 ± 0.21	20.4 ± 1.5	34.6 ± 2.7	4.1 ± 0.8	4.4 ± 0.6	12.2 ± 0.3	18 ± 17
A04	0.10	20.7 ± 4.3	13.6 ± 1.9	12.5 ± 1.0	9.9 ± 0.6	14.3 ± 1.3	20.4 ± 0.7	27.9 ± 0.9	13.5 ± 0.1	8.00 ± 0.07	17 ± 6
A05	0.10	18.6 ± 2.6	10.4 ± 3.1	30.8 ± 2.1	3.6 ± 0.6	30.4 ± 2.9	0.48 ± 0.06	—	0.62 ± 0.09	4.95 ± 0.28	14 ± 12
A06	0.05	8.0 ± 1.6	4.0 ± 0.8	1.11 ± 0.02	1.01 ± 0.06	4.2 ± 0.6	4.00 ± 0.19	—	2.22 ± 0.33	8.43 ± 0.11	3.5 ± 2.4
A07	0.05	11.1 ± 2.1	8.7 ± 3.7	12.8 ± 1.4	0.69 ± 0.13	7.5 ± 2.1	26 ± 7	9.9 ± 0.6	2.31 ± 0.18	1.26 ± 0.07	10 ± 8
A08	0.10	13.9 ± 8.8	21.8 ± 6.2	5.23 ± 0.22	13.3 ± 1.2	18.3 ± 3.4	16.4 ± 1.8	22.5 ± 2.9	1.75 ± 0.14	0.85 ± 0.04	14 ± 7
A09	—	—	20.4 ± 6.2	4.9 ± 2.2	2.8 ± 0.3	10.5 ± 3.6	29.5 ± 2.8	26 ± 7	4.4 ± 0.6	4.0 ± 0.7	14 ± 11
A010	—	—	122 ± 0	12.4 ± 2.4	15.1 ± 1.8	27.2 ± 2.1	51 ± 6	6.75 ± 0.17	7.5 ± 0.1	3.51 ± 0.31	20 ± 17

Table 9-8. PMCH Emission Rates from the Microcapsule Tagged Bulk Explosives Simulant

Simulated Explosive Stick No.	PMCH Emission Rate (nl/min-stick)		
	6/29	7/23	8/14
A01	0.25 ± 0.08	0.100 ± 0.012	0.143 ± 0.025
A02	11.3 ± 0.8	0.42 ± 0.06	0.208 ± 0.006
A03	0.47 ± 0.11	13.7 ± 0.19	2.16 ± 0.06
A04	4.14 ± 0.13	5.3 ± 0.4	1.21 ± 0.09
A05	4.8 ± 0.3	0.233 ± 0.016	0.688 ± 0.043
A06	10.3 ± 1.4	0.723 ± 0.019	1.11 ± 0.19
A07	0.957 ± 0.018	0.59 ± 0.07	0.199 ± 0.011
A08	2.69 ± 0.20	0.502 ± 0.020	0.13 ± 0.09
A09	3.0 ± 0.9	0.8 ± 0.5	0.411 ± 0.063
A010	0.684 ± 0.005	1.22 ± 0.14	0.288 ± 0.021

The results are displayed in Figures 9-1 and 9-2 for the cured and uncured elastomers respectively with the total taggant lost being plotted on the vertical axis and the square root of the time elapsed since arrival at BNL being on the horizontal axis. The square root of time dependence was found to be the best fit to the data with the displayed straight line being a least squares fit to the experimental data. The $(\text{time})^{1/2}$ dependence implies a diffusion mechanism which is controlling the rate of taggant emission. What has apparently happened is that a large percentage of the microcapsules were crushed during the milling procedure and the released taggant was solubilized into the elastomer. This solubilized taggant is now being emitted at a diffusion controlled rate until most of the solubilized taggant is depleted from the elastomer. When this has happened, the taggant will be released at a rate dependent on the taggant permeation rate of the microcapsule which

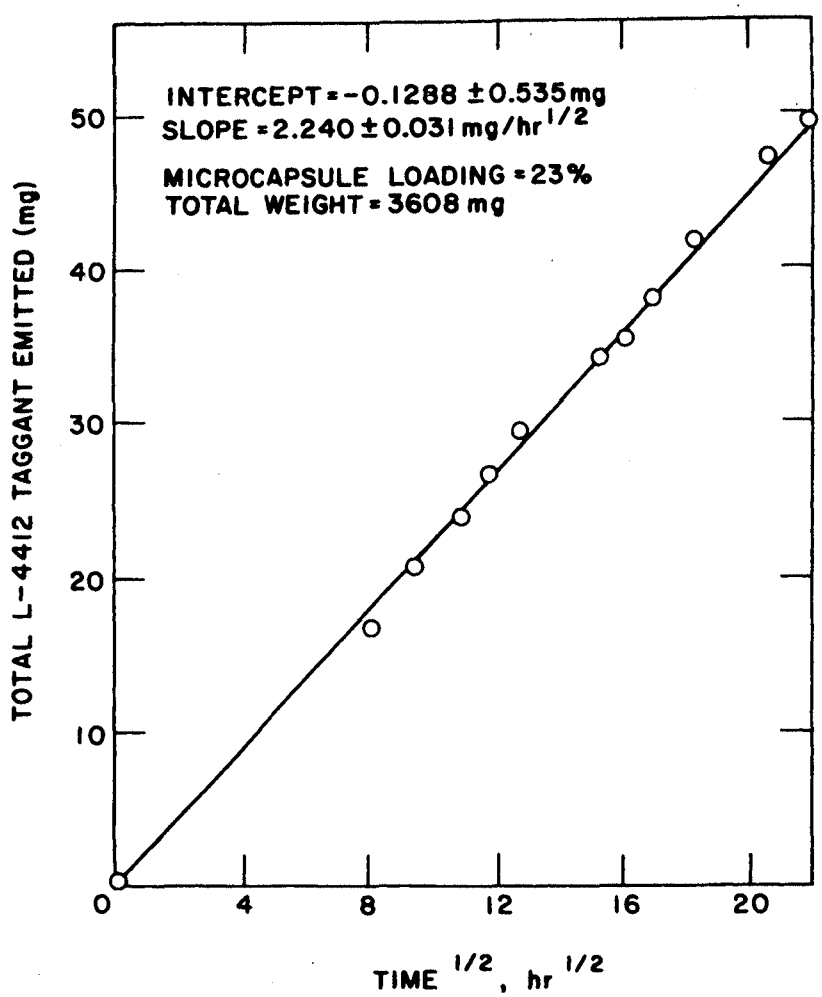

Figure 9-1. Uncured Microencapsulated Loaded Elastomer (L-22C)

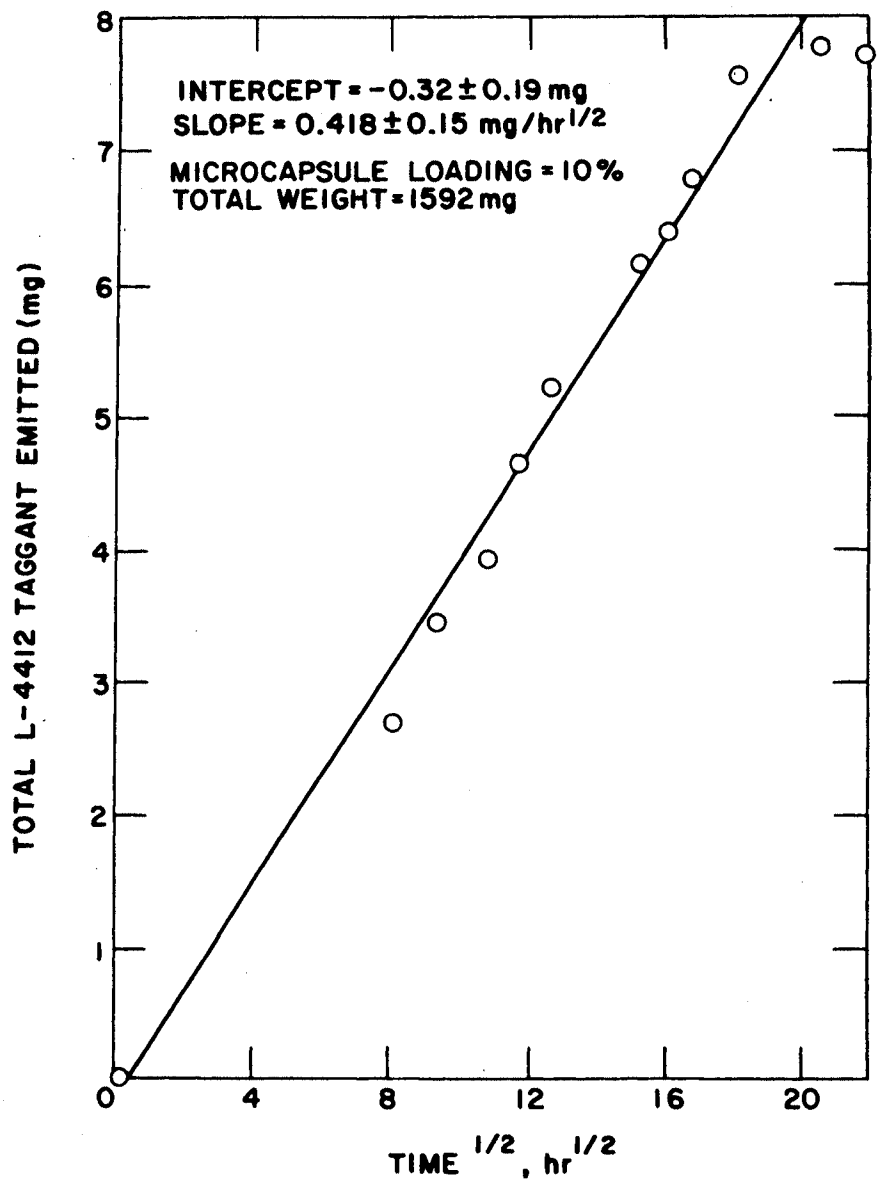

Figure 9-2. Cured Microcapsule Elastomer (L-22D)

has a no time dependence (zero order dependence). Indeed, as shown in Figure 9-2 for the cured elastomer, the rate has slowed down to the permeation rate, indicating that most of the solubilized taggant has been depleted. Of course, in the now present steady-state permeation mode, there will be a slight amount of taggant still solubilized in the elastomer which should be constant with time. This permeation rate is too low to be measured gravimetrically. The other sample, L-22C, has not yet been depleted. This is reasonable since it is solubilized with higher percentage of microcapsule and would take a longer time to be depleted assuming an equal percentage of crushed microcapsule for both samples.

This initial attempt to incorporate microcapsules into elastomers was not at all successful due to the lack of mechanical strength of the microcapsule used in preparation of the tagged end closure.

Presently, the principal result of the microencapsulated taggant emission rate determinations is that it is possible to fabricate a microencapsulated taggant with the required emission rate and lifetime, a successful example of which is the L-4445 PDCH containing microcapsule. This has been successfully used to vapor tag bulk explosives, as demonstrated by their successful use in two field tests (Senum et al., 1979c and Senum et al., 1978b). The first and second field tests involved the detection of these tagged explosives inside various luggage items with the use of a baggage examiner. The third field test involved the detection of these bulk explosives on a DC-9. (See Appendix D for descriptions of these field tests.)

X. CONCLUSION

Twenty-one fluorinated chemical compounds have been evaluated for use as vapor taggants for the predetonation detection of explosives. These fluorinated compounds (potential vapor taggants) were examined with respect to several requirements necessary for the successful predetonation detection of vapor-tagged explosives. Vapor taggants were examined for three methods of explosives vapor tagging:

- Solubilizing vapor taggants into blasting cap end closures,
- Blending of blasting cap end closure with microencapsulated vapor taggants, and
- Blending of packaged, cap-sensitive explosives with microencapsulated vapor taggants.

The first method represents the primary focus of this program. All three methods are intended to accomplish predetonation detection of explosives by the subsequent slow release of the vapor taggant from the tagged explosive with the consequent detection of the taggant vapor.

Common to these three vapor tagging methods are several general requirements for vapor taggants. The first requirement was that candidate vapor taggant molecular properties allow detection at the required sensitivity. This specification required the use of fluorinated compounds that have a high sensitivity to electron capture detection (ECD) and led to the initial selection of the 21 potential vapor taggants. A low ambient background, to ensure the detection of the vapor taggant in all detection scenarios, was the second requirement. The third general requirement was for low toxicity; this eliminated OFN, PFP, and HFB as vapor taggants. Other vapor taggants, especially the

other fluoroaromatics, may also be eliminated for this reason because toxicity data were not available for all of the proposed taggants and these compounds as a class are those most likely to be toxic. The fourth general requirement was that the selected vapor taggants have a negligible adsorption loss onto surfaces that might be present in detection scenarios. This led to the elimination of OFN, OFT, and DFBP as potential vapor taggants. Several other potential vapor taggants were eliminated for other reasons: FC-77 was eliminated because it is not a pure compound but rather a mixture of compounds; FC-78, E-1, and E-2 were eliminated because of their thermal instability in the Palladium catalyst used in the ECD detection apparatus; PFX was not considered in great detail due to its relative scarcity and high cost. The 10 remaining proposed vapor taggants were examined with respect to each of the requirements for the specific explosives tagging technique.

A. SOLUBILIZATION OF THE VAPOR TAGGANT INTO THE BLASTING CAP END CLOSURE

The specific requirement for a vapor taggant for blasting cap end closure solubilization is that the vapor taggant have a sufficient solubility in the end closure and an emission rate from the tagged blasting cap so as to ensure a 0.5- to 5-nl/min emission rate over a 5-year period after fabrication. This requires a 5 percent by weight minimum solubility of the vapor taggant chemical into the end closure. If the vapor taggant did not have an acceptable solubility in the present end closures, then it was rejected even though it might have an initial acceptable emission rate. Eventually the taggant would be depleted from the end closure before its required 5-year lifetime due to its low solubility.

1. Present End Closures

The acceptability of the 10 remaining potential vapor taggants as solubilized into the presently used end closures is given in Table 10-Part A. There are no acceptable vapor taggant chemicals meeting all selection criteria for the duPont Buna or Hercules Kraton end closures and only one marginal candidate, OFCP, for the Atlas rubber end closure. If the emission lifetime requirement is lowered from 5 years to years, an acceptable vapor taggant for Hercules Kraton end closures would be PFD. Nonetheless, there is no acceptable taggant for the duPont Buna end closure. Based on the results of this study, it is improbable that a vapor taggant exists which will vapor tag all three present end closures.

2. Substitute End Closures

The replacement of the present end closure with a substitute end closure would allow a single vapor taggant to be used for the three blasting cap manufacturers. The acceptability results are tabulated i Table 10-1, Part B, for the taggant-Viton/Fluorel and Fluorosilicone combinations. Most of the 10 taggants have an acceptable solubility i the substitute end closure; however, the resulting taggant emission rates for these taggant-substitute end closure combinations are below the required 0.5- to 5-nl/min specification. Again, if the emission lifetime requirement is relaxed to 3 years instead of 5 years, then th combinations, L-4412 with Viton or Fluorel, are acceptable in terms of both solubility and emission rate.

In conclusion, for the technique of taggant solubilization into t blasting cap end closure, there exists no single perfluorocarbon tagga chemical that would vapor tag blasting caps using the present end closure as manufactured by three different manufacturers: duPont, Atlas,

Table 10-1. Acceptability of Various Taggant End Closure Combinations

	Solubility Requirement			Emission Rate Requirement		
A. Currently Manufactured End Closures						
Taggant	DuPont Buna-N	Atlas Natural Rubber	Hercules Kraton	DuPont Buna-N	Atlas Natural Rubber	Hercules Kraton
PDCB	no	no	no	no	no	no
PMCH	no	no	no	no	no	no
DDCH	no	no	no	no	no	no*
PFD	no	no	no*	no	no	no*
DFCH	no	yes	no	no	no	no
OFCP	no	yes	no	no	marginal	no
PFO	-	-	-	-	-	-
PFPT	-	-	-	-	-	-
FC-72	no	no	no	no	no	no
L-4412	no	no	-	no	no	-
B. Substitute End Closures						
Taggant	Viton or Fluorel	Fluorosilicone 35	Fluorosilicone 70	Viton or Fluorel	Fluorosilicone 35	Fluorosilicone 70
PDCB	yes	yes	yes	no	no	no
PMCH	yes	yes	yes	no	no	no
PDCH	yes	yes	yes	no	no	no
PFD	no	-	-	no	no	no
DFCH	yes	-	-	no	no	no
OFCP	yes	-	-	no	no	no
PFO	no	-	-	no	no	no
PFPT	no	-	-	no	no	no
FC-72	yes	yes	no	no	no	no
L-4412	no	-	-	no*	no	no

*Acceptable taggant end closure combinations if the emission lifetime requirement is lowered to 3 years from 5 years.

and Hercules. The taggant OFCP is available for only the rubber end closure as used by Atlas. The substitute end closures Viton or Fluorel, however, can be vapor tagged with L-4412 taggant and would provide a marginal method for the vapor tagging of blasting caps. Viton or Fluorel fluoroelastomer must be substituted for the presently used end closures.

B. BLENDING OF PACKAGED, CAP-SENSITIVE EXPLOSIVES WITH MICROENCAPSULATED VAPOR TAGGANTS

Over 50 microencapsulated taggant samples were examined for the suitability with respect to the specified taggant emission rate, namely 1 to 10 nl/g-min. Most microcapsules were experimentally found with to be unacceptable. Only one of the investigated microencapsulated samples, L-4445 (supplied by 3M) provided an acceptable PDCH taggant constant emission rate when mixed with simulated explosives. The L-4445 microcapsule was used to vapor tag some simulated bulk explosives and successfully demonstrated the viability of vapor tagging of explosives in two demonstrations (Senum et al., 1979c and Senum et al., 1978b). (See Appendix D.) The demonstrations involved the detection of the vapor tagged explosives (1) aboard an aircraft by grab bag sampling at the outflow valves and (2) in luggage by means of a baggage examiner. The results of these demonstrations indicate a successful predetonation detection of concealed explosives vapor tagged by microencapsulated vapor taggant incorporation into simulated explosives.

C. MICROENCAPSULATED VAPOR TAGGANTS IN BLENDED BLASTING CAP END CLOSURES

Two samples of the elastomer used by Atlas for their end closure were blended with L-4500 microencapsulated PDCH vapor taggant in an attempt to prepare vapor tagged blasting caps. The results indicated

that the microencapsulated taggants were crushed during the elastomer's milling process. With this initial attempt it was not possible to vapor tagged blasting cap elastomers by this technique. Further experimental work is needed before the viability of this technique can be determined.

D. DETECTION OF VAPOR TAGGED EXPLOSIVES CONTAINED IN BARRIERS

The detectability of vapor tagged explosives was experimentally determined not to be hindered by the containment of the explosives within four common barriers: a styrofoam filled box, a suitcase, an attache case, and a heat-sealed plastic bag. This was due to the relative lack of airtightness of these barriers. Two other barriers--a sealed new paint can and a zip-locked plastic bag--did have a significant degree of airtightness.

These results have been further corroborated by two field experiments involving the detection of vapor tagged explosives in various luggage items (Dietz et al., 1978b and Senum et al., 1979b). The various types of baggage, ranging from a soft suitcase to an aluminum suitcase with a rubber gasket, did not exhibit a degree of airtightness significant enough to impede the detection of the vapor taggant. More experimental details can be found in specific reports (see Appendix D).

The field experiments verified the conclusions of the theoretical model of barrier enclosed explosives: The taggant concentration within briefcases and suitcases from a 1-nl/min tagged explosive is of the order of parts per billion. This allows real-time continuous detection of the taggants using a taggant detection with a parts per trillion limit of detection and a sampling system having a dilution factor up to 1000.

Another conclusion of the model is that the taggant concentration attained in a moderately sized room 15 minutes following introduction of

a severe barrier containing a taggant source of 1-nl/min emission rate (placed in the room 1 hour earlier) is sufficient to allow detection by a concentrating detection scheme. A moderate barrier, such as a suitcase or box, would allow almost real-time continuous detection under the same circumstances.

It was determined by the experimental work done on this program and discussed in this report that it is feasible and technically implementable to vapor tag explosives for predetonation detection and to detect the resulting vapor in several operational scenarios.

XI. REFERENCES

3M Company, "Fluorinert Electronic Liquids," Technical Manual (1976).

Anesthesia, 19, 167, (London) (1964).

Bansal, K.M., and R.W. Fessenden, J. Chem. Phys., 59, 1760 (1973).

Biol.-Med., Izv. Sib. Otd. Akad. Nauk SSSR, Ser. Biol.-Med. Nauk, 3, 91 (1965).

Christodoulides, A.A., and L.G. Christophorou, Chem. Phys. Lett., 61, 553 (1979).

Christodoulides, A.A., L.G. Christophorou, R.Y. Pai, and C.M. Tung, J.Chem. Phys., 74, 1156 (1979).

Christodoulides, A.A., R. Schumacher, and R.N. Schindler, Ber. Bunsen Ges., 80, 965 (1976).

Christodoulides, A.A., R. Schumacher, and R.N. Schindler, Int. J. Chem. Kinet., 10, 1215 (1978).

Christodoulides, A.A., R. Schumacher, and R.N. Schindler, L. Naturforsh., 30a, 811 (1975a).

Christodoulides, A.A., R. Schumacher, and R.N. Schindler, J. Phys. Chem., 79, 1904 (1975b).

Christophorou, L.G., Chem. Rev., 76, 409 (1976).

Christophorou, L.G., D.L. McCorkle, and D. Pittman, J. Chem. Phys., 60 (1974).

Compton, R.N., L.G. Christophorou, C.S. Hurst, and P.W. Reinhardt, J. Chem. Phys., 45, 4634 (1966).

Davis, F.J., R.N. Compton, and D.R. Nelson, J. Chem. Phys., 59, 2324 (1972).

Dietz, R.N., et al., "Summary Report of the Brookhaven Explosive Tagging Program," BNL-21041, Law Enforcement Assistance Administration Contract No. LEAA-J-IAA-011-4 (February 1976a).

Dietz, R.N., E.A. Cote, and R.W. Goodrich, "Air Mass Movements Determined by Real-Time Frontal Chromatography of Sulfur Hexafluoride, in Measurement, Detection, and Control of Environmental Pollutants," IAEA-SM-206/21 pp. 277-299 (September 1976b).

Dietz, R.N., E.A. Cote, and R.W. Goodrich, "Development and Application of Sulfur Hexafluoride Measurement Capabilities at Brookhaven," Brookhaven National Laboratory Report BNL-21087 (March 1976c).

Dietz, R.N., R.W. Goodrich, and E.A. Cote, "Detection of Perfluorinated Taggants in Electric Blasting Caps by Electron Capture Monitors," Proceedings, New Concepts Symposium and Workshop on Detection and Identification of Explosives, (November 1978a). (NTIS:PB 296055)

Dietz, R.N., G.I. Senum, and R.W. Goodrich, "Evaluation of Detection of Tagged Blasting Caps Utilizing the U.S. Customs Service Automated Baggage Examiner and the Brookhaven Continuous Electron Capture Monitors," Brookhaven National Laboratory, Report No. BNL-24959 (1978b).

Dietz, R.N., and J.D. Smith, "Calibration in Air Monitoring," Calibration of Permeation and Diffusion Devices by an Absolute Pressure Method, American Society for Testing and Materials, ASTM STP 598, pp. 164-179 (1976).

Dilley, J.V., "Acute Inhalation Toxicity of Perfluorodecalin, Octafluorotoluene, and Perfluorohexylsulfurpentafluoride in Rats," Final Report, SRI International Project LSD-8044 (May 1979).

DuPont, "Freon, C-51-12 Fluorocarbon," Technical Bulletin EL-13, E.I. duPont de Nemours & Co., Inc., Wilmington, Delaware (1968a).

DuPont, "Compatibility of Plastics and Elastomers with Freon E2 and Freon E3 Fluorocarbon Liquids," Technical Bulletin EL-8C, E.I. DuPont de Nemours & Co., Inc., Wilmington, Delaware (1968b).

DuPont, "Toxicity Studies with the Freon E Series Fluorocarbons," Technical Bulletin S-38, E.I. duPont de Nemours & Co., Inc. (1968c).

Fessenden, R.W., and K.M. Bansal, J. Chem. Phys., 53, 3468 (1970).

Gant, K.S., and L.G. Christophorou, J.Chem. Phys., 65, 2977 (1976).

Grimsrud, E.P., and S.H. Kim, Anal. Chem., 51, 537 (1979).

Grimsrud, E.P., and D.A. Miller, Anal. Chem., 50, 1141 (1978).

Grimsrud, E.P., and R.G. Stebbins, J. Chrom., 155, 19 (1978).

Harland, P.W., and J.C.J. Thynne, Int. J. Spectrom. Ion Phys., 10, 11 (1973).

Harland, P.W., and J.C.J. Thynne, J. Phys. Chem., 75, 3517 (1970).

Huntingdon, "Acute Toxicity Tests for the Flutec PP Fluids," Huntingdon Research Centre, Huntingdon, England (April 1970).

I.S.C. Chemicals Limited, "Technical Properties of Flutec Liquids," Avonmouth, England (1974).

Johnson, J.P., L.G. Christophorou, and J.G. Carter, J. Chem. Phys., 67, 2196 (1976).

Lagomarsino, R.J., Letter to George A. Welford, Environmental Measurement Laboratory, N.Y. (October 11, 1977).

Lapik, A.S., and L.N. Zimina, Izv. Sib. Otd. Akad. Nauk SSSR, Ser. Biol. Med. Nauk, 3, 81-3 (1967).

List, R.J., Smithsonian Meteorological Tables, Smithsonian Miscellaneous Collections, Volume 114, Smithsonian Institution Press, Washington, D.C., Table 107 (1971).

Lovelock, J.E., and A.J. Watson, J. Chrom., 158, 123 (1978).

McReynolds, J.H., G.A. St. John, and M. Arbor, "Determination of the Concentration of Explosive Vapors from Parcels and Letters," Final Report, U.S. Postal Service Contract No. 74-00810, Stanford Research Institute (January 1975).

Miller, D.A., and E.P. Grimsrud, Anal. Chem., 51, 851 (1979).

Mortelmans, K.E., and N. Marx, "In Vitro Microbiological Mutagenicity Assays of Perfluoro-1,2-dimethylcyclobutane (PDCB)," Appendix, SRI International Project LSC-8044 (May 1979).

Mortelmans, K.E., and V.F. Simmon, "In Vitro Microbiological Mutagenicity Assays of Eight Fluorocarbon Taggant Samples," Final Report, SRI International Project LSC-8044 (February 1979).

Mothes, K.G., E. Schultes, and R.N. Schindler, J. Phys. Chem., 76, 3758 (1972).

Naff, W.T., C.O. Cooper, and R.N. Compton, J. Chem. Phys., 49, 2784 (1978).

Pai, R.Y., L.G. Christophorou, and A.A. Christodoulides, J. Chem. Phys., 70, 1169 (1979).

Pate, C.T., "Characterization of Vapors Emanating from Explosives," Final Report, Law Enforcement Assistance Administration Contract No. J-LEAA-025-73 (June 1976).

Patterson, P.L., J. Chrom., 134, 15 (1977).

Prins, W., Equilibrium Swelling Due to Sorption in the Solid-Gas Interface, Volume 2, Edited by E. Allison Flood, Marcel Dekker, New York (1967).

Sauers, I., L.G. Christophorou, and J.G. Carter, J. Chem. Phys., 71, 3016 (1979).

Senum, G.I., E.M. Ferreri, M.W. Greene, R.P. Gergley, and R.N. Dietz," The Effect of Taggant Vapor Adsorption and Containment on the Predetonation Detection of Explosives, Brookhaven National Laboratory Report BNL-27150 (October 1979a).

Senum, G.I., R.P. Gergley, E.A. Cote, and R.N. Dietz, "Detection of Tagged Explosives in a DC-9 Aircraft via Sampling of the Air Exhaust," Brookhaven National Laboratory Report No. BNL-26612 (July 1978b).

Senum, G.I., R.P. Gergley, E.A. Cote, and R.N. Deitz, "Detection of Vapor Taggants used for Explosive Predetonation Detection in a Boeing 727 Aircraft," Brookhaven National Laboratory Report BNL-27099 (October 1979).

Senum, G.I., R.P. Gergley, M. Greene and R.N. Dietz, "Vapor Tagging of Electric Blasting Caps with Perfluorinated Compounds," Proceedings, New Concepts Symposium and Workshop on Detection and Identification of Explosives, (November 1978a). (NTIS:PB 296055)

Senum, G.I., R.W. Goodrich, and R.N. Dietz, "Detection of Vapor Tagged Simulated Bulk Explosives Utilizing the U.S. Customs Service Automated Baggage Examiner and the Brookhaven Continuous Electron Capture Monitor," Brookhaven National Laboratory, Report No. BNL-26782 (1979c).

Schultes, E., A.A. Christodoulides, and R.N. Schindler, Chem. Phys., 8, 354 (1975).

Schumacher, R., C. Lygris, and R.N. Schindler, Z. Phys. Chem. N.F., 107, 250 (1977).

Schumacher, R., H.R. Sprunken, A.A. Christodoulides, and R.N. Schindler, J. Phys. Chem., 82, 2248 (1978).

Singh, H.B., L.J. Salas, H. Shiegeishi, and A.H. Smith, "Fate of Halogenated Compounds in the Atmosphere," EPA-600/3-78-017 (1978).

Thynne, J.C.J., Dyn. Mass. Spectrom., 3, 67 (1972).

Toy, M.S., R.S. Stringham, and S.M. Toy, "An Evaluation of Potential Taggant Polymer Combinations for Detection Tagging of Blasting Caps," Science Applications Inc., SAI-78-508-SV (1978).

APPENDIX A

Scenario Taggant Concentrations from Barrier Enclosed Vapor Tagged Explosives: Solution of the Two Coupled Differential Equations

APPENDIX A

Scenario Taggant Concentrations from Barrier Enclosed Vapor Tagged Explosives: Solution of the Two Coupled Differential Equations

As a result of the mathematical development for barriers, two coupled differential equations were solved that have two different initial conditions: zero initial taggant concentration or a non-zero initial taggant concentration inside the barrier.

A1. Zero Initial Taggant Concentration Inside the Barrier (no time delay):

The two coupled differential equations for the $V_{en}(t)$, the volume of the taggant inside the enclosure, and $V(t)$, the volume of the taggant inside the barrier, are

$$dV_{en}(t)/dt = R_{cap} - (k/V_{en})V_{en}(t) + (k/V_{ch})V(t) \qquad \text{(A-1)}$$

and

$$dV(t)/dt = (k/V_{en})V_{en}(t) - (k/V_{ch} + R_{ex}/V_{ch})V(t) \qquad \text{(A-2)}$$

(equations (5-18) and (5-19) of the main text,) with the initial conditions

$$V_{en}(t = 0) = 0 \qquad \text{(A-3)}$$

and

$$V(t = 0) = 0 \qquad \text{(A-4)}$$

The best method for solving these coupled equations is by Laplace transforms. Defining $f(s)$ and $g(s)$ as the Laplace transforms of $V(t)$ and

$V_{en}(t)$, respectively, we obtain (using the initial conditions and equations (A-5) and (A-6)),

$$sg(s) = (R_{cap}/s) - (k/V_{en})g(s) + (k/V_{ch})f(s) \qquad \text{(A-5)}$$

and

$$sf(s) = (k/V_{en})g(s) - (k/V_{ch} + R_{ex}/V_{ch})f(s) \qquad \text{(A-6)}$$

Solving explicitly for f(s) we obtain

$$f(s) = \frac{k\ R_{cap}}{V_{en}s\left[(s + k/Vch + R_{ex}/V_{ch})(s + k/V_{en}) - k^2/(V_{en}V_{ch})\right]} \qquad \text{(A-7)}$$

The inverse Laplace transform of this expression for f(s) is then simply the solution for V(t).

Before explicitly writing the solution, it is convenient to define two dimensionless parameters:

$$\gamma = V_{en}/V_{ch} \qquad \text{(A-8)}$$

the ratio of the enclosure volume to the scenario volume and

$$\beta = k/R_{ex} \qquad \text{(A-9)}$$

the ratio of the barrier air exchange rate to the scenario ventilation rate. The parameter γ is a known quantity for any defined system whereas β is unknown unless the barrier constant is known.

The solution for the scenario taggant concentration as obtained from the inverse Laplace transform is thus

$$V(t) = \frac{R_{cap}V_{ch}}{R_{ex}}\left[1 - \frac{r_2\exp(-r_1t) - r_1\exp(-r_2t)}{r_2 - r_1}\right] \qquad \text{(A-10)}$$

in which

$$\begin{matrix} r_1 \\ r_2 \end{matrix} = (R_{ex}/V_{ch})\Big[(\beta + \beta/\gamma + 1) \tag{A-11}$$

$$\mp \left[(\beta + \beta/\gamma + 1)^2 - 4\beta/\gamma\right]^{1/2}\Big]/2$$

A2. <u>Non-Zero Initial Taggant Concentrations</u>

The differential equations for the non-zero situation are the same but the initial conditions are different:

$$V(t = 0) = 0 \tag{A-12}$$

and

$$V_{en}(t = 0) = V \tag{A-13}$$

As before, defining f(s) and g(s) as the Laplace transforms of V(t) and $V_{en}(t)$, respectively, we obtain:

$$sg(s) - V = R_{cap}/s - (k/V_{en})\, g(s) + (k/V_{ch})\, f(s) \tag{A-14}$$

and

$$sf(s) = (k/V_{en})g(s) - (k/V_{ch} + R_{ex}/V_{ch})f(s) \tag{A-15}$$

Again solving for f(s) yields

$$f(s) = \frac{(k/V_{en})(R_{cap}/s + V)}{(s + k/V_{en})(s + k/V_{en} + R_{ex}V_{ch}) - k^2/V_{en}V_{ch}} \tag{A-16}$$

Now f(s) can be expressed as two terms

$$f(s) = f_1(s) + f_2(s) \tag{A-17}$$

where

$$f_1(s) = \frac{k\ R_{cap}}{sV_{en}\left[(s + k/V_{en})(s + k/V_{en} + R_{ex}/V_{ch}) - k^2/V_{en}V_{ch}\right]} \quad \text{(A-18)}$$

and

$$f_2(s) = \frac{kV}{V_{en}\left[(s + k/V_{en})(s + k/V_{en} + R_{ex}/V_{ch}) - k^2/V_{en}V_{ch}\right]} \quad \text{(A-19)}$$

The concentration of taggant V(t) for the time delay case is expressed as a sum of two functions

$$V(t) = V_1(t) + V_2(t) \quad \text{(A-20)}$$

in which $V_1(t)$ and $V_2(t)$ are the inverse Laplace transforms of $f_1(s)$ and $s_2(s)$. Then $V_1(t)$ is simply the expression for the taggant concentration without time delay:

$$V_1(t) = \frac{R_{cap}V_{ch}}{R_{ex}} \left[1 - \frac{r_2 \exp(-r_1 t) - r_1 \exp(-r_1 t)}{r_2 - r_1}\right] \quad \text{(A-21)}$$

in which r_1, r_2, β, and γ have been defined previously.

$V_2(t)$ can also be determined from the inverse transform and it is found to be

$$V_2(t) = \frac{kV}{V_{en}} \left[\frac{\exp(-r_1 t) - \exp(-r_2 t)}{r_2 - r_1}\right] \quad \text{(A-22)}$$

thus the taggant volume in a scenario with time delay is

$$V(t) = \frac{R_{cap}V_{ch}}{R_{ex}} \left[1 - \frac{r_2 \exp(-r_1 t) - r_1 \exp(-r_2 t)}{r_2 - r_1}\right] \quad \text{(A-23)}$$

$$+ \frac{kV}{V_{en}} \left[\frac{\exp(-r_1 t) - \exp(-r_2 t)}{r_2 - r_1}\right]$$

APPENDIX B

Taggant Emission Rates from Vapor Tagged Blasting Caps: Mathematical Solution of the Diffusion Model

APPENDIX B

Taggant Emission Rates from Vapor Tagged Blasting Caps: Mathematical Solution of the Diffusion Model

The diffusion equations which were developed in order to predict taggant emission rate are as follows:

1. Differential Equation of Fickian Diffusion

$$D\nabla^2 C = \partial C/\partial t \qquad \text{(B-1)}$$

2. The Initial Conditions

$$C(r, z, t = 0) = 0 \text{ for all } r < r_o \text{ and } 0 < z < z_o, \qquad \text{(B-2)}$$

i.e., the end closure is uniformly solubilized

3. The Boundary Condition

(a) $(\partial C/\partial r) = 0$ for all $0 < z < z_o$, at $r = r_o$ (B-3)

i.e., no taggant emission from the sides of the end closure

(b) $(\partial C/\partial z) = 0$ for all $r < r_o$ at $z = o$, (B-4)

i.e., no taggant emission from the back of the end closure

(c) $(\partial C/\partial z) = - h(C - C_e)$, at $z = z_o$ (B-5)

i.e., taggant emission only from the front end of the end closure and it is governed by mass transfer

For equations B-1 through B-5:

D = taggant/substrate diffusion constant (cm^2/sec)

C = taggant concentration as a function of position inside the end closure i.e., $C = C(r, z, t)$ (g taggant/cm^3 end closure)

∇^2 = Laplacian

t = time (sec)

C_o = initial taggant concentration (g taggant/cm^3 end closure)

r_o = radius of the end closure (cm)

z_o = length of the end closure (cm)

C_e = taggant concentration in the air surrounding the tagged blasting cap, assumed to be constant (g taggant/cm^3 air)

h = mass transfer coefficient (cm^{-1})

The solution of the equation is as follows:

B1. <u>Transformation of Boundary Condition (C)</u>

In order to simplify boundary condition (C), a relative concentration is defined;

$$C^*(r, t) = C(r, t) - C_e \qquad \text{(B-6)}$$

This changes the equations into the following

1. $D\nabla^2 C^* = \partial C^*/\partial t$ (B-7)
2. $C^*(r, t = o) = C_o - C_e$ (B-8)
3. (a) $(\partial C^*/\partial r)_{r = r_o} = 0$ (B-9)
   (b) $(\partial C^*/\partial z)_{z = o} = 0$ (B-10)
   (c) $(\partial C^*/\partial z)_{z = z_o} = - hC^*$ (B-11)

B2. Transformation into Cylindrical Coordinates

The obvious coordinate system for the solution of this problem is cylindrical coordinates since the end closure is a cylinder of height z_o and radius r_o. The Laplacian ∇^2 expressed in cylindrical coordinates is

$$\nabla^2 = (1/r)\left[\partial/\partial r(r\partial/\partial r) + (1/r)\partial^2/\partial\theta^2 + r\partial^2/\partial z^2\right] \qquad \text{(B-12)}$$

Thus the differential equation becomes

$$(D/r)\left[\partial/\partial r(r\partial C^*/\partial r) + (1/r)\partial^2 C^*/\partial\theta^2 + r\partial^2 C^*/\partial z^2\right] = \partial C^*/\partial t \qquad \text{(B-13)}$$

We can further notice that

$$\partial C^*/\partial\theta = 0 \qquad \text{(B-14)}$$

$$\partial C^*/\partial r = 0 \qquad \text{(B-15)}$$

i.e., there is no angular or radial dependence of the taggant concentration due to the initial uniform solubilization of the end closure with taggant and due to the requirement that the taggant emission be only at the end of the end closure.

The differential equation then reduces to a one-dimensional problem:

$$D(\partial^2 C^*/\partial z^2) = \partial C^*/\partial t \qquad \text{(B-16)}$$

B3. Separation of Variables

In order to solve the partial differential equation (eq. B-16) we assume a solution of the form

$$C^*(z, t) = Z(z)T(t) \tag{B-17}$$

so as to transform the partial differential equation into two ordinary differential equations:

$$dT/dt = - b^2DT \tag{B-18}$$

$$d^2Z/dz^2 = - b^2Z \tag{B-19}$$

in which b^2 is a yet undetermined separation constant.

B4. Solution of the Two Ordinary Differential Equations

The equation for the time dependence of the taggant concentration can be simply solved to yield

$$T(t) = T_o \exp (- b^2Dt) \tag{B-20}$$

in which T_o is another yet undetermined constant.

The spatial dependence of the concentration can also similarly be solved to yield

$$Z(z) = A \sin bz + B \cos bz \tag{B-21}$$

in which both A and B are undetermined constants. Both A and B can be determined by application of the boundary conditions now expressed in terms of Z(z):

$$(dZ/dz)_{z = o} = 0 \tag{B-22}$$

$$(dZ/dz)_{z = z_o} = - hZ \tag{B-23}$$

Application of the first boundary condition (eq. B-22) leads to value for the constant A, i.e., A = 0. Similarly application of the second boundary condition (eq. B-23) leads to an expression for b, i.e.,

$$bz_o = hz_o \cot bz_o \tag{B-24}$$

If we now define a dimensionless parameter $\lambda = (hz_o)^{-1}$ we see that the solution of eq. B-24 is a series of numbers x_n for which

$$b = x_n/z_o \tag{B-25}$$

and

$$x_n = \cot x_n \tag{B-26}$$

These numbers x_n are a function of λ and are tabulated in Table B-1. The spatial solution is then

$$Z(z) = B \cos (z\, x_n/z_o) \tag{B-27}$$

with the time solution being now

$$T(t) = T_o \exp\left[- x_n^2\, Dt/z_o^2\right] \tag{B-28}$$

with the value b substituted in.

B5. The Complete Solution

The solution for $C^*(r,z,t)$ can be expressed as

$$C^*(z,t) = \sum_{n=1}^{\infty} d_n \exp\left(- x_n^2\, Dt/z_o^2\right) \cos (zx_n/z_o) \tag{B-29}$$

in which d_n are coefficients which have to be determined. The solution for C^* is expressed as a series since there are an infinite number of solutions for the time

Table B-1. Tabulation of x_n as a Function of λ (Source: Handbook of Mathematical Functions, Milton Abromowitz and Irene A. Stegun, eds., National Bureau of Standards Report No. AMS-55, (1964), p. 225.)

ROOTS x_n OF $\cot x_n = \lambda x_n$ — **Table 4.20**

λ	x_1	x_2	x_3	x_4	x_5	x_6	x_7	x_8	x_9
0.00	1.57080	4.71239	7.85398	10.99557	14.13717	17.27876	20.42035	23.56194	26.70354
0.05	1.49613	4.49148	7.49541	10.51167	13.54198	16.58639	19.64394	22.71311	25.79232
0.10	1.42887	4.30580	7.22811	10.20026	13.21418	16.25936	19.32703	22.41085	25.50638
0.15	1.36835	4.15504	7.04126	10.01222	13.03901	16.10053	19.18401	22.28187	25.38952
0.20	1.31384	4.03357	6.90960	9.89275	12.93522	16.01066	19.10552	22.21256	25.32765
0.25	1.26459	3.93516	6.81401	9.81188	12.86775	15.95363	19.05645	22.16965	25.28961
0.30	1.21995	3.85460	6.74233	9.75407	12.82073	15.91443	19.02302	22.14058	25.26392
0.35	1.17933	3.78784	6.68698	9.71092	12.78621	15.88591	18.99882	22.11960	25.24544
0.40	1.14223	3.73184	6.64312	9.67758	12.75985	15.86426	18.98052	22.10377	25.23150
0.45	1.10820	3.68433	6.60761	9.65109	12.73907	15.84728	18.96619	22.09140	25.22062
0.50	1.07687	3.64360	6.57833	9.62956	12.72230	15.83361	18.95468	22.08147	25.21190
0.55	1.04794	3.60834	6.55380	9.61173	12.70847	15.82237	18.94523	22.07333	25.20475
0.60	1.02111	3.57756	6.53297	9.59673	12.69689	15.81297	18.93734	22.06653	25.19878
0.65	0.99617	3.55048	6.51508	9.58394	12.68704	15.80500	18.93065	22.06077	25.19373
0.70	0.97291	3.52649	6.49954	9.57292	12.67857	15.79814	18.92490	22.05583	25.18939
0.75	0.95116	3.50509	6.48593	9.56331	12.67121	15.79219	18.91991	22.05154	25.18563
0.80	0.93076	3.48590	6.47392	9.55486	12.66475	15.78698	18.91554	22.04778	25.18234
0.85	0.91158	3.46859	6.46324	9.54738	12.65904	15.78237	18.91168	22.04447	25.17943
0.90	0.89352	3.45292	6.45368	9.54072	12.65395	15.77827	18.90825	22.04151	25.17684
0.95	0.87647	3.43865	6.44508	9.53473	12.64939	15.77459	18.90518	22.03887	25.17453
1.00	0.86033	3.42562	6.43730	9.52933	12.64529	15.77128	18.90241	22.03650	25.17245

λ^{-1}	x_1	x_2	x_3	x_4	x_5	x_6	x_7	x_8	x_9	$\langle\lambda\rangle$
1.00	0.86033	3.42562	6.43730	9.52933	12.64529	15.77128	18.90241	22.03650	25.17245	1
0.95	0.84426	3.41306	6.42987	9.52419	12.64138	15.76814	18.89978	22.03424	25.17047	1
0.90	0.82740	3.40034	6.42241	9.51904	12.63747	15.76499	18.89715	22.03197	25.16848	1
0.85	0.80968	3.38744	6.41492	9.51388	12.63355	15.76184	18.89451	22.02971	25.16650	1
0.80	0.79103	3.37438	6.40740	9.50871	12.62963	15.75868	18.89188	22.02745	25.16452	1
0.75	0.77136	3.36113	6.39984	9.50353	12.62570	15.75553	18.88924	22.02519	25.16254	1
0.70	0.75056	3.34772	6.39226	9.49834	12.62177	15.75237	18.88660	22.02292	25.16055	1
0.65	0.72851	3.33413	6.38464	9.49314	12.61784	15.74921	18.88396	22.02066	25.15857	2
0.60	0.70507	3.32037	6.37700	9.48793	12.61390	15.74605	18.88132	22.01839	25.15659	2
0.55	0.68006	3.30643	6.36932	9.48271	12.60996	15.74288	18.87868	22.01612	25.15460	2
0.50	0.65327	3.29231	6.36162	9.47749	12.60601	15.73972	18.87604	22.01386	25.15262	2
0.45	0.62444	3.27802	6.35389	9.47225	12.60206	15.73655	18.87339	22.01159	25.15063	2
0.40	0.59324	3.26355	6.34613	9.46700	12.59811	15.73338	18.87075	22.00932	25.14864	3
0.35	0.55922	3.24891	6.33835	9.46175	12.59415	15.73021	18.86810	22.00705	25.14666	3
0.30	0.52179	3.23409	6.33054	9.45649	12.59019	15.72704	18.86546	22.00478	25.14467	3
0.25	0.48009	3.21910	6.32270	9.45122	12.58623	15.72386	18.86281	22.00251	25.14268	4
0.20	0.43284	3.20393	6.31485	9.44595	12.58226	15.72068	18.86016	22.00024	25.14070	5
0.15	0.37788	3.18860	6.30696	9.44067	12.57829	15.71751	18.85751	21.99797	25.13871	7
0.10	0.31105	3.17310	6.29906	9.43538	12.57432	15.71433	18.85486	21.99569	25.13672	10
0.05	0.22176	3.15743	6.29113	9.43008	12.57035	15.71114	18.85221	21.99342	25.13473	20
0.00	0.00000	3.14159	6.28319	9.42478	12.56637	15.70796	18.84956	21.99115	25.13274	∞
*		$\left[\frac{(-5)2}{3}\right]$	$\left[\frac{(-5)1}{2}\right]$	$\left[\frac{(-5)1}{2}\right]$	$\left[\frac{(-5)1}{2}\right]$	$\left[\frac{(-5)1}{2}\right]$	$\left[\frac{(-5)1}{2}\right]$	$\left[\frac{(-5)1}{2}\right]$	$\left[\frac{(-5)1}{2}\right]$	

$\langle\lambda\rangle$ = nearest integer to λ.

For $\lambda^{-1} > .20$, the maximum error in linear interpolation is $(-4)7$; five-point interpolation gives 5D.

For $\lambda^{-1} \leq .20$,

$$x_1 = \frac{1}{\sqrt{\lambda}}\left[1 - \frac{1}{6\lambda} + \frac{11}{360\lambda}2 - \frac{1}{432\lambda}3 + \ldots\right].$$

and spatial dependence equations. The full solution can be expressed as a linear combination of these solutions as by the principle of superposition.

The coefficients d_n can be determined with the use of the initial condition:

$$C^*(z,t = o) = C_o - C_e = \sum_{n=1}^{\infty} d_n \cos (zx_n/z_o) \qquad \text{(B-30)}$$

and making use of the orthogonality of the spatial solutions to give

$$d_n = \frac{(C_o - C_e)(\sin x_n)/x_n}{(0.5 + (\sin 2x_n)/4x_n)} \qquad \text{(B-31)}$$

Therefore, the full solution can be written as

$$C^*(z,t) = (C = C_o) \sum_{n=1}^{\infty} \frac{\sin x_n \exp (- x_n^2 Dt/z_o^2) \cos (z\, x_n/z_o)}{x_n(1/2 + (\sin 2x_n)/4x_n)} \qquad \text{(B-32)}$$

B6 Total Amount of Taggant as a Function of Time Alone

The quantity $C^*(z,t)$ is the taggant concentration in the end closure as a function of position and time, the total amount of taggant, $S^*(t)$, in the end closure as function of time alone is then simply

$$S^*(t) = \int_0^{z_o} dz \int_0^{2\pi} d\theta \int_0^{r_o} r dr C^*(z,t) \tag{B-33}$$

$$= r_o^2 z_o (C_o - C_e) \sum_{m=1}^{\infty} \frac{\sin^2 x_m \exp(-x_m^2 Dt/z_o^2)}{x_m^2 (1/2 + (\sin 2x_m)/4x_m)} \tag{B-34}$$

Thus, the total amount of taggant remaining on the end closure per unit volume as a function of time is

$$C^*(t) = S^*(t)/r_o^2 z_o = (C_o - C_e) \sum_{m=1}^{\infty} \frac{\sin^2 x_m \exp(-x_m^2 Dt/z_o^2)}{x_m^2 (1/2 + (\sin 2x_m)/4x_m)} \tag{B-35}$$

A check on this solution is to see if it reduces to the assumed initial condition (eq. B-8). Thus setting t = 0 we obtain

$$C^*(t = 0) = (C_o - C_e) \sum_{m=1}^{\infty} \frac{\sin^2 x_m}{x_m^2 (1/2 + (\sin 2x_m)/4x_m)} \tag{B-36}$$

and making note the identity

$$\sum_{m=1}^{\infty} \frac{\sin^2 x_m}{x_m^2 (1/2 + (\sin 2x_m)/4x_m)} = 1 \tag{B-37}$$

we obtain

$$C^*(t = 0) = C_o - C_e \tag{B-38}$$

which is eq (B-8), thus verifying the solution.

Equation (B-35) is the total amount taggant remaining per unit volume end closure, $C^*(t)$ can thus be reexpressed as

$$C^*(t)/C^*(o) = \sum_{m=1}^{\infty} \frac{\sin^2 x_m \exp(-x_m^2 Dt/z_o^2)}{x_m^2 (1/2 + (\sin 2 x_m)/4 x_m)} \qquad \text{(B-39)}$$

in which $C^*(t)/C^*(o)$ can be regarded as the fractional amount of taggant remaining at time t in the end closure, that is, if $C^*(t)/C^*(o) = 0.4$, only 40 percent of the original taggant loading is present in the end closure or equivalently, the end closure has lost 60 percent of its original loading.

The parameter λ is related to the mass transfer coefficient. An increasing λ corresponds to a situation where the rate of mass transfer becomes more rate limiting. The two limiting cases for λ are

- $\lambda \longrightarrow \infty$ or equivalently $h = 0$, i.e.,
  No mass transfer across the interface, then $C^*(t)/C^*(0) = 1$ for all time, i.e., there is no loss of taggant from the plug. This is easily seen in boundary condition (C) with $h = 0$,

  $$(dC^*/dz)_{z = z_o} = 0, \qquad \text{(B-40)}$$

  no emission of taggant from the end of the end closure.

- $\lambda = 0$ or equivalently $h \longrightarrow \infty$, i.e.,

there is no impediment to mass transfer at the interface, the loss of taggant is solely dependent on the rate of taggant diffusion in the end closure. In this case,

$$\frac{C^*(t)}{C^*(0)} = \frac{8}{\pi^2} \sum_{n=0}^{\infty} \frac{\exp\left[-(2n+1)^2 \pi^2 Dt/4z_o^2\right]}{(2n+1)^2} \qquad \text{(B-41)}$$

since when $\lambda \longrightarrow 0$, then $x_n \longrightarrow (2n - 1)\pi/2$. This again can be seen in boundary condition (C) which take the form

$$(C^*(t))_{z = z_o} = 0 \qquad \text{(B-42)}$$

when $h \longrightarrow \infty$.

B7. Diffusion Limited Case

It is expected that diffusion will be the rate determining step in the model for many taggants. This corresponds to the situation when $\lambda = 0$ as discussed above, and equation (B-41) is then the appropriate expression for $C^*(t)/C(0)$, the fractional amount of taggant remaining. This expression, however, is difficult to evaluate when Dt/z_o^2 is less than 1, many terms are required for the suitable convergence of expression (B-41). An alternative expression can be derived which has excellent convergence in this regime by the use of theta function transformations. Recognizing that

$$\theta_2(0/t) = 2 \sum_{n=0}^{\infty} \exp\left[i \pi t(n + 1/2)^2\right] \qquad \text{(B-43)}$$

and that

$$\theta_2(0/t) = (-it)^{-1/2}\, \theta_4(0/-1/t) \qquad \text{(B-44)}$$

for which

$$\theta_4(\theta/t) = \sum_{n=-\infty}^{\infty} (-1)^n \exp\left[i\pi n^2 t\right] \tag{B-45}$$

we see that

$$2\sum_{n=0}^{\infty} \exp\left[-x(n+1/2)^2\right]$$

$$= (\pi/x)^{1/2} \sum_{n=-\infty}^{\infty} (-1)^n \exp\left[-\pi^2 n^2/x\right] \tag{B-46}$$

Integrating both sides with respect to x from y to ∞ yields

$$\sum_{n=0}^{\infty} \frac{\exp\left[y(n+1/2)^2\right]}{(n+1/2)^2} = \pi^{1/2} \sum_{n=-\infty}^{\infty} (-1)^{n+1}\, n\pi \left[\mathrm{erf}\,(n\pi/y^{1/2})\right.$$

$$\left. + y^{1/2} \exp\,(-n^2\pi^2/y)/n\pi\right] \tag{B-47}$$

With some algebra and the fact that

$$\lim_{y\to 0} \sum_{n=1}^{\infty} (-1)^{n+1}\, n\, \mathrm{erf}(n\pi/y^{1/2}) = 1/4 \tag{B-48}$$

gives us

$$\frac{C^*(t)}{C^*(0)} \approx 1 - (2/z_o)(Dt/\pi)^{1/2} \tag{B-49}$$

an expression valid for small Dt/z_o^2. The $(Dt/z_o)^{1/2}$ dependence of $C^*(t)/C^*(0)$ can be explicitly seen in Figures 8-4 and 8-5 for the $\lambda = 0$ curve (diffusion limited curve).

B8. Expressions for the Taggant Emission Rates

The taggant emission rate from a tagged blasting cap is simply the negative of the time derivative of the taggant concentration inside the end closure. Therefore, taking the time derivative of expression (B-46) for $C^*(t)/C^*(0)$ yields

$$dC^*(t)/dt = -(C_o - C_e)/z_o(D/\pi t)^{1/2}$$

$$\left(1 + 2\sum_{n=1}^{\infty} (-1)^n \exp(-n^2 z_o^2/Dt)\right) \qquad \text{(B-50)}$$

and alternatively

$$dC^*(t)/dt = -\frac{2(C_o - C_e)}{z_o^2} (D/\pi t)$$

$$\sum_{n=o}^{\infty} \exp\left(-(n + 1/2)^2 \pi^2 Dt/z_o^2\right) \qquad \text{(B-51)}$$

Expressions (B-50) and (B-51) are identical to one another; however, expression (B-50) has good convergence when $Dt/z_o^2 < 1$, and (B-51) has good convergence when $Dt/z_o^2 > 1$.

APPENDIX C

Taggant Concentrations in Detection Scenarios from Vapor Tagged Explosives Enclosed in Various Barriers: Theoretical Modeling of the Adsorption Losses

APPENDIX C

Taggant Concentrations in Detection Scenarios from Vapor Tagged Explosives Enclosed in Various Barriers: Theoretical Modeling of the Adsorption Losses

In vapor tagging of explosive products, there is a requirement that vapor taggants be volatile. This ensures that there will be negligible taggant adsorption losses on various surfaces present in scenarios, e.g., clothing inside suitcases, and packing material in boxes. This appendix describes a suitable adsorption loss term and determines the effect of adsorption losses on the detectability of nonvolatile taggants. This discussion is appropriate to the detection of explosive vapors, such as EGDN and TNT, from bulk explosives. These natural vapors are relatively non-volatile and adsorption losses are an important sink for these vapors.

Two cases of a detection scenario are considered: one without barriers and one with barriers, such as suitcases and boxes.

C1. No Barrier Case

The vapor concentration present in a detection scenario is a result of a balance between the vapor sources and the vapor sinks (losses). Thus the rate of increase of the volume of vapor taggant in the scenario is simply

$$dV_o(t)/dt = (\text{sources}) - (\text{sinks}) \qquad \text{(C-1)}$$

The only source present is the vapor emission rate from the vapor source (e.g., a tagged blasting cap, a permeation source in bulk explosive, or the inherent explosive vapors). For the explosive vapor, the emission rate would be equivalent to vapor evaporation rate from the explosives.

Define

$$(\text{sources}) = R_{cap}. \tag{C-2}$$

There are two sinks to be considered. First, the loss of vapor from the scenario due to the ventilation of the scenario is simply $V_o(t)\ R_{ex}/V_{ch}$ in which R_{ex} is the ventilation rate. The quantity (V_{ch}/R_{ex}) is equal to the turnover time t_v of the scenario, which is the time required to completely replace the air in the scenario with fresh air. The second sink is a loss of taggant due to irreversible adsorption. This is best expressed using the BET adsorption isotherm

$$V_{ad} = v_m\ c(p/P_o)/[1 + c(p/P_o)] \tag{C-3}$$

where: V_{ad} = the amount of adsorbate,

v_m = the volume of gas necessary to cover the entire surface with a completely adsorbed monolayer,

c = an empirical constant,

p = the partial pressure of the adsorbate, and

P_o = the equilibrium vapor pressure of the adsorbate.

This can also be expressed as

$$V_{ad} = v_m\ cV_o(t)(P_{ext}/V_{ch}P_o)/[1 + cV_o(t)P_{ext}/V_{ch}P_o] \tag{C-4}$$

or more conveniently as

$$V_{ad} = av_mV_o(t)/(1 + aV_o(t)) \tag{C-5}$$

The rate of loss due to adsorption is then:

$$R_{ad} = dV_{ad}/dt = \frac{av_m dV_o(t)/dt}{[1 + aV_o(t)]^2} \tag{C-6}$$

and the complete equation is

$$dV_o(t)/dt = R_{cap} - V_o(t)/t_v - av_m/[1 + V_o(t)]^2 \cdot dV_o(t)/dt \quad \text{(C-7)}$$

This equation has a steady-state solution of $R_{cap}\ t_v$, which also is the case without adsorption. The equation for $V_o(t)$ has to have this limit because the adsorption sites will be saturated and consequently adsorption loss will become negligible after a sufficient time.

This differential equation (eq. C-7) can be solved explicitly to yield the following solution,

$$\ln\left(1 - \frac{V_o(t)}{t_v R_{cap}}\right) - \frac{a^2 v_m V_o(t)}{(1 + at_v R_{cap})(1 + aV_o(t))}$$

$$- \frac{av_m}{(1 + at_v R_{cap})^2} \ln\left[\frac{1 + aV_o(t)}{1 - V_o(t)/t_v R_{cap}}\right] = - t/t_v \quad \text{(C-8)}$$

however, this exact solution is cumbersome. Another solution can be obtained for $V_o(t)$ in terms of a power series expansion

$$V_o(t) = a_o + a_1 t + a_2 t^2 + a_3 t^3 + \ldots \quad \text{(C-9)}$$

for which:

$$a_o = 0 \quad \text{(C-10)}$$

$$a_1 = R_{cap}/(1 + av_m) \quad \text{(C-11)}$$

$$a_2 = \frac{R_{cap}}{(1 + av_m)^2}\left[\frac{2v_m a^2 R_{cap}}{1 + av_m} - \frac{1}{t_v}\right] \quad \text{(C-12)}$$

This solution for the initial condition $V_o(t = o) = 0$ is a realistic condition for most laboratory experiments.

This is compared with solution for the no adsorption case

$$V_o(t) = R_{cap}\ t + \ldots$$

where the initial rate of taggant increase has been attenuated by the factor $(1 + av_m)$. More explicitly:

$$(1 + av_m) = (1 + v_m c\ P_{ext}/V_{ch}P_o) \qquad \text{(C13)}$$

due to adsorption losses. The attenuation due to adsorption is greatest when

- v_m is large -- a large surface is available for adsorption
- p_o is small -- the more nonvolatile an adsorbate is.

The attenuation can be further quantified if v_m, c, and p_o are known for particular adsorbates and surfaces. The factors a and v_m can be obtained experimentally from a least squares fit of any experimental system if sufficient experimental detection precision is available at initial times.

C2. Barrier Case

The equations for the case with a non-negligible barrier enclosing the explosive vapor source is more complicated. The differential equations for this situation are:

$$dV_{en}(t)/dt = R_{cap} - kV_{en}(t)/V_{en} + kV(t)/V_{ch} - av_m/(1 + aV_{en}(t))^2 \cdot dV_{en}(t)/dt \qquad \text{(C-14a)}$$

and

$$dV(t)/dt = kV_{en}(t)/V_{en} - kV(t)/V_{ch} - V(t)/t_v - a'v'_m/(1 + a'V(t))^2 dV(t)/dt \qquad \text{(C-14b)}$$

These equations include an adsorption loss inside the barrier (eq. C-14a) and an adsorption loss in the scenario and on the outside of the barrier (eq. C-14b). This last term can, in most practical cases, be neglected so that the relevant equations become

$$dV_{en}(t)/dt = R_{cap} - kV_{en}(t)/V_{en} + kV(t)/V_{ch} - av_m/(1 + aV_{en}(t))^2\ dV_{en}(t)/dt \qquad \text{(C-15a)}$$

and

$$dV(t)/dt = kV_{en}(t)/V_{en} - kV(t)/V_{ch} - V(t)/t_v \qquad \text{(C-15b)}$$

Again, it is possible to obtain the few leading terms in the power series development for V(t),

$$V(t) = a_o + a_1 + a_2t^2 + a_3t^3 + \ldots \qquad \text{(C-16)}$$

Specifically

$$a_o = a_1 = 0 \qquad \text{(C-17)}$$

$$a_2 = \frac{k\ R_{cap}}{V_{en}\ (1 + av_m)} \qquad \text{(C-18)}$$

The same attenuation factor of the initial vapor emission rate, i.e., $(1 + av_m)$, occurs in the barrier case as in the no-barrier case. Thus the same conclusions can be applied here as stated for the no-barrier case. These equations (both eq. C-14 and C-15) have the correct limiting values, i.e., $V(t \longrightarrow \infty) = t_vR_{cap}$.

C3. Conclusion

The effect of adsorption losses is to effectively attenuate the vapor emission rate R_{cap} by a factor $(1 + av_m)$ during the initial part of the detection period, i.e., $t < t_v$. This adsorption attenuation $(1 + av_m)$ can be related to known physical parameters and thus realistic estimates can be made regarding the detectability of explosives vapor. Almost all explosive vapors are exceedingly nonvolatile, thus the attenuation due to adsorption should be large. If the vapor taggants are fairly volatile, however, the attenuation factor due to adsorption should be near unity, essentially no adsorption loss of the vapor taggant.

APPENDIX D

Evaluation and Field Testing of Vapor Taggants for Predetonation Detection of Explosives (Reports Completed by Brookhaven National Laboratory)

1. "Evaluation of Detection of Tagged Blasting Caps Utilizing the U.S. Customs Service Automated Baggage Examiner and the Brookhaven Continuous Electron Capture Monitors." D-3

2. "Detection of Vapor Tagged Simulated Bulk Explosives Utilizing the U.S. Customs Service Automated Baggage Examiner and the Brookhaven Continuous Electron Capture Monitor." D-23

3. "Detection of Tagged Explosives in a DC-9 Aircraft via Sampling of the Air Exhaust." D-67

4. "Detection of Vapor Taggants Used for Explosive Predetonation Detection in a Boeing 727 Aircraft." D-95

BNL-24959
LIMITED DISTRIBUTI

EVALUATION OF DETECTION OF TAGGED BLASTING CAPS UTILIZING THE U. S. CUSTOMS SERVICE AUTOMATED BAGGAGE EXAMINER AND THE BROOKHAVEN CONTINUOUS ELECTRON CAPTURE MONITORS

Russell N. Dietz, Gunnar I. Senum, Robert W. Goodrich

August 1978
Test Date: July 19, 1978

INFORMAL REPORT

Research sponsored by the
Bureau of Alcohol, Tobacco, and Firearms
of the U.S. Treasury Department
under the auspices of the Aerospace Corporation

BROOKHAVEN NATIONAL LABORATORY
UPTON, NEW YORK 11973

Abstract

Utilizing the Brookhaven electron capture continuous monitors and the U. S. Customs Service Automated Baggage Examiner, these tests conclusively demonstrated that a tagged blasting cap of the design emission rate (1 nℓ/min) can be adequately and reliably detected in 15 minutes or less after being placed within a typical suitcase.

Abstract

Utilizing the Brookhaven electron capture continuous monitors and the U. S. Customs Service Automated Baggage Examiner, these tests conclusively demonstrated that a tagged blasting cap of the design emission rate (1 nℓ/min) can be adequately and reliably detected in 15 minutes or less after being placed within a typical suitcase.

Introduction

We have hypothesized for some time[1] that tagged blasting caps having an emission rate of about 1 nanoliter per minute (nℓ/min) would be sufficient for detection in a suitcase if an extraction of some of the air in the suitcase could be automatically performed and transferred to one of the Brookhaven semi-continuous[2,3] or continuous[4] electron capture monitors.

This paper reports the results of several tests devised to validate the detection capability of tagged blasting caps contained in suitcases which were moving on a typical conveyor belt system.

Experimental

Details on the fabrication and performance of tagged blastings[1,5,6] and of the latest versions of the Brookhaven electron capture taggant monitors[3,4] have been provided in earlier reports. Basically, vapor tagging of electric blasting caps has been accomplished by dissolving certain electronegative compounds (taggants) within the existing or new material end closures of the caps--tailoring the loading to have an emission rate of about 1 nℓ/min at 1 year. Under those conditions, detection in various scenarios has been postulated to be quite feasible even for caps 5 to 10 years old. This tagging technique, using sulfur hexafluoride, has been patented[7] and a similar method utilizing perfluorocarbon compounds has been filed for a patent.[8]

The two detection instruments contained electron capture detectors but processed the sampled air in two different fashions. The semi-continuous instrument was applicable only to the detection of sulfur hexafluoride (SF_6), utilizing a packed column (frontal chromatography) to delay the elution of interfering oxygen while measuring the SF_6.[3] The continuous instrument[4] was used to detect SF_6 and perfluorocarbon compounds by selectively

(catalytically) destroying interfering compounds while preserving the taggant compounds for detection. Further details will be published elsewhere.

A device for extracting a fraction of the air within suitcases and packages while continuously processing these items on a conveyor belt was developed for the U. S. Customs Service.[9] Measuring about 3 feet high by 3 feet wide and straddling the suitcase conveyor belt for about 8 feet of length, the tunnel-like device contained five weighted fingers which slightly depressed suitcases as they passed through the system, expelling some of the air from the suitcase which was lying on its side. At the same time, two spring-loaded arms containing air sampling tubes ran along the seams of the suitcases, collecting a fraction of the expelled air.

As shown in Table 1, seven different suitcases, each containing a different tagged blasting cap, were used in these tests.

Results and Discussion

SF_6 Semi-Continuous Monitor. A series of suitcase scans were made with the semi-continuous instrument as shown in Table 2 and Figures 1 through 4. In Figure 1, the step indicated as the background room concentration of SF_6 was equivalent to 27 pp 10^{12} -- about 50 times the present tropospheric concentration. Obviously the room concentration was elevated because of the number of SF_6 tagged caps present in a nearby portion of the room. Assuming an air exchange rate for the room of once every 40 minutes and a total SF_6 emission rate of 100 nℓ/min, an approximate SF_6 concentration of 20 pp 10^{12} can be calculated--in very good agreement with the measured room concentration.

Two peaks were indicated in the scan of Figure 1--one for suitcase No. 3 and one for suitcase No. 1, corresponding to measured concentrations of 170 and 19 pp 10^{12}, respectively. Based on estimated suitcase concentrations assuming an accumulation for 1 hour with no losses (probably high by a factor of 3 to 10),

a dilution factor (estimated suitcase concentration divided by measured concentration from conveyor belt device) of several hundred was computed as shown in Table 2, last column.

Ten minutes later, at 11:50 A.M., suitcases Nos. 3 and 2 were passed through the device and the response was as shown in Figure 2. Again the presence of the tagged blasting caps in the suitcases was immediately evidenced by the peaks on the recorder trace. The high measured concentrations were not unexpected, considering the high emission rates of the caps--66 nℓ/min in suitcase 2 and 30 nℓ/min in suitcase 3. And again the calculated dilution factors were in the same range as the previous test.

Figure 3 showed the traces obtained for suitcases Nos. 1 and 4, which contained tagged blasting caps having emissions rates of 2.5 and 1.1 nℓ/min, respectively, as determined by chromatographic analysis (more reliable than the gravimetrically determined values). In spite of the sloping baseline, even the 1.1 nℓ/min tagged cap in suitcase No. 4 was clearly detected. The cap had been in the suitcase for just 13 minutes when the test was performed. Assuming that all of the emitted SF_6 from the cap was retained by the suitcase during the 13 minutes, the dilution factor was calculated to be 70--i.e., about 1.4% extraction efficiency. That suitcase was screened again 6 minutes later on the baggage examiner, and, as shown in Figure 4, was quite readily detected. The extraction efficiency was estimated to be 1.9%

Continuous Perfluorocarbon Monitor. To demonstrate the potential of continuous on-line screening of suitcases, several tests were performed in the afternoon using the Brookhaven continuous electron capture monitor. As shown in Table 3, the estimated dilution factors were similar to those obtained in the morning using the semi-continuous monitor. Furthermore, for suitcases

Nos. 1 and 2, the measured concentrations as extracted by the baggage device were nearly the same, whether the measurement was performed within 1 hour after placing the cap in the suitcase (Table 2) or within 3 hours (Table 3). This result confirms our predictions[10] for poorly sealing containers such as suitcases--namely, that within several tens of minutes after being placed in a suitcase, the rate of loss of taggant vapors from the suitcase balances with the rate of emission from the cap and there is no further increase in vapor concentration within the suitcase.

The results of several suitcase scans are shown in Figures 5,6, and 7 and a standard for SF_6 at about 300 pp 10^{12} is shown in Figure 8. It should be noted that the sensitivities for the perfluorocarbon taggants, PDCB (perfluorodimethylcyclobutane) and PMCH (perfluoromethylcyclohexane) were about 2/5 and 3/5, respectively, of that for SF_6. A number of problems were subsequently discovered in the continuous instrument including temperature cycling of detector and reactor ovens and a leak in the detector inlet connection which compromised the results to some extent. However, the principal of using the Baggage Examiner with a continuous electron capture monitor was adequately demonstrated.

Conclusions

The purpose of these measurements was to test the feasibility of automatically screening baggage for a hidden bomb containing a tagged electric blasting cap. The most definitive tests of the capability to detect tagged explosives were those performed with suitcase No. 4--Figures 3 and 4. In just 13 and 19 minutes, respectively, after placing a 1 nℓ/min tagged blasting cap in the suitcase, the presence of the cap was readily indicated. Proven techniques[11] for increasing the signal-to-noise ratio by more than

an order of magnitude will still further increase the detectability of tagged explosives by the approach described here.

Acknowledgment

The authors would like to thank Chris Pate of the Aerospace Corporation and Dale Mitchell of the Customs Service for their time and effort in preparation for these tests. Thanks also go to Bob Gergley for the fabrication of the tagged blasting caps.

References

1. Dietz, R.N., et al. Summary report of the Brookhaven Explosives Tagging Program. BNL 21041. February 1976.

2. Dietz, R.N., Cote, E.A., and Brown, R.M. A portable electron capture gc for tracing air pollutants. BNL 16512. April 1972.

3. Dietz, R.N., Cote, E.A., and Goodrich, R.W. Air mass movements determined by real-time frontal chromatography of sulfur hexafluoride. In Measurement, Detection, and Control of Environmental Pollutants, IAEA-SM-206/21, September 1976, pp. 277-299.

4. Dietz, R.N., Cote, E.A., and Goodrich, R.W. Ultra trace determination of sulfur hexafluoride and perfluorocarbons for atmospheric tracing. Presented at 174th American Chemical Society Meeting, Chicago, August 1977.

5. Senum, G.I. Evaluation of SF_6 Tagged Blasting Caps. Monthly progress letter reports to the Federal Aviation Administration. March through November 1977.

6. Senum, G.I. Evaluation of Vapor Taggants and Substrates for the Tagging of Blasting Caps. Monthly progress letter reports to the Aerospace Corporation, July 1977 through June 1978.

7. Dietz, R.N., et al. Tagging explosives with sulfur hexafluoride. U.S. Patent No. 3,991,680, November 16, 1976.

8. Dietz, R.N. and Senum, G.I. Perfluorocarbon vapor tagging of blasting cap detonators. Patent application. BNL 78-01, S-49,614. January 1978.

9. Mitchell, D. Automated baggage examiner. U.S. Customs Service Internal Report, 1977.

10. Senum, G.I. Expected taggant concentrations in scenarios from tagged blasting caps in various barriers. Brookhaven internal report, July 1978.

11. Lovelock, J.E. Solute switching and detection by synchronous demodulation in gas chromatography. J. Chromatogr. 112, 29-36 (1975).

TABLE I

Tagged Blasting Caps Placed in Suitcases

Suitcase	Tagged Cap Taggant	Rate, nℓ/min Grav.	Rate, nℓ/min Chrom.	Time placed in Suitcase
1	SF_6	6.3	2.5	1030
2	SF_6	66	---	1040
3	SF_6	30	---	1040
4	SF_6	0.73	1.1	1147
5	PMCH	26	---	1040
6	PDCB	27	---	1030
7	PMCH	7.0	5	1348

Suitcase 1. Small blue case, hard sides (30 ℓ)
2. Large, soft, side zipper (100 ℓ)
3. 1 Suiter, brown, soft (50 ℓ)
4. 1 Suiter, brown, soft (40 ℓ)
5. Large, soft, side zipper (100 ℓ)
6. Full size, brown, semi-soft (120 ℓ)
7. Medium, soft, side zipper (80 ℓ)

TABLE 2

Detection of Tagged Blasting Caps Contained in Suitcases
(Brookhaven SF_6 Semi-Continuous Monitor)

Test Time	Suitcase[a]	Figure	Elapsed Time, min.[b]	SF_6 Concentration, pp 10^{12} Room	Suitcase[c]	Device[d]	Dilution Factor
1135	1	--	65	--	5,000	11	450
1135	2	--	55	--	40,000	130	310
1140	3	1	60	27	36,000	170	210
1140	1	1	70		5,000	19	260
1150	3	2	70	24	36,000	94	380
1150	2	2	70		40,000	94	430
1200	1	3	90	14	5,000	13	380
1200	4	3	13		360	5	70
1206	4	4	19	14	520	10	50

[a]The suitcases and the tagged caps within them are described in Table 1.
[b]Time duration from placement of cap in suitcase to sampling time.
[c]Concentration in suitcase estimated as 1 hour accumulation with no losses.
[d]Concentration outside suitcase as extracted by the baggage examiner.

TABLE 3

Detection of Tagged Blasting Caps Contained in Suitcases
(Brookhaven Continuous Perfluorocarbon Monitor)

Test Time	Suitcase	Figure	Elapsed Time, min.	Taggant Concentration, pp 10^{12}			Dilution Factor
				Taggant	Suitcase	Device	
1330	1	--	180	SF_6	5,000	20	250
1332	1	--	182	SF_6	5,000	20	250
1334	2	5	174	SF_6	40,000	90	440
1336	3	--	176	SF_6	36,000	20	1800
1340	5	6	180	PMCH	15,000	220	70
1343	6	7	193	PDCB	13,000	450	30
1414	1	--	224	SF_6	5,000	30	110

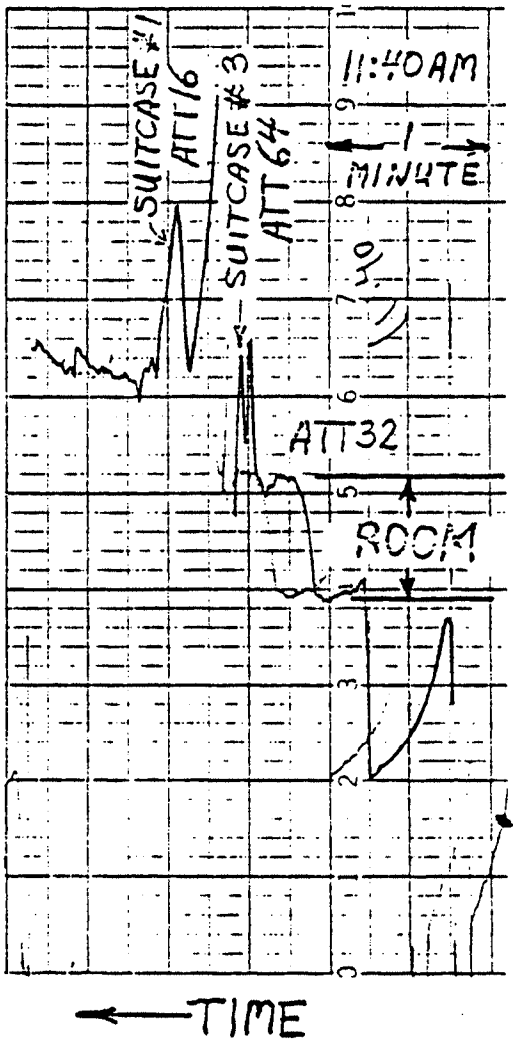
SUITCASE #1
ATT16
SUITCASE #3
ATT64
11:40AM
1
MINUTE
ATT32
ROOM
TIME

Figure 1

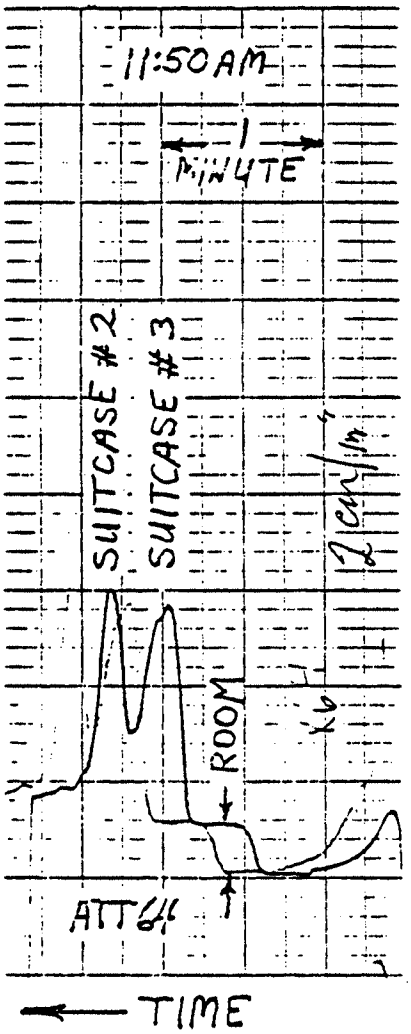

Figure 2

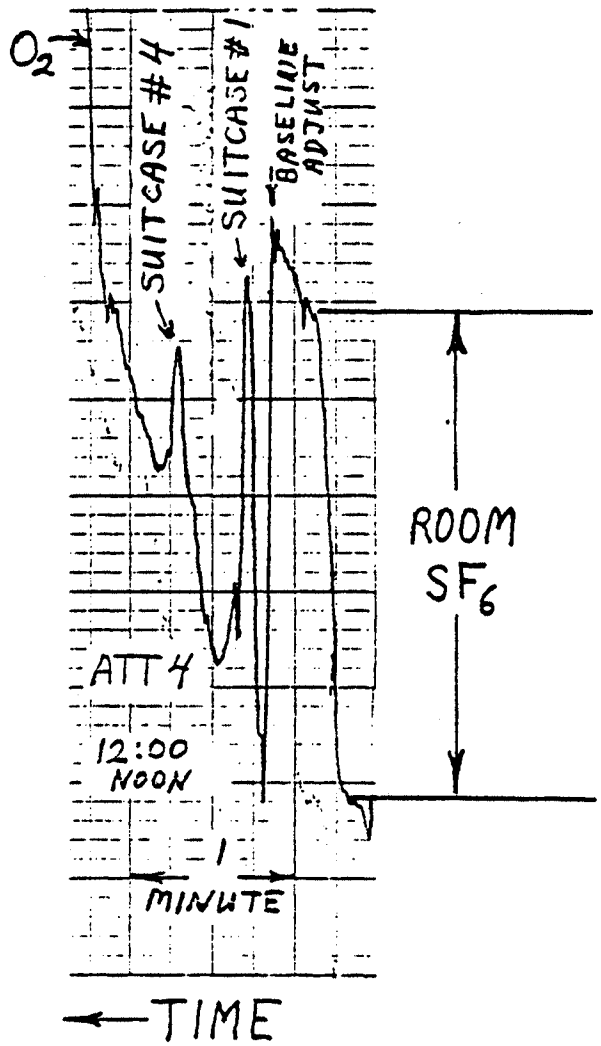
O_2
SUITCASE #4
SUITCASE #1
BASELINE ADJUST
ROOM SF_6
ATT 4
12:00 NOON
1 MINUTE
TIME

Figure 3

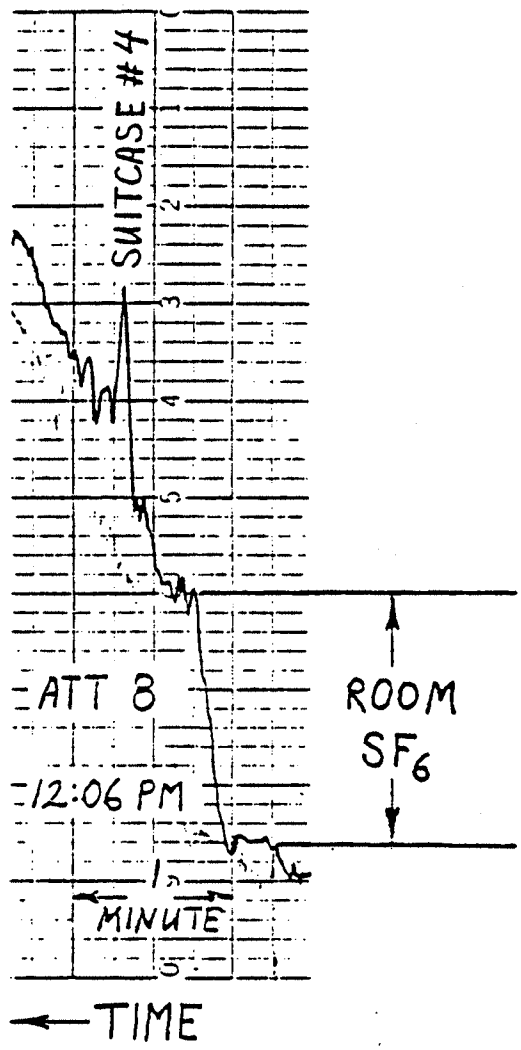

Figure 4

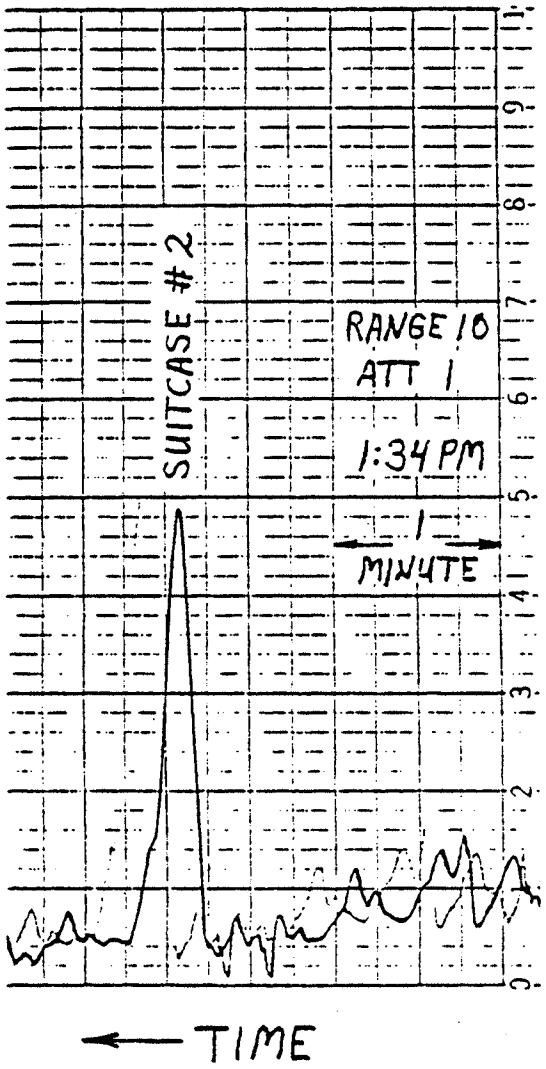

Figure 5

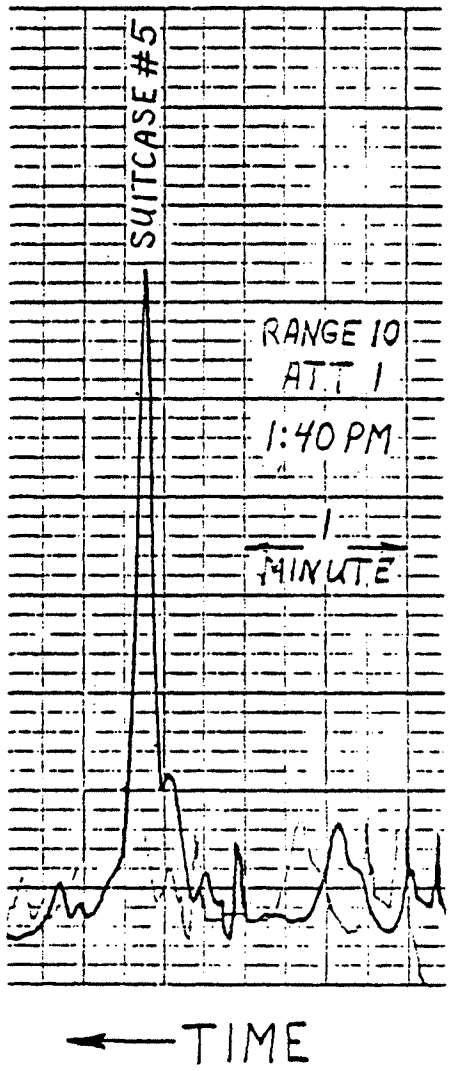

Figure 6

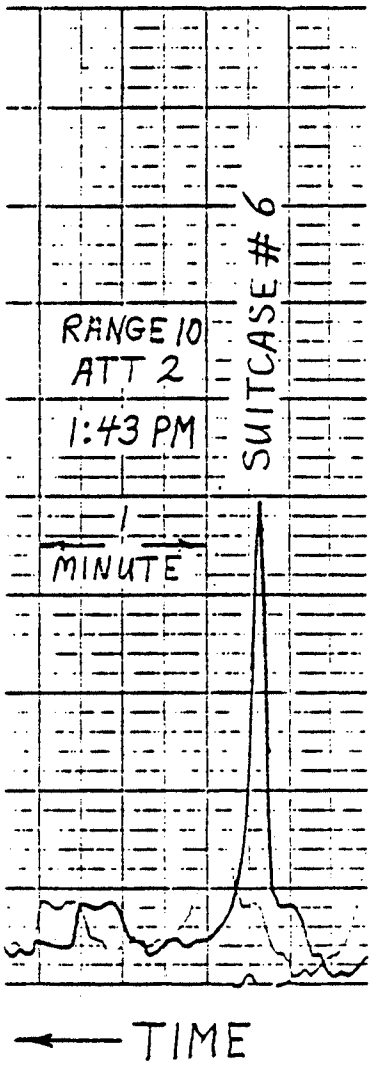

Figure 7

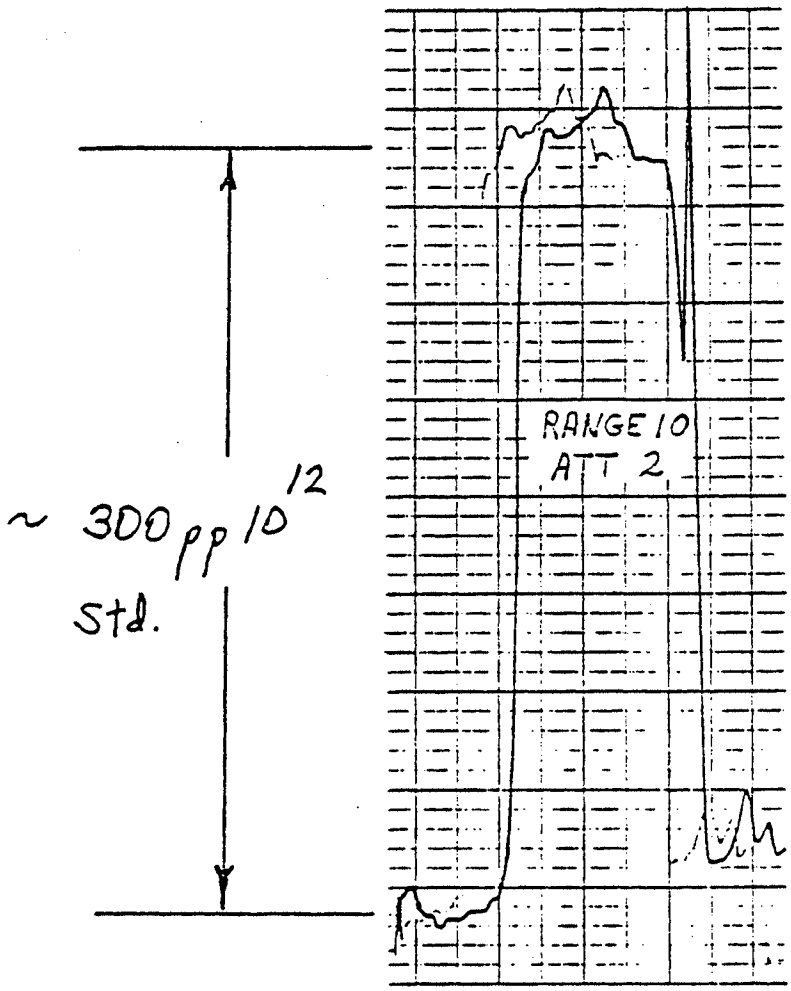

Figure 8

BNL-26782
LIMITED DISTRIBUTION

DETECTION OF VAPOR TAGGED SIMULATED BULK EXPLOSIVES UTILIZING THE U. S. CUSTOMS SERVICE AUTOMATED BAGGAGE EXAMINER AND THE BROOKHAVEN CONTINUOUS ELECTRON CAPTURE MONITOR

Gunnar I. Senum, Robert W. Goodrich, and Russell N. Dietz

August 1979
Test date: May 2 and 3, 1979

Research sponsored by the
Bureau of Alcohol, Tobacco and Firearms
of the U.S. Department of the Treasury
under the direction of The Aerospace Corporation

INFORMAL REPORT

B R O O K H A V E N N A T I O N A L L A B O R A T O R Y

A S S O C I A T E D U N I V E R S I T I E S , I N C.

under contract No. EY-76-C-02-0016 with the

UNITED STATES DEPARTMENT OF ENERGY

ABSTRACT

A demonstration using the U.S. Customs Service baggage examiner and the Brookhaven electron capture continuous monitor has conclusively demonstrated the feasibility of detecting a vapor tagged stick of bulk explosive contained inside various pieces of baggage within at least 7 minutes after the introduction of the tagged explosive into the luggage.

By examining 11 different types of luggage that were empty or filled with clothing or makeup, it was possible to determine an extraction coefficient range of 0.0003 to 0.311 with an average of 0.05 for the baggage examiner, i.e., the taggant concentration at the output of the examiner was approximately 5% of the taggant concentration present inside the examined baggage.

The simulated bulk explosives had been vapor tagged by the incorporation of microencapsulated perfluorodimethylcyclohexane (PDCH) at 0.05% to 0.10% by weight in the bulk simulated explosives, which would typify the expected taggant loading in commercial bulk explosives.

N O T I C E

This report was prepared as an account of work sponsored by the United States Government. Neither the United States nor the United States Department of Energy, nor any of their employees, nor any of their contractors, subcontractors, or their employees, makes any warranty, express or implied, or assumes any legal liability or responsibility for the accuracy, completeness or usefulness of any information, apparatus, product or processes disclosed, or represents that its use would not infringe privately owned rights.

INTRODUCTION

This is the second in a series of reports[1] demonstrating the detectability of vapor tagged bulk explosives in various detection scenarios. In this demonstration, the tagged bulk explosives were placed in various pieces of luggage, and the vapor taggant was extracted by the U.S. Customs Service Automated Baggage Examiner and subsequently detected by the Brookhaven continuous electron capture monitor. This controlled access detection scenario is relevant to the predetonation detection of explosives at airports, buildings or controlled entry sites, with the baggage examiner providing rapid sampling of every luggage or package item as it passes through the examiner. The baggage examiner is designed to be bolted to a luggage conveyor system.

This detection system, the baggage examiner and the Brookhaven monitor, had been used previously in detection of tagged blasting caps which had been placed in pieces of luggage;[2] however, these earlier demonstrations used SF_6 as a vapor taggant, a substance no longer considered as a potential taggant. Since then, the vapor tagging of explosives has progressed to the point where there are several potential vapor taggants detectable with the Brookhaven monitor. One such vapor taggant, perfluorodimethylcyclohexane (PDCH), has now bee incorporated into some simulated bulk explosives at the low concentrations which would be typical of vapor tagged explosives. Consequently, the vapor taggant emission rates from these explosives are typical of the proposed tagging techniques and provide a realistic demonstration of the capability of vapor tagged explosives. However no attempts were made to employ detection counter measures by contamination of the vapor sources, i.e., the presences of high conentrations of Freons, but such counter measures would not make the lug gage items undetectable, rather more detectable.

BACKGROUND

A piece of luggage containing a vapor tagged explosive will provide two impediments to the detection of the vapor taggant from that luggage. The first impediment is loss of the taggant due to physical adsorption of the vapor taggant on various adsorptive surfaces present inside the luggage, i.e., clothes, etc. This loss can be minimized[3] by using vapor taggants which are relatively volatile, e.g., perfluorodimethylcyclobutane (PDCB), perfluoromethylcyclohexane (PMCH), and perfluorodimethylcyclohexane (PDCH). The second impediment is the containment of the vapor taggant within the luggage. Some items of luggage might be sufficiently airtight so as to slightly or significantly reduce the rate of vapor taggant extraction by the baggage examiner. However, in a series of laboratory experiements involving luggage such as briefcases, suitcases, sealed boxes, etc., this impediment has also been shown[3] to be negligible. A variant of this impediment is to enclose the vapor tagged explosive in an airtight barrier, such as a plastic bag, a sealed paint can, etc., and place that in the luggage. Such barriers were also examined and although several barriers e.g., a sealed paint can and a ziplocked plastic bag, did provide a significant degree of airtightness, the majority of common barriers have a negligible degree of airtightness.

PDCH was chosen as a potential vapor taggant because of its high responsivity to detection by the Brookhaven monitor, i.e., high responsivity to the electron capture detector (ECD). One advantage of the ECD is its simplicity, allowing the vapor taggant detector to be made into a small, portable, and inexpensive unit.[4] The detection sensitivity for real-time vapor taggant detection is presently circa a part per trillion (1 ppt or 1 pp 10^{12}) of vapor taggant in air. Concentration techniques allow the detection sensitivity to be increased by two to four orders of magnitude depending on the method.[5]

There are several methods to incorporate vapor taggants into explosives;[6] two of which are of the greatest practicality. The first practical method is to incorporate the vapor taggant into the blasting cap, which is used to detonate the explosive. Either the vapor taggant is directly solubilized into the end plug of the blasting cap[3,7-12] or the end plug is blended with taggant-containing microcapsules.[6] The second method is to blend microspheres into th bulk explosives at concentrations of 0.05% to 0.10% by weight. The taggant will then permeate out of the microsphere at a known rate. Both microcapsule methods allow a tagging lifetime up to 5 years after incorporation.

EXPERIMENTAL

The procedure used during the demonstration was to place the tagged bulk explosives in various pieces of luggage and subsequently to pass the piece of luggage through the baggage examiner. A description of the luggage used in th demonstration is given in Table 1 along with the contents of the luggage.

The baggage examiner and the Brookhaven monitor (Figure 1) are identical to those used in the previous demonstration with tagged blasting caps.[2] Brief ly, the baggage examiner extracts a fraction of air from within each baggage item as it passes through the examiner on a conveyor belt. Measuring about 3 feet high by 3 feet wide and straddling the baggage conveyor belt for about 8 feet of length (Figure 1a), the tunnel-like device contains five weighted fingers (Figure 1b) which slightly depress the baggage items as they pass through the system (Figure 1c), expelling some of the air from each of the baggage items which is lying on its side. The suitcases are also guided by a spring-loaded arm on each side of the conveyor belt. At the same time, contained at the end of one of the weighted fingers and at the end of each of the two spring-loaded arms are three air sampling manifolds that collect a fraction of the air extracted from the baggage. The air from the sampling manifolds is

subsequently fed into the Brookhaven monitor for detection of the vapor taggant. The three air sampling manifolds were each fabricated from a 4 inch length of tubing which had been slightly flattened. Small holes had been drilled along the flattened surface and one end of the tubing was sealed and the other end was connected to the intake port of the Brookhaven monitor. The three sections of connecting 1/8" tubing from the three sampling manifolds to the intake port of the monitor were all the same length. This was to ensure that the sampled air from each of the sampling manifolds arrived simultaneously at the monitor intake port. Further details about the baggage examiner can be found elsewhere.[13]

The Brookhaven monitor used in these demonstrations is a real-time continuous detector for the PDCH vapor taggant used to tag the bulk explosives. Commonly occurring compounds that are also sensitive to ECD such as ambient Freons, oxygen, etc., are selectively removed by the monitor. Thus the monitor detects the various perfluorinated vapor taggants, e.g., PDCB, PMCH, and PDCH; but does not detect most interferant substances. More specific detail can be found in other reports.[5,14]

The output of the Brookhaven monitor was displayed on a strip-chart recorder, and the threshold alarm, a red light and a buzzer, was set to trigger when the output of the monitor was greater than 28% of the full-scale output of the monitor, i.e., when a PDCH concentration greater than a certain threshold was detected. This threshold concentration was not the same throughout the demonstration, but varied with attenuation settings on the monitor. The unit housing the threshold alarm was located at the point along the conveyer belt where the previously examined luggage would be if the alarm was triggered (see Figure 1d) due to the presence of a vapor tagged explosive in that particular piece of luggage.

The microcapsule tagged bulk explosive simulants used in this demonstration were prepared for The Aerospace Corporation and are described in Table 2. The amount of microencapsulated taggant that was blended into each sample and a description of the tagged explosive wrapping are given. These samples were simulants in the sense that the EGDN or TNT had been excluded during manufacture and a closely chemically related but inert compound had been substituted. The PDCH emission rates from these samples have now been recorded for 6 months and the chromatographically determined emission rates are tabulated in Table 3 with the averaged emission rates in Table 3a. The taggant emission rates show rather large variations. The large fluctuations between different determinations and the large relative standard deviations are inherent to the microcapsule tagged samples and not the chromatographic analysis technique. These fluctuations may be due to the large temperature dependence of the emission rate because the analysis were done without temperature regulation. The reasons for these large fluctuations are a subject of investigation by Aerospace and microcapsule manufacturers. Nonetheless, the apparent consistency of the PDCH taggant emission rate demonstrates the ability to tag bulk explosives by incorporation of microencapsulated taggant into the explosive. Another potential taggant, PMCH, is present as an impurity in PDCH at about 5% to 20% depending on the source of PDCH. Thus, the PDCH tagged samples are also emitting PMCH and the emission rates of PMCH as determined chromatographically are given in Table 4.

The calibration of the Brookhaven monitor was done with tagged blasting caps with known measured PDCH emission rates. These standard caps were placed for circa 1 to 2 min in a tube connected to the intake port of the monitor. The resulting recorder display for the standard taggant emission output is shown in Figure 2. The PDCH concentration entering the monitor is calculated

from the PDCH emission rate of the standard divided by the intake port flow rate (approximately 2 L/min). The resulting calibration factors (ppt/mV) are given in Table 5 as derived from the measured monitor response (mV) to each of the standard cap concentration (ppt) resulting from each standard cap. Figure 3 shows a plot of the calibration data revealing linearity over two orders of magnitude of taggant concentration. The positive intercept can be bucked out electronically as a zero offset.

Given also in Table 5 is the response of the monitor to SF_6 as determined with the use of an SF_6 tagged cap. The resulting calibration indicates that the monitor has a greater sensitivity for SF_6 compared to PDCH which is in agreement with previous results[2].

RESULTS AND DISCUSSION

During the 2 day period, many demonstrations and experiments were done with the baggage examiner and the Brookhaven monitor. These can be broadly distinguished into three areas and these will be discussed individually.

Feasibility Demonstration

The objective of the demonstration was to show the feasibility of detecting tagged bulk simulated explosives in various pieces of luggage. A clothing filled suitcase with no tagged simulated bulk explosives was conveyed through the baggage examiner to ascertain that, indeed, it initially contained no vapor taggant nor interfering substances. A resulting recorder trace is shown in Figure 4a with the arrow indicating the time at which the suitcase was placed on the conveyor belt; the strip chart shows that no vapor taggant nor interferant was present. Then a vapor tagged bulk simulated explosive (stick A010) was then placed in the clothing filled suitcase. It was again conveyed through the examiner, and the resulting monitor response is shown in Figure 4b

and Figure 4c for 1 minute and 8 minutes, respectively, after placement of the vapor tagged explosive. The time delay between the passage of the suitcase into the examiner (the arrow) and the occurrence of the peak was indicative of the residence time of the taggant from the manifold to the detector—about 20 seconds. The horizontal line in Figure 4b and all subsequent figures represents the threshold which, if surpassed, would trigger the threshold alarm. As seen in Figure 4d, the threshold level was surpassed and the alarm indicated the presence of a tagged stick of explosive in the suitcase at only 8 minutes after placement of the explosive in the suitcase.

The feasibility demonstration was repeated three more times as is shown in Figures 4e, f, and g and in Figure 5. In each instance, the suitcase was examined 7 to 8 minutes after the introduction of the tagged explosive into the suitcase. The baggage examiner was able to extract the vapor taggant from within the suitcase and present it to the detector at sufficiently large concentration so as to set off the monitor's threshold alarm. Thus, it is entirely feasible to detect a vapor tagged bulk explosive contained inside a suitcase within 7 to 8 minutes after the introduction of the explosive into the suitcase with the use of the Customs Service baggage examiner and the Brookhaven monitor.

The taggant concentrations as measured by the monitor for these feasibility demonstrations are tabulated in Table 6.

Extraction Coefficents

A semi-quantitative measure of the extraction ability of the baggage examiner can be formulated in terms of an extraction coefficient. This is defined as the ratio of the extracted taggant concentration as measured by the taggant monitor to the taggant concentration inside the luggage. The latter quantity

can be calculated from the taggant emission rate (with its large associated error) of the enclosed explosive, from the duration for which the explosive has been in the luggage and a rough estimate of the internal volume of the luggage.

On the first day of the demonstration, 10 pieces of luggage that were either empty or filled with clothing or makeup (luggage pieces 1 through 10 in Table 1) each had a stick of tagged explosive placed within it in the early morning. Three and one half hours later, these pieces of luggage were conveyed through the baggage examiner; the resulting monitor responses are given in Figure 6. The extracted taggant concentrations as measured by the monitor were sufficient to trigger the threshold for all 10 pieces of luggage, with the threshold level represented by the horizontal lines in Figure 6. The extraction coefficient for each of the ten luggage pieces has been calculated and is given in Table 7, with the coefficants ranging from .0003 to .123, i.e., the taggant concentration detected by the monitor was 8 to 3000 more dilute than the taggant concentration inside the pieces of luggage.

In the afternoon of the first day, three tagged blasting caps were placed in three pieces of luggage for the purpose of recording the taggant concentrations in the luggage as a function of elapsed time. Thus each luggage piece was conveyed through the baggage examiner at half hour intervals throughout the afternoon. The resulting monitor responses are shown in Figures 7 through 9. The taggant concentrations as measured by the monitor and the consequent extraction coefficients are tabulated in Table 8. As is expected, the taggant concentrations inside the luggage pieces increase linearly with time because the tagged caps have a constant taggant emission rates.

Further determinations of the extraction coefficient of the baggage examiner for various pieces of luggage continued the following day. The vapor tagged bulk explosives were placed in the luggage, and they were periodically

sampled by the baggage examiner throughout the day. The results for six pieces of luggage are displayed in Figures 10 through 16. The taggant concentrations as measured by the monitor and the calculated extraction coefficients are given in Table 9. For all the pieces of luggage the baggage examiner was able to extract a sufficient quantity of taggant to trigger the threshold alarm. The taggant concentrations inside the pieces of luggage increased linearly throughout the day with the exception of the last measurements taken in the late afternoon which were exceptionally low for all the luggage pieces determined at that time. This was apparently due to a gradual heating of the monitor which probably caused the catalyst to operate at a higher temperature. This allowed some of the taggant to be destroyed by the catalyst and thus could have been the cause of the monitors reduced detection sensitivity for the vapor taggants.[5] In no case was equilibrium between the vapor taggant emission rate and the taggant diffusion rate from the baggage established.

Figure 15(d) shows an example of the use of a hand-held probe to sniff at the seams of a suitcase in order to search for vapor taggant. The measured concentration was reduced four-fold because the probe was connected at the fourthinput of the taggant monitor intake manifold with the other three inputs open to the ambient air, i.e., the other three were not disconnected from the baggage examiner. Nevertheless, a hand examination of a suitcase is sufficient to detect the presence of a tagged explosive in the suitcase.

Figure 16 displays the situation when a tagged explosive is removed from the suitcase. Just before removal (Figure 16(c)) a taggant concentration of 418 ppt was detected by the baggage examiner monitor. A minute after the removal of the tagged explosive but with the suitcase remaining closed, the taggant concentration dropped to 127 ppt (Figure 16 (e)). At 90 minutes after removal (Figure 16 (f)), the taggant concentration was still the same, 157 ppt,

i.e., very little taggant has diffused out of the suitcase. After the suitcase was opened and aired for 10 minutes, the taggant concentration dropped below the detection limit of the monitor. Thus, it is possible to detect a suitcase that previously contained a tagged stick of explosive as long as the suitcase remains closed after the removal of the tagged explosive. This also suggests the diffusion from suitcases is very slight and points out the value of a vapor extraction mechanism.

The extraction coefficient for each piece of luggage is tabulated in Table 10. The coefficients range from a low of 0.0003 for a make-up case to a high of 0.156 for a rigid two-suiter suitcase. The overall extraction coefficient, an average of 11 different pieces of luggage, is $.05 \pm .07$, i.e., the taggant concentration measured by the monitor is approximately 5% of the taggant concentration inside the luggage. These extraction coefficients are greater than those determined previously[2] with essentially the same baggage examiner and monitor. The increased efficiency is due to the use of a different air sampling manifold which was designed for more efficient sampling.

Brookhaven Monitor Sensitivities.

The ultimate sensitivity of the Brookhaven taggant monitor varied throughout the demonstration. Initially the sensitively was affected by the cycling of a pop valve within the taggant monitor which regulated the monitor's internal pressure. This cycling introduced a periodic signal into the monitor output (see especially Figures 4(a) and 4(c)), which reduced the ultimate sensitivity of the monitor to circa 15 ppt PDCH at a signal to noise ratio (S/N) of 2. Later during the first day of the demonstration, this cycling was minimized by electronic filtering which at best increased the sensitivity to 5 ppt (see Figure 4(e)); however, through the two demonstration days, the sensitivity averaged at circa 10 ppt PDCH at S/N of 2.

Upon return to Brookhaven National Laboratory (BNL) after the demonstration the cycling of the pop valve was eliminated by replacement of the pop valve and substitution of a more powerful instrument pump in the monitor. Also, since the demonstration, the pulse width and voltage of the electron capture detector within the monitor has been optimized for maximum sensitivity and this has consequently improved the sensitivity by circa 25%. Thus the Brookhaven taggant monitor presently has a PDCH sensitivity of circa 3 to 4 pp at S/N = 2. During the demonstration the zero drift baseline stability of the monitor was determined to be approximately 1 ppt/min as measured over a 22 minute interval.

CONCLUSION

It has been shown in this demonstration that with the use of the U.S. Customs baggage examiner and the Brookhaven taggant monitor, it is entirely feasible to detect a vapor tagged stick of explosive in various pieces of luggage within no more than 7 minutes after placement within a piece of luggage. This is illustrated in Figures 4 and 5 for tagged explosives with emission rates of 20 and 3.5 nL/min respectively.

With the use of 11 different pieces of luggage it has been possible to determine the overall extraction coefficient of the baggage examiner to be 0.05 ± 0.07, i.e., the monitor measured a taggant concentration of circa 5% of the taggant concentration within the examined luggage.

The results of these demonstrations, in addition to the previous test and demonstration, [1,2] show the feasibility of predetonation detection via the use of vapor tagged explosives.

ACKNOWLEDGMENTS

The authors would like to thank Chris Pate and Robert Moler of The Aerospace Corporation for their assistance in arranging this demonstration.

also thank the U.S. Customs Service for use of their baggage examiner. Thanks also go to Bob Gergley for determining the emission rates of the tagged simulated bulk explosives and to Ed Cote for determining the emission rates of the standard caps.

REFERENCES

1. Senum, G.I., Gergley, R.P., Cote, E.A., and Dietz, R.N. Detection of Tagged Explosives in a DC-9 Aircraft via Sampling of the Air Exhaust, BNL 26612, July 1979.
2. Dietz, R.N., Senum, G.I., and Goodrich, R.W. Evaluation of Detection of Tagged Blasting Caps Utilizing the U.S. Customs Service Automated Baggage Examiner and the Brookhaven Continuous Electron Capture Monitor, BNL 24959, August 1978.
3. Senum, G.I. Evaluation of Vapor Taggants and Substrates for the Tagging of Blasting Caps. Monthly progress letter reports to The Aerosopace Corporation. July 1977 through March 1979.
4. Dietz, R.N., Cote, E.A., and Brown, R.M. A Portable Electron Capture GC for Tracing Air Pollutants. BNL 16512, April 1972.
5. Dietz, R.N., Goodrich, R.W., and Cote, E.A. Detection of Perfluorinated Taggants in Electric Blasting Caps by Electron Capture Monitors, Proc. New Concepts Symposium and Workshop on Detection and Identification o Explosives, November 1978.
6. Moler, R.B. Summary of Current Research on Explosives Detection and Identification, Proc., New Concepts Sympsoium and Workshop on Detection and Identification of Explosives, November 1978.
7. Dietz, R.N., et al. Summary Report of the Brookhaven Explosives Tagging Program. BNL 21041, February 1976.
8. Senum, G.I. Evaluation of SF_6 Tagged Blasting Caps. Monthly progress letter reports to the Federal Avaiation Administration. March throug November 1977.

9. Dietz, R.N., et al. Tagging Explosives with Sulfur Hexafluoride. U.S. Patent No. 3,991,680, November 16, 1976.

10. Dietz, R.N. and Senum, G.I. Perfluorocarbon Vapor Tagging of Blasting Cap Detonators. Patent Application. BNL 78-01, S-49,614, SN-9623. February 1979.

11. Toy, M.S., Stringham, R.S. and Toy, S.M. An Evaluation of Potential Taggant Polymer Combinations for Detection Tagging of Blasting Caps. Science Applications, Inc., SAI-78-508-SV. 1978.

12. Senum, G.I., Gergley, R.P., Greene, M., and Deitz, R.N. Vapor Tagging of Electric Blasting Caps with Perfluorinated Compounds, Proc., New Concepts Symposium and Workshop on Detection and Identification of Explosives. November 1978.

13. Mitchell, D. Automated baggage examiner. U.S. Customs Service Internal Report. 1977.

14. Goodrich, R.W. and Dietz, R.N. Portable Continuous Monitor for Perfluorinated Compounds. In preparation.

Table 1

Luggage Description

Luggage #	Type	Contents	Internal Volume (liter)
1	Two-suiter	Clothes	100
2	Two-suiter, rigid	Clothes	100
3	Soft-sided, zippered	Clothes	40
4	Makeup case	Makeup	40
5	Alum. Two-suiter	Empty	150
6	Two-suiter	Clothes	100
7	Two-suiter	Clothes	100
8	Top-zippered	Clothes	40
9	Soft-sided, zippered	Clothes	40
10	Overnite, soft-sided	Clothes	40
11	Attache case	Empty	20
13	Soft-sided, zippered	Empty	40
15	Soft-sided, zippered	Empty	40

Table 2

Microcapsule Tagged Bulk Explosive Simulants

Simulated Explosive Stick number	PDCH Microcapsule Weight Percent	Cartridge Wrapper (Dimensions in inches)	Enclosure
A01	0.05	White plastic	Wrapped in polyethylene
A02	0.05	1 x 12 waxed paper	Wrapped in newspaper
A03	0.10	1 x 12 waxed paper	Wrapped in newspaper
A04	0.10	1 1/2 x 12 waxed paper	Wrapped polyethylene bag
A05	0.10	1 x 8 waxed paper	Wrapped in newspaper
A06	0.05	1 x 8 waxed paper	Tied polyethylene bag
A07	0.05	2 x 14 waxed cartridge	Wrapped in newspaper
A08	0.10	2 x 14 waxed cartridge	Wrapped in newspaper
A09	0.05	2 x 5 waxed cartridge	Tied polyethylene bag
A010	0.10	2 x 5 waxed cartridge	None

Table 3

PDCH Emission Rate from the Microcapsule
Tagged Bulk Explosives Simulants

Sample #	Loading %	PDCH Emission Rate nL/min 1/23-25	3/1	3/29	4/18-19	5/11-14	6/19-20	6/29	7/21	8/14
A01	0.05	——	1.74 ± 0.33	7.2 ± 1.1	1.52 ± 0.22	2.49 ± 0.35	0.91 ± 0.20	2.3 ± 0.7	.63 ± .04	1.31 ± .29
A02	0.05	20.3 ± 5.4	10.2 ± 1.1	8.38 ± 0.25	6.02 ± 0.07	16 ± 4	2.53 ± 0.20	——	.99 ± .14	1.13 ± .35
A03	0.10	23.5 ± 3.3	3.96 ± 0.32	48.7 ± 2.3	2.91 ± 0.21	20.4 ± 1.5	34.6 ± 2.7	4.1 ± 0.8	4.4 ± .6	12.2 ± .3
A04	0.10	20.7 ± 4.3	13.6 ± 1.9	12.5 ± 1.0	9.9 ± 0.6	14.3 ± 1.3	20.4 ± 0.7	27.9 ± 0.9	13.5 ± 3.1	8.00 ± .07
A05	0.10	18.6 ± 2.6	10.4 ± 3.1	30.8 ± 2.1	3.6 ± 0.6	30.4 ± 2.9	0.48 ± .06	——	.62 ± .09	4.95 ± .28
A06	0.05	8.0 ± 1.6	4.0 ± 0.8	1.11 ± 0.02	1.01 ± 0.06	4.2 ± 0.6	4.00 ± 0.19	——	2.22 ± .33	8.43 ± .11
A07	0.05	11.1 ± 2.1	8.7 ± 3.7	12.8 ± 1.4	0.69 ± 0.13	7.5 ± 2.1	26 ± 17	9.9 ± 0.6	2.31 ± .18	1.26 ± .07
A08	0.10	13.9 ± 8.8	21.8 ± 6.2	5.23 ± 0.22	13.3 ± 1.2	18.3 ± 3.4	16.4 ± 1.8	22.5 ± 2.9	1.75 ± .14	.85 ± .04
A09	——	——	20.4 ± 6.2	4.9 ± 2.2	2.8 ± 0.3	10.5 ± 3.6	29.5 ± 2.8	26 ± 7	4.4 ± .6	4.0 ± .7
A010	——	——	122 ± 30	12.4 ± 2.4	15.1 ± 1.8	27.2 ± 2.1	51 ± 6	6.75 ± 0.17	7.5 ± 1.1	3.51 ± .31

Table 3a

Averaged PDCH Emission Rates

Sample #	Averaged PDCH Emission Rate, (nL/min)
A01	1.6 ± 0.7
A02	9 ± 7
A03	18 ± 17
A04	17 ± 6
A05	14 ± 12
A06	3.5 ± 2.4
A07	10 ± 8
A08	14 ± 7
A010	14 ± 11
A10	20 ± 17

Table 4

PMCH Emission Rates from the Microcapsule Tagged Bulk Explosive Simulants

Simulated Explosive Stick No.	PMCH Emission Rate (nL/min)		
	6/29	7/23	8/14
A01	0.25 ± .08	0.100 ± .012	.143 ± .025
A02	11.3 ± 0.8	.42 ± .06	.208 ± .006
A03	0.47 ± 0.11	1.37 ± .19	2.16 ± .06
A04	4.14 ± 0.13	5.3 ± .4	1.21 ± .09
A05	4.8 ± 0.3	.233 ± .016	.688 ± .043
A06	10.3 ± 1.4	.723 ± .019	1.11 ± .19
A07	0.957 ± .018	.59 ± .07	.199 ± .011
A08	2.69 ± 0.20	.502 ± .020	.13 ± .09
A09	3.0 ± 0.9	.8 ± .5	.411 ± .063
A010	0.684 ± .005	1.22 ± .14	.288 ± .021

Table 5

Standards

PDCH Standards

Standard Cap No.	Measured Voltage (mV)	PDCH[a] Concentration (ppt)	Calibration factor(ppt/mV)
L-58	248	—	—
L-16	132	217	1.64
L-406	1024	1535	1.50
L-404	864	1378	1.59
L-16	96	217	2.26
L-56	12	30	2.50
L-404	896	1378	1.54
L-58	148	—	—
L-16	104	217	2.09
			1.87 ± 0.40

SF_6 Standard

114	408	350	1.16

[a]ppt represents parts per trillion, i.e., parts per 10^{12}.

Table 6

Feasibility Demonstration

Suitcase No.	Elapsed time, min	Simulated Explosive Stick No.	Measured tagged Concentration(ppt)	Figure Reference
13	1	A010	15	4 a,b,c,d
	8	A010	94	4 a,b,c,d
13	7	A010	380	4 e,f,g
13	7	A06	131	5 a,b,c
13	7	A06	130	5 d,e,f

Table 7

Extraction Coefficients
(Figure 6)

Suitcase No.	Simulant No.	Elapsed Time (min)	Measured PDCH (ppt)	Suitcase conc.(pbb)	Extraction coefficient
1	A09	223	213	31.2	0.0068
2	A010	215	150	43.0	0.0035
3	A06	209	94	18.3	0.0051
4	A04	213	39	121.0	0.0003
5	A07	204	449	13.6	0.0330
6	A08	217	47	30.4	0.0015
7	A02	222	344	20.0	0.0167
8	A05	207	636	72.5	0.0088
9	A03	211	733	95.0	0.0077
10	A01	212	2094	17.0	0.1232

Table 8

Extraction Coefficients
as Calculated with the Use of Tagged
Blasting Caps

Elapsed Time (min)	Measured Concentration (ppt)	Suitcase Concentration (ppb)	Extraction Coefficient
A. Suitcase No. 13, Tagged Cap No. L-406, (Figure 7)			
13	11.2	1.03	.0109
29	22.4	2.29	.0098
60	52.4	4.74	.0110
89	56.1	7.03	.0080
119	142	9.40	.0151
B. Suitcase No. 15, Tagged Cap No. 114, (Figure 9)			
24	16.2	0.60	.0271
53	20.9	1.32	.0158
83	37.1	2.08	.0179

Table 9

Extraction Coefficients for
Various Pieces of Luggage

Elapsed Time (min)	Measured Concentration (ppt)	Suitcase Concentration (ppb)	Extraction Coefficient
A. Suitcase No. 2, Sample No. A07, (Figure 10)			
53	219	5.3	.0414
103	439	10.3	.0426
172	643	17.2	.0374
227	576	22.7	.0254
338	86	33.8	--
B. Suitcase No. 3, Sample No. A05, (Figure #11).			
46	2,450	16.1	.152
C. Suitcase No. 3, Sample No. A03, (Figure #11).			
19	2,660	8.55	.311
D. Suitcase No. 5, Sample No. A05, (Figure #12).			
25	209	2.33	.0897
33	325	3.08	.105
71	419	6.62	.0633
126	643	11.8	.0547
194	673	18.1	.0372
234	501	21.8	.0229
E. Suitcase No. 6, Sample No. A08, (Figure #13).			
54	67.3	7.56	.0089
80	97.2	11.2	.0087
173	142	24.2	.0059
230	209	32.2	.0065
335	209	46.9	.0045
F. Suitcase No. 8, Sample No. A03, (Figure #14).			
47	913	21.2	.0043
178	179	80.1	.0022
G. Suitcase No. 9, Sample No. A06, (Figure #15).			
49	808	4.28	.1888
70	1590	6.13	.259
175	1795	15.3	.117
H. Suitcase No. 13, Sample No. A02, (Figure #16).			
13	418	2.93	.1429

Table 10

Summary of the
Extraction Coefficient

Luggage #	Extraction Coefficient
1	0.0068
2	0.030 ± 0.016
3	0.156 ± 0.153
4	0.0003
5	0.064 ± 0.029
6	0.0063 ± 0.0030
7	0.0167
8	0.0051 ± 0.0034
9	0.0077
10	0.1232
13	0.033 ± 0.054
Overall (41 measurements, 12 different pieces of luggage)	0.05 ± 0.07

Figure 1

(a)

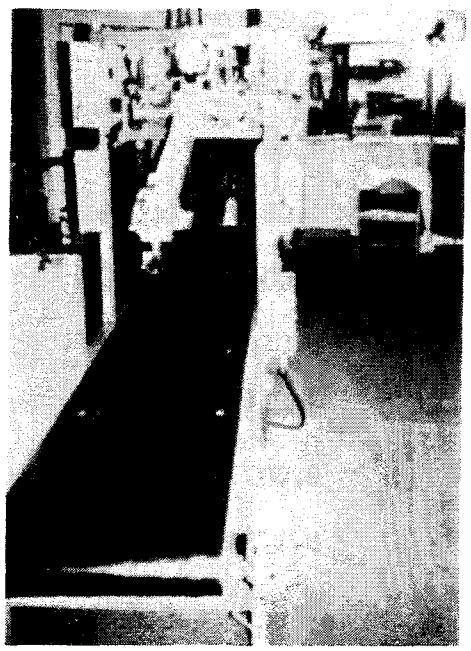

(b)

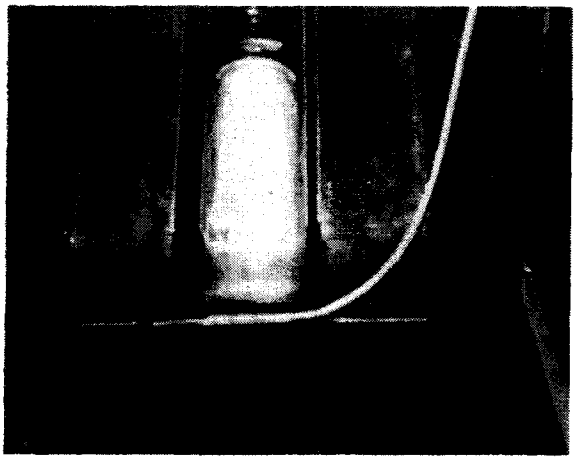

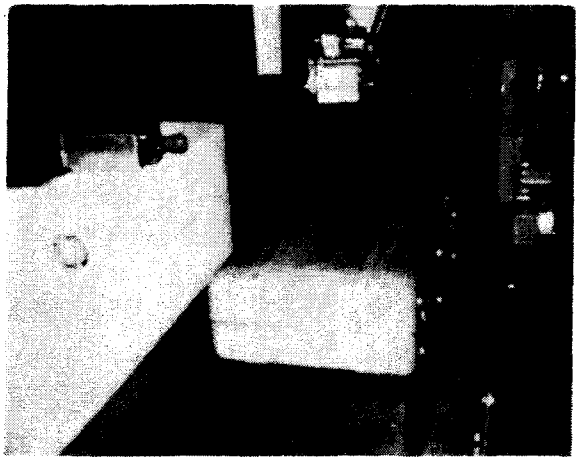

(d)

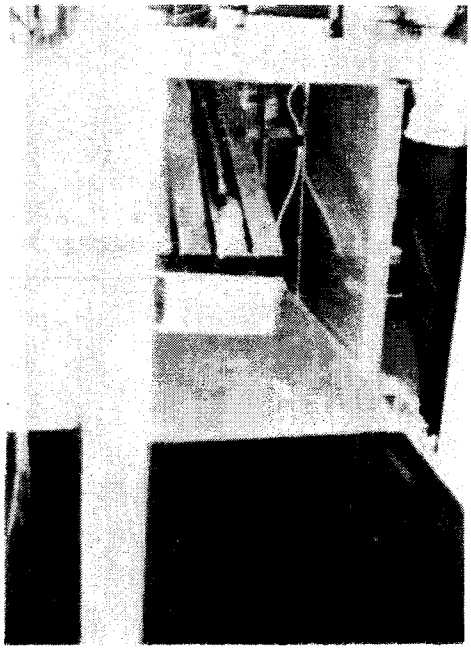

(c)

STANDARDS

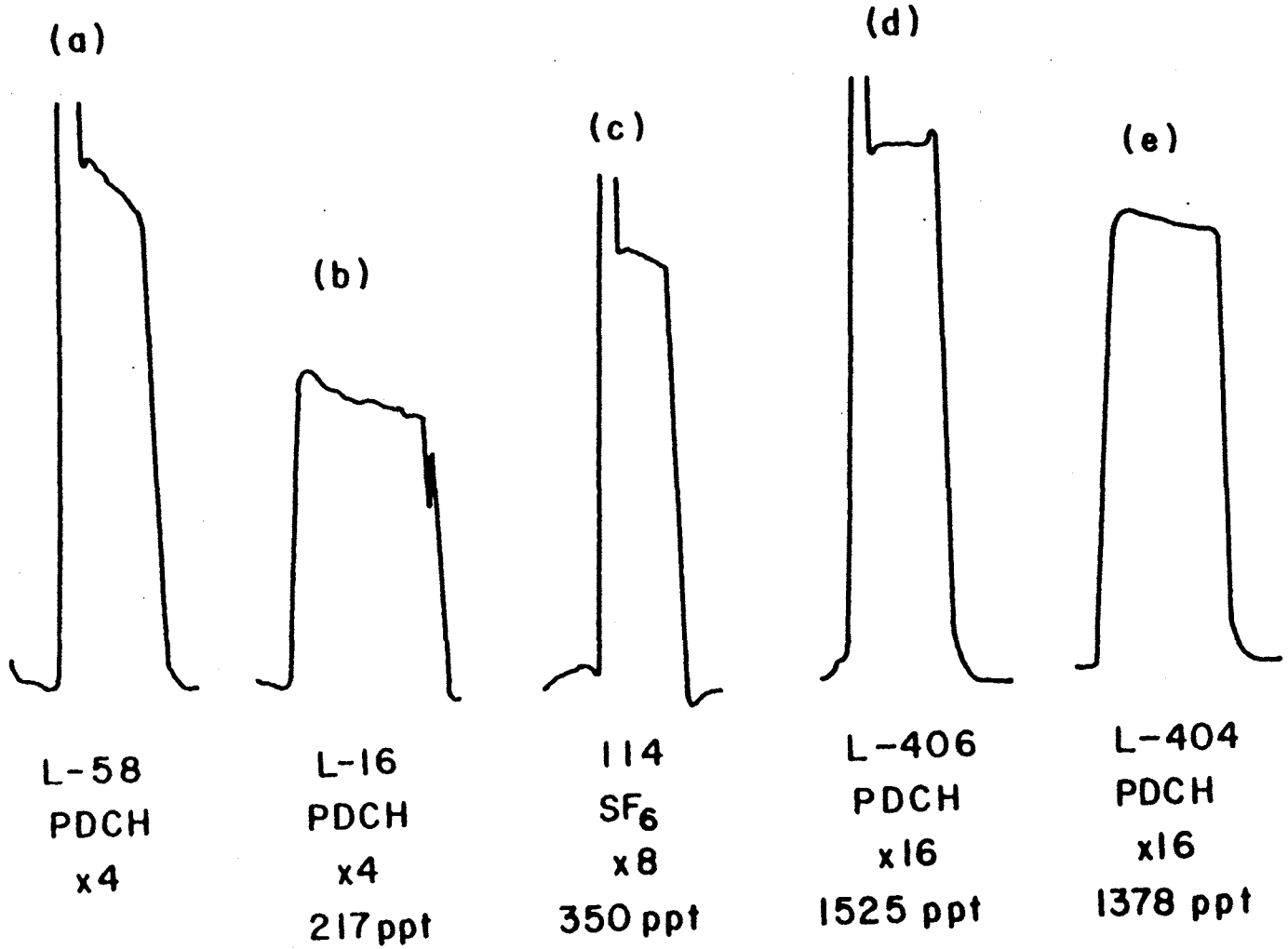

Figure 2

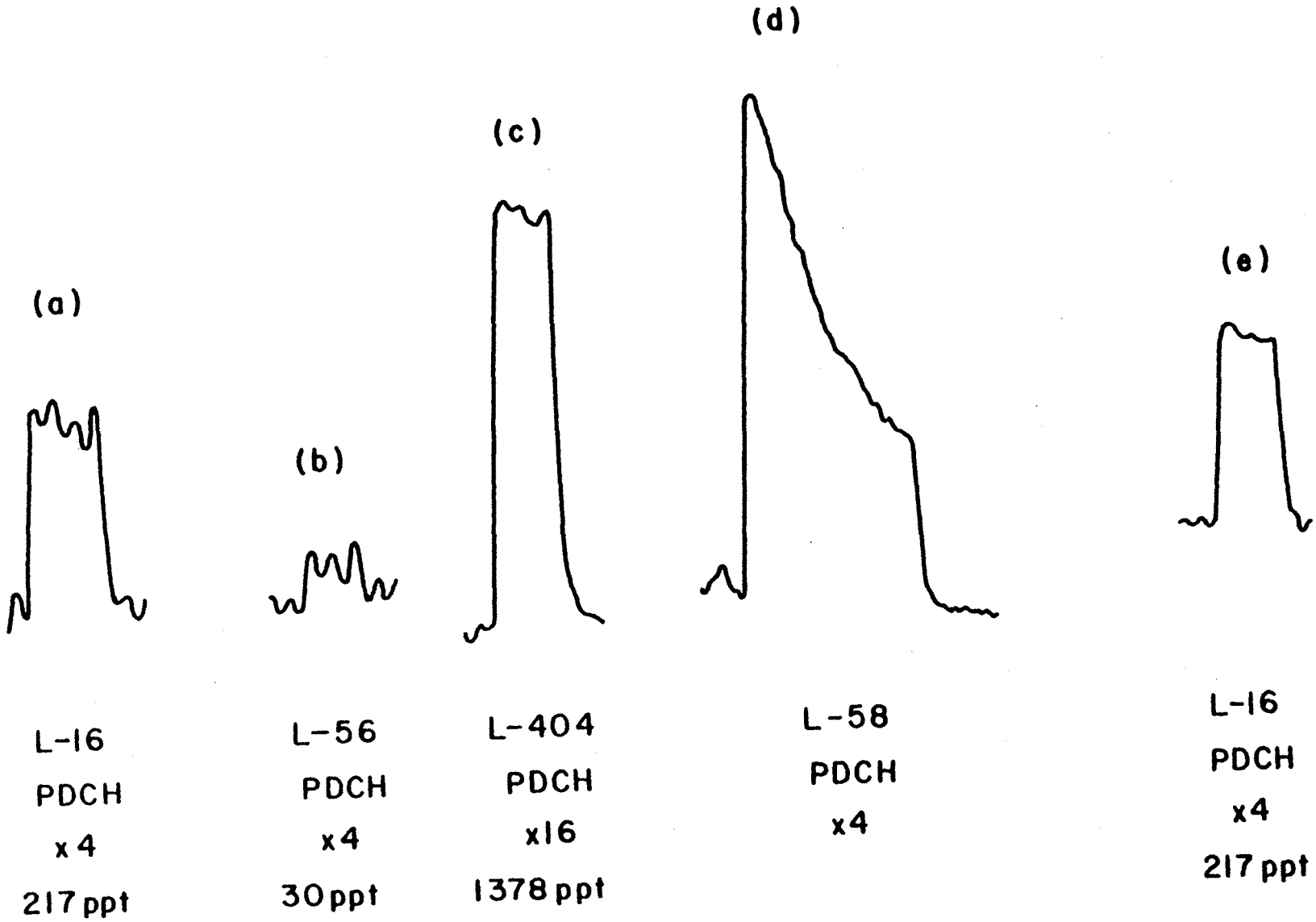

Figure 2
Continued

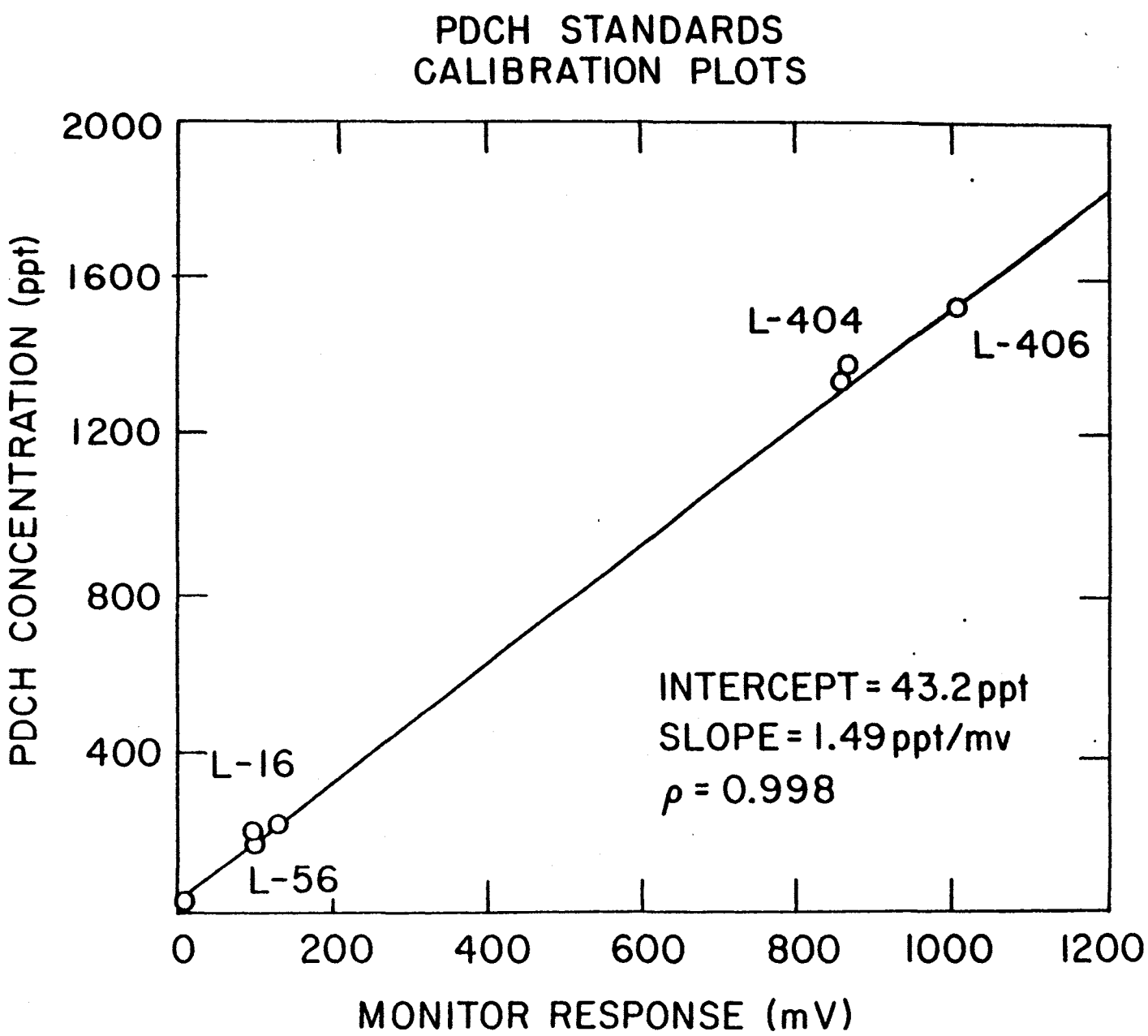
PDCH STANDARDS
CALIBRATION PLOTS
PDCH CONCENTRATION (ppt)
2000
1600
1200
800
400
0
200
400
600
800
1000
1200
MONITOR RESPONSE (mV)
L-404
L-406
L-16
L-56
INTERCEPT = 43.2 ppt
SLOPE = 1.49 ppt/mv
ρ = 0.998

Figure 3

Figure 4

SUITCASE #13

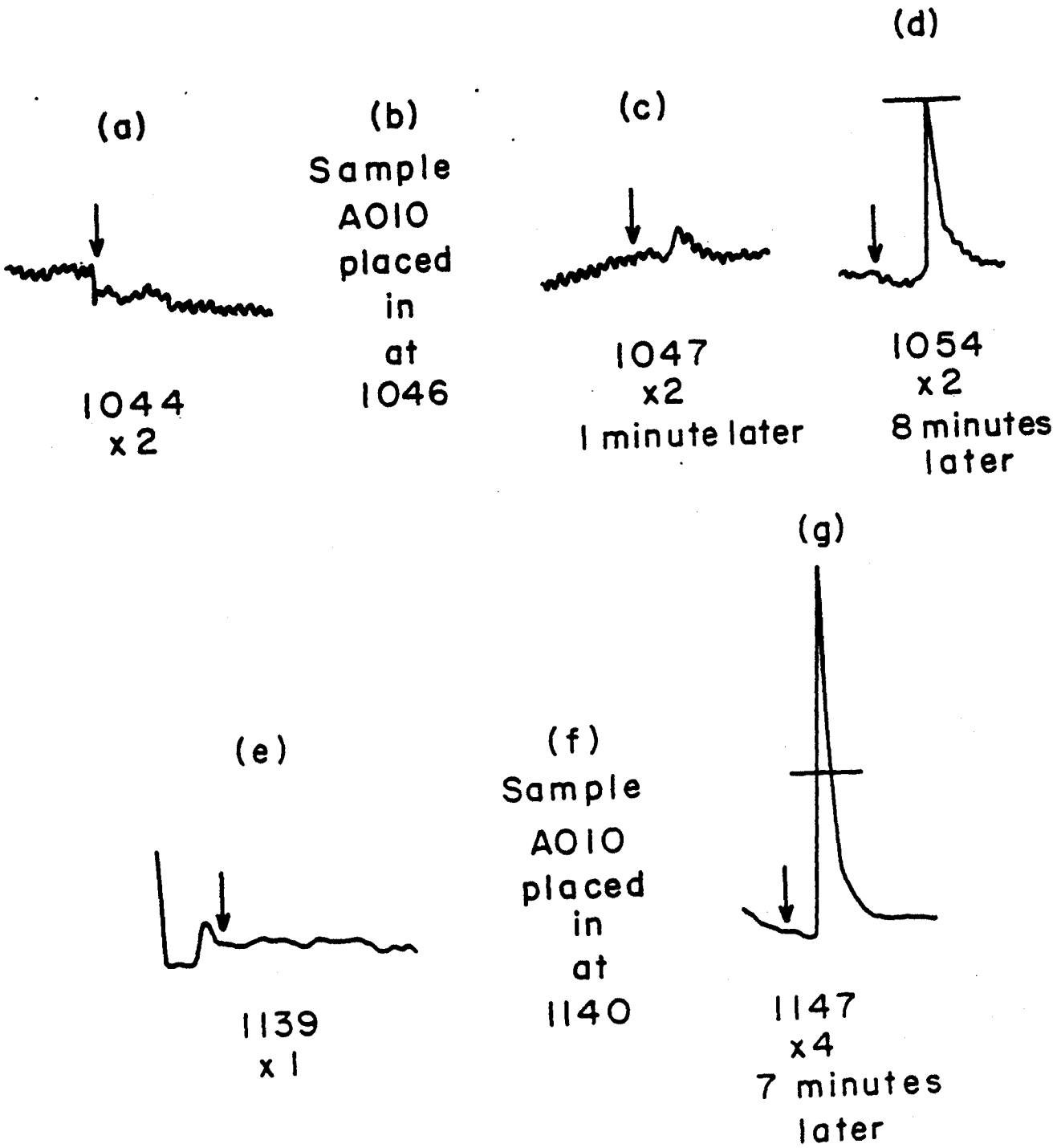

Figure 5

SUITCASE #13

(a)

1345
x1

(b)

Sample
A06
placed
in
at
1346

(c)

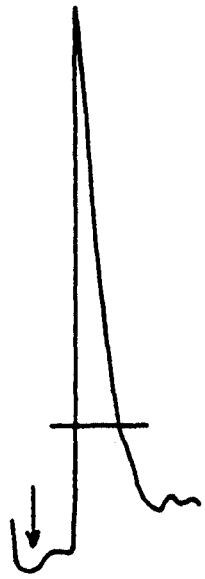

1353
x1
7 minutes later

(d)

1415
x1

(e)

Sample
A06
placed
in
at
1416.5

(f)

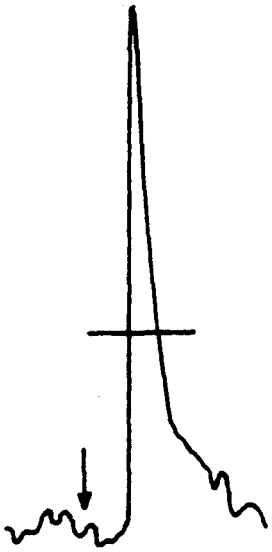

1423.5
x1
7 minutes later

Figure 6

SUITCASE SCANS

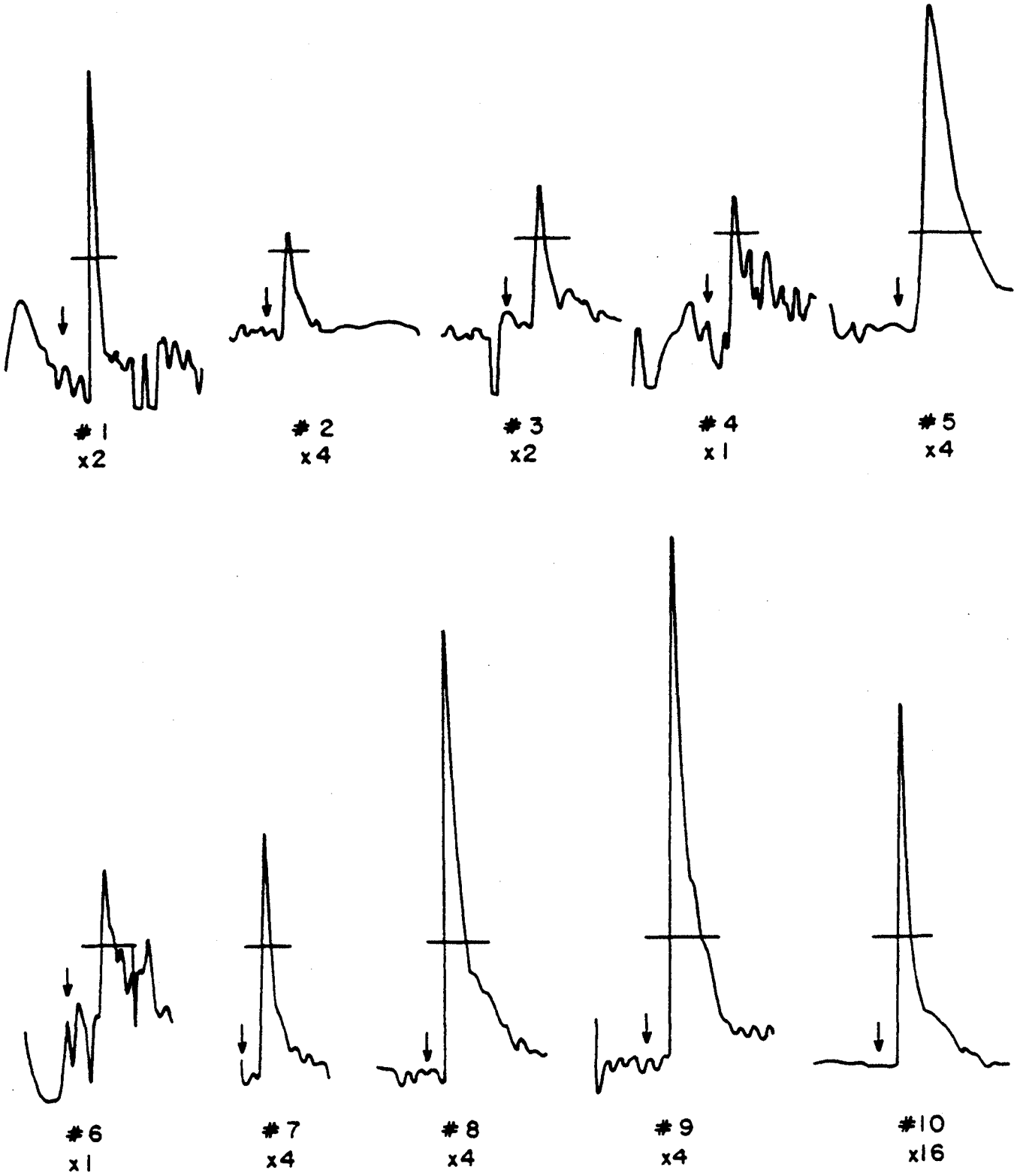

Figure 7

SUITCASE #13
SCALE ATTENUATION = 2

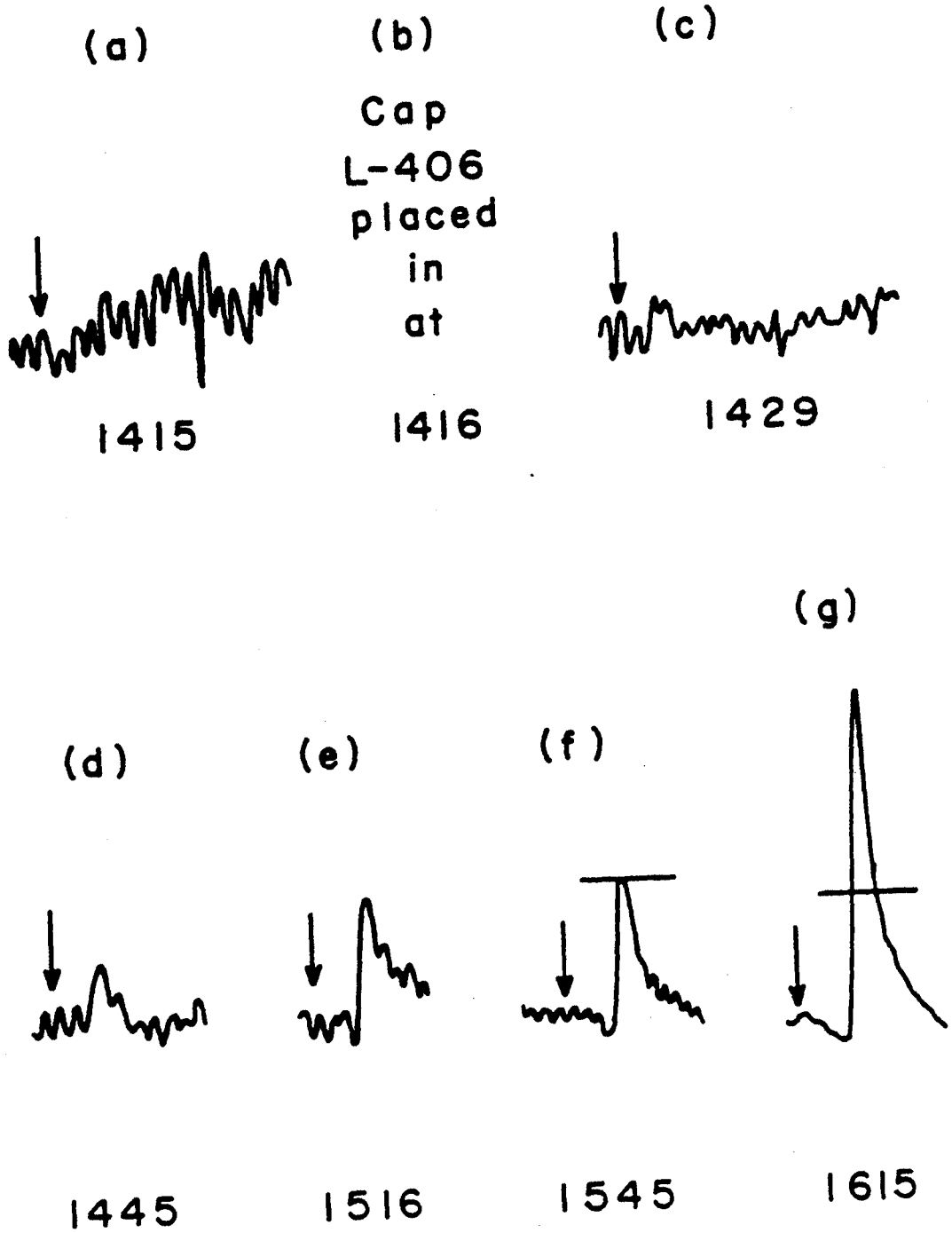

Figure 8

SUITCASE # 14
SCALE ATTEUATION = 2

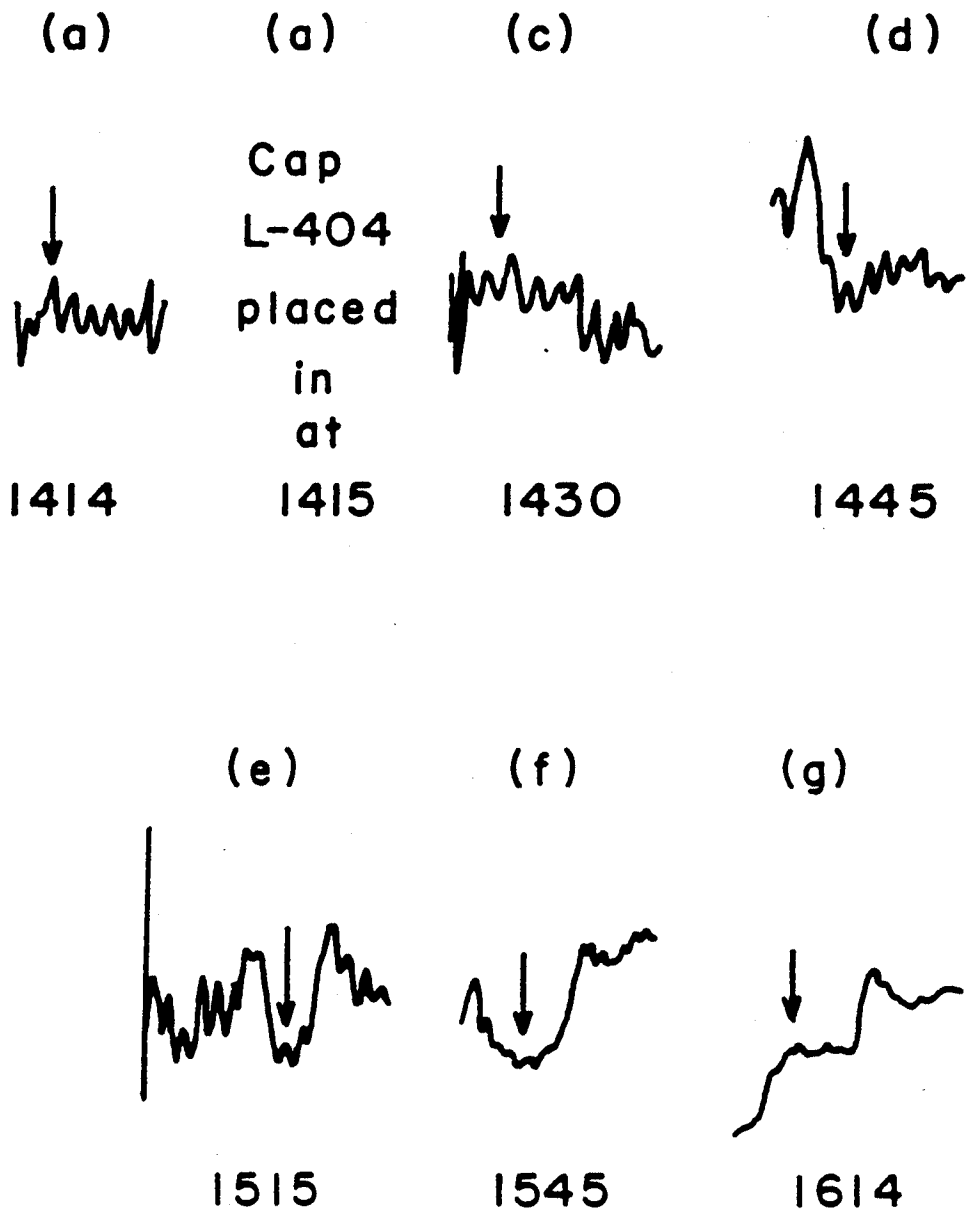

Figure 9

SUITCASE #15

SCALE ATTENUATION = 2

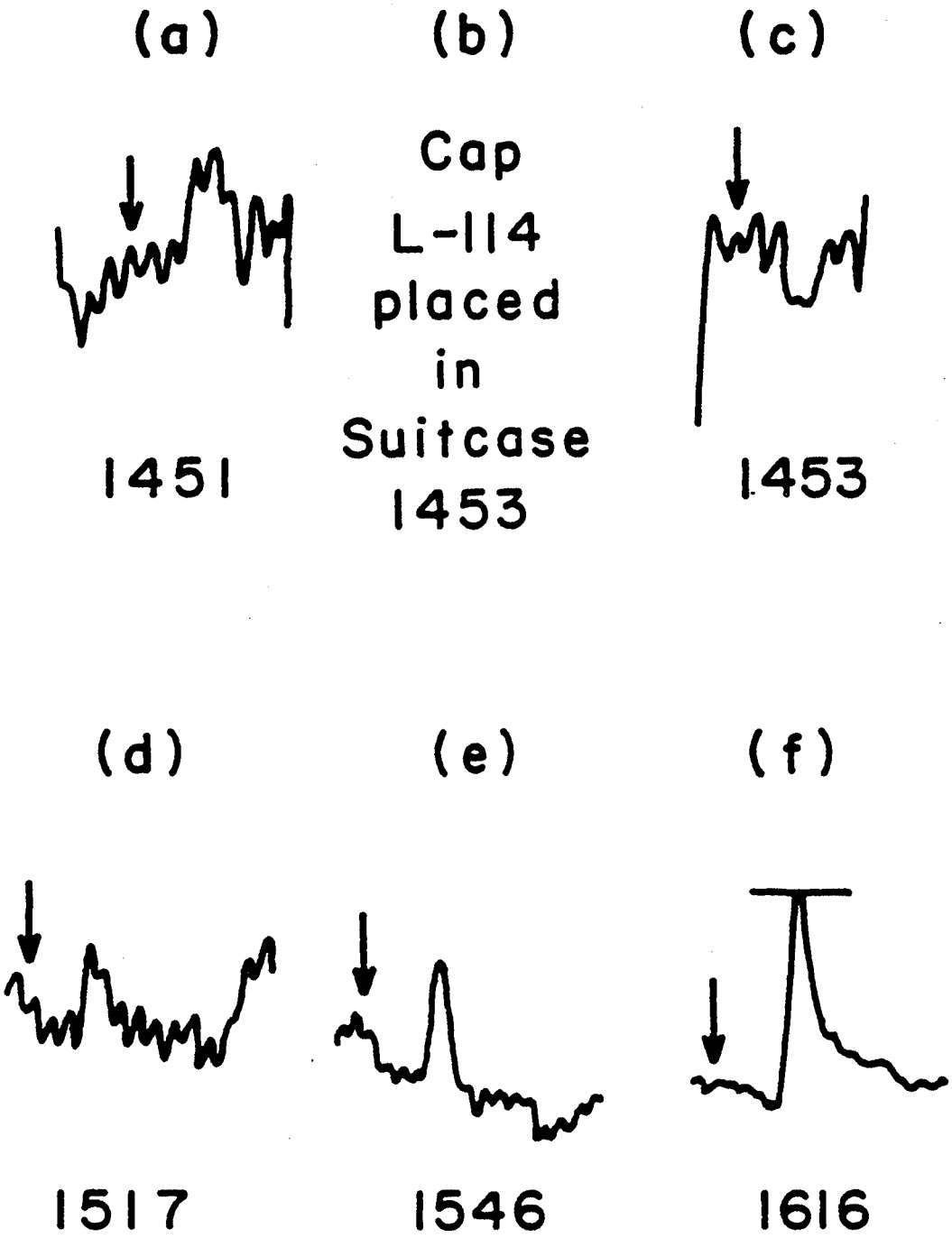

Figure 10

SUITCASE # 2

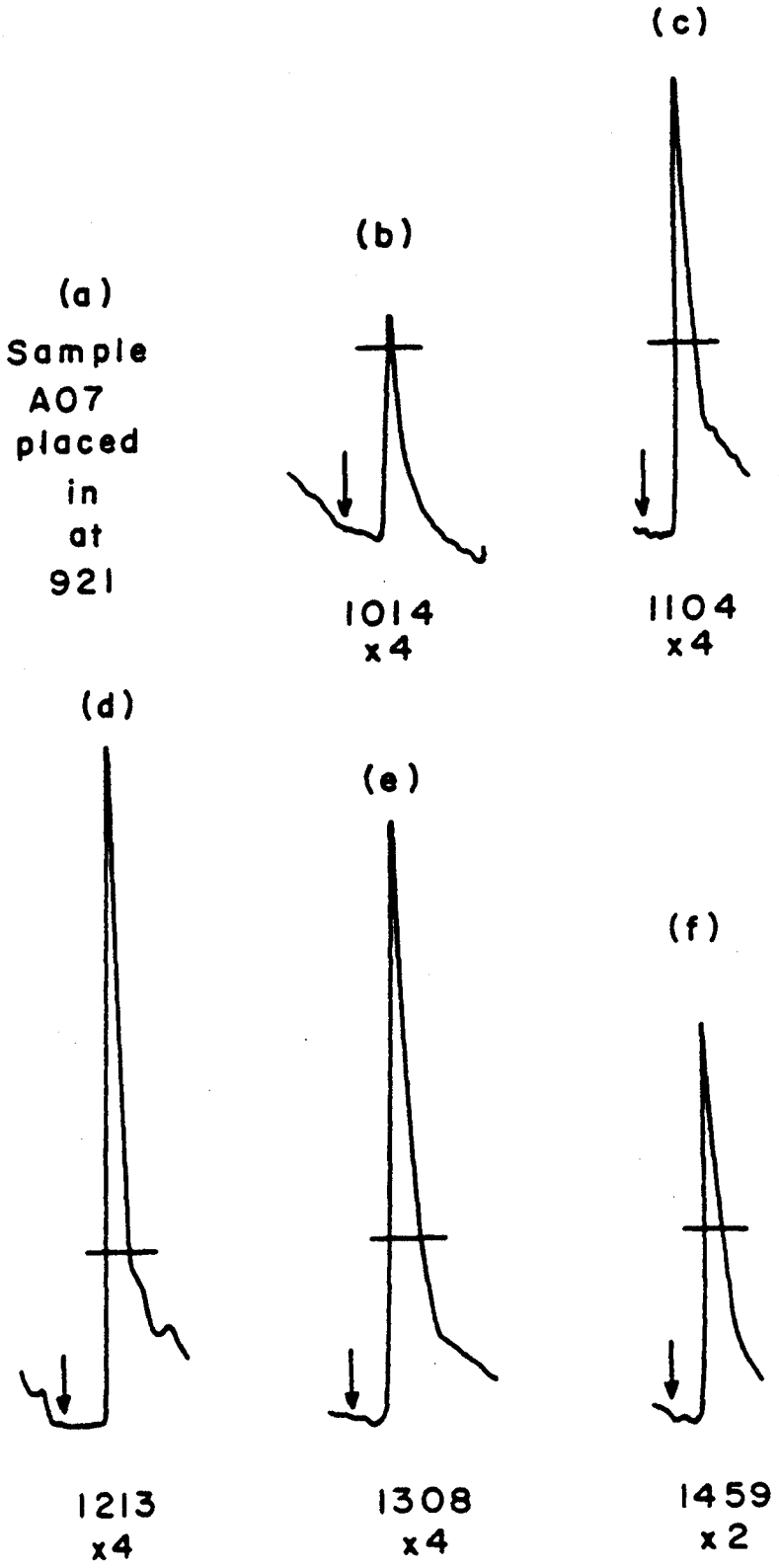

Figure 11

SUITCASE #3

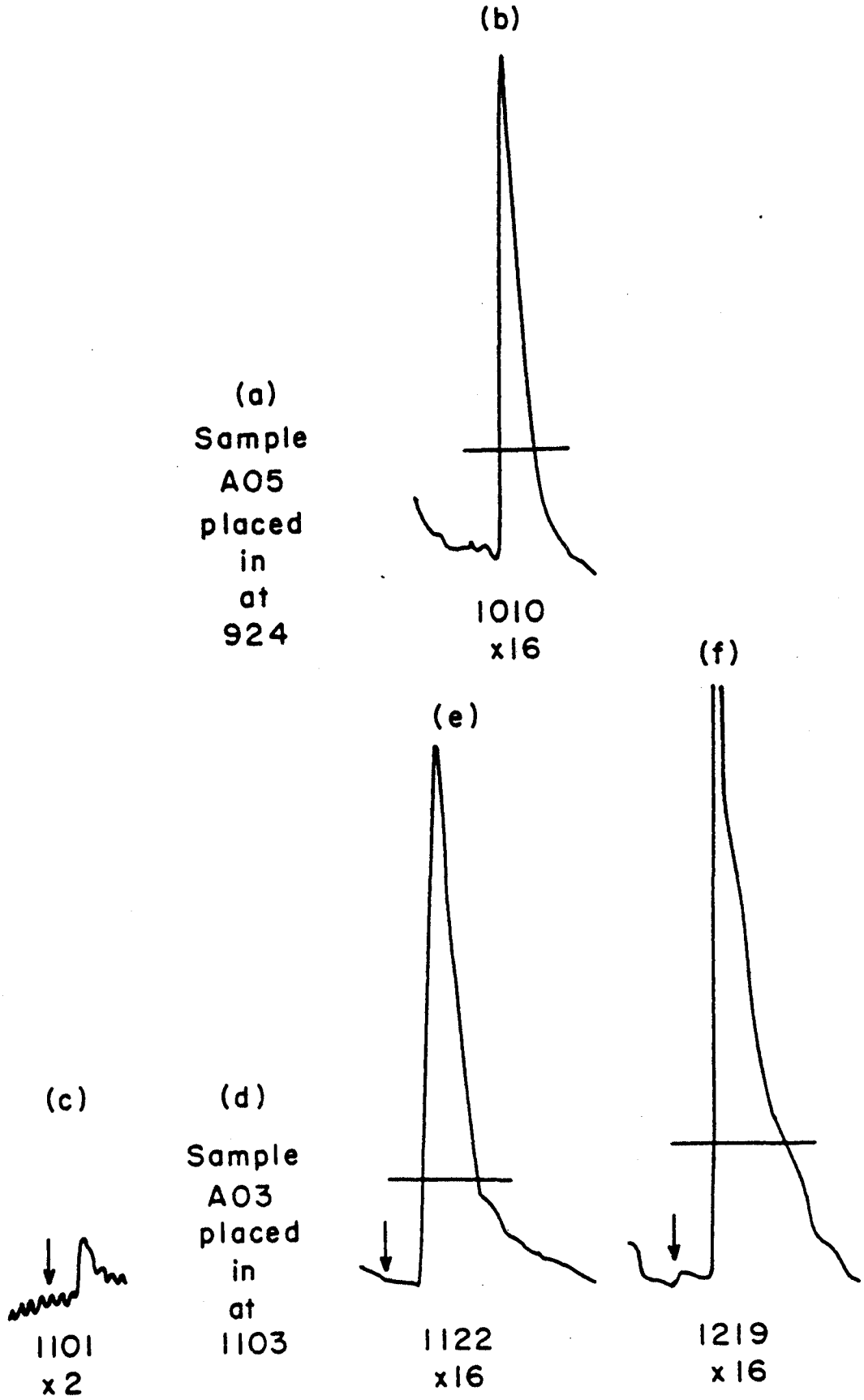

Figure 12

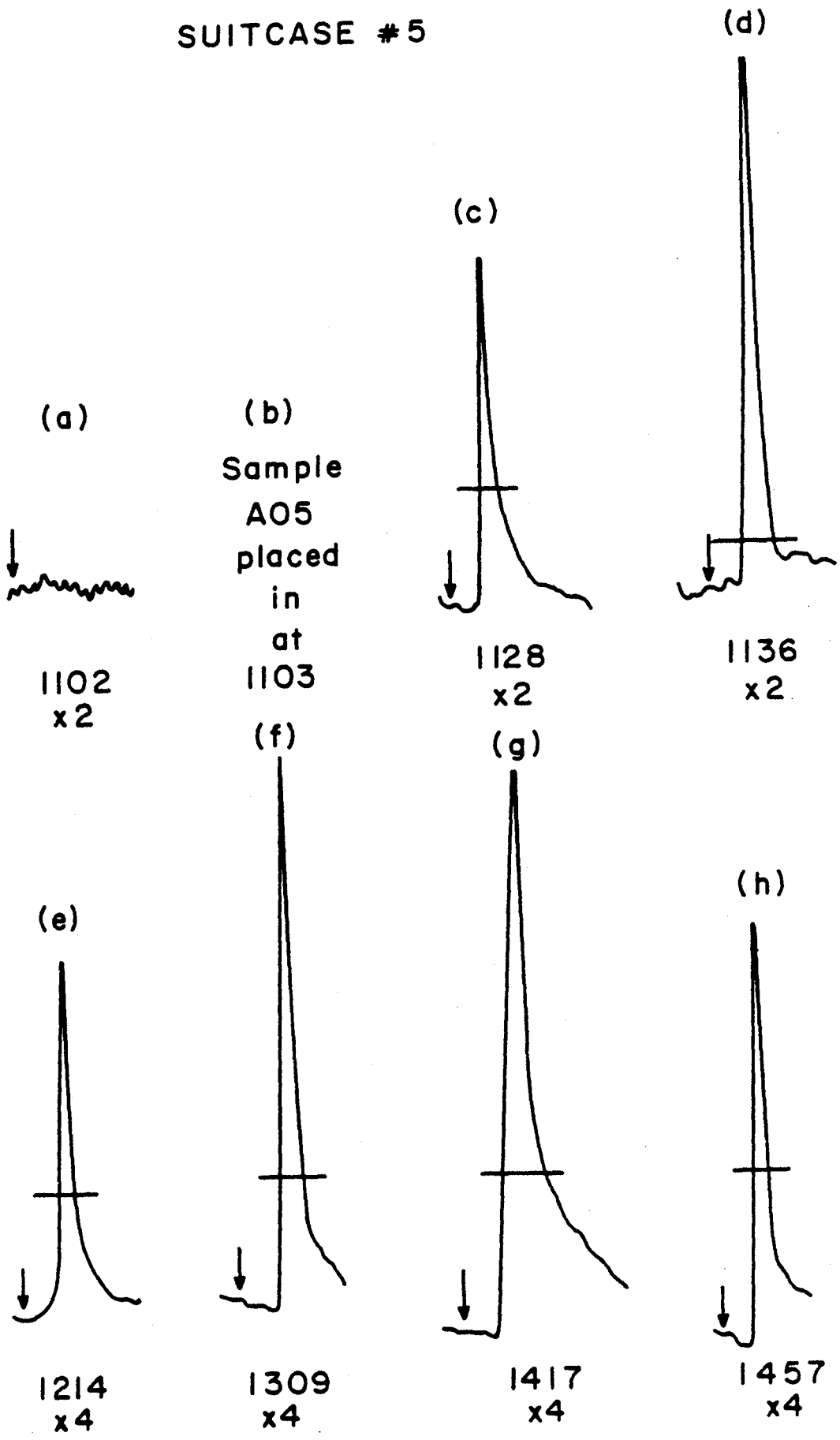
SUITCASE #5
(a)
1102
x2
(b)
Sample
A05
placed
in
at
1103
(c)
1128
x2
(d)
1136
x2
(e)
1214
x4
(f)
1309
x4
(g)
1417
x4
(h)
1457
x4

Figure 13

SUITCASE #6

(a)

Sample A08 placed in at 922

(b)

1016
x2

(c)

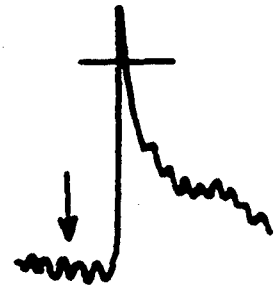

1042
x2

(d)

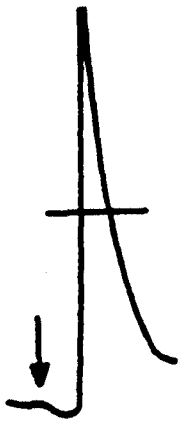

1215
x2

(e)

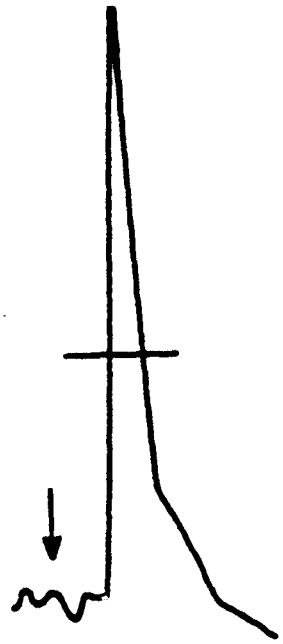

1312
x2

(f)

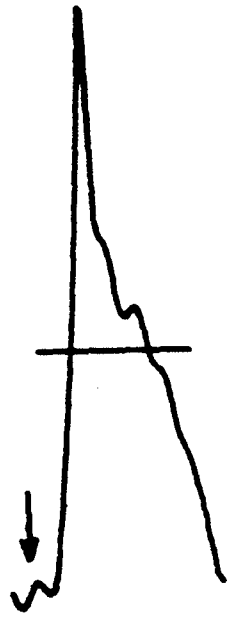

1457
x2

Figure 14

SUITCASE #8

(a)

Sample
A03
placed
in
at
921

(b)

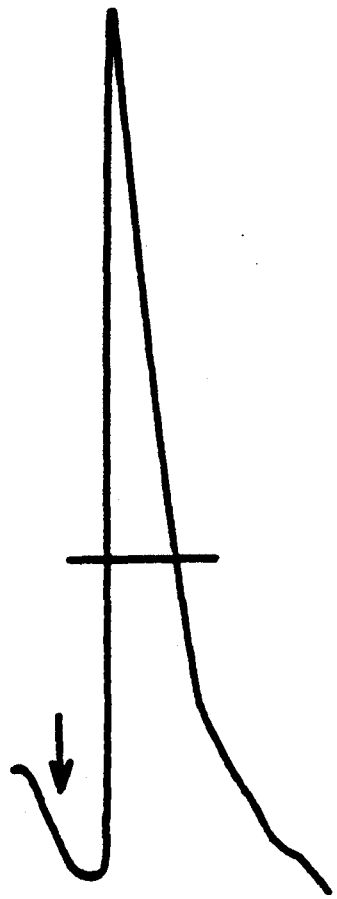

1008
x8

(c)

1219
x16

Figure 16

SUITCASE #13

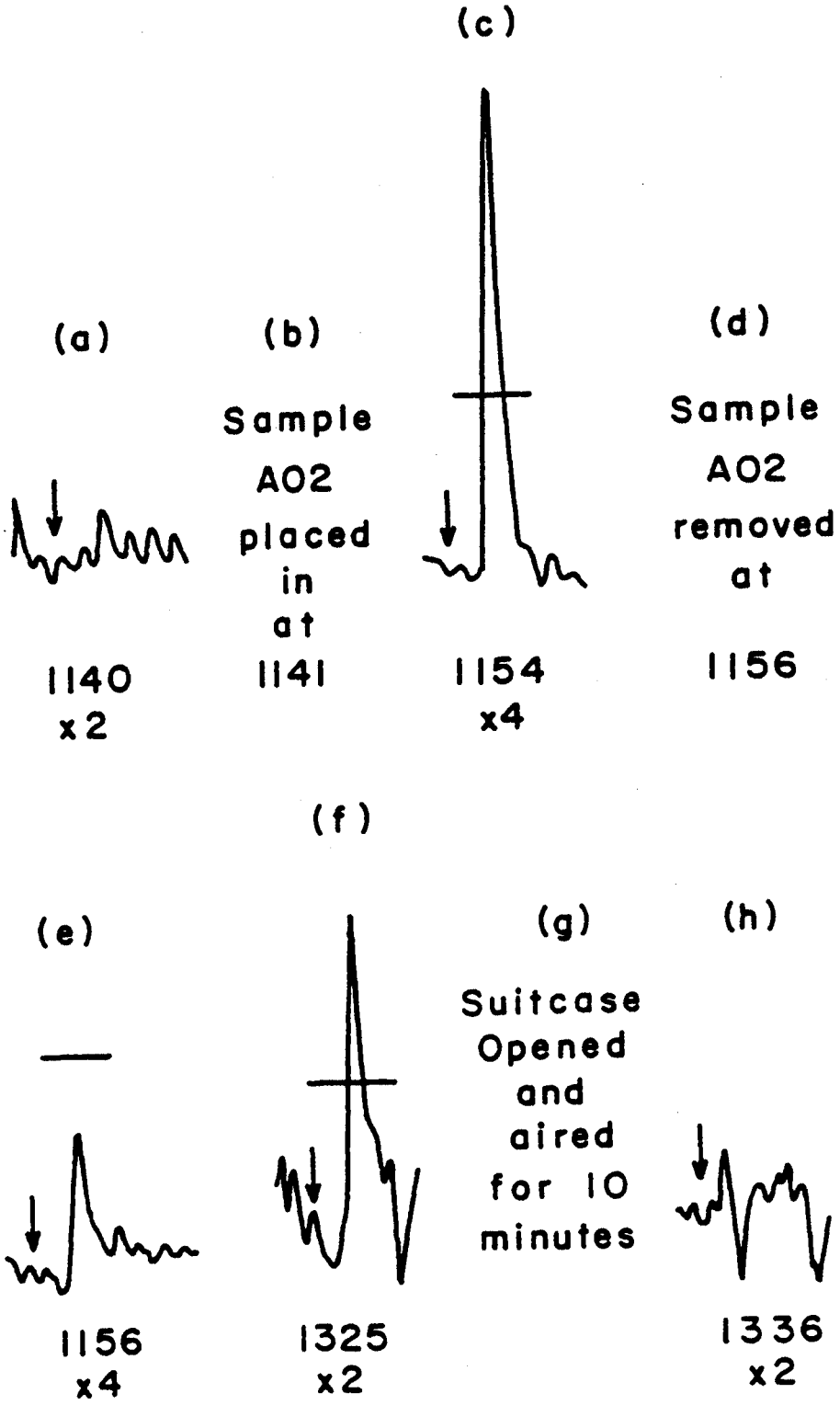

BNL-26612
LIMITED DISTRIBUTION

DETECTION OF TAGGED EXPLOSIVES IN A DC-9 AIRCRAFT VIA SAMPLING OF THE AIR EXHAUST

Gunnar I. Senum, Robert P. Gergley, Edgar A. Cote and Russell N. Dietz

July 1979

Test date: May 23, 1979

Research sponsored by the
Bureau of Alcohol, Tobacco, and Firearms
of the U.S. Treasury Department
under the auspices of the Aerospace Corporation

INFORMAL REPORT

BROOKHAVEN NATIONAL LABORATORY
UPTON, NEW YORK 11973

NOTICE

This report was prepared as an account of work sponsored by the United States Government. Neither the United States Government nor any agency thereof, or any of their employees, makes any warranty, expressed or implied, or assumes any legal liability or responsibility for any third party's use, or the results of such use, of any information, apparatus, product or process disclosed, or represents that its use by such third party would not infringe privately owned rights.

Abstract

Experiments to determine the feasibility of detecting vapor tagged explosives placed on a DC-9 aircraft have been performed. Taggant vapor concentrations were measured at the DC-9 ventilation outflow valve from simulated tagged explosives placed in either the passenger or baggage compartments. The taggant concentration from the aircraft reached a steady state concentration within 15-20 minutes after the placement of the tagged explosives in the passenger compartment. This steady state concentration of about 7.5 parts-per-trillion taggant in air is sufficiently great so as to be detected by a portable real-time continuous taggant detector. The taggants, PDCH and PMCH, had been incorporated as microencapsulated PDCH at 0.05 to 0.10% by weight in the bulk simulated explosives, typifying the expected taggant loading in commercial bulk explosives.

Introduction

The ultimate success of any vapor tagging technique for predetonation detection of explosives is dependent on the ability to detect the vapor taggants in various detection scenarios. A scenario of great interest is the detection of explosives on an aircraft, especially at the convenient time between passenger loading and take-off. The vapor tagged explosives will have had circa 0-30 minutes in which to release the vapor taggant into the aircraft (in either the passenger or baggage compartment) before detection. Thus the feasibility of the technique is dependent on ability to detect the taggant vapor at concentrations present in the first thirty minutes at either inside the aircraft or at the ventilation outflow port.

The vapor tagging of explosives has now progressed to the point where there are several potential vapor taggants with a suitable detection technique. One such vapor taggant, PDCH, has now been incorporated into some simulated bulk explosives at low concentrations which would be typical of vapor tagged explosives. Consequently the vapor taggant emission rates from these explosives are typical of the proposed tagging techniques. This report summarizes the results of an experiment in which these tagged bulk explosives were placed inside a DC-9 aircraft and the vapor taggant concentrations in air samples collected at the DC-9 ventilation outflow port were determined as a function of elapsed time.

Background

A scenario containing a vapor tagged explosive will provide two impediments to the detection of the vapor taggant in or from that scenario. The first impediment is loss of the taggant due to physical adsorption of the vapor taggant on various adsorptive surfaces present in the scenario, i.e., clothes, curtains, rugs, etc. This loss can be minimized as has been shown[1] with the use

of vapor taggants which are relatively volatile, e.g., perfluorodimethylcyclobutane (PDCB), perfluoromethylcyclohexane (PMCH), and perfluorodimethylcyclohexane (PDCH). The second impediment is the containment of the vapor taggant within any barrier enclosing the tagged explosive, e.g., the tagged explosives may be placed in a briefcase which is then left in the scenario. The briefcase or any other barrier may be sufficiently airtight so as to slightly or significantly reduce the rate of vapor taggant to escape into the scenario. However, in a series of laboratory experiments involving barriers such as briefcases, suitcases, sealed boxes and heat sealed plastic bags,this impediment has also been shown[1] to be negligible. Although, several barriers did provide a significant air-tightness, e.g., a sealed paint can and a zip-locked plastic bag, the majority of common barriers have a negligible degree of air-tightness.

With these impediments minimized the detection of vapor taggants becomes dependent on the degree of scenario air mixing and the scenario ventilation rate. The vapor taggant will be constantly diluted and removed from the scenario by the inflow and outflow of ventilation air and consequently after a sufficiently long time a steady state taggant concentration will be reached in the scenario. As a result of this ventilation, the taggant concentration can be shown[2] to have the following time dependence, i.e.,

$$C(t) = C(\infty)\ [1 - \exp\ (- t/t_v)] \qquad (1)$$

in which C(t) is the scenario taggant concentration at time t (elapsed time after the introduction of the tagged explosive), $C(\infty)$ is the aforementioned steady state concentration and t_v is the ventilation turnover time. The two quantities $C(\infty)$ and t_v can be further expressed as

$$C(\infty) = R_{source}/R_{ventilation} \qquad (2)$$

and

$$t_v = V_{ch}/R_{ventilation} \qquad (3)$$

in which R_{source} is the vapor taggant emission rate from the tagged explosive, $R_{ventilation}$ is the scenario ventilation rate and V_{ch} is the volume of the scenario. Thus if R_{source}, $R_{ventilation}$ and V_{ch} are known, then the taggant concentration within the scenario can be predicted. This functional dependence is derived under the assumption of uniform mixing of the taggant within the scenario. The effect of an air tight barrier surrounding the tagged explosive is to slow the rate of release of the taggant in the scenario, but the same steady state concentration will be reached after a longer elapsed time. Further discussion and equations for this effect is given in reference 2.

Previously, Dravniks et. al.,[3] have obtained the attenuation factors r for a tagged source in various aircraft in order to determine taggant detector sensitivity requirements. The attentuation factor r is simply

$$r = C(t)/R_{source} \tag{4}$$

and those obtained by Dravniks apparently have the functional dependence of C(t) as given in equation (1) although not explicitly displayed. However Dravniks did not use a specific taggant nor a specific detection system since his purpose was to determine sensitivity requirement. The purpose of this experiment was to examine the feasibility of detecting a proposed vapor taggant (PDCH) on a DC-9 aircraft using a proposed detection method (Electron Capture Detection, ECD).

A reason PDCH (perfluorodimethylcyclohexane) was chosen as a potential vapor taggant is its high sensitivity towards ECD detection. One advantage of ECD is its simplicity, allowing the vapor taggant detector to be made into a small, portable, and inexpensive unit[4]. The detection sensitivity for real-time vapor taggant detection is presently approximately one part-per-trillion of vapor taggant in air. Concentration techniques allows the detection sensitivity

to be increased by two to four orders of magnitude depending on the method[5].

There are several methods to incorporate vapor taggants into explosives[6], of which two are of the greatest practicality. The first method is the incorporation of the vapor taggant into the blasting cap which is used to detonate the explosive. The vapor taggant is either directly solubilized into the end plug of the blasting cap[1,7-11] or else the end plug can be blended with taggant-containing microspheres[6]. The other method is to blend microspheres into the bulk explosives at concentrations of 0.05-0.10% by weight. The taggant will then permeate out of the microspheres at a known rate. Both methods allow a tagging lifetime up to 5 years after incorporation.

Experimental

The microcapsule tagged bulk explosive simulants used in this experiment were prepared for the Aerospace Corporation and are described in Table 1 along with the amount of microencapsulated taggant which had been blended into each sample. These samples were simulants in the sense that the EGDN or TNT had been excluded during manufacture and an inert compound had been substituted. The PDCH emission rates from these samples have now been followed for a period of six months and the chromatographically determined emission rate are tabulated in Table 2. The taggant emission rates have been more or less constant with no apparent decrease in the rate. The large fluctuations between different determinations and the large relative standard deviations are inherent to the microcapsule tagged samples and not the chromatographic analysis technique. These fluctuations may be due to the large temperature dependence of the emission rate since the analysis were done without temperature regulation. Nonetheless, the apparent constancy of the PDCH taggant emission rate demonstrates the ability to tag bulk explosives by incorporation of

microencapsulated taggant into the explosive. Another potential taggant, PMCH, is present as an impurity in PDCH at about 5-20% depending on the source of PDCH. Thus the PDCH tagged samples are also emitting PMCH and the emission rates of PMCH as determined chromatographically are given in Table 3.

Two aircraft, both DC-9, were available for the experiment after the completion of their scheduled runs in the late evening. The tagged explosives were to be placed on board the DC-9 aircraft and the aircraft air was to be sampled at the ventilation outflow port on the underside of the aircraft. It was initially decided to take air samples in two-liter air sampling bags for subsequent analysis at BNL since the expected PDCH taggant concentrations were too low for real-time continuous sampling. The air sampling bags and the tagged bulk explosives were shipped separately to the experimental site in order to avoid any contamination of the sample bags by the PDCH tagged samples. Before the experiment all the air sampling bags were filled with ultra-high purity air and several were analyzed for PDCH in order to check for the absence of PDCH. Several bags were used as internal blanks, i.e., remained unused during the experiment in order to check for cross contamination of the bags during their return to BNL.

The first aircraft to be made available was at 11:30 P.M. Two air samples of the ambient aircraft were taken before the start of the experiment. Three tagged explosive samples (#A04, A07 and A08) were wrapped in some newspaper and placed in the passenger compartment on row 8, seat C, more or less in the center of the aircraft. The aircraft was sealed with only the air recirculation fans ventilating the aircraft since the engines were not running. The distribution of air in the aircraft in the recirculation pump mode is shown in Figure 1. When the engines and consequently the turbocompressors are on, the ventilation

rate is increased and the ventilation pattern is changed as can be seen in the comparison of the two ventilation modes in Figure 1. The ventilation rate was calculated from a measurement of the air velocity with an anemometer at the outflow valve. After the aircraft was sealed air samples were taken from the outflow valve every two minutes with 50 seconds required to fill a 1 liter air sampling bag. Nineteen air sample bags were filled for a total of 40 minutes of sampling.

The second aircraft to become available was at 1:00 A.M. Six tagged explosive samples (#A04, A07, A08, A02, A05 and A06) were wrapped in some newspaper and placed in the baggage hold. The aircraft was sealed as before with only the air recirculation pumps providing the ventilation. Air samples were then taken every two minutes with 90 seconds required to fill the two liter air sampling bags. Seventeen air samples were filled for a total of 34 minutes of sampling.

The air sample bags were shipped back to BNL for PMCH and PDCH analysis. This was performed on a laboratory chromatograph system which is schematically outlined in Figure 2, with the following procedure. Air was withdrawn from the air sample bag so as to fill a 40 cc sample loop which was injected into a N_2 carrier gas. The PMCH and PDCH is subsequently collected on a concentrator trap. The concentrator trap is then isolated and rapidly heated so as to thermally desorb the PMCH and PDCH into another carrier stream which is backflushing through the trap. This carrier stream with the PMCH and PDCH is then passed through a Pd catalyst column (3% Pd on Molecular Sieve 5A) with a small added amount of H_2. This combusts any oxygen and ambient Freons which might be in the sample after concentration which would interfere with the analysis. Following the Pd column, the taggant sample passes through a Nafion

permeation drier which removes water and any other freon combustion products. The PMCH and PDCH sample is then chromatographed on a six foot 1/8" porosil F column and subsequently detected by an electron capture detector. The resulting PMCH and PDCH chromatographic peaks are integrated with a computing integrator. The analysis is calibrated with a periodic analysis of a ten parts-per-trillion standard of PDCH in air which also contain PMCH. The resulting PMCH and PDCH vapor taggant concentrations for both sets of air sampling bags are given in Tables 4 and 5. An experimental uncertainity was obtained for several air samples which were analyzed in duplicate or triplicate and this is given also in the Tables.

Results and Discussion

A. Tagged Explosives in the Passenger Compartment

It is evident from a plot of the measured PDCH and PMCH taggant concentrations (Figures 3 and 4) that the taggant concentration in the aircraft in this instance follows the time dependence as described by equation (1). The solid line in both figures is a least mean square fit of equation (1) to the measured taggant concentrations. The resulting fitted values of the steady state concentration, $C(\infty)$, and the ventilation turnover time, t_v, are given in the top half of Table 6. The ventilation turnover time should be identical for both taggants since this is independent of the choice of taggants as shown in equation (3). The fitted turnover times of 6.3 ± 0.6 minutes for PMCH and 5.46 ± 0.25 minutes for PDCH are indeed in good agreement with each other.

The steady state concentrations, $C(\infty)$, and the ventilation turnover time, t_v, can also be predicted from a knowledge of the taggant emission rate, the ventilation rate and the aircraft volume as given in equations (2) and (3). The

comparison between these measured and predicted quantities is given in Table 7. The predicted values of the steady state concentrations for both taggants are a factor of about four lower than the measured value whereas the predicted value of the ventilation turnover time is in good agreement with the measured values. At present, it is felt that the measured aircraft taggant concentrations are more accurate than the predicted estimates. No explanation can be given for the discrepancy in the predicted and measured steady state concentrations until further experiments have been done with the tagged explosives placed in various parts of the passenger compartment.

As mentioned previously the aircrafts were ventilated with only the air recirculation system in these experiments at a rate of 600 to 700 cubic feet per minute. Realistically, when an aircraft is loaded, it will be ventilated by the turbocompressors at a higher ventilation rate about 1.5 fold higher[3]. Thus the steady state taggant concentration will be proportionally reduced according to the proportional increase in the ventilation rate. The ventilation turnover time will be similarly reduced. Thus the taggant concentration in the aircraft will reach a lower steady state concentration in a shorter period of time when the turbocompressors are used when compared to the results in this study.

B. Tagged Explosives in the Baggage Compartment.

Figures 5 and 6 display the PMCH and PDCH taggant concentrations when the tagged explosives are placed in the baggage compartment. In this case, the taggant concentration increases linearly with time. The PMCH concentrations in Figure 6 are offset by a constant amount which was due to an interfering compound present during the chromatographic analysis. The rate of taggant increase is given in Table 6 as determined from a least squares analysis. These results

indicate that the ventilation turnover time is very long for the baggage compartment when compared to the passenger compartment, i.e., the baggage compartment is not as well ventilated as the passenger compartment. Thus the length of the sampling time (circa 35 minutes) was not long enough for the taggant concentrations to start to approach the steady state concentration.

In this case, when the duration of the sampling time is less than the ventilation turnover time, i.e., $t/t_v < 1$, the equation of the taggant concentration, equation (1), can be approximated as

$$C(t) \approx (C(\infty)/t_v)t = (R_{source}/V_{ch})t \quad . \tag{5}$$

The measured rate of taggant growth can now be compared to a predicted rate of growth, i.e., R_{source}/V_{ch} and this comparison is given in the bottom of Table 7. In this case the predicted rate of growth is from four to ten times greater than the measured values. As in the passenger compartment case, it is the measured value which is felt to be more accurate. Apparently, this discrepancy can be ascribed to the poor ventilation of the baggage compartment and possibly more experiments with the explosives in different parts of the baggage compartment would further clarify the discrepancy.

Conclusions

The main conclusion is that it is entirely feasible to detect vapor tagged explosives which have been placed in a DC-9 aircraft, either in the passenger or the baggage compartment. The aircraft taggant concentration as measured at the ventilation outflow valve is six ppt in ten minutes after the placement of three tagged sticks of dynamite in the passenger compartment. Similarly the aircraft taggant concentration is 1.5 ppt in ten minutes when six tagged sticks are tagged with taggant containing microcapsule appropriate to a tagging lifetime of up to five years with constant taggant emission rates in the range 0.5 to 30

nanoliters per minute. These taggant concentrations are in the detectability range of portable real-time continuous taggant detectors, i.e., taggant concentrations greater than 1 ppt. Lower concentrations can be detected with semi-continuous portable instruments[5].

The ventilation rates and internal volume of a DC-9 allow the maximum taggant concentration to be reached within two to three ventilation turnover times, i.e., 12 to 18 minutes after the tagged explosives have been placed on-board the aircraft in the passenger compartment. The ventilation distribution in the baggage compartment is poorer and consequently the taggant concentration is lower when compared to the passenger compartment.

Acknowledgments

The authors would like to thank Chris Pate and Bob Moler of the Aerospace Corporation for their assistance in these experiments.

References

1. Senum, G.I. Evaluation of Vapor Taggants and Substrates for the Tagging of Blasting Caps. Monthly progress letter reports to the Aerospace Corporation, July 1977 through March 1979.

2. Senum, G.I. Expected Taggant Concentrations in Scenarios from Tagged Blasting Caps in Various Barriers. Brookhaven Internal Report, July 1978.

3. Dravniks, A., Brabet, R. and Stanley, T.A. Evaluating Sensitivity Requirements for Explosives Vapor Detector Systems. DOT Report No. FAA-RD-72-23.

4. Dietz, R.N., Cote, E.A. and Brown, R.M. A Portable Electron Capture GC for Tracing Air Pollutants. BNL 16512. April 1972.

5. Dietz, R.N., Goodrich, R.W. and Cote, E.A. Detection of Perfluorinated Taggants in Electric Blasting Caps by Electron Capture Monitors, Proc. New Concepts Symposium and Workshop on Detection and Identification of Explosives, November 1978.

6. Moler, R.B. Summary of Current Research on Explosives Detection and Identification, Proc. New Concepts Symposium and Workshop on Detection and Identification of Explosives, November 1978.

7. Dietz, R.N., et. al. Summary Report of the Brookhaven Explosives Tagging Program. BNL 21041. February 1976.

8. Senum, G.I. Evaluation of SF_6 Tagged Blasting Caps. Monthly progress letter reports to the Federal Aviation Administration. March through November 1977.

9. Dietz, R.N., et. al. Tagging Explosives with Sulfur Hexafluoride. U.S. Patent No. 3,991,680, November 16, 1976.

10. Dietz, R.N. and Senum, G.I. Perfluorocarbon Vapor Tagging of Blasting Cap Detonators. Patent Application. BNL 78-01, S-49,614, SN-9623, February 1979.

11. Toy, M.S., Stringham, R.S. and Toy, S.M. An Evaluation of Potential Taggant Polymer Combinations for Detection Tagging of Blasting Caps, Science Applications, Inc., SAI-78-508-SV.

Table 1

Microcapsule Tagged Bulk Explosive Simulants
(Power Primer Formula)

Sample #	PDCH Microcapsule Weight Percent	Cartridge Wrapper Dimensions	Wrapper Designation
A01	0.05	White plastic	Power Primer
A02	0.05	1" x 12" waxed paper	Powerdyn X
A03	0.10	1" x 12" waxed paper	Powerdyn X
A04	0.10	1 1/2" x 12" waxed paper	Extra Gelatin
A05	0.10	1" x 8" waxed paper	Permissible Gelatin
A06	0.05	1" x 8" waxed paper	Permissible Gelatin
A07	0.05	2" x 14" waxed cartridge	Floridyn
A08	0.10	2" x 14" waxed cartridge	Floridyn
A09	0.05	2" x 5" waxed cartridge	Super Prime #16L
A10	0.10	2" x 5" waxed cartridge	Super Prime #16L

Table 2

PDCH Emission Rate from the Microcapsule
Tagged Bulk Explosives Simulants

Sample #	Loading %	PDCH Emission Rate nℓ/min						
		1/23-25	3/1	3/29	4/18-19	5/11-14	6/19-20	6/29
A01	0.05	-----	1.74 ± 0.33	7.2 ± 1.1	1.52 ± 0.22	2.49 ± 0.35	0.91 ± 0.20	2.3 ± 0.7
A02	0.05	20.3 ± 5.4	10.2 ± 1.1	8.38 ± 0.25	6.02 ± 0.07	16 ± 4	2.53 ± 0.20	-----
A03	0.10	23.5 ± 3.3	3.96 ± 0.32	48.7 ± 2.3	2.91 ± 0.21	20.4 ± 1.5	34.6 ± 2.7	4.1 ± 0.8
A04	0.10	20.7 ± 4.3	13.6 ± 1.9	12.5 ± 1.0	9.9 ± 0.6	14.3 ± 1.3	20.4 ± 0.7	27.9 ± 0.9
A05	0.10	18.6 ± 2.6	10.4 ± 3.1	30.8 ± 2.1	3.6 ± 0.6	30.4 ± 2.9	0.48 ± .06	-----
A06	0.05	8.0 ± 1.6	4.0 ± 0.8	1.11 ± 0.02	1.01 ± 0.06	4.2 ± 0.6	4.00 ± 0.19	-----
A07	0.05	11.1 ± 2.1	8.7 ± 3.7	12.8 ± 1.4	0.69 ± 0.13	7.5 ± 2.1	26 ± 17	9.9 ± 0.6
A08	0.10	13.9 ± 8.8	21.8 ± 6.2	5.23 ± 0.22	13.3 ± 1.2	18.3 ± 3.4	16.4 ± 1.8	22.5 ± 2.9
A09	----	-----	20.4 ± 6.2	4.9 ± 2.2	2.8 ± 0.3	10.5 ± 3.6	29.5 ± 2.8	26 ± 7
A10	----	-----	122 ± 30	12.4 ± 2.4	15.1 ± 1.8	27.2 ± 2.1	51 ± 6	6.75 ± 0.17

Table 3

PMCH Emission Rates from the Microcapsule Tagged Bulk Explosive Simulants

Sample #	PMCH Emission Rate (nℓ/min)
	6/29
A01	0.25 ± .08
A02	11.3 ± 0.8
A03	0.47 ± 0.11
A04	4.14 ± 0.13
A05	4.8 ± 0.3
A06	10.3 ± 1.4
A07	0.957 ± .018
A08	2.69 ± 0.20
A09	3.0 ± 0.9
A10	0.684 ± .005

Table 4

Experiment #1
Tagged Explosives Placed in the Passenger Compartment (Row 8, Seat C)

Sampling Bag #	Elapsed Time (min)	Measured Taggant Concentrations (ppt) PMCH	PDCH
65	1	0.340	1.83 ± .05
66	3	0.707	3.72
67	5	1.15	4.82
68	7	1.19	5.61
69	9	1.40	6.21
70	11	1.54	7.20
71	13	1.65	7.03
72	15	1.57	6.91 ± .12
57	17	0.781	3.65 ± .03 (bag deflated)
56	19	1.69	7.44
55	21	1.65	7.19
54	23	1.74	7.56
53	25	1.81	7.75
62	27	1.80	7.63
61	29	1.84	7.68
60	31	1.82	7.83 ± .04
59	34	1.86	7.69 ± .23
Tagged Explosives removed from plane at 35:20			
58	37	1.74	8.51 ± .002
73	40	2.01	8.78 ± .01

Table 5

Experiment #2
Tagged Explosives Placed in the Baggage Compartment

Sampling Bag #	Elapsed Time (min)	Measured Taggant Concentrations (ppt) PMCH	PDCH
35	1	0.389	0.108 ± .017
34	3	0.644	0.520
33	5	0.520	0.671
32	7	0.448	0.965
31	9	0.564	1.30
16	11	0.599	1.67
17	13	0.447	1.91 ± .02
18	15	0.504	1.99 ± .03
19	17	0.558	2.45
20	19	0.737	2.68
21	21	0.861	3.39
22	23	0.929	3.54 ± .25
23	25	0.974	3.46 ± .04
24	27	0.982	3.43
25	29	1.07	3.76
11	31	1.17	4.23
12	33	1.04	4.43

Table 6

Calculated Results

I. Experiment #1 (Passenger Compartment)
Samples A04, A07 and A08

	Taggant	
	PMCH	PDCH
Time Constant, t_v (min)	6.3 ± 0.6	5.46 ± 0.25
Steady State Concentration, C(∞)(ppt)	1.80 ± 0.05	7.69 ± 0.09
Emission Rate, R_{cap} (nℓ/min)	7.8 ± 0.4	43 ± 7
Ventilation Rate, R_{ex} (ℓ/min)	19,700	
Aircraft Volume (liters)	156,000	

II. Experiment #2 (Baggage Compartment)
Samples A04, A07, A08, A02, A05 and A06

	Taggant	
	PMCH	PDCH
Intercept (ppt)	0.33 ± 0.06	0.00 ± 0.10
Rate of Growth (ppt/min)	0.0228 ± .0028	.134 ± .005
Emission Rate, R_{cap} (nℓ/min)	34 ± 3	84 ± 10
Ventilation Rate, R_{ex} (ℓ/min)	16,500	
Aircraft Volume (liters)	156,000	

Table 7

Comparison of Measured and Predicted Results

I. Experiment #1 (Passenger Compartment)

Taggant	Steady State Concentration, $C(\infty)$, ppt Measured	Predicted
PMCH	1.80 ± 0.05	0.40
PDCH	7.69 ± 0.09	2.18

Taggant	Ventilation Turnover Times, t_v, minutes Measured	Predicted
PMCH	6.3 ± 0.6	7.92
PDCH	5.46 ± 0.25	7.92

II. Experiment #2 (Baggage Compartment)

Taggant	Rate of Taggant Growth, ppt/minute Measured	Predicted
PMCH	0.0228 ± .0028	.218
PDCH	0.134 ± .005	.538

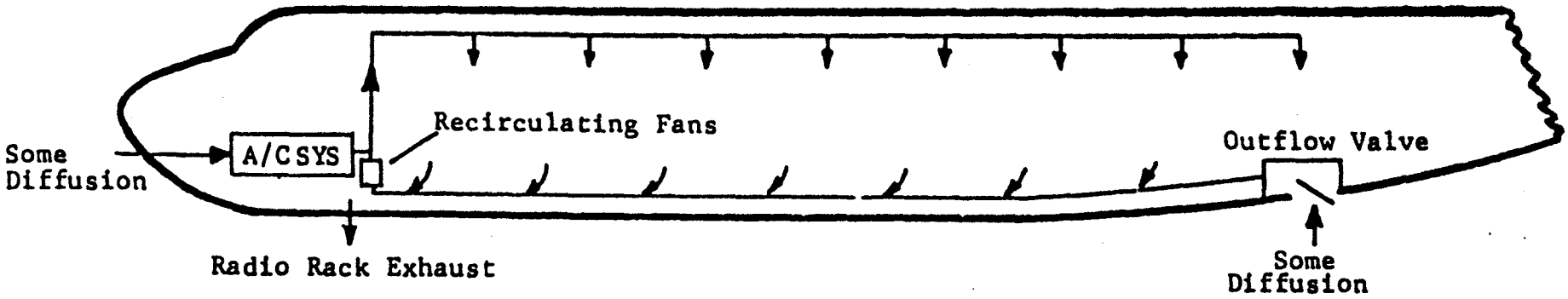

Air Flow with Recirculating Fans On

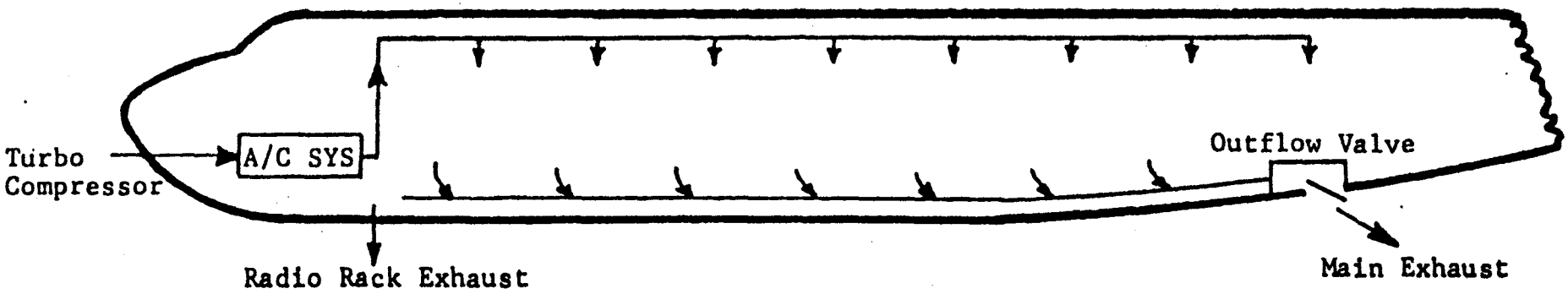

Air Flow with Turbo-Compressors On

AIR CIRCULATION WHILE TAXIING

Figure 1

No Negative #

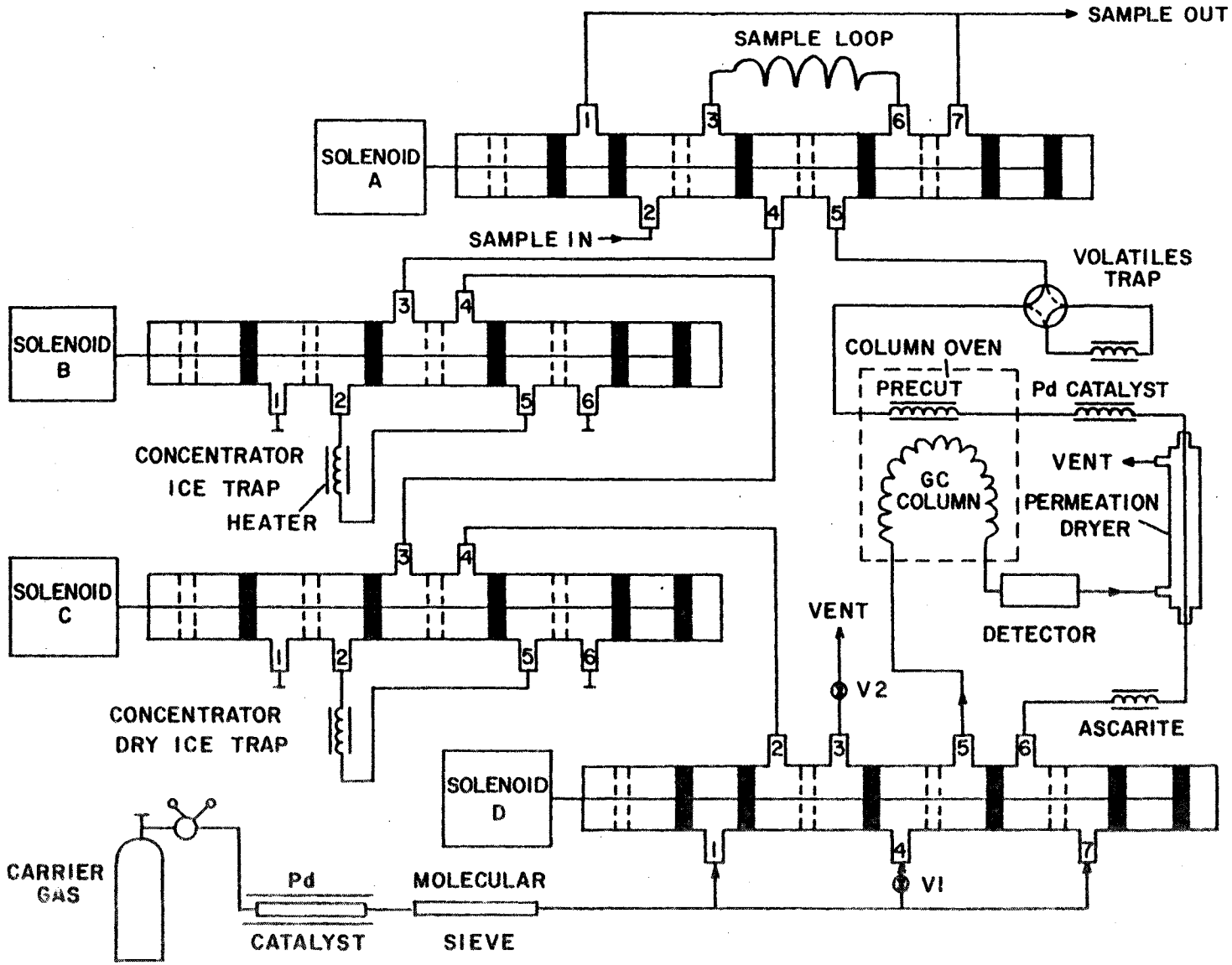
SAMPLE OUT
SAMPLE LOOP
SOLENOID A
SAMPLE IN
VOLATILES TRAP
SOLENOID B
COLUMN OVEN
PRECUT
Pd CATALYST
CONCENTRATOR ICE TRAP
HEATER
GC COLUMN
VENT
PERMEATION DRYER
SOLENOID C
VENT
DETECTOR
V2
CONCENTRATOR DRY ICE TRAP
ASCARITE
SOLENOID D
CARRIER GAS
Pd
MOLECULAR
V1
CATALYST
SIEVE

Figure 2

Figure 3

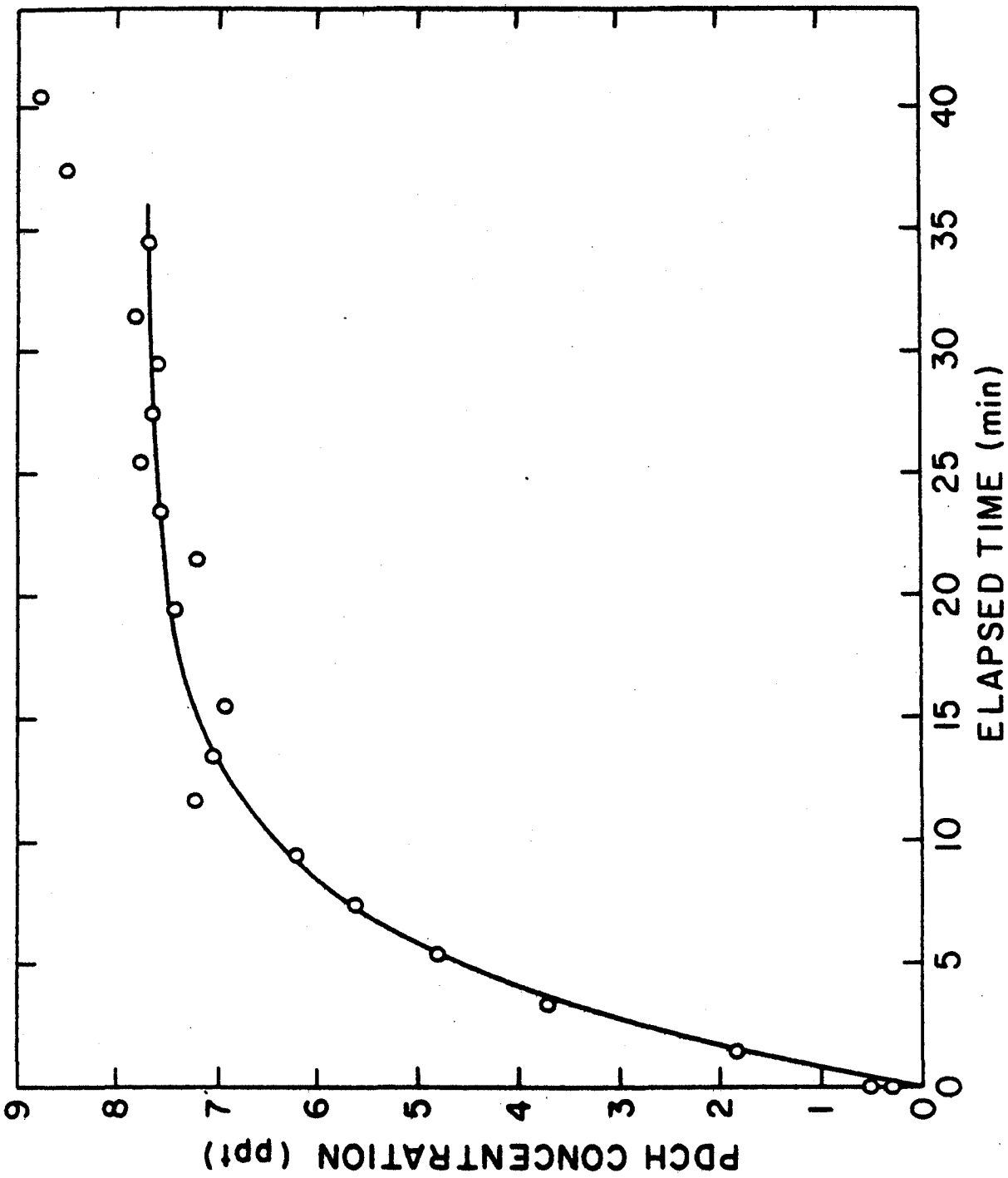
PDCH CONCENTRATION (ppt)
0
1
2
3
4
5
6
7
8
9
ELAPSED TIME (min)
0
5
10
15
20
25
30
35
40

MEASURED TAGGANT CONCENTRATIONS
AT A DC9 OUTFLOW VALVE
AS A FUNCTION OF ELAPSED TIME
TAGGED EXPLOSIVES IN
THE PASSENGER COMPARTMENT

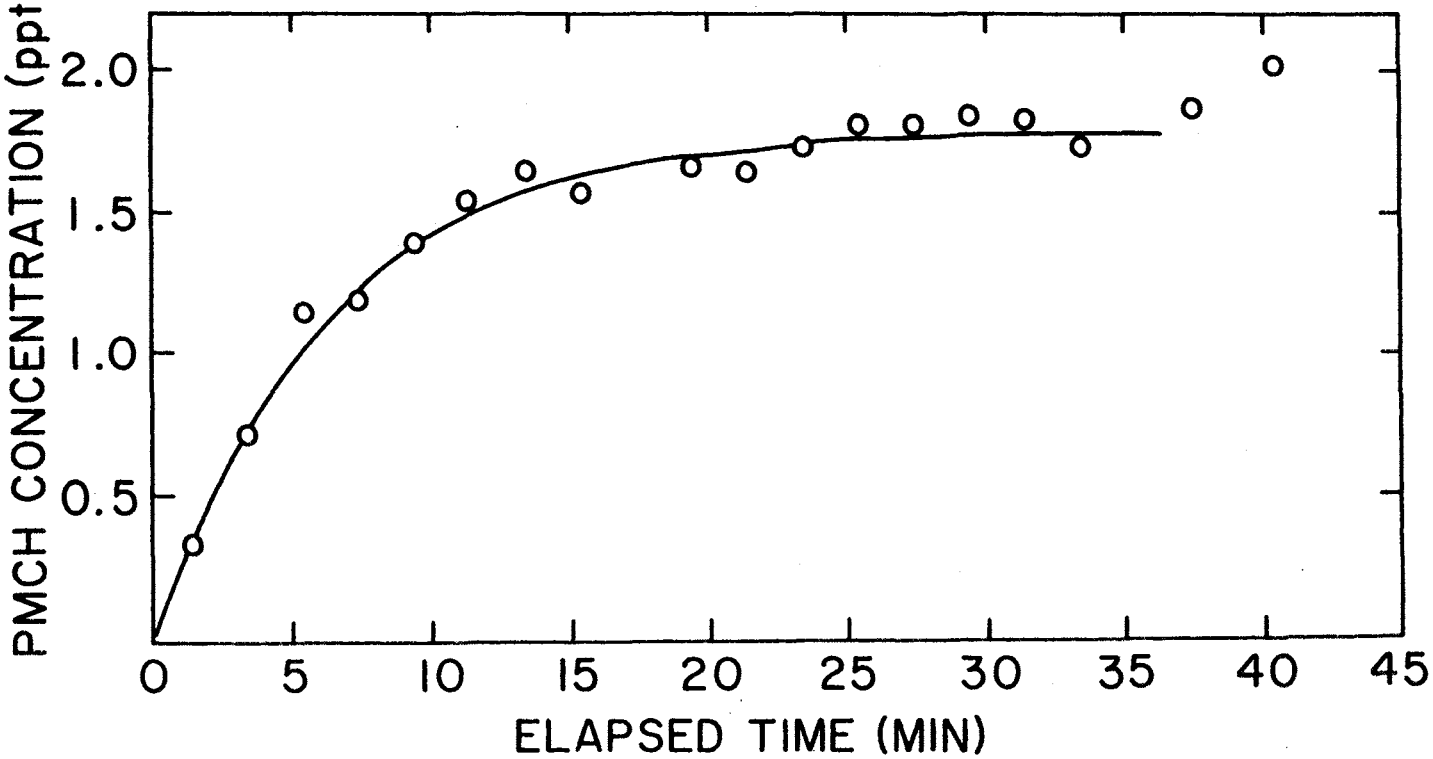

Figure 5

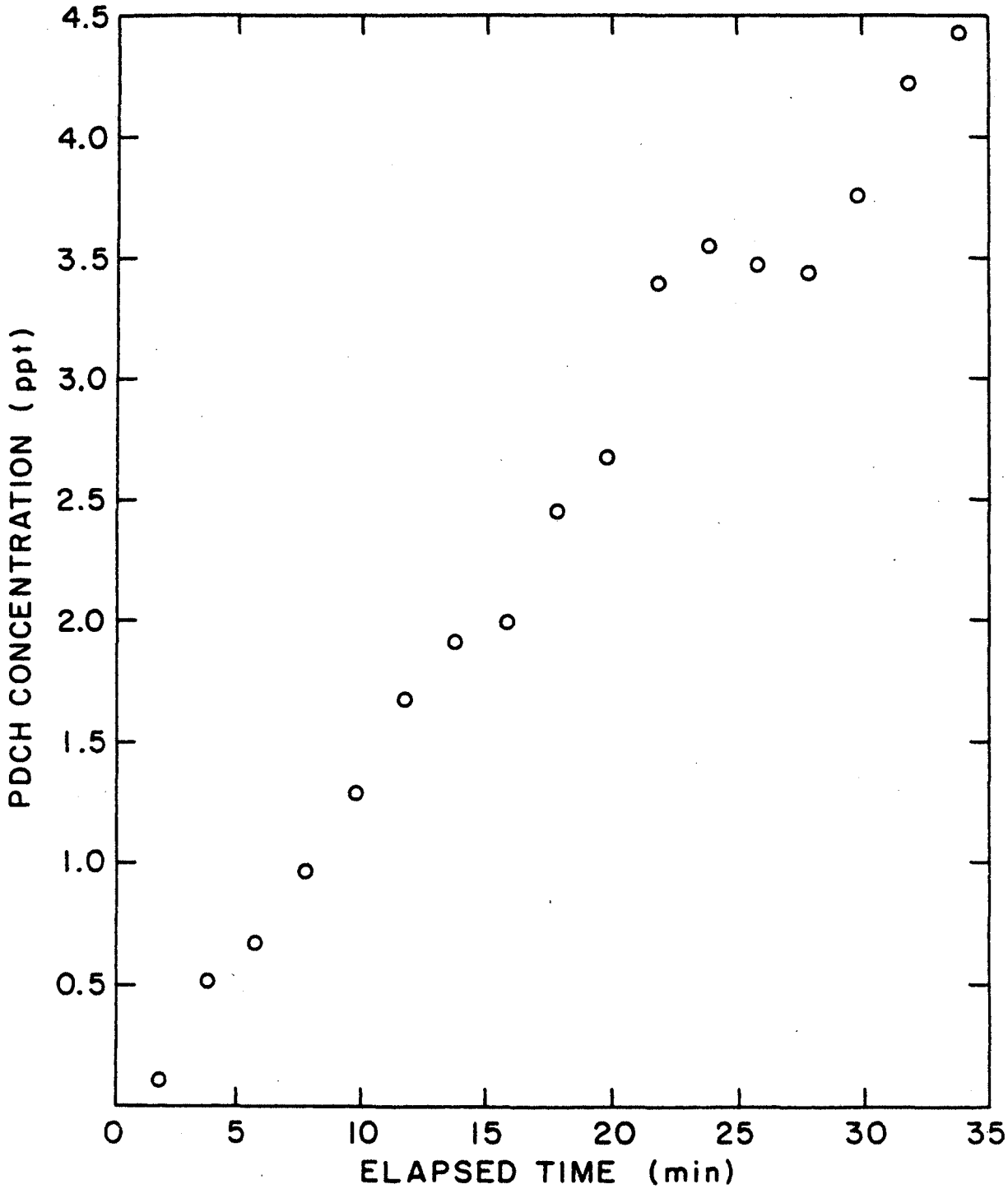
4.5
4.0
3.5
3.0
2.5
2.0
1.5
1.0
0.5
PDCH CONCENTRATION (ppt)
0
5
10
15
20
25
30
35
ELAPSED TIME (min)

MEASURED TAGGANT CONCENTRATIONS
AT A DC9 OUTFLOW VALVE
AS A FUNCTION OF ELAPSED TIME
TAGGED EXPLOSIVE IN
THE BAGGAGE COMPARTMENT

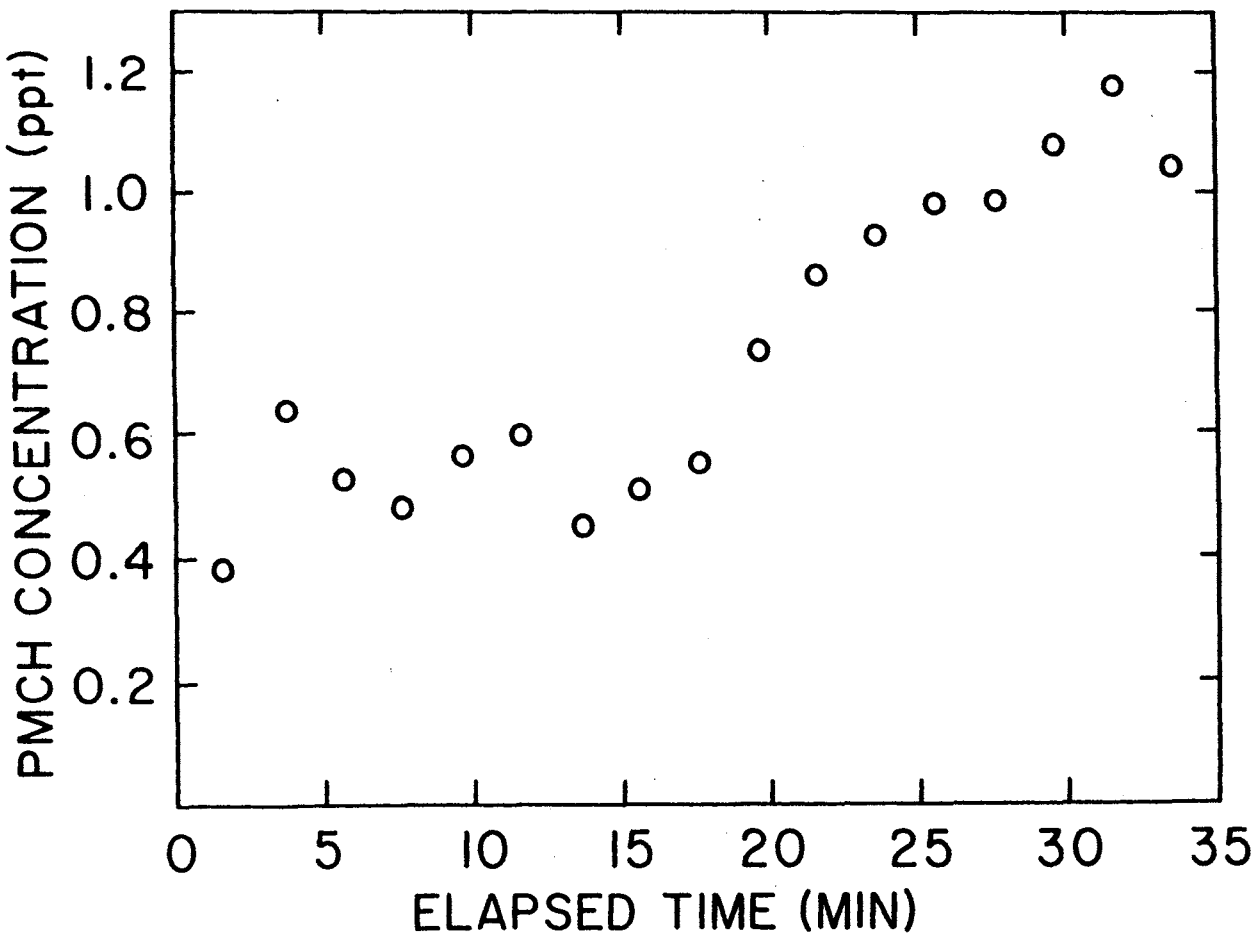

Figure 6

BNL-27099
LIMITED DISTRIBUTION

DETECTION OF VAPOR TAGGANTS USED FOR EXPLOSIVE PREDETONATION DETECTION IN A BOEING 727 AIRCRAFT

Gunnar I. Senum, Robert P. Gergley, Edgar A. Cote, and Russell N. Dietz

Environmental Chemistry Division
Department of Energy and Environment

October 1979

Test Date: September 12, 1979

Research sponsored by the
Bureau of Alcohol, Tobacco and Firearms
of the U.S. Department of the Treasury
under the direction of The Aerospace Corporation

Informal Report

BROOKHAVEN NATIONAL LABORATORY

ASSOCIATED UNIVERSITIES, INC.

UPTON, NEW YORK 11973

ABSTRACT

Experiments to determine the feasibility of detecting vapor taggants from a Boeing 727-100 aircraft have been performed using perfluoromethylcyclohexane (PMCH) and perfluorodimethylcyclohexane (PDCH) as vapor taggants for the pre-detonation detection of explosives. Using a vapor taggant source of PMCH and PDCH which approximates a single (1/2 lb) stick with 0.05 percent by weight of taggant- containing microcapsules, the taggant chemicals were detectable at 86.6 parts per 10^{15} (ppq) within 10 minutes after source placement in the forward cargo compartment. The No. 1 engine of the Boeing 727 aircraft was at idle thrust on the runway with both air compressors (air pacs) running. After the source placement and closure of all hatches and doors the aircraft was pressurized to approximately 0.1 psig. The total measured air flow of cabin air through the aircraft was 1494 $\pm$ 152 ft^3/min. Taggant vapor concentrations were measured at the Boeing 727 ventilation outflow valve from a vapor taggant source placed in the front baggage compartment with the result that the taggant concentration in the front baggage compartment did not reach a steady state concentration during a 90-minute experiment. Taggant vapor concentrations were measured simultaneously in the passenger compartment and the rear baggage compartment with the use of a preconcentrator (The Brookhaven Atmospheric Tracer Sampler - BATS), a portable automatic air sampler; the vapor taggants emitted from a source in the front baggage compartment were not found to be above the ambient background levels in either the passenger compartment or the rear baggage compartment. Thus, under these test conditions, the best sampling point for detecting vapor tagged explosives on the Boeing 727 is at the ventilation outflow valve.

I. INTRODUCTION

The ultimate success of any vapor tagging technique for predetonation detection of explosives is dependent on the ability to detect the vapor taggants in various detection scenarios. A scenario of great interest is the detection of explosives on an aircraft, especialy between cargo and passenger loading and take-off times, when the vapor tagged explosives will have had only a short period of time in which to release the vapor taggant into the aircraft (in either the passenger or baggage compartment) before any detection is attempted. Thus, the feasibility of the technique is dependent on ability to detect the taggant vapor at concentrations present in the first few minutes with air sampling locations either inside the aircraft or at the ventilation outflow port.

An aircraft scenario using a DC-9 has been previously examined and the results discussed in an earlier report.[1] The results, however, had a degree of uncertainty due to the measurement of a higher taggant steady state concentration than predicted. A major source of experimental error was believed to be the measurement of total air flow. The vapor taggant source of the DC-9 experiment was several sticks of microencapsulated perflourodimethylcyclohexane (PDCH) tagged simulated explosive. There was a degree of uncertainty associated with the emission rate from the PDCH taggant source because of its temperature dependence. Two experiments were performed in the previous study,[1] one with the vapor tagged simulated explosives placed in the passenger compartment of the aircraft and the other with the explosives placed in the baggage compartment. There was sufficient air mixing in the passenger compartment to detect the vapor taggant in the ventilation outflow valve. However, the ventilation in the baggage compartment to the rest of the aircraft was determined to

be nonhomogeneous; the taggant concentrations measured at the outflow valve were lower than those measured for the passenger compartment for the same taggant source. Consequently, further experiments were needed for tagged explosives placed in the aircraft baggage hold to confirm nonhomogeneous mixing between passenger and cargo areas. The previous aircraft experiments were performed with the DC-9 aircraft being ventilated with only one air pac unit powered by the auxiliary power unit (see Fig. 1). This is the normal situation used during passenger and cargo loading.

II. BACKGROUND

As aircraft containing a vapor tagged explosive will provide two impediments to the detection of the vapor taggant in or from the aircraft. The first impediment is loss of the taggant due to physical adsorption of the vapor taggant on various adsorptive surfaces present in the aircraft, i.e., clothes, carpeting, etc. This loss can be minimized[2] by using vapor taggants that are relatively volatile, e.g., perfluorodimethylcyclobutane (PDCB), perfuoromethylcyclohexane (PMCH), and perflurodimethylcyclohexane (PDCH). The second impediment is the container or barrier surrounding the tagged explosive, e.g., luggage and boxes. Some containers can be sufficiently airtight so as to slightly or significantly reduce the rate of vapor taggant release into the aircraft. However, in a series of laboratory experiments involving barriers such as briefcases, suitcases, and sealed boxes, the effect has been shown[2] to be negligible due to the lack of airtightness of these barriers.

Two barriers, a sealed paint can and a zip-locked plastic bag, did provide a significant airtightness and with careful handling these barriers could be effective.

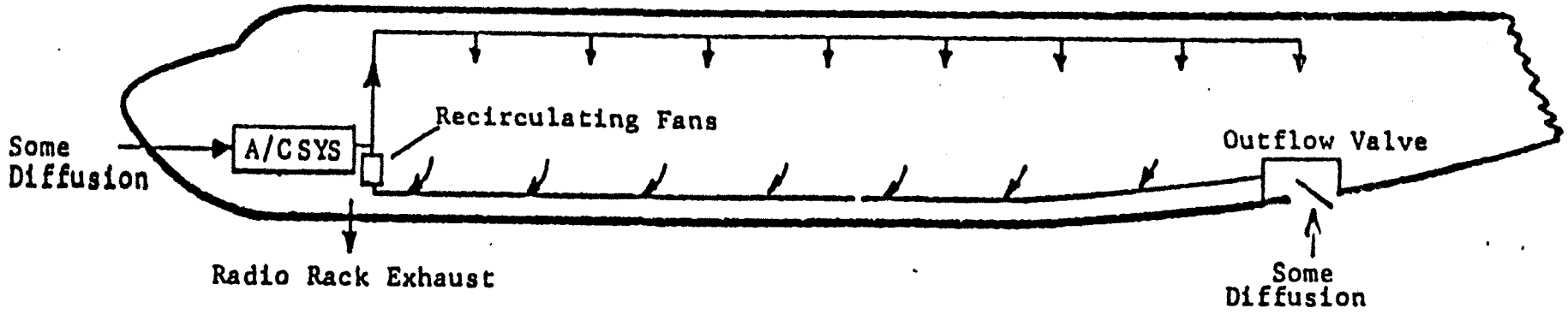

Air Flow with Recirculating Fans On

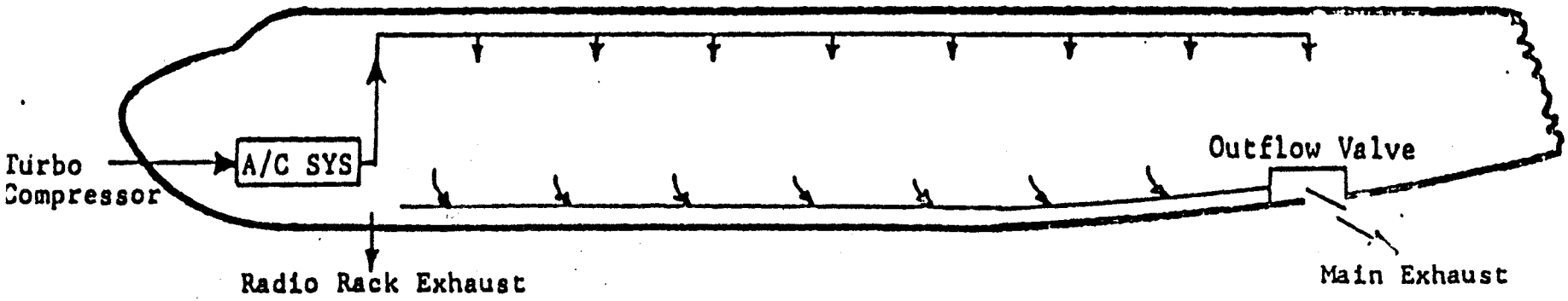

Air Flow with Turbo-Compressors On

Figure 1

No Negative #

With these impediments minimized, the detection of vapor tagged explosives become dependent on the degree of aircraft air mixing and the aircraft ventilation rate. The vapor taggant will be constantly diluted and removed from the aircraft by the inflow and outflow of ventilation air, and after a sufficiently long time, a steady-state taggant concentration will be reached inside the aircraft. As a result of this ventilation, the taggant concentration can be shown[3] to have the following time dependence:

$$C(t) = C(\infty)\ [1 - \exp\ (-\ t/t_v)] \tag{1}$$

where: $C(t)$ = the aircraft taggant concentration at a time t (elapsed time after the introduction of the tagged explosive),

$C(\infty)$ = the aforementioned steady state concentration and

t_v = the ventilation turnover time.

The two quantities $C(\infty)$ and t_v can be further expressed as

$$C(\infty) = R_{source}/R_{ventilation} \tag{2}$$

and

$$t_v = V_{ch}/R_{ventilation} \tag{3}$$

where:

R_{source} = the vapor taggant emission rate from the tagged explosive,

$R_{ventilation}$ = the aircraft ventilation rate, and

V_{ch} = the volume of the aircraft.

Thus if R_{source}, $R_{ventilation}$ and V_{ch} are known; then the taggant concentration within the aircraft can be predicted assuming homogeneous air mixing.

This functional dependence is derived under the assumption of uniform mixing of the taggant within the aircraft. The effect of an airtight barrier surrounding the tagged explosive is to slow the rate of taggant release into the aircraft, but the same steady-state concentration will be reached after a

longer elapsed time. Further discussion and equations for this effect is given in reference 3.

For the explosive predetonation detection experiment on the Boeing 727 aircraft PDCH was chosen as the vapor taggant due to its high sensitivity toward electron capture detector (ECD) detection. The ECD method was used because of its simplicity: the vapor taggant detector can be made as a small, portable, and relatively inexpensive unit.[4] The detection sensitivity for real-time continuous vapor taggant detection is presently 1 ppt of vapor taggant in air. Concentration techniques allow the detection sensitivity to be increased by two to four orders of magnitude depending on the method.[5]

III. EXPERIMENTAL

The aircraft used in the experiment was a Boeing 727-100, identification number FAA-N40, manufacturer's serial number 19854, as provided by the National Aviation Facilities Experimental Center (NAFEC) at Atlantic City, New Jersey. The aircraft was placed on a remote site at the airport so that one engine could be turned on and the ventilation turbocompressors could be used in the experiment. It was decided to place the taggant source in the front baggage hold of the aircraft and to sample for the taggant at one of the ventilation outflow valves on the underside of the aircraft (see Figure 1) by periodically collecting 2-liter Saran air samples in same manner as was done previously.[1]

The ventilation rate of the aircraft was measured during the experiment at all of the outflow valves on the aircraft by a 4 in. Davis vane anemometer (Model A/2). The combined ventilation rate through both rear outflow valves and the radio rack post was measured to be 1493 $\pm$ 153 ft^3/min.

The source of vapor taggant consisted of a pressurized cylinder mixture with a 5.14 $\pm$ 0.11 mL/min flow of a 2 ppm source of PDCH and a 0.2 ppm source of PMCH in UHP air controlled by a small pressure restrictor and measured by a bubble flowmeter before and after the experiment. Consequently, the PDCH taggant emission rate was $(10.3 \pm 0.2) \times 10^{-9}$ liters per minute and the PMCH taggant emission rate was $(1.0 \pm 0.2) \times 10^{-9}$ liters per minute which is comparable to the taggant emission rates of vapor tagged bulk explosives.[1] The pressurized cylinder, however, provided a more stable source of vapor taggant in terms of a constant emission rate than the vapor tagged bulk simulated explosives using microencapsulated PMCH and PDCH previously used due to their emission rate fluctuations as a function of storage temperature.

It was initially decided to take air samples in 2-liter air sampling bags for subsequent analysis at BNL because the expected PMCH and PDCH taggant concentrations were too low for real-time continuous taggant vapor monitoring by the Brookhaven Continuous Electron Capture Detector (CECD). Included were two Brookhaven Atmospheric Tracer Samplers (BATS) used to collect air samples inside the passenger compartment and in the rear baggage hold. Once the taggant source and the two BATS units were placed in the aircraft, the aircraft was sealed, the ventilation turbocompressors were turned on, and the experiment began.

The air sampling bags and taggant source were brought separated to the experimental site separately in order to avoid any contamination of the sample bags by the taggant source. Before the experiment, all the air sampling bags were cleaned and filled with ultrahigh purity air and several were analyzed for PDCH and PMCH residuals in order to guarantee the absence of these taggants.

Several bags were used as internal blanks and remained unused during the experiment in order to check for cross contamination of the bags during their return to BNL.

The BATS unit is an adsorption sampler which collects up to 23 air samples for subsequent analysis by gas chromatographic (GC) techniques. An internal pump sequentially draws an air sample through an adsorbent packed stainless steel sampling tube (23) where the compounds of interest are adsorbed onto Ambersorb, a Rohm and Haas proprietary adsorbant contained therein. The BATS unit is versatile in that it can be programmed to take a preselected number of samples (1 to 23) for a preselected sampling time (1 to 24 hours) and will automatically record by means of a self-contained printer the sample data consisting of sample number, time and flow. Also, the sampler can be preprogrammed to turn on within a 24-hour period over 7 days to provide timed sequential sampling. The sampler is battery powered and is portable (20 lb) and contained within a weatherproof aluminum case 13 in. wide x 9 in. deep x 7 in. high). Recovery of the adsorbed vapor taggant sample is accomplished by thermal desorption using direct resistive heating of the sample tube under the control of an external programmer.

An illustration of the BATS unit is given in Figure 2. The BATS units, as used in the experiment, were programmed to start simultaneously at the commencement of the experiment and to take 5-minute air samples every 5.25 minutes during the 2-hour duration of the experiment. The airflow rate through each sampling tube was 70 mL/ min. Approximately 350 mL of air was sampled through each sampling tube.

At the end of the experiment, the air sampling bags and the two BATS units were returned to BNL for analysis. The BATS units were analyzed directly by

Figure 2

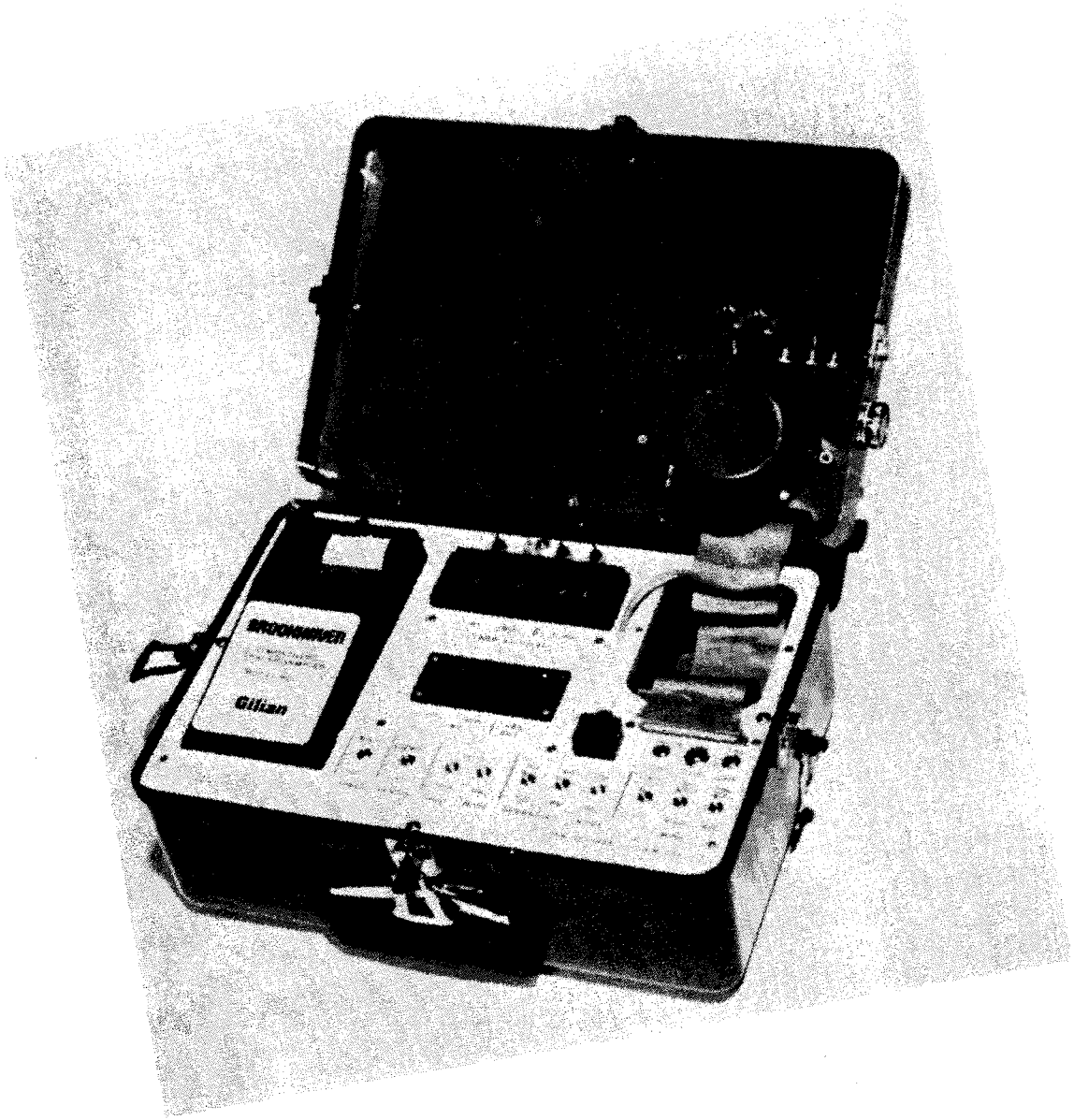

gas chromatographic analysis; however, the air sampling bags could not be similarly analyzed without preconcentration due to the expected low taggant concentrations of approximately 10^{-14} parts per part. The analysis was accomplished by concentrating approximately 400 mL of each air sample into an adsorption trap of the BATS unit, which was subsequently desorbed and chromatographically analyzed.

IV. RESULTS AND DISCUSSION

The expected steady-state taggant concentration, $C(\infty)$ and turnover time, t_v, can be calculated according to equations (2) and (3) from the measured taggant emission rate (10.3×10^{-9} L/min), aircraft ventilation rate (42280 $\pm$ 4300 L/min), and the aircraft internal volume (233,696 liters). Consequently, a steady-state concentration 243 $\pm$ 24 ppq and turnover time 5.5 minutes are calculated. This very short calculated turnover time indicates that the steady-state concentration is reached within 10 minutes after the taggant source has been placed within the aircraft. Thus, it is nearly impossible to extract an experimentally determined turnover time as was done in the previous study[1] from the concentrations measured from the bag and BATS samples, because these air samples were 2- and 5-minute averages. Consequently, all of the measured taggant concentrations should approach the steady-state taggant concentration assuming efficient air mixing within the aircraft.

The calculated steady-state taggant concentration of 243 $\pm$ 24 ppq is an order of magnitude above ambient PDCH background concentration of 23.8 $\pm$ 2.5 ppq as measured during 1977 in Chester, New Jersey, by the Department of Energy Environmental Measurement Laboratory.[6]

In independent experiments performed by Brookhaven, ambient background concentrations of several taggants were measured, i.e., PMCH - 2.7 $\pm$ 0.3 ppq,

PDCH - 30.3 $\pm$ 1.7 ppq, and PDCB - 7.9 $\pm$ 1.8 ppq. The air samples used to generate the above data were collected at Yaphank, a rural site in central Long Island, New York during September 1979.[7] These ambient background concentrations of PMCH and PDCH must be subtracted from measured concentrations in the aircraft air samples, because ambient air was used to ventilate the aircraft during the experiment. The resultant value after background subtraction will reflect the contribution of PDCH due to the vapor source placed into the forward cargo area.

The analysis for the PMCH and PDCH taggant concentrations in the sampling bags and in the desorbed samples from the BATS units were done chromatographically, in the same manner as previously.[4] The analysis were calibrated with a 1×10^{-13} parts per part standard of PDCH and a 0.11×10^{-13} parts per part concentration of PMCH. The analysis of the aircraft air bag samples used the BATS units as preconcentrators. Analyses were standardized by preconcentrating the above standards in the same manner as the aircraft air bag samples. The precision of the PMCH and PDCH analysis was approximately 10 to 15 percent based on multiple analyses of the standards.

Air samples were simultaneously collected for subsequent laboratory analysis in three locations of the aircraft: (1) passenger compartment - BATS system in the center of the cabin; (2) rear cargo compartment - BATS system in the center of the compartment; and (3) rear outflow valve of the aircraft - grab bag air samples. The results of the laboratory analyses of the air samples collected from each location are discussed below.

A. Passenger Compartment Air Samples - BATS System

The PMCH and PDCH taggant concentrations measured in the passenger compartment using BATS unit No. 1 are given in Table 2. The elapsed time is

calculated from the starting time of the experiment and is the midpoint time of the 5-minute sampling period. The measured concentrations are also displayed in Figure 3 for PMCH and in Figure 4 for PDCH as a function of experimental elapsed time. This experiment also yielded an estimate of the ambient background concentrations of PMCH and PDCH from the least squares intercepts in Figures 3 and 4 as 0.3 $\pm$ 0.7 ppq and 24 $\pm$ 4 respectively. This ambient concentration of PDCH is in good agreement with the previous measurements of the ambient background. The ambient PMCH concentration is, however, less than the previously measured ambient concentrations. The measured PMCH and PDCH concentrations do not have the calculated steady-state concentration of 243 $\pm$ 24 ppq, but rather the measured concentrations increase linearly with time starting from the ambient PMCH and PDCH concentration. This result indicates that there is poor mixing of air between the front baggage hold in which the taggant source was located and the passenger compartment where the air samples were taken (see below). However, this result is not unexpected because it is known that the ventilation air flows from the passenger compartment around the cargo compartment and exits through the outflow valves. Consequently it should be difficult for the taggant vapors to diffuse into the passenger compartment against the flow of ventilation air. Thus, it is unlikely that a vapor tagged explosive, which has been placed in the front baggage hold can be detected by attempting to sample air in the passenger compartment. Based on this aircraft airflow stream, a better sampling location is at the ventilation outflow valve, which was also done in this experiment with the bag sampling (see below).

Figure 3

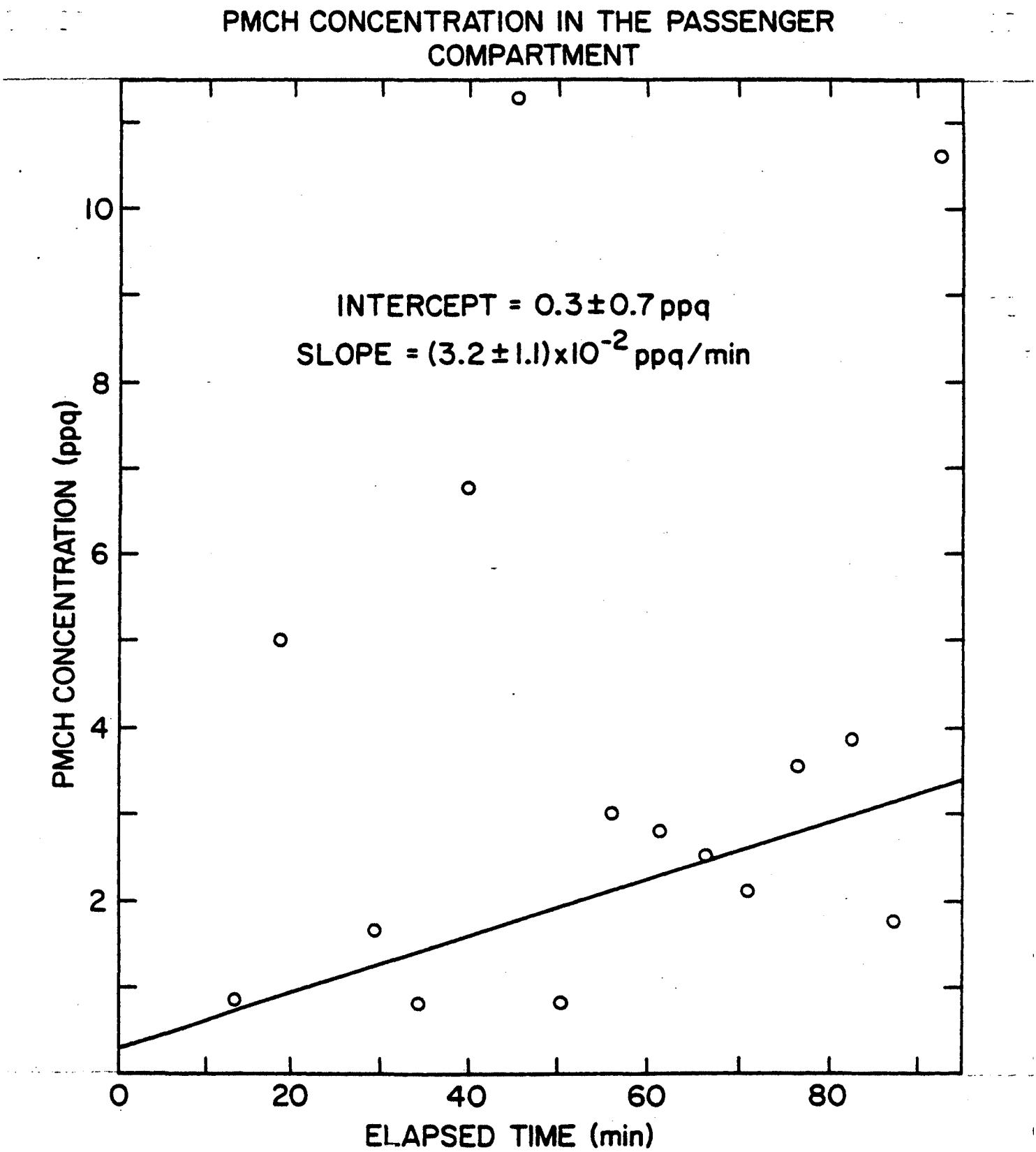
PMCH CONCENTRATION IN THE PASSENGER COMPARTMENT
INTERCEPT = 0.3 ± 0.7 ppq
SLOPE = (3.2 ± 1.1) x 10^-2 ppq/min
PMCH CONCENTRATION (ppq)
ELAPSED TIME (min)
0
20
40
60
80
2
4
6
8
10

Figure 4

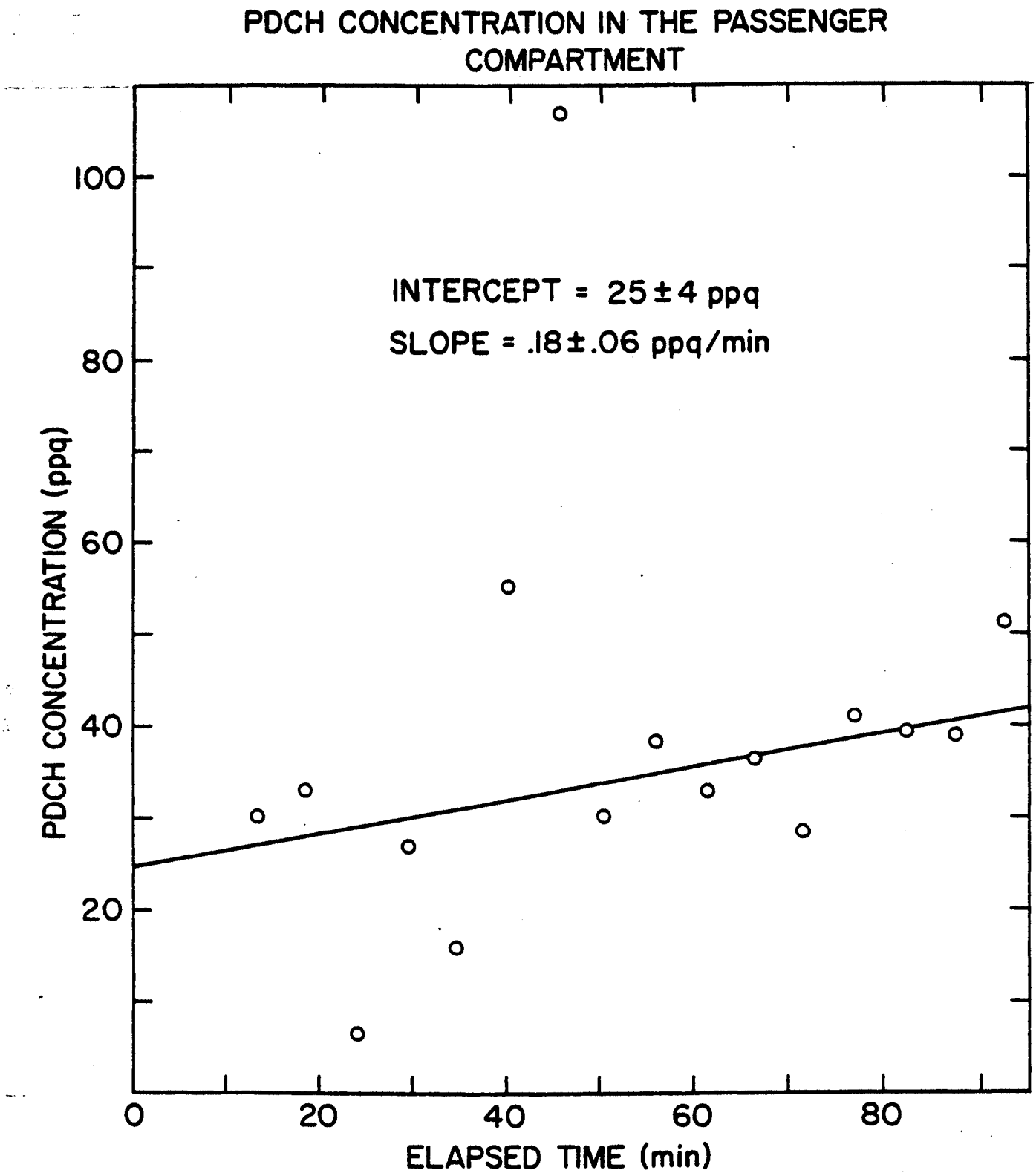
PDCH CONCENTRATION IN THE PASSENGER COMPARTMENT
INTERCEPT = 25 ± 4 ppq
SLOPE = .18 ± .06 ppq/min
PDCH CONCENTRATION (ppq)
100
80
60
40
20
0
20
40
60
80
ELAPSED TIME (min)

B. Rear Cargo Compartment Air Samples - BATS System

Unfortunately, BATS unit No. 2, which was placed in the rear baggage hold, had malfunctioned, and only two air samples were taken; 5-min and a 2-hr air samples. Nonetheless, the measured PDCH concentrations, as given in Table 3, are near the ambient background concentration 22.2 ppq, indicating that no taggant was transported from the front baggage hold into the rear baggage hold.

C. Rear Outflow Valve of Aircraft - Grab-Bag Samples

The PMCH and PDCH taggant concentrations as measured in the air sampling bags taken at the rear aircraft ventilation outflow valve are given in Table 4 and displayed in Figure 5 for PMCH and in Figure 6 for PDCH. The measured concentrations are approximately constant over the 2-hr period of the experiment. However, all of the measured concentrations are greater than the taggant ambient background concentrations. A measured steady-state concentration of 40.5 $\pm$ 35.0 ppq for PDCH and 14.1 $\pm$ 10.0 ppq for PMCH is obtained from an average of the measured concentrations, 70.8 $\pm$ 33.3 - 30.3 $\pm$ 1.7 ppq for PDCH and 16.8 $\pm$ 9.7 - 2.7 $\pm$ 0.3 ppq for PMCH minus the taggant ambient backgrounds as given in Table 1. The measured PDCH steady-state concentration of 40.5 $\pm$ 35.0 ppq is not in agreement with the calculated value of 243 $\pm$ 24 ppq. Likewise, the measured PMCH steady-state concentration of 14.1 $\pm$ 10.0 ppq is not in agreement with the calculated value of 25 ppq. The calculated value of the steady-state vapor taggant concentration using equation 2 is 243 $\pm$ 24 ppq for PDCH and 25 $\pm$ 2.5 ppq for PMCH. The observed taggant concentrations with background subtractions in the air samples from the outflow valve were: 40.5 $\pm$ 35 ppq for PDCH and 14.1 $\pm$ 10.0 ppq for PMCH. These measured concentrations are understandably low because the cargo compartments of the Boeing 727-100 were designed to be airtight. The cargo compartments of the Boeing 727-100 are

Figure 5

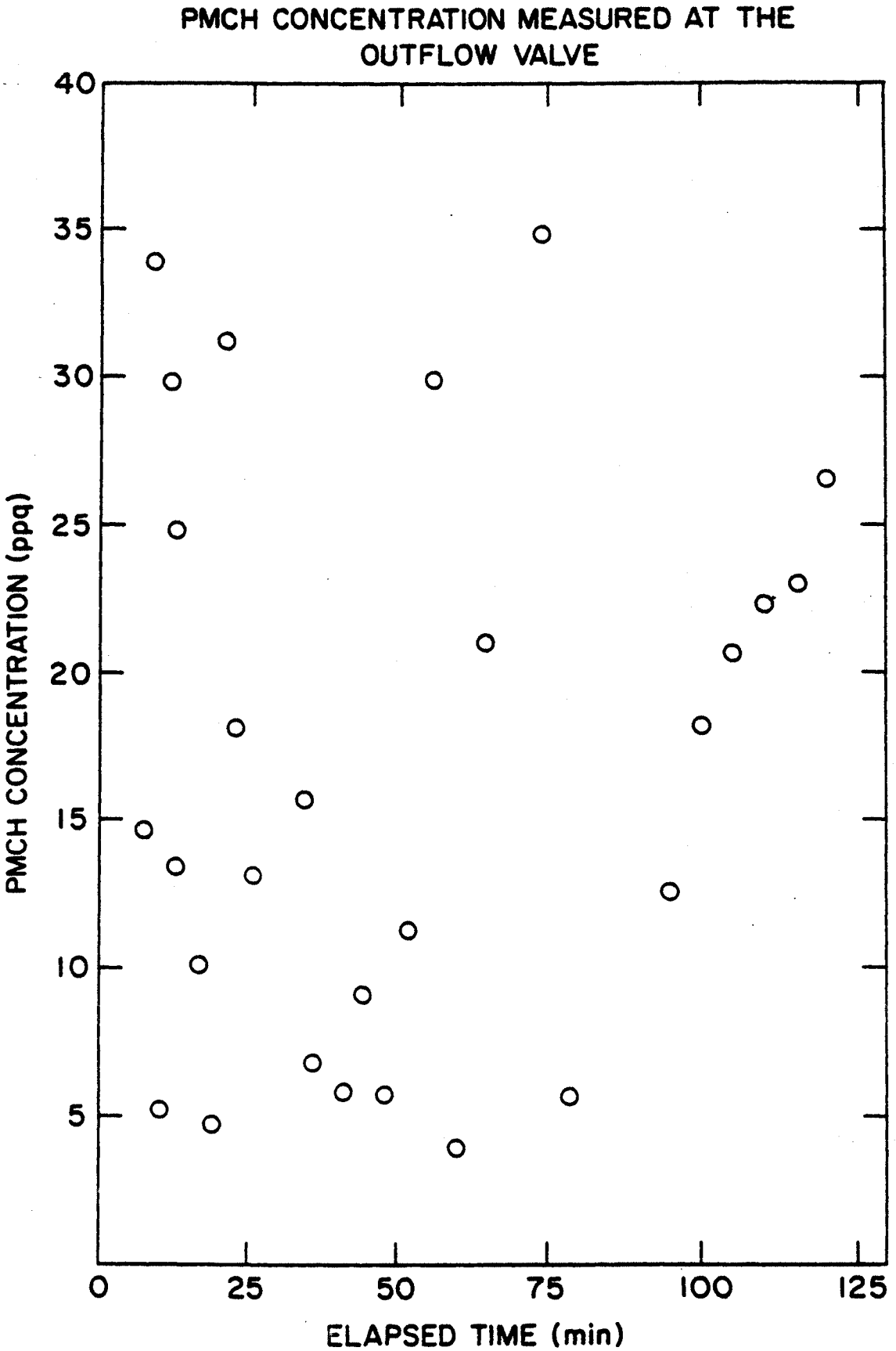
PMCH CONCENTRATION MEASURED AT THE OUTFLOW VALVE
PMCH CONCENTRATION (ppq)
40
35
30
25
20
15
10
5
0
25
50
75
100
125
ELAPSED TIME (min)

Figure 6

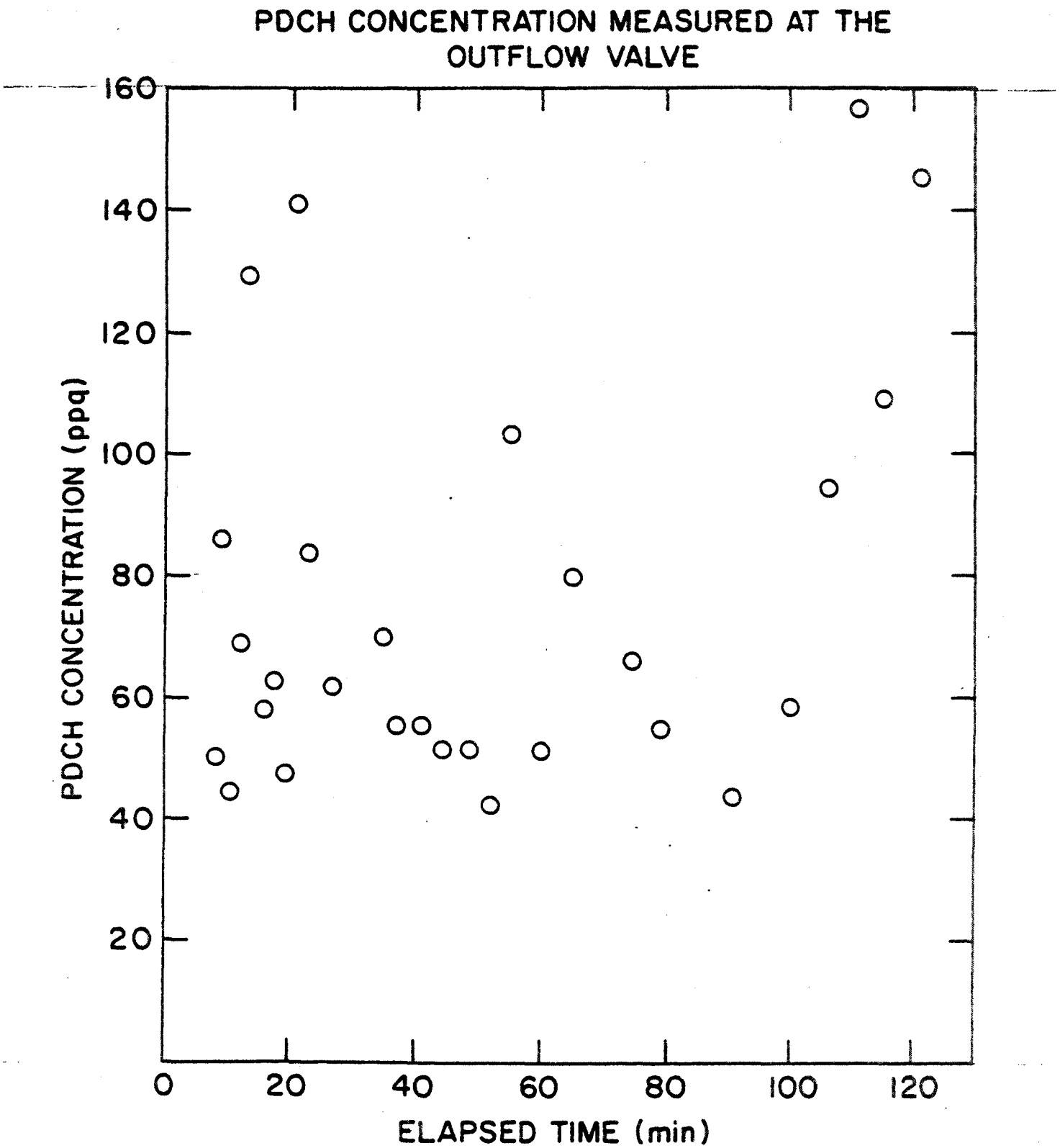
PDCH CONCENTRATION MEASURED AT THE OUTFLOW VALVE
PDCH CONCENTRATION (ppq)
160
140
120
100
80
60
40
20
0
20
40
60
80
100
120
ELAPSED TIME (min)

subject to the Federal Air Regulation No. 25 and have been constructed as class "D" compartments. The class D aircraft fabrication requirements stipulate that cargo air is not to mix with cabin air. This aircraft design feature is a fire protection measure. In the event of a fire in the cargo compartments, the air tight seal of the cargo compartments will not allow sufficient air (oxygen) to enter the compartment to sustain combustion. Also, toxic gases from such fires will not mix with cabin air.

V. CONCLUSIONS

A vapor taggant source equivalent to a single stick of explosive, vapor tagged with microencapsulated perfluorocarbon chemicals such as PMCH or PDCH has been used to determine the feasibility of detecting vapor taggants from a Boeing 727-100 aircraft. With a vapor taggant source placed in the forward cargo compartment, the suitability of three sampling locations has been investigated. Two air sampling locations show no significant vapor taggant penetration. The passenger area sampling location is upstream of the cargo compartment ventilation pattern of the aircraft. Consequently only ambient background PMCH and PDCH taggant concentrations were observed. Similarly, the rear cargo compartment was found to contain only ambient background concentrations of PMCH and PDCH. This result indicates air mass isolation between the forward and rear cargo compartments of the Boeing 727 aircraft. Results indicate that the sampling of the rear outflow valve of the aircraft is the preferred position.

Despite the aircraft design specification requiring air mass isolation of the cargo compartments, there is significant penetration of taggant vapors into the air stream exiting the aircraft from the rear outflow valve. However, the air mass mixing in the entire aircraft is nonhomogeneous. The calculated steady-state concentrations of PMCH and PDCH were consequently not attained.

Another major conclusion of the experiment is that the scenario when a taggant vapor source is placed in the forward cargo compartment of a Boeing 727 aircraft requires the measurement of parts per quadrillion (10^{15}) quantities of the vapor taggant. To attain a reasonable confidence level for tagged explosive detection in such a scenario, use of an automated preconcentration technology, capable of vapor taggant enrichment factors of 10^2 to 10^4, is required prior to sample delivery to a sensor with a lower limit of detection at 1 ppt.

ACKNOWLEDGMENTS

The authors would like to thank C.T. Pate and R.B. Moler of The Aerospace Corporation and G. Carp and T. Tsacoumis of the Federal Aviation Administration for arranging these experiments, and to C.T. Pate and E.K. Achter for their assistance during the experiment. Appreciation is expressed to Kurt Schilling of NAFEC for his assistance.

REFERENCES

1. Senum, G.I., Gergley, R.P., Cote, E.A., and Dietz, R.N. Detection of Tagged Explosives in a DC-9 Aircraft via Sampling of the Air Exhaust, BNL 26612, July 1979.

2. Senum, G.I. Evaluation of Vapor Taggants and Substrates for the Tagging of Blasting Caps. Monthly progress letter reports to The Aerospace Corporation, July 1977 through March 1979.

3. Senum, G.I., E.M. Ferreri, M.W. Greene, R.P. Gergley and R.N. Dietz. The Effect of Taggant Vapor Adsorption and Containment on the Predetonation Detection of Explosives, October 1979.

4. Dietz, R.N., Cote, E.A., and Brown, R.M. A Portable Electron Capture GC for Tracing Air Pollutants. BNL 16512, April 1972.

5. Dietz, R.N., Goodrich, R.W., and Cote, E.A. Detection of Perfluorinated Taggants in Electric Blasting Caps by Electron Capture Monitors, Proc., New Concepts Symposium and Workshop on Detection and Identification of Explosives, November 1978.

6. Lagomarsino, R.J., Department of Energy, Environmental Measurements Laboratory, memo to G.A. Welford, Department of Energy, Analytical Chemistry Division, October 1977.

7. Dietz, R.N., Cote, E.A., Unpublished data, 1979.

TABLE 1

Ambient Taggant Concentrations
Yaphank, N.Y. - September 1979

Sample Vol., L	Concentration, pp 10^{15}		
	PDCB	PMCH	PDCH
15.9	10.1	4.0	32.9
16.1	9.9	3.2	32.4
16.7	6.5	2.7	30.3
17.0	9.3	2.7	28.3
30.2	7.1	2.5	29.3
30.2	5.4	2.7	29.3
30.2	7.3	2.5	29.4
Average	7.9 ± 1.8	2.7 ± 0.3	30.3 ± 1.7

TABLE 2

Measured Taggant Concentrations in the Passenger Compartment
BATS Unit No. 1

Elapsed Time (min)	PMCH (ppq)	PDCH (ppq)
8.5	----	----
13.5	0.85	30.1
18.5	4.99	32.9
24.0	----	6.3
29.5	1.57	26.8
34.5	.80	16.9
40	6.77	55.2
45.5	11.3	107
50.5	.81	30.1
56	3.01	37.9
61.5	2.81	32.9
66.5	2.53	36.4
71.5	2.11	27.8
77.0	3.54	41.1
82.5	3.87	39.6
87.5	1.76	39.1
92.5	10.7	51.6

TABLE 3

Measured Concentrations as Collected by the BATS Units

Taggant	BATS No. 1 Rear Baggage Compartment Concentration in ppq 10:25 am	10:30 to 12:47 pm	BATS No. 2 Passenger Compartment INTERCEPT (Ambient Concentration ppq)	SLOPE (ppq/min)
PDCH	19.9	22.2	25 ± 4	0.18 ± 0.06
PMCH	---	2.3	0.3 ± 0.7	3.2 ± 1.1 x 10^{-}

TABLE 4

PMCH and PDCH Vapor Taggant Concentrations as Measured at the Ventilation Outflow Valve of a Boeing 727 Aircraft

Elapsed Time (min)	Taggant Concentrations ppq PMCH	PDCH		Averaged Concentrations
7.92	14.6	49.8		PMCH: 16.8 ± 9.7 ppq
9.25	33.9	86.5		PDCH: 75.8 ± 33.3 ppq
10.52	5.2	44.2		
11.92	29.8	68.9		
13.25	24.8	129.4		
14.52	974.4	4192	deleted	
15.92	13.4	58.4		
17.42	10.1	62.7		
19.08	4.7	47.0		
20.75	31.2	141.9		
22.75	18.1	83.6		
26.75	13.0	61.7		
34.75	15.6	69.7		
37.42	6.8	55.7		
41.08	5.8	55.4		
44.75	9.1	51.4		
48.42	5.7	51.5		
52.08	11.2	42.0		
55.75	29.9	103.3		
60.42	3.9	51.2		
65.08	21.0	79.8		
69.75	314.8	482.2	deleted	
74.42	34.8	65.9		
79.08	5.6	54.8		
90.42	12.5	43.2		
100.83	18.1	58.8		
105.83	20.6	94.1		
110.83	22.2	157.0		
115.83	23.0	109.2		
120.17	26.5	145.5		